12-2014

Dissection of Gray Leaf Spot of Maize Through Functional Genomics

Robert Louis Hirsch
University of Arkansas, Fayetteville

Dissection of Gray Leaf Spot of Maize Through Functional Genomics

Dissection of Gray Leaf Spot of Maize Through Functional Genomics

A dissertation submitted in partial fulfillment
of the requirements for the degree of
Doctor of Philosophy in Plant Science

by

Robert Louis Hirsch
Tulane University
Bachelor of Arts in English and Religious Studies, 2007
University of Arkansas
Master of Science in Plant Pathology, 2010

December 2014
University of Arkansas

This dissertation is approved for recommendation to the Graduate Council

_____
Dr. Burton Bluhm
Dissertation Director

_____
Dr. Frederick Spiegel
Committee Member

_____
Dr. Michael Evans
Committee Member

_____
Dr. Won-Bo Shim
Committee Member

_____
Dr. James Correll
Committee Member

ABSTRACT

Gray leaf spot, caused by *Cercospora zeae-maydis*, is a devastating disease of maize that reduces yields and increases management costs. *C. zeae-maydis* penetrates maize leaves through stomata, but the biological and molecular bases of this process are poorly understood. The goal of this research was to elucidate the biological parameters of stomatal infection in *C. zeae-maydis,* and to identify and characterize novel genetic pathways involved in stomatal sensing and pathogenesis. Histopathological observations of a GFP-expressing strain of *C. zeae-maydis* during infection of maize indicated that the fungus responded to host-derived stomatal cues during the infection process. *C. zeae-maydis* was observed exhibiting tropism toward non-host stomata, which ultimately implicated molecular oxygen as a possible stomatal chemoattractant. To explore the role of circadian rhythmicity in gray leaf spot, the putative central circadian oscillator gene *FRQ* in *C. zeae-maydis* was functionally disrupted and characterized. Interestingly, *FRQ* deletion strains were non-pathogenic when inoculated on maize leaves. Histological observations suggested that *FRQ* deletion strains failed to form appressoria in association with maize stomata. In order to identify other novel genes involved in pathogenesis, a collection of 1228 insertional mutants was created and assayed for infectious development. Ten mutants were identified, including one that was disrupted in *RJP1*, a putative epigenetic regulator of gene expression. In a related study, thirty-one genes were selected for functional disruption based on sequence similarity to known fungal regulatory genes. Analysis of these mutants indicated that *GPA2*, which encodes a putative G protein alpha subunit, was required for pathogenesis. Lastly, gene expression analysis during pre-penetration infectious development revealed widespread transcriptional reprogramming. Key findings from this research include the discovery of novel pathogenesis-related genes and potential roles for oxygen sensing and the fungal circadian clock in foliar pathogenesis. Furthermore, this research illuminated a previously

unrecognized level of complexity underlying the regulation of stomatal infection during gray leaf spot of maize and established a foundation for future molecular investigations.

ACKNOWLEDGEMENTS

First and foremost, I would like to thank Dr. Burt Bluhm for his advice and guidance during my Ph.D. degree program. Dr. Bluhm's mentorship has been invaluable to my development both as a person and as a scientist. I would like to thank the members of my graduate committee: Dr. Jim Correll, Dr. Fred Spiegel, Dr. Mike Evans, Dr. Won-Bo Shim and Dr. Rick Bennett, the head of the Plant Pathology Department. Their research suggestions and support of my academic development were deeply appreciated. Also, thanks are due to the U.S. National Science Foundation for funding this research.

The members of my lab have been instrumental in the success of my research program. I would like to thank Mr. John Ridenour and Mr. Jon Smith for providing their knowledge of molecular biology, and Ms. Kara Troglin, Ms. Shantae Wilson and Mr. Brant Smith for their constant hard work and diligence. I am continually impressed by the teamwork exhibited by the members of the Bluhm lab, and I am indebted to them for their help.

Finally, I am very fortunate to have such a caring family. I would like to thank Mom, Dad, Augie and especially my wife Christal for their support and encouragement during the course of my degree. I could not have completed this process without them.

TABLE OF CONTENTS

CHAPTER 1: INTRODUCTION

Fungi Sense And Respond To Their Chemical Environment Through A Variety Of Mechanisms

Fungi occupy most ecological niches on the planet and have developed complex sensory mechanisms that facilitate their evolutionary success and global presence (Bahn et al., 2007). Similar to higher eukaryotes, fungi sense many environmental stimuli, including light, chemicals, surface topography, gravity and electric fields (Bahn et al., 2007). As sessile organisms, fungi are frequently challenged by environmental stimuli that require the immediate elicitation of physiological responses, such as nutrient acquisition and the maintenance of cellular homeostasis.

Like most eukaryotes, fungi utilize transmembrane receptor proteins to sense various chemicals in their surroundings. The G protein-coupled receptors (GPCRs) comprise one of the largest families of transmembrane proteins, and their role in sensing pheromones and nutrients has been studied at length (Li et al., 2007). GPCRs bind to heterotrimeric signaling complexes comprised of Gα, Gβ, and Gγ subunits, which are released by the GPCRs following recognition of the appropriate chemical signal. The heterotrimers then disassociate into Gα and Gβγ subunits, which trigger the expression of downstream regulatory genes (Li et al., 2007). For example, the yeast *Saccharomyces cerevisiae* secretes two different mating pheromones, which are detected by cells of opposite mating types by the GPCRs Ste2 and Ste3 (Versele et al., 2001). Once the pheromones bind to their target GPCRs, the Gα subunit Gpa1 disassociates from the Gβγ dimer and activates a mitogen-activated protein kinase cascade, which halts the cell cycle and promotes fusion with strains of the opposite mating-type (Versele et al., 2001). Homologs of the *S. cerevisiae* pheromone GPCRs are present in *Schizosaccharomyces pombe, Aspergillus*

nidulans, Neurospora crassa, and *Ustilago maydis*, (Bolker et al., 1992; Takanaka et al., 1993; Seo et al., 2004; Kim and Borkovich, 2004; Bahn et al., 2007) which shows a broad conservation of GPCR-mediated signaling throughout many fungi.

Glucose is a preferred carbon-based energy source for many organisms and fungi have developed several distinct mechanisms to sense and transport this important molecule. In *S. cerevisiae*, the GPCR Gpr1 senses sucrose and glucose, which activates the G protein heterotrimer containing the Gα subunit Gpa2. Gpa2 then triggers the cyclic AMP-dependent expression of Protein Kinase A, a regulatory enzyme involved in numerous cellular processes, including transcription, metabolism, and mitosis (Xue et al., 1998; Lorenz et al., 2000; Lemaire et al., 2004). The filamentous ascomycete fungi *A. nidulans* and *N. crassa* contain putative Gpr1 homologs, but their roles in sugar sensing are currently unknown (Bahn et al., 2007). Hexose transporters also play important functions in carbohydrate sensing and transport, including the HXT (hexose transporter) family of proteins in *S. cerevisiae*. Most characterized HXTs display an affinity for specific carbohydrates and may function synergistically to mediate the interaction between fungi and their nutrient sources (Forsberg and Ljunghajl, 2001). Recently, putative fructose hexokinases were characterized in the ascomycete pathogens *Botrytis cinerea*, *A. fumigatus, and Fusarium verticillioides* (Rui and Hahn, 2007; Fleck and Brock, 2010; Kim et al., 2011c). Hexokinases are broadly conserved multifunctional enzymes involved in the initiation of glycolysis and function as potential glucose sensors in taxonomically diverse organisms (Harrington and Bush, 2003; Santangelo, 2006). Similar to observations of predicted *F. verticillioides HXK1* homologs in the pathogenic fungi *Botrytis cinerea* and *A. fumigatus, HXK1* of *F. verticillioides* regulated carbohydrate-specific catabolism and virulence during infection of host tissue (Rui and Hahn, 2007; Fleck and Brock, 2010; Kim et al., 2011c). Despite the

importance of carbohydrate sensing and intracellular sugar transport during crucial biological processes in fungi, the transduction of nutritional signals during growth and development remains poorly understood.

Fungi are the principle consumers of organic matter in many ecosystems and they have evolved a diverse array of enzymes designed to degrade complex plant polymers (Baldrian et al., 2012). Many fungi survive saprophytically on plant debris by secreting enzymes that break down and actively transport the subsequent products through the hyphal cell membrane. In many environments, fungi in the phylum Basidiomycota are described colloquially as "white-rots" or "brown-rots" based on their preference for degrading either lignin or cellulose (and hemicellulose), common molecules that comprise woody plant tissues (Kogel-Knabner, 2002). Lignin is a polymer of aromatic alcohols and is a major component of plant secondary cell walls (Crawford, 1981). Within each plant cell, lignin acts a structural support between the cellulose, hemicellulose and pectin components that also comprise most plant material (Crawford, 1981). White-rot fungi produce enzymes that catalyze the degradation of lignin resulting in organic matter rich in undigested cellulose, which is white in color (Hatakka, 1994). White-rot fungi produce numerous lignin-modifying enzymes like lignin peroxidases, manganese peroxidases, and many phenol-oxidases, which catalyze the breakdown of lignin by oxidative rather than hydrolytic mechanisms (Hatakka, 2005).

Brown-rot fungi are basidiomycetes that form a dense mycelium in decaying organic matter and preferentially metabolize cellulose, leaving the brownish lignin matrix visible to the unaided eye (Goodell, 2003). Cellulose is a polysaccharide containing thousands of $\beta(1\rightarrow4)$ linked D-glucose units, which act as important structural components of the primary cell walls in plants (O'Sullivan, 1997). As a straight chain polymer comprising approximately 40-50% of

plant biomass, cellulose contributes to cell wall tensile strength and stem rigidity (O'Sullivan, 1997). The breakdown of cellulose and hemicellulose provides fungi with glucose molecules and other carbohydrates needed for glycolysis, and is thus an important mechanism of primary metabolism for many fungi (Barelle et al., 2006). Recently, the capacity of many fungi to degrade cellulose into individual glucose monomers has driven the development of fungi as bioreactors for the production of biofuels. The ubiquitous saprophytic ascomycete *Hypocrea japonica* (*Trichoderma reesei*) has been the subject of decades of genetic research focused on elucidating the pathways underlying lignocellulosic enzyme production (Hakkinen et al., 2014). *H. japonica* contains multiple lignocellulose degrading enzymes, including nine characterized cellulases, 15 characterized hemicellulases, and at least 42 predicted genes with lignocellulose degrading activity (Hakkinen et al., 2014), highlighting the diversity of enzymes that fungi utilize to break down organic substrates.

Light Is A Major Environmental Stimulus

The diurnal fluctuations of light and dark are one of the most dependable environmental cycles present since the evolution of life, and many organisms have evolved sensory mechanism that respond to transitions from light to dark or fluctuations in light intensity. The filamentous zygomycete fungus *Phycomyces blakesleeanus* displays striking physiological changes in response to light, and was one of the earliest established model species for the study of fungal photosensing. Prior to spore dispersal, *P. blakesleeanus* forms numerous sporangiophores that grow up to ten centimeters in length (Cerdá-Olmedo and Lipson, 1987). The sporangiophores grow toward blue and near-UV light within a very large intensity range, similar to that of the human eye (Galland, 1990). The first phototropism-defective *Phycomyces* mutants were developed by Dr. Max Delbruck (Bergman et al., 1973), and the underlying genes in the mutant

strains were named "*mad*" in honor of Dr. Delburck (Bergman et al., 1973). Ten *mad* genes (*madA-madJ*) involved in photosensing have been subsequently identified from genomic analysis of the mutant strains (Cerdá-Olmedo, 2001). The *mad* mutations are pleotropic in *P. blakesleeanus*, but detailed characterization of multiple targeted gene-deletion strains indicate that phototransduction depends on the synchronized function of multiple proteins and is not centralized through a single mechanism (Cerdá-Olmedo, 2001; Idnurm et al., 2006; Sanz et al., 2009; Corrochano and Garre, 2010).

The prevailing models of fungal light sensing were generated, in large part, from the elucidation of light sensing by *N. crassa*. During incubation in diurnal light conditions, mycelia of *N. crassa* develop alternating bands of conidia corresponding to growth during times of darkness. This phenotype provided a visual cue to select mutants defective in photosensing during the establishment of the *Neurospora* system in the 1950's and 1960's (Davis and Perkins, 2002). Specifically, the *band* (*bd*) mutation resulted in the formation of easily measurable bands of conidia, and *bd* has been incorporated into nearly every *N. crassa* strain utilized for circadian biology research (Sargent and Woodward, 1969; Belden et al., 2007). When exposed to light, the blue-light photoreceptor protein White Collar-1 (WC-1) forms a heterodimer with White Collar-2 (WC-2) to form the White Collar Complex (WCC). The WCC acts as a transcription factor that regulates multiple downstream processes, including the induction of conidiation, the orientation of perithecia, production of secondary metabolites and circadian rhythms (reviewed by Baker et al., 2011). While recent comparative genomic analyses have identified numerous putative photoreceptors analogous to opsins, phytochromes and cryptochromes in related fungi, the WC-1/WC-2 system appears broadly conserved in form and function in multiple taxa of fungi (Idnurm and Heitman, 2005; Idnurm et al., 2006). Putative WC-1 orthologs are known to

regulate conidiation, secondary metabolism, formation of sexual structures and pathogenesis in ascomycete fungi, hyphal differentiation and sporocarp development in basiodiomycetes, and secondary metabolism and phototropism in zygomycetes (Bahn et al., 2007; Ruiz-Roldan et al., 2008). *N. crassa* also contains a second blue-light photoreceptor designated VIVID, which is less conserved in fungi (Schwerdtfeger and Linden, 2003; Chen et al., 2010). The existence of multiple blue-light photosensory mechanisms indicates that light responsiveness is a complex process that may be regulated differently in various fungi. Furthermore, the associated downstream effectors remain poorly characterized and represent an intriguing area of current research.

Fungi As Plant Pathogens

Few fungi have more of a direct effect on society than plant pathogens (Agrios, 1997). Pathogenic fungi rarely have major ecological impacts in natural environments because host plants are often broadly dispersed, thereby reducing the likelihood of disease epidemics (Dinoor and Eshed, 1984). Also, non-fatal reductions in plant vigor and seed yield are often difficult to attribute to a single biotic variable (Dinoor and Eshed, 1984). Notable exceptions to this paradigm often involve pathogens introduced from other ecosystems, like the American chestnut blight pathogen *Cryphonectria parasitica*, and *Ophiostoma novo-ulmi*, the causal agent of Dutch elm disease (Anderson et al., 2004). These two pathogens decimated American chestnut and elm tree populations across the country during the last century, and significantly altered the composition of flora in American forests (Anderson et al., 2004). Agricultural practices like no-till farming and monoculture cropping strategies combined with society's dependence on a steady food supply have compounded the potential impacts of plant disease epidemics (Fisher et al., 2012). Fungal plant pathogens cause billions of dollars in annual crop losses to growers in

all agricultural regions of the world (Oerke et al., 1999), making pathogenic fungi an important area of study.

Fungal plant pathogens utilize diverse colonization strategies related to whether the pathogens kill host cells or utilize special mechanisms to keep host cells alive to complete their lifecycle. Many common plant pathogens like rust fungi, powdery mildews and downy mildews are obligate biotrophs, which require a continuous interaction with a living host for growth and reproduction (Brown and Hovmoller, 2002; Mendgen and Hahn, 2002). Facultative biotrophs, like the maize smut pathogen *U. maydis,* can grow independently of maize, but must infect maize to form reproductive structures (Gan et al., 2012). Biotrophic pathogens acquire nutrients from host cells through specialized infection structures called haustoria. For example, following foliar penetration by the bean rust pathogen *Uromyces fabae,* haustorial mother cells are formed after hyphae contact a host mesophyll cell (Harder and Chong, 1991). The haustorial mother cell penetrates through the plant cell wall and invaginates the host plasma membrane, forming a mature haustorium that facilitates the transfer of hexose sugars, amino acids and water into the fungal hyphae (Heath and Skalamera, 1997; Voegele and Mendgen, 2003). Once the haustorium is formed, *U. fabea* relies on the infected cell for nutrition (Voegele and Mendgen, 2003). Plant resistance against biotrophic pathogens is typically mediated through a gene-for-gene recognition of the pathogen. In gene-for-gene defense interactions, effectors produced by the pathogen are detected by corresponding resistance (or "R") genes, which trigger defense responses that limit pathogen infection (Glazebrook, 2005). In response to biotrophic pathogens, plants degrade their own infected cells in a type of apoptosis called hypersensitive cell death (HR; Kerr et al., 1972; Ellis et al., 1991). The HR separates the pathogen from its nutrient source, effectively

preventing the establishment of the parasitic relationship and prevents the pathogen from invading adjacent healthy cells.

In contrast to biotrophic pathogens that rely on a parasitic relationship with their hosts, necrotrophs can only acquire nutrients from dead or dying plant cells. Necrotrophic fungi typically secrete low molecular weight toxins or reactive oxygen species that elicit cell death (Walton, 1996; Friesen et al., 2008; Tudzynski and Kokkelink, 2009). For example, the gray mold fungus *B. cinerea* causes host cell death by producing oxidative bursts during cuticle penetration and subsequent lesion formation on bean leaves (von Tidedemann, 1997; Tudzynski and Kokkelink, 2009). *B. cinerea* also secretes a suite of cell wall-degrading enzymes that aid in necrosis and the establishment of lesions during colonization. Recently, differential expression of six different pectinases was observed during foliar infection by *B. cinerea*, and two of the enzymes were required for full virulence (Williamson et al., 2007). Genomic comparisons indicate that pathogens exhibiting necrotrophic colonization like *Magnaporthe oryzae* and *Fusarium graminearum* contain 138 and 103 genes encoding putative cell wall-degrading enzymes, respectively (Horbach et al., 2011). Compared to the 38 genes encoding cell wall-degrading enzymes in the facultative biotroph *U. maydis* (Kamper et al., 2006), the importance of degrading host tissue by necrotrophs is clear. Unlike the gene-for-gene resistance strategies observed with biotrophic pathogens (which typically result in HR), some necrotrophic pathogens have evolved inverse gene-for-gene relationships with dominant host sensitivity/susceptibility genes. For example, the wheat pathogen *Stagonospora nodorum* secretes several host-selective toxins that interact with host gene products to induce disease (Friesen et al., 2007; Friesen et al., 2008a,b). In addition to resistance/susceptibility genes, hosts utilize signaling molecules like jasmonic acid (JA) to regulate other defense responses that do not involve apoptosis

(Glazebrook, 2005). In Arabidopsis, mutants with reduced JA signaling are susceptible to *B. cinerea* (Thomma et al., 1998), and the transcription factor *JIN1* regulates the expression of many JA-responsive genes (Lorenzo et al., 2004). However, *jin1* mutant plants are more resistant to *B. cinerea*, suggesting the existence of multiple JA-dependent signaling cascades that have different effects on defense responses against necrotrophic pathogenesis (Lorenzo et al., 2004).

While distinct pathogenic classifications like biotrophy and necrotrophy delineate opposite modes of the infection spectrum, many hemibiotrophic fungi utilize aspects of both modes during the course of host infection and colonization. After penetrating the host leaf, *Colletotrichum* species avoid host recognition as hyphae asymptotically colonize surrounding cells. During colonization of host tissue, fungi disguise their presence by chitin deacetylation, which provides resistance to fungal cell well-degrading enzymes produced by the host (El Gueddari et al., 2002). Another example of active suppression of host defenses during biotrophic growth occurs during latent colonization and growth by *C. gloeosporioides*. After initial colonization, *C. gloeosporioides* expresses the nitrogen starvation-induced gene *CgDN3*, which appears to serve as a compatibility determinant that suppresses host-mediated HR (Stephenson et al., 2000). Between 48 and 72 hours post-inoculation, *Colletotrichum* species shift to a necrotrophic phase of growth. During this transition, smaller secondary hyphae develop and pierce the plasma membrane of host cells and rapidly degrade the cellular contents (Munch et al., 2008). During the transition to necrotrophic growth, *Colletotrichum* species secrete numerous cell wall-degrading enzymes that likely provide the pathogen with nutrients prior to conidiogenesis (Wijesundera et al., 1989; Herbert et al., 2004). In support of these initial observations, a recent comparative transcriptomic analysis showed that *Colletotrichum* species

expressed specific classes of genes during transitions between biotrophic and necrotrophic growth (O'Connell et al., 2012).

Stomata As Avenues Of Entry For Plant Pathogenic Fungi

Fungal pathogens have evolved a wide range of strategies to infect plants. Many fungi utilize specialized structures called appressoria to penetrate the cuticle or to infect through natural openings such as stomata (Zeng et al., 2010). In *Magnaporthe oryzae,* for example, germ tubes grow without specific direction before forming appressoria, which generate enormous turgor pressure to directly penetrate the cuticle and enter the mesophyll (de Jong et al., 1997). In *M. oryzae*, the regulation of appressorium formation depends on host physiology and environmental factors, such as hydrophobicity of the contact surface (Lee and Dean, 1994), surface hardness (Xiao et al., 1994), and the presence of plant cutin monomers (Gilbert et al., 1996). Unlike the direct penetration strategy utilized by *M. oryzae*, many plant pathogens infect host tissue through stomata, natural openings on the leaf surface that facilitate gas exchange and transpiration. Germinating spores of rust fungi such as *Puccinia graminis f.sp. tritici* exhibit thigmotropic growth in response to wheat leaf topography (Johnson, 1934; Lewis and Day, 1972). When hyphae of *P. graminis f.sp. tritici* encounter ridges on the leaf surface, such as guard cells of stomata, they form appressoria. Appressorium formation typically leads to penetration through the stomatal cavity and the development of subsequent infection structures like penetration pegs and substomatal vesicles (Allen et al., 1991). However, with few exceptions, appressorium formation leads to infection only when formed over stomates (Dodman, 1979). Similar to what is observed in *P. graminis f.sp. tritici*, hyphae of the bean rust fungus *Uromyces appendiculatus* undergoes thigmo-differientation after contact with stomatal ridges on host leaves or topographically accurate replicas of the leaf surface (Wynn, 1976;

Wynn, 1981; Wynn and Staples, 1981; Hoch et al., 1987). Furthermore, experiments with synthetic surfaces indicated that encountering a 5µm ridge induced hyphae to form appressoria, which corresponded to the average height of the bean guard cells (Hoch et al., 1987). Mechanosensitive calcium channels have been hypothesized to regulate aspects of thigmo-differientation in *U. appendiculatus* and other fungi, but the specific mechanisms regulating thigmotropism and stomatal sensing in plant pathogenic fungi are poorly understood (Zhou et al., 1991; Watts et al., 1998).

Infection through stomata is a common infection strategy among members of the genus *Cercospora*, although the phenomenon appears to be more intricate than a purely thigmotropic response. In 1916, Pool and McKay postulated that open stomata of sugar beet exert an attractive force to developing germ tubes of *Cercospora beticola*. Subsequent observations of stomatal tropism suggested that infection is humidity and moisture dependent (Rathaiah, 1976), which was linked to hydrotropic growth toward respiring stomates (Solel and Minz, 1971; Wallin and Loonan, 1971). Interestingly, *C. beticola* can penetrate through stomata without the development of appressoria (Rathaiah, 1977). However, a thorough mechanistic and genetic understanding of how fungi infect leaves via stomata is currently unavailable for any ascomycete fungus.

Gray Leaf Spot Of Maize

Gray leaf spot of maize is a devastating foliar disease present throughout the maize growing regions of the world (Dunkle and Levy, 2000; Ward et al., 1997, 1999; Latterell and Rossi, 1983). Two anamorphic *Cercospora* species cause gray leaf spot of maize, *C. zeae-maydis* and *C. zeina* (Crous et al., 2006; Goodwin et al., 2001; Dunkle and Levy, 2000). *C. zeae-maydis* is present in North America, South America and Asia, while *C. zeina* has been found in

South America, the Eastern United States, China and Africa (Liu and Xu, 2013; Mesiel et al., 2009; Okori et al., 2003; Dunkle and Levy, 2000). *C. zeae-maydis* was first reported by Tehon and Daniels in 1924 in Illinois, and the disease increased in severity in the U.S. Southeast beginning in the mid-1970's and Midwest in the 1980's (Ward et al., 1999; de Nazareno et al., 1992; Beckman and Payne, 1983). *C. zeae-maydis* overwinters on crop debris, and widespread adoption of reduced tillage is theorized to have greatly increased overwintering potential (Payne and Waldron, 1983; Payne et al., 1987; de Nazareno et al., 1993). Gray leaf spot can significantly reduce maize yields when the environment is conducive for disease (Ward et al., 1999). Severe infections commonly reduce yields by 10% to 25%, and epidemics can cause losses of 100% due to lodging and/or premature plant death (Latterell and Rossi, 1983).

C. zeae-maydis has evolved an intricate infection strategy to infect maize and cause disease (reviewed by Kim et al., 2011a). The disease cycle of *C. zeae-maydis* begins in the spring after overwintering on crop residue. The pathogen then forms conidia that are dispersed by wind or rain onto developing maize plants (Ward et al., 1999; Payne and Waldron, 1983). Once spores encounter host tissue, pathogenesis can be categorized into four distinct stages: germination, infection, colonization and sporulation. Germination of conidia occurs in conditions near 100% relative humidity, (Rupe et al., 1982; Thorson and Martinson, 1993) between zero and three days after germination. Developing hyphae (germ tubes) emerge from conidia and grow across the leaf surface until they sense stomata and reorient their growth accordingly. Upon encountering stomata (one to five days after germination), infection begins when hyphae develop into swollen, globular appressoria. Appressoria potentially serve as scaffolds that guide a penetration peg between the guard cells and into the stomatal pore. After entering the mesophyll through stomata, *C. zeae-maydis* grows intracellularly and rapidly

colonizes host tissue. At some point during this stage of infection, the fungus shifts to a necrotrophic growth habit. Necrotic growth is delineated by the major veins, giving gray leaf spot its characteristic rectangular lesions. After lesions form (more than seven days after germination), sporulation occurs when erumpent conidiophores bearing conidia egress through stomatal pores within the necrotic lesions. Macroscopically, regions of sporulation give gray leaf spot its characteristic coloration (Ringer and Grybauskas, 1995). Conidia are spread by wind and rain as secondary inoculum to nearby plants, thus initiating a polycyclic progression of disease throughout the growing season. Additionally, *C. zeae-maydis* can sporulate via microcycle conidiation (Lapaire and Dunkle, 2003), in which conidia are produced directly from conidia, without an intervening vegetative growth stage. Microcycle conidiation in *C. zeae-maydis* was observed on trichomes of soybean (*Glycine max*) and Johnsongrass (*Sorghum halepense*), which could facilitate disease spread over long distances, as non-host plants may serve as a repository of viable inoculum (Lapaire and Dunkle, 2003). *C. zeae-maydis* and other related *Cercospora* species also produce cercosporin, a phytotoxin that has been hypothesized to aid colonization (Daub et al., 2006; Daub and Ehrenshaft, 2000; Gwinn et al., 1987). When exposed to sunlight, cercosporin generates active oxygen species that damage host cell membranes (Daub and Ehrenshaft, 2000). Although components of the disease cycle of gray leaf spot are well established, many intriguing questions remain about how the fungus navigates leaf surfaces, senses and enters stomata, and colonizes host tissues.

Functional Genomics In *C. zeae-maydis*

The recent increase of genetic and genomic resources for *C. zeae-maydis* make it a tractable system to study stomatal infection. Most importantly, the United States Department of Energy's Joint Genome Institute sequenced and annotated the *C. zeae-maydis* genome in 2011

(http://genome.jgi-psf.org/Cerzm1/Cerzm1.home.html). Additionally, several recently characterized genes provide footholds for the molecular dissection of critical biological functions. *CZK3*, a mitogen-activated protein kinase kinase kinase, was the first functionally characterized gene in *C. zeae-maydis* (Shim and Dunkle, 2002, 2003). Targeted disruption of *CZK3* suppressed the expression of cercosporin biosynthetic genes and abolished cercosporin production. Furthermore, *CZK3* disruption mutants grew more quickly than the wild type in culture, lacked the ability to produce conidia, and elicited small chloritic flecks as opposed to lesions during infection of maize. The genetic regulation of light-related processes like blue light photoreception and repair of UV-damaged DNA were elucidated by the characterization of *PHL1*, a cryptochrome/6-4 photolyase-like gene (Bluhm and Dunkle, 2008). Aside from increasing conidiation and reducing cercosporin biosynthesis in culture, *PHL1* was dispensable for pathogenesis. However, when the fungus was exposed to natural light, *PHL1* was required for photoreactivation and the induction of genes involved in repairing UV-induced DNA damage. To identify differentially expressed genes during vegetative, infectious, and reproductive stages of growth, Bluhm and associates in 2008 generated a collection of 27,551 Expressed Sequence Tags (ESTs). Analysis of the EST library uncovered the diversity and novelty of *C. zeae-maydis* genes expressed in different environmental and biological settings, and provided a sequence resource that was valuable for subsequent genome sequencing and annotation. Recently, the Bluhm lab identified and characterized *CRP1* (Kim et al., 2011b), a homolog of the *white collar-1* family of blue light photoreceptors studied extensively in the model fungus *N. crassa* (Crosthwaite et al., 1997; Lee et al., 2003; Liu and Bell-Pedersen, 2006). *CRP1* disruption mutants were unable to orient hyphal growth toward stomata during infection, and therefore failed to cause disease, making *CRP1* the first characterized gene that affects

stomatal tropism during fungal pathogenesis. Based on the function of *CRP1* in *C. zeae-maydis* and the elucidation of photoreception in other pathogenic microbes (Idnurm and Crosson, 2009), light has been hypothesized to regulate significant aspects of host sensing and infection. The role of light in fungal growth and development has been recently corroborated by studies showing that circadian rhythms regulate hyphal melanization in the soybean pathogen *Cercospora kikuchii* (Bluhm et al., 2010), and broader circadian regulation has been implicated in pathogenicity and immune responses in the Arabidopsis/*Hyaloperonospora arabidopsidis* and Arabidopsis/*Pseudomonas syringae* pathosystems (Wang et al., 2011; Zhang et al., 2013).

Project Rationale And Long-Term Goals

Although gray leaf spot causes substantial losses to global agriculture, a basic question underlying infection remains unanswered: How does the pathogen sense stomata, form appressoria, and initiate disease? Preliminary observations in the Bluhm lab suggest foliar infection by *Cercospora* species, specifically *C. zeae-maydis*, is a finely tuned biological process regulated by uncharacterized biological and genetic parameters. The goal of my Ph.D. dissertation research was to describe stomatal tropism and appressorium formation, and elucidate molecular mechanisms underlying pathogenesis.

Objectives

The specific objectives of this research were to:

1. Define stomatal tropism and appressorium formation in *C. zeae-maydis*.
2. Elucidate the role of circadian rhythmicity underlying pathogenicity in *C. zeae-maydis*.
3. Identify the transcriptome underlying foliar infection in *C. zeae-maydis*.

4. Create genetic resources to dissect stomatal tropism, appressorium formation and infection through functional genomic approaches.

Chapter Two of this dissertation describes the experiments performed to address the first objective, Chapter Three describes experiments to address the second objective, continued in this format until Chapter Five. Chapter Six presents a summary of the research, as well as potential research directions that can be pursued following the conclusion of this research project.

References

Allan, E. A., Hazen, B. E., Hoch, H. C., Kwon, Y., Leinhos, G. M. E., Staples, R. C., Stumpf, M. A. and Terhune, B. T. 1991. Appressorium formation in response to topographical signals by 27 rust species. *Phytopathology* 81:323-331.

Anderson, P.M., Cunningham, A.A., Patel, N.G., Morales, F.J., Epstein, P.R., and Daszak, P. 2004. Emerging infectious diseases of plants: pathogen pollution, climate change and agrotechnology drivers. *Trends Eco Evo* 19:535-544.

Agrios, G.N. 1997. Plant Pathology, 5th edition. Academic Press, USA.

Bahn, Y-S., Xue, C., Idnurm A., Rutherford, J.C., Heitman, J,, Cardenas, M.E. 2007. Sensing the environment: lessons from the fungi. *Nat. Rev. Microbiol.* 5:57-69.

Baker, C.L., Loros J.J., and Dunlap, J.C. 2011. The circadian clock of *Neurospora crassa*. *FEMS Microbiol Rev* 36:95-110.

Baldrian, P., Kolank, M., Stursova, M., Kopecky, J., Valaskova, V. Vetrovsky, T. et al., 2012. Active and total microbial communities in forest soil are largely different and highly stratified during decomposition. *ISME J* 6:248-258.

Barelle, C.J., Priest, C.L., MacCallum, D.M., Gow, N.A.G., Odds, F.C., and Brown, A.J.P. 2006. Niche-specific regulation of central metabolic pathways in a fungal pathogen. *Cell Microbiol* 8:961-971.

Beckman, P. M. and Payne, G. A. 1983. Cultural techniques and conditions influencing growth and sporulation of *Cercospora zeae-maydis* and lesion development in corn. *Phytopathology* 73:286-289.

Belden, W.J., Larrondo, L.F., Froehlich, A.C., Shi, M., Chen, C-H., Loros, J.L. and Dunlap, J.C. 2007. The *band* mutation in *Neurospora crassa* is a dominant allele of *ras-1* implicating RAS signaling in circadian output. *Genes Dev*. 21:1494-1505.

Bergman K, Eslava AP, Cerdá-Olmedo E. 1973. Mutants of *Phycomyces* with abnormal phototropism. *Mol Gen Genet*. 123:1-16.

Bluhm, H.B. and Dunkle, L.D. 2008. PHL1 of *Cercospora zeae-maydis* encodes a member of the photolyase/cryptochrome family involved in UV protection and fungal development. *Fun Gen Biol* 45:1364-1372.

Bluhm, H.B., Dhillon, B., Lindquist, E.A., Kema, G.H.J., Goodwin, S.B. and Dunkle, L.D. 2008. Analysis of expressed sequence tags from the maize foliar pathogen *Cercospora zeae-maydis* identify novel genes expressed during vegetative, infectious, and reproductive growth. *BMC Gen* 9:523.

Bluhm, B.H., Burnham, A.M. and Dunkle, L.D. 2010. A circadian rhythm regulating hyphal melanization in *Cercospora kikuchii*. *Mycologia* 102:1221-1228.

Bölker, M., Urban, M. & Kahmann, R. 1992. The a mating type locus of *U. maydis* specifies cell signaling components. *Cell* 68:441-450

Brown, J.K., and Hovmoller, M.S. 2002. Aerial dispersal of pathogens on the global and continental scales and its impact on plant disease. *Science* 297:537-541.

Cerdá-Olmedo, E. and Lipson, E.D. 1987. *Phycomyces* (Cold Spring Harbor Lab. Press, Woodbury, NY).

Cerdá-Olmedo, E. 2001. *Phycomyces* and the biology of light and color. *FEMS Microbiol. Rev*. 25:503-512.

Chandran, D., Inada, N., Hather, G., Kleindt, C.K. and Wildermuth, M.C. 2010. Laser microdissection of *Arabidopsis* cells at the powdery mildew infection site reveals site-specific processes and regulators. *Proc Natl Acad Sci USA* 107:460-465.

Chen, C-H., DeMay, B.S., Gladfelter, A.S., Dunlap, J.C., Loros, J.J. 2010. Physical interaction between VIVID and white color complex regulates photoadaptation in *Neurospora*. *Proc Natl Acad Sci USA* 107:16715-16720.

Corrochano, L.M., Garre, V. 2010. Photobiology in the Zygomycota: multiple photoreceptor genes for complex responses to light. *Fungal Genet Biol* 47:893-899.

Crawford, R.L. 1981. *Lignin biodegradation and transformation*. New York: John Wiley and Sons.

Crosthwaite, S.K., Dunlap, J.C. and Loros, J.L. 1997. *Neurospora wc*-1 and *wc*-2: Transcription, photoresponses and the origins of circadian rhythmicity. *Science* 276:763.

Crous, P.E., Groenewald J.Z., Groenewald M., Caldwell P., Braun U. and Harrington T.C. 2006. Species of *Cercospora* associated with grey leaf spot of maize. *Stud Mycol* 55: 189-197.

Daub, M.E. and Ehrenshaft, M. 2000. The photoactivated *Cercospora* toxin cercosporin: contributions to plat disease and fundamental biology. *Annu Rev Phytopathol* 38:461-490.

Daub, M.E., Herrero, S. and Chung, K-R. 2006. Photoactivated perylenequinone toxins in fungal pathogenesis of plants. *FEMS Microbiol Let* 252:197-206.

Davis, R.H., and Perkins, D.D. 2002. Neurospora: a model of model microbes. *Nat Rev Gen* 3:7-13.

de Jong, J.C., McCormack, B.J., Smirnoff, N. and Talbot, N.J. 1997. Glycerol generates turgor in rice blast. *Nature* 389:244–245.

de Nazareno, N.R.X., Lipps, P.E. and Madden, L.V. 1992. Survival of *Cercospora zeae-maydis* in corn residue in Ohio. *Plant Dis* 76:560-563.

de Nazareno, N.R.X., Lipps, P.E. and Madden, L.V. 1993. Effect of levels of corn residue on the epidemiology of gray leaf spot of corn in Ohio. *Plant Dis* 77:67-70.

Dinoor, A., and Eshedm N. 1984. The role and importance of pathogens in natural plant communities. *Annu Rev Phytopathol* 22:443-466.

Dodman, R. L. 1979. How the defenses are breached. Pages 135-153 in: Plant Disease: An Advanced Treatise, Vol. 4. J. G. Horsfall and E. B. Cowling, eds. Academic Press, New York.

Dunkle, L.D. and Levy, M. 2000. Genetic relatedness of African and United States populations of *Cercospora zeae-maydis*. *Phytopathology* 90:486–490.

El Gueddari, N.E., Rauchhaus, U., Moerschbacher, B.M., Deising, H.B. 2002. Developmentally regulated conversion of surface-exposed chitin to chitosan in cell walls of plant pathogenic fungi. *New Phytol* 156:103-112.

Ellis, R.E., Yuan, J.Y., and Horvitz, H.R. 1991. Mechanisms and functions of cell death. *Annu Rev Cell Biol* 7: 663-698.

Fisher, M.C., Henk D.A, Briggs, C.J., Brownstein, J.S., Madoff, L.C., McCraw, S.L., Gurr, S.J. 2012. Emerging fungal threats to animal, plant and ecosystem health. *Nature* 484: 186-194.

Forsberg, H., Ljungdahl, P.O. 2001. Sensors of extracellular nutrients in *Saccharomyces cerevisiae*. *Curr Genet* 40:91-109.

Friesen, T.L., Faris, J.D., Solomon, P.S., Oliver, R.P. 2008a. Host-specific toxins: effectors of necrotrophic pathogenicity. *Cell Microbiol* 10:1421-1428.

Freisen, T.L., Zhang, Z.C., Solomon, P.S., Oliver, R.P., and Faris, J.D. 2008b. Characterization of the interaction of a novel Stagonospora nodorum host-selective toxin with a wheat susceptibility gene. *Plant Physiol* 146:682-293.

Friesen, T.L., Meinhardt, S.H., Faris, J.D. 2007. The *Stagonospora nodorum*-wheat pathosystem involves multiple proteinaceaous host-selective toxins and corresponding host sensitivity genes that interact in an inverse gene-for-gene manner. *Plant J* 51:681-692.

Fu, J., Hettler, E. and Wickes B.L. 2006. Split marker transformation increases homologous integration frequency in *Cryptococcus neoformans*. *Fungal Genet Biol* 43:200–212.

Galland P., 1990. Phototropism of the *Phycomyces* sporangiophore: A comparison with higher plants. *Photochem Photobiol*.52:233-240.

Gan, P.H.P., Dodds, P.N., and Hardham, A.R. 2012. Plant infection by biotrophic fungal and oomycete pathogens. *Sig Comm Plant* 11:183-212.

Goodell, B. 2003. Brown-rot fungal degradation of wood: our evolving view. In: *Wood deterioration and preservation: advances in our changing world*. Eds. Goodell, B, Nicholas, D.D., Schultz, T.P. Pages:97-118.

Goodwin, S.B., Dunkle, L.D. and Zismann, V.L. 2001. Phylogenetic analysis of *Cercospora* and *Mycosphaerella* based on the internal transcribed spacer region of ribosomal DNA. *Phytopathology* 91:648-658.

Gilbert, R.D., Johnson, A.M. and Dean, R.A. 1996. Chemical signals responsible for appressorium formation in the rice blast fungus *Magnaporthe grisea*. *Physiol Mol Plant Pathol* 48:335-346.

Glazebrook, J. 2005. Contrasting mechanisms of defense against biotrophic and necrotrophic pathogens. *Annu Rev Phytopathol* 43:205-227.

Gwinn, K.D., Stelzig, D.A., and Brooks, J.L. 1987. Effects of corn plant-age and cultivar on resistance to *Cercospora zeae-maydis* and sensitivity to cercosporin. *Plant Dis* 71:603-606.

Hacquard, S., Delaruelle, C., Legue, V., Tisserant, E., Kohler, A., Frey, P., Martin, F. and Duplessis, S. 2010. Laser capture microdissection of uredinia formed by *Melampsora larici-populina* revealed a transcriptional switch between biotrophy and sporulation. *Mol Plant-Microbe Interact* 23:1275-1286.

Hainen, M., Valkonen, M.J., Westerholm-Parvinen, A., Aro, N., Arvas, M., Vitikainen, M., Penttila, M., Saloheimo, M., and Pakula, T.M. 2014. Screening of candidate regulators for cellulase and hemicellulose production in Trichoderma reesei and identification of a factor essential for cellulose production. *Biotechnol Biof* 7:14.

Hatakka, A. 1994. Lignin-modifying enzymes from selected white-rot fungi: production and role from in lignin degradation. *FEMS Microbiol Rev* 13:125-135.

Hatakka, A. 2005. Biodegradation of lignin. Biopolymers Online.

Harder DE, Chong J. 1991. Rust haustoria. In: Mendgen, K., Lesemann, D-E., eds. *Electron microscopy of plant pathogens*. Berlin, Germany: Springer, 235-250.

Harrington, G.N. and Bush, D.R. 2003. The bifunctional role of hexokinase in metabolism and glucose signaling. *Plant Cell* 15:2493-2496.

Heath, M.C.,, and Skalamera, D. 1997. Cellular interactions between plants and biotrophic fungal parasites. *Adv Bot Res* 24:195-225.

Herbert, C., O'Connell, R., Gaulin, E., Salesses, V., Esquerre-Tugaye, M.T., Dumas, B. 2004. Production of a cell wall-associated endopolygalacturonase by *Colletotrichum lindemuthianum* and pectin degradation during bean infection. *Fungal Genet Biol* 41:140-147.

Hoch, H.C, Staples R.C. 1987. Structural and chemical changes among the rust fungi during appressorium development. *Annu Rev Phytopathol*. 25:231-247.

Horbach, R., Navarro-Quesada, A.R., Knogge, W., and Deising, H.B. 2011. When and how to kill a plant cell: Infection strategies of plant pathogenic fungi. *J Plant Physiol* 168:51-62.

Idnurm A., Rodriguez-Romero, J., Corrochano, L.M., Sanz, C., Iturriaga E.A., Eslava, A.P., Heitman, J. 2006. The *Phycomyces* madA gene encodes a blue-light photoreceptor for phototropism and other light responses. *Pub Nat Sci Acad USA* 103:4546-4551.

Idnurm, A., Crosson, S. 2009. The photobiology of microbial pathogenesis. *PLoS Patho* 5:e1000470.

Idnurm, A., and Heitman, J. 2005. Light controls growth and development via a conserved pathway in the fungal kingdom. *PLoS Biol* 3(4): e95.

Johnson T. 1934. A tropic response in germ tubes of uredospores of *Puccinia graminis tritici*. *Phytopathology* 24:80–82.

Kamper, J., Kahmann, R., Bolker, M., Ma, L.J., Brefort, T., Saville, B.J., et al. 2006. Insights from the genome of the biotrophic fungal plant pathogen *Ustilago maydis*. *Nature*. 444:97-101.

Kerr, J.F., Wyllie, A.H., and Currie, A.R. 1972. Apoptosis: a basic biological phenomenon with wide-ranging implications in tissue kinetics. *Br J Cancer* 26:239-257.

Kim, H. and Borkovich, K. A. 2004. A pheromone receptor gene, pre-1, is essential for mating type-specific directional growth and fusion of trichogynes and female fertility in *Neurospora crassa*. *Mol. Microbiol*. 52:1781-1798.

Kim, H., Ridenour, J. B., Dunkle, L. D. and Bluhm, B. H. 2011a. Regulation of pathogenesis by light in *Cercospora zeae-maydis*: An updated perspective. *Plant Pathol J* 27:103-109.

Kim, H., Ridenour, J. B., Dunkle, L. D. and Bluhm, B. H. 2011b. Regulation of stomatal tropism and infection by light in *Cercospora zeae-maydis*: Evidence for coordinated host/pathogen responses to photoperiod? *PLoS Pathogens* 7(7): e1002113.

Kim, H., Smith J.E., Ridenour, J.B., Woloshuk, C.P., Bluhm, B.H. 2011c. *HXK1* regulates carbon catabolism, sporulation, fumonisin B_1 production and pathogenesis in *Fusarium verticillioides*. *Microbiology* 157: 2658-2669.

Kogel-Knabner, I. 2002. The macromolecular organic composition of plant and microbial resides as inputs to soil organic matter. *Soil Biol and Biochem* 34:139-162.

Lapaire, C.L. and Dunkle, L.D. 2003. Microcycle conidiation in *Cercospora zeae-maydis*. *Phytopathology* 93:193-199.

Latterell, F.M., and Rossi, A.E. 1983. Gray leaf spot of maize: A disease on the move. *Plant Dis* 67:842-847.

Lee, Y-H. and Dean, R.A. 1994. Hydrophobicity of contract surface induces appressorium formation in *Magnaporthe grisea*. *FEMS Microbiol Lett* 115:71-75.

Lee, K., Dunlap, J.C. and Loros, J.L. 2003. Roles for white collar-1 in circadian and general photoperception in *Neurospora crassa*. *Genetics* 163:103-114.

Lemaire, K., Van de Velde, S., Van Dijck, P. & Thevelein, J.M. 2004. Glucose and sucrose act as agonist and mannose as antagonist ligands of the G protein-coupled receptor Gpr1 in the yeast *Saccharomyces cerevisiae*. *Mol. Cell* 16:293-299.

Li, L., Wright, S.J., Krystofova, S., Park, G., and Borkovich, K.A. 2007. Heterotrimeric G protein signaling in filamentous fungi. *Annu Rev Microbiol* 61:423-452.

Liu, Y. and Bell-Pedersen, D. 2006. Circadian rhythms in *Neurospora crassa* and other filamentous fungi. *Eukary Cell* 8:1184-1193.

Liu K. and Xu X. 2013. First report of gray leaf spot of maize cause by *Cercospora zeina* in China. *Plant Dis* 97:12.

Lorenz, M.C., Pan, X., Harashima, T., Cardenas, M.E., Xue, Y., Hirsch J.P., and Heitman, J. 2000. The G protein-coupled receptor Gpr1 is a nutrient sensor that regulates pseudohyphal differentiation in *Saccharomyces cerevisiae*. *Genetics* 154:609-622.

Lorenzo, O., Chico, J.M., Sanchez-Serrano, J.J., and Solano R. 2004. JASMONATE-INSENSITIVE1 encodes a MYC transcription factor essential to discriminate between different jasmonate-regulated defense responses in Arabidopsis. *Plant Cell* 16:1938-50.

Loros, J. J. and J. C. Dunlap. 2001. Genetic and molecular analysis of circadian rhythms in *Neurospora*. *Annu Rev Physiol* 63:757–794.

Lewis, B.G. and Day, J.R. 1972. Behavior of uredospore germ-tubes of *Puccinia graminis tritici* in relation to the fine structure of wheat leaf surfaces. *Trans Br Mycol Soc* 58:139–45.

Meisel, B., Korsman, J., Kloppers, F.J. and Berger, D.K. 2009. *Cercospora zeina* is the causal agent of grey leaf spot disease of maize in southern Africa. *Eur J Plant Pathol* 124: 577–583.

Mendegen, K., and Hahn, M. 2002. Plant infection and the establishment of fungal biotrophy. *Trends Plant Sci* 7:352-356.

Munch, S., Lingner, U., Floss, D.S., Ludwig, N., Sauer, N., and Deising, H.B. 2008. The hemibiotrophic lifestyle of *Colletotrichum* species. *J Plant Pathol* 165:41-51.

O'Connell, R.J., Thon, M.R., Hacquard, S., Amyotte, S.G., Kleemann, J. et al. 2012. Lifestyle transitions in plant pathogenic *Colletotrichum* fungi deciphered by genome and transcriptome analysis. *Nature Gen* 44:1060-1065.

Oerke, E-C., Dehne, H-W, Schonbeck, F., and Weber, A. 1999. *Crop production and crop protection: estimated losses in major food and cash crops*. Elsevier Science, Amsterdam, The Netherlands.

Okori, P., Fahleson, J., Rubaihayo, P. R., Adipala, E. and Dixelius, C. 2003. Assessment of genetic variation among East African *Cercospora zeae-maydis*. *Afri Crop Sci J* 11:75-85.

O'Sullivan, A.C. 1997. Cellulose: the structure slowly unravels. *Cellulose* 4:173-207.

Ramsay, K., Jones, M.G. and Wang, Z. 2006. Laser capture microdissection: a novel approach to microanalysis of plant-microbe interactions. *Mol Plant Pathol* 7:429-435.

Rathaiah, Y. 1976. Infection of sugarbeet by *Cercospora beticola* in relation to stomatal condition. *Phytopathology* 66:737-740.

Rathaiah, Y. 1977. Stomatal tropism of *Cercospora beticola* in sugarbeet. *Phytopathology* 67:358-362.

Ringer, C.E. and Grybauskas, A.P. 1995. Infection cycle components and disease progress of gray leaf spot on field corn. *Plant Dis* 79:24-28.

Rupe, J.C., Siegel, M.R. and Hartman, J.R. 1982. Influence of environment and plant maturity on gray leaf spot of corn caused by *Cercospora zeae-maydis*. *Phytopathology* 72:1587-1591.

Ruiz-Roldan, M.C., Garre, V., Guarro, J., Marine, M., Roncero, M.I.G. 2008. Role of the white collar 1 photoreceptor in carotenogenesis, UV resistance, hydrophobicity, and virulence of *Fusarium oxysporum*. *Eukaryot Cell* 7:1227-1230.

Santangelo, G. M. 2006. Glucose signaling in *Saccharomyces cerevisiae*. *Microbiol Mol Biol Rev* 70:253-282.

Sanz, C., Rodriguez-Romero, J., Idnurm, A., Christie, J.M., Heitman, J., Corrochano, L.M., Eslava, A.P. 2009. Phycomyces MADB interacts with MADA to form the primary photoreceptor complex for fungal phototropism. *Proc Natl Acad Sci USA* 106:7095-7100.

Sargent, M.L. and Woodward, D.O. 1969. Genetic determinants of circadian rhythmicity in *Neurospora*. *J Bachteriol*. 97:861-866.

Schwerdtfeger, C., Linden, H. 2003. VIVID is a flavoprotein and serves as a fungal blue light

photoreceptor for photoadaptiation. *EMBO* 22:4846-4855.

Seo, J. A., Han, K. H. & Yu, J. H. 2004. The gprA and gprB genes encode putative G protein-coupled receptors required for self-fertilization in *Aspergillus nidulans*. *Mol Microbiol* 53:1611-1623.

Shim, W-B. and Dunkle, L.D. 2002. Identification of genes expressed during cercosporin biosynthesis in *Cercospora zeae-maydis*. *Phys Mol Plant Pathol* 61: 237-248.

Shim, W-B. and Dunkle, L.D. 2003. CZK3, a MAP kinase kinase kinase homolog in *Cercospora zeae-maydis*, regulates cercosporin biosynthesis, fungal development, and pathogenesis. *Mol Plant-Microbe Interact* 16:760-768.

Solel, Z. and Minz, G. 1971. Infection process of *Cercospora beticola* in sugarbeet in relation to susceptibility. *Phytopathology* 61:463-466.

Stephenson, S.A., Gatfiled, J., Rusu, A.G., Maclean, D.J., AMnners, J.M. 2000. *CgND3*: an essential pathogenicity gene for *Colletotrichum gloeosporioides* necessary to avert a hypersensitive-like response in the host *Stylosanthes guianensis*. *Mol Plant-Microbe Interact* 13:929-941.

Tanaka, K., Davey, J., Imai, Y., Yamamoto, M. 1993. *Schizosaccharomyces pombe* map3+ encodes the putative M-factor receptor. *Mol. Cell. Biol.* 13:80-88.

Tehon, L.R. and Daniels, E. 1925. Notes on the parasitic fungi of Illinois: II. *Mycologia* 17:240-249.

Thomma, B.P.H.J., Eggermont, K., Penninckx, I.A.M.A., Mauch-Mani, B., Vogelsang, R., et al. 1998. Separate jasmonate-dependent and salicylate-dependent defense-response pathways in Arabidopsis are essential for resistance to distinct microbial pathogens. *Proc Natl Acad Sci USA*. 95:15107-15111.

Thorson, P.R. and Martinson, C.A. 1993. Development and survival of *Cercospora zeae-maydis* germlings in different relative humidity environments. *Phytopathology* 83:153-157.

von Tiedemann, A. 1997. Evidence for a primary role of active oxygen species in t induction of host cell death druing infection of bean leaves with Botrytis cinerea. *Physiol Mol Plant Pathol* 50:151-166.

Tremblay, A., Li, S., Scheffler, B.E. and Matthews, B.A. 2009. Laser capture microdissection and expressed sequence tag analysis of uredinia formed by *Phakopsora pachyrhizi*, the causal agent of Asian Soybean Rust. *Physio Mol Plant Pathol* 73:163-174.

Tremblay, A., Hosseini, P., Alkharouf, N.E., Li, S. and Matthews, B.A. 2010. Transcriptome analysis of a compatible response by *Glycine max* to *Phakopsora pachyrhizi* infection. *Plant Sci* 179:183-193.

Tudzynski, P., and Kokkelink, L. 2002. *Botrytis cinerea*: molecular aspects of a necrotrophic life style. H.B. Deising (Ed.), Plant Relationships V (2nd ed.), Springer-Verlag, Berlin, Heidelberg. Pages: 29-50.

Payne, G.A., Duncan, H.E. and Adkins, C.R. 1987. Influence of tillage in development of gray leaf spot and number of airborne conidia of *Cercospora zeae-maydis*. *Plant Dis* 71:329-332.

Payne, G.A. and Waldron, J.K. 1983. Overwintering and spore release of *Cercospora zeae-maydis* in corn debris in North Carolina. *Plant Dis* 67:87-89.

Pool, V.. and McKay, M.B. 1916. Relation of stomatal movement to infection by *Cercospora beticola*. *J Agric Res* 5:1011-1038.

Versele, M., Lemaire, K. & Thevelein, J. M. 2001. Sex and sugar in yeast: two distinct GPCR systems. *EMBO Rep*. 2:574-579.

Voegele, R.T., and Mendgen, K. 2003. Rust haustoria: nutrient uptake and beyond. *New Phytol* 159:93-100.

Wallin, J.R. and Loonan, D.V. 1971. Effect of leaf wetness duration and air temperature on *Cercospora beticola* infection in sugarbeet. *Phytopathology* 61:546-549.

Walton, J.D. 1996. Host-selective toxins: agents of compatibility. *Plant Cell* 8:1723-1233.
Wang, Z., Gerstein, M. and Snyder, M. 2009. RNA-seq: a revolutionary tool for transcriptomics. *Nat Rev Genet* 10:57-63.

Wang, W., Barnaby, J.Y., Tada, Y., Li, H., Tor, M., Caldelari, D., Lee, D-u., Fu, X-D. and Dong, X. 2011. Timing of plant immune responses by a central circadian regulator. *Nature* 470:110-114.

Watts, H.J., Very, A-A., Perera, T.H.S., Davies, J., Gow, N.A.R. 1998. Thigmotropism and stretch-activated channels in the pathogenic fungus *Candida albicans*. *Microbiology* 144:689-695.

Ward, J.M.J., Laing, M.D. and Rijkenbert, F.H.J. 1997. Frequency and timing of fungicide applications for the control of gray leaf spot of maize. *Plant Dis* 81:41-48.

Ward, J. M. J., Stromberg, E. L., Nowell, D. C., and Nutter, F. W. 1999. Gray leaf spot: A disease of global importance in maize production. *Plant Dis* 83:884-895.

Wijesundera, R.L.C., Bailey, J.A., Byrde, R.J.W., and Fielding, A.H. 1989. Cell wall degrading enzymes of *Colletotrichum lindemuthianum*: their role in the development of bean anthracnose. *Physiol Mol Plant Pathol* 34:403-413.

Williamson, B., Tudzynski, B., Tudzynski, P., and van Kan, J.A.L. 2007. *Botrytis cinerea*: the cause of grey mould disease. *Mol Plant Pathol* 8:561-580.

Wynn, W.K. 1976. Appressorium formation over stomates by the bean rust fungus: response to a surface contact stimulus. *Phytopathology* 66:136-146.

Wynn, W.K. 1981. Tropic and taxic resposnes of pathogens to plants. *Annu Rev Phytopathol* 19:237-255.

Wynn, W.K., Staples, R.C. 1981. Tropisms of fungi in host recognition. In: Staples, R.C., Toenniessen, G.H. eds. *Plant disease control resistance and susceptibility*. New York, USA: John Wiley and Sons: 45-69.

Xaio, J-Z., Watanabe, T., Kamakura, T., Ohshima A., and Yamaguchi, I. 1994. Studies on cellular differentiation of *Magnaporthe grisea*. Physicochemical aspects of substratum surfaces in relation to appressorium formation. *Physiol Mol Plant Pathol* 44:227-236.

Xue, Y., Batlle, M. & Hirsch, J. P. 1998. GPR1 encodes a putative G protein-coupled receptor that associates with the Gpa2p G alpha subunit and functions in a Ras-independent pathway. *EMBO J*. 17:1996-2007.

Zeng, W., Melotto, M. and He, S.Y. 2010. Plant stomata: a checkpoint of host immunity and pathogen virulence. *Curr Opin Biot* 21:599-603.

Zhang, C., Xie, Q., Anderson, R.G., Ng, G., Seitz N.C., et al. 2013. Crosstalk between the circadian clock and innate immunity in Arabidopsis. *PLoS Pathog* 9: e1003370. doi:10.1371/journal.ppat.1003370

Zhou X.L., Stumpf, M.A., Hoch, H.C., Kung, C. 1991. A mechanosensitive channel in whole cells and in membrane patches of the fungus *Uromyces*. *Science* 253:1415-1417.

CHAPTER II: STOMATAL TROPISM BY *CERCOSPORA ZEAE-MAYDIS* INVOLVES REPSONSES TO AN UNKNOWN ATTRACTANT

Summary

Cercospora zeae-maydis causes gray leaf spot of maize, one of the most widespread and destructive foliar diseases of maize in the world. The penetration of maize leaves through stomata is a critical, yet poorly defined component of pathogenesis in *C. zeae-maydis*. Observations that *C. zeae-maydis* can grow toward distant stomata during infection led to the hypothesis that the fungus responds to an unknown chemical cue emanating from stomata. To test this hypothesis, histological examinations of stomatal infection were performed with epifluorescence and confocal microscopy. During infection, hyphae exhibiting stomatal tropism did not form branches, which was consistent with heightened apical dominance. However, upon encountering artificial stomata on topographically accurate acrylic leaf replicas, *C. zeae-maydis* neither displayed stomatal tropism nor formed appressoria, which indicated that thigmotropic cues were not sufficient to elicit pre-penetration infectious development. During infection of non-host plants, *C. zeae-maydis* exhibited stomatal tropism and formed appressoria over stomata, which suggested that a broadly conserved chemical cue emanating from stomata elicited a chemotropic response. Stomatal tropism and appressorium formation in *C. zeae-maydis* were impaired when atmospheric oxygen levels were disturbed, thus implicating oxygen sensing in pathogenicity. When exposed to an oxygen gradient, *C. zeae-maydis* formed appressorium-like structures *in vitro*, linking morphological differentiation to environment oxygen concentration. Lastly, gene-deletion strains lacking the blue light photoreceptor *CRP1* did not display stomatal tropism during infection, linking light reception and stomatal sensing. Thus, this study characterized stomatal tropism during infection by *C. zeae-maydis* and implicated oxygen

sensing as a determinant of virulence, thus providing a new conceptual framework for the molecular dissection of foliar pathogenesis.

Introduction

The fungal genus *Cercospora* is one of the largest and most ubiquitous groups of plant pathogenic fungi. There are over 3000 named species of *Cercospora* (Crous and Braun, 2003; Aptroot, 2006), which occupy most agricultural regions and infect a wide range of important plant species (Goodwin et al., 2001; Groenewald et al., 2006; Cheewangkoon et al., 2009; To-Anun et al., 2011). *Cercospora* species generally exhibit narrow host specificity, and because species are difficult to distinguish morphologically, many species were traditionally named based on host-plant association (Chupp, 1954; Ellis, 1971). The two causal agents of gray leaf spot of maize, *C. zeae-maydis* and *C. zeina*, are only known to infect maize (Ward, 1999; Crous et al., 2006). *Cercospora* diseases frequently cause significant agricultural losses because commercially deployed germplasm often lacks effective genetic resistance (e.g., Nevill, 1981; Poland et al., 2008; Zhang et al., 2012), and *Cercospora* species can develop resistance to fungicides (Kirk et al., 2012; Zhang et al., 2012a; Zhang et al., 2012b; Trkulja et al., 2013).

Although many species of *Cercospora* are reported to infect their hosts through stomata, the process is poorly understood at the molecular level. In 1916, Poole and McKay postulated that open stomata exert a chemical signal that attracts hyphae of *C. beticola* (Poole and McKay, 1916). Subsequent investigations into stomatal tropism of *C. beticola* suggested that hydrotropism was involved in stomatal sensing (Vestal, 1933), and that tropic hyphae formed more readily following periods of drying and wetting during incubation (Rathaiah, 1977). During periods of prolonged wetness, *C. beticola* exhibited a drastic reduction in stomatal tropism and penetrated stomata at approximately 1% efficiency compared to cycles of nighttime wetness and daytime drying (Rathaiah, 1977). Also, *C. beticola* responded to stomatal aperture by either directly entering open stomata with hyphae, or forming small appressoria between the

stomatal guard cells (Rathaiah, 1976). In contrast, *C. zeae-maydis* has not been observed to penetrate stomata without forming appressoria (Kim et al., 2011a). Prior to appressorium formation, *C. zeae-maydis* reorients growth toward distant stomata by an uncharacterized mechanism, and forms appressoria on approximately 75% of stomata intercepted by hyphae (Kim et al., 2011b). Unlike rust fungi, in which appressorium formation over stomata is triggered thigmotropically (Lewis and Day, 1972; Dodman, 1979; Allen et al., 1991), the ability of *Cercospora* species to sense stomata from a distance appears to require a unknown chemoattractant cue.

Stomatal emissions have been linked to aspects of abiotic stress responses and defense against pathogens (Oikawa and Lerdau, 2013), but the responses of pathogenic fungi to plant exudates remains unknown. The microenvironment of the leaf boundary layer is enveloped in numerous volatile organic compounds (VOCs) involved in plant-to-plant signaling, abiotic stress, and defense against pathogens (Holopainen, 2004). Plants emit approximately 1 Pg of carbon (peta gram=10^{15}g) in the form of VOCs annually (Guenther et al., 1995), some of which could function as elicitors of fungal pathogenic development (Holopainen, 2004; Oikawa and Lerdau, 2013). Since the relationship between VOCs and fungal stomatal sensing remains uncharacterized, the identification of a volatile host signal that elicits tropic growth will greatly expand the models of host-pathogen interactions. Furthermore, identification of host sensory mechanisms may explain the species diversity among members of the genus and the tendency for narrow host specificity among individual *Cercospora* species (Crous et al., 2006).

In this study, fungal development underlying surface sensing, host and non-host stomatal tropism, appressorium formation, and responses to atmospheric oxygen were assessed in *C. zeae-maydis and C. beticola*. Hyphal growth and mycelial formation was significantly different on

host plant, non-host plant and synthetic medium, demonstrating a previously uncharacterized sensory capacity by *C. zeae-maydis*. Hyphal growth and branching on maize leaves were significantly different from hyphae growing on topographically accurate leaf replicas, which indicated that *C. zeae-maydis* relies on non-thigmotropic sensing mechanisms during stomatal infection. Discovery of stomatal tropism during non-host interactions led to the hypothesis that stomatal tropism is cued by a conserved stomatal exudate, which led to the subsequent identification of molecular oxygen as a potential stomatal attractant. Incubating maize plants inoculated with *C. zeae-maydis* in an atmosphere enriched with oxygen reduced appressorium formation on stomata. However, *C. zeae-maydis* developed significantly more appressorium-like structures *in vitro* when inoculated in a water agar medium enriched in oxygen, indicating a response to oxygen gradients. Lastly, blue-light photosensing was shown to affect stomatal sensing during infection. These findings have led to the formulation of new hypotheses regarding sensory mechanisms in *C. zeae-maydis* regulating pathogenic development during foliar infection of maize.

Materials and Methods

Strains and culture conditions. *C. zeae-maydis* (strain SCOH1-5) was obtained from the Bluhm lab stocks and utilized as the wild-type strain. *C. zeae-maydis* strain *Δcrp1-40*, a strain with a targeted disruption of *CRP1* derived from SCOH1-5, was created in a previous study (Kim et al., 2011b). *C. beticola* (strain S1) was isolated from diseased sugar beet leaves collected in Montana, USA. GFP-reporter strains SCOH1-5-GFP3 and Δ*crp1-40*GFP1 of *C. zeae-maydis,* along with S1-GFP of *C. beticola,* were created for this study and are described in greater detail below. Strains were maintained on V8 agar medium and incubated at room temperature in the dark to promote conidiation. Conidia were harvested with sterile water and

quantified with a hemocytometer. Acrylic leaf replicas created following the protocol described by Wynn (1976) were kindly provided by Dr. Larry Dunkle (UDSA-ARS, Purdue University, West Lafayette, IN) and utilized for this study. Briefly, leaf replicas were created by developing a rubberized negative of a leaf surface and stamping the rubber negative into layers of molten plastic from Petri dishes. After cooling, the plastic disks with the imprinted leaf surface were removed from the negative, washed with soap and water, and utilized for inoculations.

Nucleic acid manipulations and fungal transformation. Plasmid gGFP containing the *GFP* gene driven by the *trpC* promoter and hygromycin resistance gene, HYG^R, driven by the *gpdA* promoter was acquired from the Fungal Genetics Stock Center (Kansas City, MO; McClusky et al., 2003). Plasmid pBYR48, containing the *GPF* gene driven by the *trpC* promoter and geneticin resistance gene , GEN^R, driven by the *trpC* promoter was obtained from the Bluhm laboratory stocks. Plasmid DNA was isolated with a Fermentas Plasmid Mini-prep kit (Thermo Fisher Scientific, Glen Burnie MA). The gGFP plasmid was transformed into protoplasts of *C. zeae-maydis* SCOH1-5 and *C. beticola* strain S1, and pBYR48 was transformed into protoplasts of Δ*crp1-40* as previously described (Kim et al., 2011b). After transformation, strains expressing GFP were visually selected with the DFP-1 Dual Fluorescent Protein Flashlight (NightSea Corporation, Bedford, MD) and subsequently cultured on V8 medium with hygromycin (150 μg/ml) or geneticin selection (400 μg/ml) as appropriate.

Nutrient and surface effects on mycelium growth. Mycelium development on different surfaces was determined by inoculating conidia of the SCOH1-5-GFP3 strain (10^2 conidia in 1 mL H_20) onto the surface of Petri dishes containing CM or 0.2 × PDA, maize and beet leaves as described below, or on artificial leaf replicas. Cultures were incubated in a growth chamber maintained at 23°C with a 14:10 light:dark photoperiod with a light intensity at leaf

level of 300 μmol m^{-2} s^{-1}. Cultures were observed every 24 hours after inoculation. Measurements of hyphal branching and length were performed with the image analysis program ImageJ as described below (http://imagej.nih.gov/ij/). One hundred colonies were observed and quantified, and the experiment was repeated three times.

Hyphal growth, stomatal tropism and appressorium formation on leaf surfaces. The two GFP-reporter strains of *C. zeae-maydis* (SCOH1-5-GFP3, Δ*crp1-40*GFP1) and the GFP-reporter strain of *C. beticola* S1-GFP were utilized to inoculate maize (Silver Queen) and beet (Detroit Dark Red). Three maize plants (three to four weeks after emergence) were inoculated with 10 ml of a conidium suspension (10^5 conidia/ml) of strains SCOH1-5-GFP3 and *Δcrp1-40*GFP1 of *C. zeae-maydis,* and S1-GFP of *C. beticola.* Concurrently, three beet plants were inoculated with SCOH1-5-GFP3 and S1-GFP. The conidial suspensions for all inoculations were amended with 0.01% Triton X-100 and plants were inoculated with an atomizer attached to an air compressor until inoculum run-off. Mock-inoculated control plants were sprayed with the same Triton X-100 solution but contained no conidia. Inoculations were performed three times with similar results.

After inoculation, maize plants inoculated with *C. zeae-maydis* strains SCOH1-5-GFP3, Δ*crp1-40*GFP1, and *C. beticola* strain S1-GFP were placed in incubation chambers made of wire mesh wrapped in opaque plastic to maintain free moisture on plants and increase humidity. To prevent the physical crossover of inoculum, maize plants from each inoculation were placed in separate incubation chambers. The incubation chambers were of sufficient size to surround the inoculated plants but not touch the leaves. The chambers containing inoculated maize plants were placed in a large growth chamber for five days. The growth chamber was maintained at 23°C with a 14:10 light:dark photoperiod with a light intensity at leaf level of 300 μmol m^{-2} s^{-1}.

Beet plants inoculated with *C. beticola* S1-GFP, *C. zeae-maydis* SCOH1-5-GFP3, and Δ*crp1-40*GFP1 were incubated in similar wire mesh incubation chambers for five days in the greenhouse at the University of Arkansas, Fayetteville. The experimental design included three maize and three beet plants per strain and each experiment was repeated three times. The plants were positioned utilizing a completely randomized design during incubation.

To visualize hyphal development on leaf surfaces, infected leaves from each inoculated plant were collected five days after inoculation. Prior to histological analysis of fungal growth on the leaf surface, three leaves were removed from each three inoculated plants (nine leaves total) and combined as one sample prior to observation and image acquisition. Small leaf sections (1.5 cm × 4.0 cm) were excised from each leaf for histological examination. Hypha/stomata interaction events were selected for analysis if there was no physical contact/overlap between different hyphae, and if the target hypha physically encountered a stomatal guard cell. Three inoculations yielded a total of 100 hypha/stomate interaction events, which were observed and recorded for each inoculation condition. Measurements of stomatal tropism were similar between the three replications. Leaves were initially examined with a Nikon Eclipse 90i for observations and measurements, and a Nikon Eclipse 90i C1 confocal microscope for confocal imagery. Hyphal characteristics were measured with the analysis program ImageJ. ImageJ simplifies measurements of digital images by calculating the distance of complex lines, which can be utilized to trace individual hypha and measure their length. Briefly, the length of each pixel in the digital epifluorescence images was calculated by measuring the number of pixels required to trace a 200 μm line on a hemocytometer. Then, the length of each hypha was measured in pixels from the point of apical reorientation or lateral branch formation prior to stomatal interception by tracing a hypha with a line in the ImageJ

software. The length of each line was converted from pixels to metric units of length. Angles were calculated by measuring the angle formed between two lines traced between fungal hyphae (for lateral branches), or along a hypha (for apical reorientation), with the angle representing the point of hyphal reorientation or lateral branch formation. Confocal images were edited for color and clarity in Adobe Photoshop or NIS Elements.

Atmospheric oxygen enrichment. Oxygen enrichment experiments were performed by inoculating maize (Silver Queen) with strain SCOH1-5-GFP3. The inoculated plants were exposed to different atmospheres as follows: A clear plastic container with a sealable lid (Item #1334, Sistema Plastics, New Zeland) was fitted with a small port to accept 0.25 inch tubing. The three maize plants (three to four weeks old) inoculated with SCOH1-5-GFP3 as previously described were placed in the plastic container with a small area of the seal temporarily open, and 100% analytical grade oxygen was pumped into the container via 0.25 inch tubing from a pressurized tank. After five minutes of direct addition of 100% oxygen, the container seal was closed, tubing removed, and tube port sealed. This approach sustained a high level of molecular oxygen in the chamber while maintaining high humidity required for conidia germination and growth on the leaf surface following inoculation. The control experiment representing incubation in atmospheric oxygen (21%) was performed in the same manner except with compressed air as an additive. The sealed containers were then placed in a growth chamber, as previously described, to ensure consistency among inoculations performed in this study. Analytical-grade 100% oxygen or compressed air exposure was preformed five minutes daily until sampling. Each assay was performed at least three times.

***In vitro* oxygen gradient assay.** The thin-medium culture technique was adapted from Aoki et al., 1998. Briefly, 25 mL of molten water agar (50°C) was inoculated with 1.5 x 10^6

conidia of strains SCOH1-5-GFP3 and *Δcrp1-40*GFP1. A 20 µL drop of molten agar was placed on a microscope slide and quickly covered with a coverslip. Cultures were placed in a clear plastic container with a sealable lid similar to the container utilized in the oxygen enrichment plant inoculations. Chambers were flooded with either 100% oxygen or compressed air for two minutes every 24 hours and then sealed to prevent desiccation of the medium. Sealed containers were then placed in a growth chamber at 23°C and incubated in 14:10 light:dark photoperiod or total darkness for 7 days. *In vitro* appressorium formation was determined by quantifying the total amount of appressoria-like structures in 9 cm^2 of water agar medium. A total of ten replicate slides were used per isolate and all experiments were performed three times.

Results

The effects of nutrients and surfaces on mycelium growth. Several lines of evidence indicate that hyphal growth and morphology of *C. zeae-maydis* are influenced by the maize leaf environment before or during spore germination (Ward et al., 1999; Payne and Waldron, 1983). In nutrient-poor and nutrient-rich artificial culture media, conidia of *C. zeae-maydis* germinated and formed numerous hyphae radiating outward on the surface of the media and into the air after 24 hours (Fig 2.1). After 48 hours, conidia consistently formed dense mycelia (Fig 2.1). However, conidia of *C. zeae-maydis* that were inoculated on maize leaves developed fewer hyphae during the same time course. In order to quantify hyphal growth following conidium germination, the number of hyphae formed per conidium was quantified along with the length of hyphae produced 24 and 48 hours after inoculation. Interestingly, germinating conidia of *C. zeae-maydis* on maize leaves formed an average of 2.78 ± 0.09 hyphal filaments after 24 hours, and only an average of 3.29 ± 0.13 hyphal filaments 48 hours (Fig 2.1; Table 2.1). More striking was the drastic reduction in growth as measured by total hyphal branch length in the mycelium.

While germinating conidia on artificial media formed a dense mycelium after 24 hours, conidia inoculated on maize leaves developed only 244 μm ± 10 μm of hyphal filaments (Table 2.1). Surprisingly, the length of hyphae produced from a conidium on maize leaves at 48 hours (247 μm ± 13 μm) did not statistically differ from the growth 24 hours after inoculation (Table 2.1). Together, these data indicate that *C. zeae-maydis* exhibited differential germination and growth characteristics on maize leaves as compared to water agar medium. Furthermore, since water agar and the surfaces of maize leaves are both nutrient poor yet elicit distinct growth morphologies, signaling mechanisms other than nutrient acquisition may be involved in regulating growth after germination.

Hyphal growth, stomatal tropism and appressorium formation on host and non-host leaf surfaces. After germination, *C. zeae-maydis* orients hyphal growth toward stomata (Kim et al., 2011a). In this study, stomatal interception was most frequently observed after the initiation of apical reorientation of a hypha rather than the initiation of a new lateral branch. (Fig 2 B; Table 2.2). Unlike *Magnaporthe oryzae* and *Colletotrichum* species that form appressoria on small germ tubes originating from conidia (Bourette and Howard, 1990; Perfect et al., 1999), *C. zeae-maydis* often formed appressoria on lateral branches that intercepted adjacent stomata (Fig 2.2 A) as well as terminal hyphae demonstrating apical reorientation in the direction of nearby maize stomata (Fig 2.2 B). Stomatal tropism was measured as two components, the maximum distance in which hyphae intercepting stomata displayed reorientation or branch formation, and the branching angle of hyphae prior to stomatal interception (Fig 2.2 A, B). Stomatal interception was preceded by a change in hyphal growth, either developing from the formation of a lateral branch (40.5% ± 0.1 of interactions) or redirection of the hyphal tip (59.5% ± 0.1% of interactions; Table 2.2). After initiation of stomatal tropism, lateral branches developed from the

parental hyphae at an angle of 86.1° ± 1.69°, and apically dominant hyphae reoriented growth at an angle of 37.74° ± 1.67° (Fig 2.2 D). The initiation distance for hyphal reorientation and stomatal interception was 32.71 μm ± 3.65 μm for lateral branches, while the distance required for apically reoriented hyphae to intersect a stomate was 47.08 μm ± 2.95 μm (Fig 2.2 C). These experiments were conducted three times with similar results. Together, these observations demonstrate that hyphae of *C. zeae-maydis* display a consistent pattern of growth in response to distant host stomata.

Appressorium formation and maturation was initially observed as a swelling of the apical hyphal tip or the differentiation of a lateral branch that began to enlarge after the fungus physically encountered a stomatal guard cell (Fig 2.3 A). After initiation, appressoria consisted of numerous protuberances that typically rested on the stomatal guard cells (Fig 2.3 B). Appressorium maturation resulted in the development of a bulbous, hyaline, multi-lobed structure (Fig 2.3 C). Interestingly, appressoria were rarely formed away from guard cells, and multiple hyphae competing for the same stomate were never witnessed. Appressoria appeared to lay flat upon the guard cells with the approximate height of a hypha (Fig 2.3 D) as opposed to the globose, melanized appressoria formed by fungi like *M. oryzae*. Taken together, these data indicate that appressoria of *C. zeae-maydis* undergo a systematic developmental pattern in association with host stomata.

The influence of leaf surface topography on stomatal tropism and appressorium formation. To evaluate the role of leaf surface topography in infectious development in *C. zeae-maydis*, acrylic replicas of maize leaves created as described by Wynne (1976; Fig. 2.4) were inoculated with *C. zeae-maydis*. Within 24 hours after inoculation, conidia formed 3.29 ± 0.13 hyphae and produced 319 μm ± 12 μm of hyphal filaments (Fig 2.1; Table 2.1). After 48 hours,

mycelium (from a single conidium) contained an average of 6.39 ± 0.48 hyphae and 520 μm ± 45 μm of hyphal filaments (Fig 2.1; Table 2.1). After germination, *C. zeae-maydis* grew rapidly across the surface of the leaf replica; unlike on maize, which elicited appressorium formation (Fig 2.5 A). No appressoria were observed on leaf replicas despite identical incubation conditions and numerous repetitions (Fig 2.5 B). To determine if hyphae displayed tropism toward artificial stomata, the growth of hyphae that physically encountered replica stomata were quantified. During growth on artificial leaves, hyphae formed fewer lateral branches, and grew nearly straight across the surface of the replica. On leaf replicas, long unbranched hyphae encountered replica stomata approximately three times more often than lateral branches (Table 2.2). However, the lateral branching angle preceding stomatal interception was 78.43° ± 3.16° on the leaf replicas, which was similar to stomatal tropism observed on a maize leaf (Fig 2.2 D), indicating that lateral branches form at similar angles in relation to parental hyphae on maize leaves and leaf replicas. The angle of apical reorientation preceding stomatal interception on a leaf replica was 26.59° ± 2.14°, significantly less than the angle observed during stomatal tropism on maize leaves (Fig 2.2 D). While growing indiscriminately across the surface of leaf replicas, hyphae of *C. zeae-maydis* eventually encountered artificial stomata. However, hyphae displayed hyphal reorientation or lateral branching 63.05 μm ± 5.25 μm from replica stomates, which was nearly 30% farther than the distance required for stomatal tropism during pre-infectious growth on maize. The greater distance associated with branch formation on replicas likely indicates indiscriminant growth on the synthetic leaf surface rather than tropic reorientation toward distant replica stomata. These observations indicated that *C. zeae-maydis* derives cues from the leaf environment that regulate hyphal growth and development, and, unlike

many rust fungi, leaf surface topography alone is not sufficient to induce infectious growth and development.

***C. zeae-maydis* senses stomata and forms appressoria during non-host interactions.**

To determine if pre-penetration infectious development was influenced by host specificity, growth of *C. zeae-maydis* was observed during inoculations on the non-host beet. Twenty four hours after inoculation on beet (*Beta vulgaris*) leaves, conidia of *C. zeae-maydis* germinated and formed an average of 3.81 ± 0.18 hyphal branches, and produced 313 μm ± 20 μm of hyphal filaments (Fig 2.6; Table 2.1), which was statistically indistinguishable from growth on the acrylic leaf replicas (Fig 2.6; Table 2.1). After 48 hours, colonies contained an average of 4.68 ± 0.25 hyphae and 441 μm ± 26 μm of hyphal filaments (Fig 2.6; Table 2.1). The hyphal growth observed on beet leaves indicated that hyphae sensed a rigid leaf surface similar in some respects to host epidermis. However, the non-host surface was sufficiently different compared to maize leaves to elicit non-infectious growth similar to development on acrylic leaf replicas. During growth on beet leaves, *C. zeae-maydis* exhibited comparable branching to what was observed on maize leaves (Fig 2.7 A) and formed morphologically similar appressoria over beet stomates (Fig 2.7 A). Lateral branches with an average angle of 85.30° ± 2.67° preceded 45.2 % ± 0.1% of stomatal interceptions, which was similar to lateral branch formation on maize leaves (Fig 2.7 C). Apical reorientation with an average angle of 26.96° ± 2.67° preceded 54.7% ± 0.1% of stomatal interceptions, which was less than the angle formed on maize leaves (Fig 2.2 D). Unlike *C. zeae-maydis* grown on maize, which developed appressoria on 75% ± 2% of stomata encountered (Kim et al., 2011a,b), *C. zeae-maydis* development appressoria on only 61% ± 2% of beet stomata physically touching hyphae (Fig 2.7 A). Appressoria that formed on beet stomata appeared phenotypically indistinguishable to appressoria on maize (Fig 2.7 A).

Interestingly, *C. zeae-maydis* initiated stomatal tropism toward beet stomata at distance of 21.95 μm ± 3.16 μm from lateral branches, indicating that hyphae of *C. zeae-maydis* intersected beet stomata from shorter tropic branches compared to growth on maize (Fig 2.7 B). Hyphae reoriented apical growth toward beet stomata at a distance greater than what was required for tropic growth to maize stomata (Fig 2.7 B). These findings demonstrated that *C. zeae-maydis* exhibited stomatal tropism and appressoria formation on non-host stomata, and indicated that *C. zeae-maydis* was receptive to a potentially universally produced chemical cue from plant stomata.

Pre-penetration infectious development is conserved in *C. beticola.* To determine if pre-penetration growth on non-host leaves is conserved among *Cercospora* species, we evaluated *C. beticola* during infection of maize and beet leaves. Following inoculation, conidia germinated and extensively colonized the surface of maize and beet leaves. Also, *C. beticola* exhibited nearly identical stomatal tropism and appressorium formation in response to non-host maize stomata as compared to infection of beet (Fig 2.7 A). These data illustrate that *C. beticola* and *C. zeae-maydis* exhibited stomatal tropism and appressorium formation when inoculated on non-host plants. The initiation of stomatal tropism and appressorium formation on non-host stomata indicates that a conserved method of stomatal sensing is present among species of *Cercospor*a, and implicates a ubiquitous sensory cue emitted from stomata that triggers tropic growth and development.

Oxygen enrichment disrupts aspects of stomatal tropism and appressorium formation. In order to evaluate the role of oxygen in infectious development, maize plants were inoculated with the *C. zeae-maydis* SCOH1-5-GFP3 strain and placed in oxygen enrichment chambers. Similarly to maize leaves incubated in 21% O_2, stomatal interception during oxygen

enrichment was preceded by a change in directed growth. Fungi incubated in enriched oxygen exhibited similar percentages of lateral branch formation and apical reorientation preceding stomatal interception (Table 2.3). After *C. zeae-maydis* began to grow toward stomata in enriched oxygen, lateral branches developed at a similar angle to what was observed during the air incubations (Fig 2.8 B). However, tropic growth toward stomata occurred at a great distance from lateral hyphal branches, which differed significantly from the distance required for lateral branch formation when incubated in air (Fig 2.8 C). Growth in enriched oxygen had no effect on the distance for apical reorientation (Fig 2.8 C). The most striking effect of enriched oxygen on pre-infection physiology was a four-fold reduction in appressoria formed over stomata compared to the air incubation (Fig 2.8 D). Together, these results indicated that the formation of lateral branching during stomatal tropism was affected by high atmospheric concentrations of oxygen, but apical reorientation and the distances preceding hyphal reorientation were unaffected. The difference in stomatal tropism between terminal hyphae and lateral branches may be a result of the different mechanisms regulating apical growth and branch formation and warrants further exploration. Importantly, increased atmospheric oxygen concentrations significantly reduced the amount of appressoria formed on host stomata.

Oxygen gradients promote the development of appressorium-like structures *in vitro.* To determine if oxygen gradients elicited appressorium formation separately from stomatal tropism, a diffused oxygen coverslip assay was adapted from Aoki et al., 1998 for *in vitro* observations of appressorium formation in *C. zeae-maydis*. Briefly, a small amount of molten water agar medium was inoculated with conidia and placed between a microscope slide and coverslip. As the medium cooled, the inoculated drop formed a thin layer of medium with the margins exposed. During incubation in small chambers, the surrounding gas would diffuse

through the medium, creating a concentration gradient. After seven days of incubation in air (21% O_2), *C. zeae-maydis* formed a small number of truncated appressorium-like structures throughout the medium (Fig 2.9 A). However, after incubation in 100% O_2 for seven days, *C. zeae-maydis* formed approximately five-fold more appressorium-like structures (Fig 2.9 A, C). Similarly to appressoria formed on a leaf, *in vitro* appressorium-like structures were only observed forming from single parental hyphae, and formed either from hyphal apices or from small lateral branches (Fig 2.9 B). The appressorium-like structures produced *in vitro* were hyaline and exhibited similar vacuolization and cellular organization compared to appressoria formed on host stomata during infection (Fig 2.9 B). *CRP1* of *C. zeae-maydis*, an ortholog of the blue light photoreceptor *white collar-1* of *Neurospora crassa,* is required for appressorium formation as well as post-penetration infectious development (Kim et al., 2011b). Interestingly, the Δ*crp1-40* mutant failed to produce appressorium-like structures in either atmospheric condition, indicating that *CRP1* may regulate the formation of the appressorium-like structures *in vitro* as well as *in planta* (Fig 2.9 C). Taken together, these results suggested that the presence of an oxygen gradient was necessary for the formation of appressorium-like structures, and that *CRP1* regulates appressorium formation.

***CRP1* regulates multiple aspects of pre-penetration infectious development.**

Previous characterization of *CRP1* showed that appressorium formation was significantly reduced and pathogenicity was eliminated in the Δ*crp1-40* mutants, but the role of *CRP1* in stomatal tropism was not determined (Kim et al., 2011b). To explore the role of *CRP1* in stomatal tropism, growth of the Δ*crp1-40* mutant was quantified during infection of maize leaves. As previously reported during growth on the leaf surface, the *Δcrp1-40* mutant frequently grew over stomata and formed appressoria approximately 10-fold less than the wild

type (Kim et al., 2011b; Fig 2.10 A). Measurements of hyphal growth on the leaf surface revealed that the distance required for stomatal interception and hyphal branching angles were greater for the *Δcrp1-40* strain compared to the wild-type strain (Fig 2.10 B, C), suggesting indiscriminate growth on the leaf surface. Growth displayed by the *Δcrp1-40* strain was similar in many respects to the phenotype observed when the wild-type strain was grown on acrylic leaf replicas (Fig 2.2 C, D). The *Δcrp1-40* mutant formed lateral branches preceding 23.1% ± 0.1% of hyphal interceptions, which was statistically different than the hyphal branch ratios formed during infection of the wild-type strain on maize (Table 2.2). The decrease in lateral branch formation by the *Δcrp1-40* strain, combined with decreased lateral branch and apical reorientation angles preceding stomatal interception during growth on the leaf surface (Figure 2.10 B, C) indicated that *CRP1* was required for wild-type levels of stomatal tropism.

Discussion

Stomatal tropism and appressorium formation are required for pathogenesis in *C. zeae-maydis*, but prior to this work, neither phenomenon had been extensively quantified. This study represents the first systematic assessment of stomatal tropism and provides a broader perspective on stomatal infection among *Cercospora* species. A key finding from this work was the identification of two distinct methods through which hyphae reorient growth toward stomata. Modulating apical polarity and initiation of new hyphal branches are distinct mechanisms of fungal colonization and growth. Exactly how fungi initiate fungal branching, particularly establishing the site of hyphal branch initiation, is poorly understood and a long-standing subject of interest in fungal research (Harris 2008). In *C. zeae-maydis*, the stomatal chemoattractant(s) could conceivably interact with a membrane-bound receptor during pre-penetration pathogenic development, which then demarcates the site of branch initiation or induces a change in hyphal

tip polarity. In nature, fungi rarely form right-angle hyphal branches, yet *C. zeae-maydis* and *C. beticola* were observed to form them in response to distant stomata (Rathaiah, 1977; Kim et al., 2011a,b). This observation raises the question of whether the initiation of a hyphal branch in response to a stomate utilizes a different mechanism than the initiate of acute angle branches as observed in culture conditions. Together, these observations suggest the existence of an uncharacterized receptor that induces hyphal branching, a phenomenon that has not yet been described in the fungal kingdom.

The perception of light and molecular oxygen by fungi during stomatal infection combines two ubiquitous yet under-researched stimuli potentially involved in initial colonization stages of the infection process. Despite oxygen's fundamental importance to life, very little is known about fungal oxytropism (Brown, 1922; Robinson, 1973; Aoki et al., 1998). Oxygen signaling has not been investigated within the context of plant/fungal interactions, but oxygen sensing during hypoxic conditions is well studied in yeast and human pathogenic fungi. *Saccharomyces cerevisiae* adapts to anaerobic conditions by a expressing genes involved in oxygen-related functions such as respiration, heme biosynthesis and membrane biosynthesis (Zhang et al., 1999; Hon et al., 2003; Davies and Rine, 2006). Molecular oxygen is required for heme biosynthesis, and during aerobic growth, heme binds to the transcriptional activator Hap1 (Heme Activator Protein; Creusot et al., 1988; Pfiefer et al., 1989; Zhang and Guarente, 1995). In addition to regulatory genes involved in respiration, Hap1 also regulates numerous genes including ROX1 (Repressor Of hypoXic genes), which represses genes involved in hypoxic development (Zitomer et al. 1997). Relatedly, *CRP1* contains a flavin-binding light, oxygen, voltage (LOV) domain, which is a member of the PAS domain superfamily involved in environmental sensing in fungi (Crosson et al., 2003; Zoltowski et al., 2009). The interaction

between LOV domain-containing proteins and oxygen has been studied extensively in bacteria (Herrou and Crosson, 2011), but the role of fungal oxygen sensing during pathogenesis is poorly understood. Within this context, *CRP1* could represent a novel target for research into fungal oxytropism and oxygen sensing. In this study, altering concentrations of atmospheric oxygen influenced pathogenic development. When the normal atmospheric oxygen concentration was artificially enriched, the fungus was not able to efficiently identify distant stomata and was impaired in appressorium formation. Based on this prediction, light could regulate the perception and/or responsiveness to oxygen gradients released from stomata. *C. zeae-maydis* senses blue light through *CRP1*, which is predicted to be a core component of the white collar complex (WCC; Kim et al., 2011b). In model organisms, the WCC is a transcription factor that regulates responses to light and entrains the innate circadian clock (Baker et al., 2011). Thus, if *CRP1* regulates sensitivity to molecular oxygen gradients, *C. zeae-maydis* may be more sensitive to stomatal exudates when it is primed for infection, presumably at dawn. Alternatively, *CRP1* may regulate growth responses downstream from the perception of oxygen gradients, such as the initiation of hyphal branches or hyphal tip reorientation. Additionally, upon sensing molecular oxygen gradients in an *in vitro* assay, *C. zeae-maydis* grows toward higher concentrations of oxygen and forms appressorium-like structures in a process that requires a functional copy of *CRP1*. However, a more thorough molecular characterization of *CRP1* signaling and a better understanding of oxygen sensing through functional genomics are required to support this model.

Appressoria of *C. zeae-maydis* appear to differ in form and function compared to turgor-generating appressoria of other pathogenic fungi. Appressorium initiation in model fungi like *M. oryzae* is governed by cues such as chemical signals associated with the leaf surface, surface hydrophobicity and surface texture (Podila et al., 1993; Xiao et al., 1994; DeZann et al., 1999).

However, none of these cues appeared to elicit appressorium formation by *C. zeae-maydis*, either during this study or in previously published literature. In other fungi, appressoria generally form as terminal structures at the apices of small germ tubes originating from conidia (Emmett and Parbery, 1975; Bourette and Howard, 1990; Byrn et al., 1997), which contrasts starkly with the germination and growth of *C. zeae-maydis* that precedes appressorium formation during pre-penetration infectious development. Furthermore, the formation of appressoria by *C. zeae-maydis* over stomata rather than epidermal cells suggests that turgor pressure is not necessary for infection. Appressoria of model organisms like *M. oryzae* and *Colletotrichum spp*. are globose, single celled, heavily melanized structures that are capable of generating turgor pressure to drive a penetration peg through the leaf epidermis (Bourette and Howard, 1990; Perfect et al., 1999). Conversely, appressoria of *C. zeae-maydis* appear to contain many cells that aggregate into an irregular cluster over stomatal pores. Lastly, there is no visual evidence that appressoria of *C. zeae-maydis* produce melanin, which is a crucial cell wall component in other appressoria during turgor generation (Money and Ferrari, 1989). These observations strongly suggest that appressoria of *C. zeae-maydis* function differently than appressoria in other fungi, and may be associated with the transition to hemi-biotrophic growth. This conclusion is especially intriguing considering that appressoria of *C. zeae-maydis* appear structurally similar to infectious hyphae of *M. oryzae* (Bruno et al., 2004) and infection cushions produced by *Botrytis cinerea* (Leroch et al., 2011).

Cercospora species generally exhibit narrow host specificity, which is theorized to result from specificity during early stages of infection. In this study, *C. zeae-maydis* was shown to form appressoria over the stomatal pores of beet, a non-host plant. Thus, the molecular mechanisms underlying host specificity appear more likely to occur following stomatal

penetration, perhaps analogous to an effector-driven model as observed in numerous other fungal/plant interactions (Jones and Dangl, 2006). During infection, the plant perceives conserved plant-associated molecular patterns (PAMPs) and responds by triggering defense responses (Jones and Dangl, 2006). Many pathogens respond to the initiation of plant defenses by producing effectors, which increase pathogen virulence by inhibiting PAMP-triggered immunity and allow the pathogen to rapidly colonize the host (Jones and Dangl, 2006). The evolution of different effector proteins could explain the extensive speciation that has occurred in the genus *Cercospora*. For example, various *Cercospora* species are often present at a single location, and when conidia land on non-host plants and form appressoria and penetrate the substomatal cavity, there would be a consistent opportunity to test the limits of host specificity. Eventually, through horizontal gene transfer, mutation, or other genetic mechanisms, a small number of strains could overcome non-host resistance, thus allowing colonization and the eventual emergence of a *Cercospora* species with a broader host range. However, a more thorough characterization of the mechanistic basis of non-host interactions must be performed among *Cercospora* species to test this hypothesis.

Stomatal infection has been discussed as an important aspect of fungal pathogenesis for more than 100 years, but this study is the first to describe non-thigmotropic mechanisms of stomatal infection among plant pathogenic fungi. Also, this study implicates molecular oxygen as a chemoattractant, and establishes that multiple *Cercospora* species sense and respond to host and non-host stomata. Lastly, the elucidation of stomatal tropism in the *CRP1* deletion mutant contributes to the mechanistic understanding of stomatal infection in *C. zeae-maydis*.

References

Allan, E.A., Hazen, B.E., Hoch, H.C., Kwon, Y., Leinhos, G.M.E., Staples, R.C., Stumpf, M.A. and Terhune, B.T. 1991. Appressorium formation in response to topographical signals by 27 rust species. *Phytopathology* 81:323-331.

Aoki S., Ito-Kuwa S., Nakamura K., Vidotto V. and Takeo K. 1998. Oxygen as a possible tropic factor in hyphal growth of *Candida albicans. Mycoscience* 39:231-238.

Aptroot A. 2006. Mycosphaerella and its anamorphs: 2. Conspectus of Mycosphaerella. CBS Biodiversity Series 5:1-231.

Baker C.L., Loros J.L and Dunlap J.C. 2011. The circadian clock of *Neurospora crassa. FEMS Microbiol Rev* 36:95-110.

Bourett, T. and Howard, R. 1990. In vitro development of penetration structures in the rice blast fungus *Magnaporthe grisea. Can J Bot* 69: 329-342.

Brown W. 1922. On the germination and growth of fungi at various temperatures and in various concentration of oxygen and of carbon dioxide. *Ann Bot* 36: 257-283.

Bruno K.S., Tenjo F., Li L., Hamer J.E. and Xu J.R. 2004. Cellular localization and role of kinase activity of PMK1 in Magnaporthe grisea. *Eukaryot Cell* 3:1525-1532.

Byrne, J.M., Hausbeck, M.K., and Hammerschmidt, R. 1997. Conidial germination and appressorium formation of *Colletotrichum coccodes* on tomato foliage. *Plant Dis* 81:715-718.

Cheewangkoon, R., Crous, P.W., Hyde, K.D., Groenewald, J.Z., To-anan, C. 2008. Species of *Mycosphaerella* and related anamorphs on Eucalyptus leaves from Thailand. *Persoonia* 21: 77-91.

Chupp C. 1954. A monograph of the fungus genus *Cercospora*. Ithaca, New York.

Creusot, F., Verdiere, J., Gaisne, M., Slonimski, P.P. 1988. *CTP1* (*HAP1*) regulator of oxygen-dependent gene expression in yeast. Overall organization of the protein sequence displays several novel structural domains. *J Mol Biol* 204:263-276.

Crosson S., Rajagopal S. and Moffat K. 2003. The LOV domain family: photoresponsive signaling modules coupled to diverse output domains. *Biochemistry* 42:2-10.

Crous P.W. and Braun U. 2003. *Mycosphaerella* and its anamorphs. 1. Names published in Cercospora and Passalora. CBS Biodiversity Series 1:1-571.

Crous, P.W., Groenewald, J.Z., Groenewald, M., Caldwell, P., Braun, U. and Harrington, T.C. 2006. Species of *Cercospora* associated with grey leaf spot of maize. *Stud Mycol* 55:189-197.

Davies, B.S., and Rine, J. 2006. A role for sterol levels in oxygen sensing in *Saccharomyces cerevisiae*. *Genetics* 174:191-201.

DeZann, T.M., Carroll, A.M., Valent, B. and Swiegard, J.A. 1999. *Magnaporthe grisea* Pth11p is a novel plasma membrane protein that mediates appressorium differentiation in response to inductive substrate cues. *Plant Cell* 11:2013-2030.

Dodman, R.L. 1979. How the defenses are breached. Pages 135-153 in: Plant Disease: An Advanced Treatise, Vol. 4. J.G. Horsfall and E.B. Cowling, eds. Academic Press, New York.

Ellis, M.R. 1971. Dematiaceous hyphomycetes. Kew, England: Commonwealth Mycological Institute.

Emmett, R.W., and Parbery, D.G. 1975. Appressoria. *Annu Rev Phytopathol* 13:147-165.

Goodwin, S.B., Dunkle, D.L., Zismann, V.L. 2001. Phylogenetic analysis of *Cercospora* and *Mycosphaerella* based on the internal transcribed spacer region of ribosomal DNA. *Phytopathology* 91:648-658.

Groenewald M, Groenewald JZ, Braun U, Crous PW. 2006. Host range of Cercospora apii and C. beticola, and description of C. apiicola, a novel species from celery. *Mycologia* 98:275-285.

Guenther, A., Hewitt C.N., Erickson D., Fall R., Geron C., Graedel T., Harley, P., Klinger, L., Lerdau, Mckay, W.A., Pierce, T., Scholes, B., Steinbrecher, R., Tallamraju, T., Taylor, J., and Zimmerman, P. 1995. A global-model of natural volatile organic-compound emissions. *J Geophys Res* 100:8873-8892.

Harris, S.D. 2008. Branching of fungal hyphae: regulation, mechanisms and comparison with other branching systems. *Mycologia* 100: 823-832.

Herrou, J. and Crosson, S. 2011. Function, structure and mechanism of bacterial photosensory LOV proteins. *Nat Rev Microbiol* 9:713-723.

Holopainen, J.K. 2004. Multiple functions of inducible plant volatiles. *Trends Plant Sci* 9:529-533.

Hon, T., Dodd, A., Dirmeier, R., Gorman, N., Sinclair, P.R., Zhang, L., Poyon, R.O. 2003. A mechanism of oxygen sensing in yeast. Multiple oxygen-responsive steps in the heme biosynthetic pathway affect Hap1 activity. *J Biol Chem* 12:50771-50780.

Jones, J.D., and Dangl, J.L. 2006. The plant immune system. *Nature* 444: 323-339.

Kim, H., Ridenour, J.B., Dunkle, L.D. and Bluhm, B.H. 2011a. Regulation of pathogenesis by light in *Cercospora zeae-maydis*: An updated perspective. *Plant Pathol J* 27:103-109.

Kim, H., Ridenour, J.B., Dunkle, L.D. and Bluhm, B.H. 2011b. Regulation of stomatal tropism and infection by light in *Cercospora zeae-maydis*: Evidence for coordinated host/pathogen responses to photoperiod? *PLoS Pathog* 7(7): e1002113.

Kirk, W.W., Hanson, L.E., Franc, G.D., Stump, W.L., Gachango, E., Clark, G., and Steward, J. 2012. First report of strobilurin resistance in *Cercospora beticola* in sugar beet (*Beta vulgaris*) in Michigan and Nebraska, USA. *New Dis. Rep.* 26:3.

Leroch, M., Mernke, D., Koppenhoefer, D., Schneider, P., Mosbach, A., Doehlman, and G. Hahn M. 2011. Living colors in the gray mold pathogen *Botrytis cinerea*: Codon-optimized genes encoding green fluorescent protein and mCherry, which exhibit bright florescence. *App Env Biol* 77:2887-2897.

Lewis, B.G. and Day, J.R. 1972. Behavior of uredospore germ-tubes of *Puccinia graminis tritici* in relation to the fine structure of wheat leaf surfaces. *Trans Br Mycol Soc* 58:139-45.

McCluskey, K. 2003. The fungal genetics stock center: from molds to molecules. *Adv Appl Microbiol* 52:245-262.

Money, R.J. and Ferrari, M.A. 1989. Role of melanin in appressorium formation. *Exp Mycol* 13: 403-418.

Nevill, D.J. 1981. Components of resistance to *Cercospora* archidicola and *Cercosporidium personatum* in groundnuts. *Ann Appl Biol* 99: 77-86.

Oikawa, P.Y. and Lerdau, M.T. 2013. Catabolism of volatile organic compounds influences plant survival. *Trends Plant Sci* 18:695-703.

Payne, G.A. and Waldron, J.K. 1983. Overwintering and spore release of *Cercospora zeae-maydis* in corn debris in North Carolina. *Plant Dis* 67:87-89.

Perfect, S.E., Hughes, H.B., O'Connell, R.J. and Green, J.R. 1999. *Colletotrichum*: A model genus for studies on pathology and fungal-plant interactions. *Fungal Gen Biol* 27: 186-198.

Pfeifer, K., Kim, K.S., Kogan, S., Guarente, L. 1989. Functional dissection and sequence of yeast HAP1 activator. *Cell* 56:291-301.

Podila, G.K., Rogers, L.M. and Kolattukudy, P.E. 1993. Chemical signals from avocado surface wax trigger germination and appressorium formation in *Colletotrichum gloeosporioides*. *Plant Physiol.*103:267–272.

Poland, J.A., Balint-Kurti, P.J., Wisser, R.J., Pratt, R.C. and Nelson, R.J. 2008. Shades of gray: the world of quantitative disease resistance. *Trends Plant Sci*. 14:21-9

Pollack, F.G. 1987. An annotated compilation of *Cercospora* names. *Mycologia Memoir* 12:1-212.

Pool, V.W. and McKay, M.B. 1916. Relation of stomatal movement to infection by *Cercospora beticola*. *J Agric Res* 5:1011-1038.

Rathaiah, Y. 1976. Infection of sugarbeet by *Cercospora beticola* in relation to stomatal condition. *Phytopathology* 66:737-740.

Rathaiah, Y. 1977. Stomatal tropism of *Cercospora beticola* in sugarbeet. *Phytopathology* 67:358-362.

Robinson, P.M. 1973. Oxygen – positive chemotropic factor for fungi? *New Phytol* 72:1349-1456.

Shim, W-B. and Dunkle, L.D. 2003. CZK3, a MAP kinase kinase kinase homolog in *Cercospora zeae-maydis*, regulates cercosporin biosynthesis, fungal development, and pathogenesis. *Mol Plant-Microbe Interact* 16:760-768.

To-Anun, C., Hidayat, I., and Meeboon, J. 2011. Genus *Cercospora* in Thailand: Taxonomy and phylogeny (with a dichotomous key to species). *Plant Pathol Quar* 1:11-87.

Trkulja, N., Ivanovic, Z., Pfaf-Dolovac, E., Dolovac, N., Mitrovic, M., Tosevski, I. and Jovic, J. 2013. Characterization of benzimidazole resistance of *Cercospora beticola* in Serbia using PCR-based detection of resistance-associated mutations of the Beta-tubulin gene. *Euro J Plant Pathol* 135: 889-902.

Vestal, E.F. 1933. Pathogenicity, host response and control of *Cercospora* leaf spot of sugar beets. *Iowa Agric Exp Stn Bull* 168:43-72.

Ward, J.M.J., Stromberg, E.L., Nowell, D.C., and Nutter F.W. Jr. 1999. Gray leaf spot: a disease of global importance in maize production. *Plant Dis* 83: 884–895.

Weiland, J.J., and Koch, G. 2004. Sugar-beet leaf spot disease (*Cercospora beticola* Sacc.). *Mol Plant Pathol* 5:157-166.

Wynn, W.K. 1976. Appressorium formation over stomates by the bean rust fungus: Response to a surface contact stimulus. *Phytophathology* 66:136-146.

Xiao, J.-Z., Watanabe, T., Kamakura, T., Ohshima, A,. and Yamaguchi, I. 1994. Studies on cellular differentiation of *Magnaporthe grisea*. Physicochemical aspects of substratum surfaces in relation to appressorium formation. *Physiol. Mol. Plant Pathol*. 44: 227–236.

Zhang, L., and Guarente, L. 1995. Geme binds to a short sequence that serves a regulatory function in diverse proteins. *Embo J* 14:313-320.

Zhang, L., and Hach, A. 1999. Molecular mechanism of heme signaling in yeast: the transcriptional activator Hap1 serves as a key mediator. *Cell Mol Life Sci* 56:415-426.

Zhang, Y., Xu, L., Fan, X., Tan, J., Chen, W. and Xu, M. 2012a. QTL mapping of resistance to gray leaf spot in maize. *Theor Appl Genet* 125: 1797-1808.

Zhang, G.R., Newman, M.A., and Bradley, C.A. 2012b. First report of the soybean frogeye leaf spot fungus (*Cercospora sojina*) resistant to quinone outside inhibitor fungicides in North America. *Plant Disease* 96:767.

Zitmoer R.S., Carrico, P., and Deckert, J. 1997. Regulation of hypoxic gene expression in yeast. *Kindey Int* 51:507-513.

Zoltowski, B.D., Vaccaro, B. and Crane, B.R. 2009. Mechanism-based tuning of a LOV domain photoreceptor. *Nat Chem Biol* 5: 827–834.

Figures

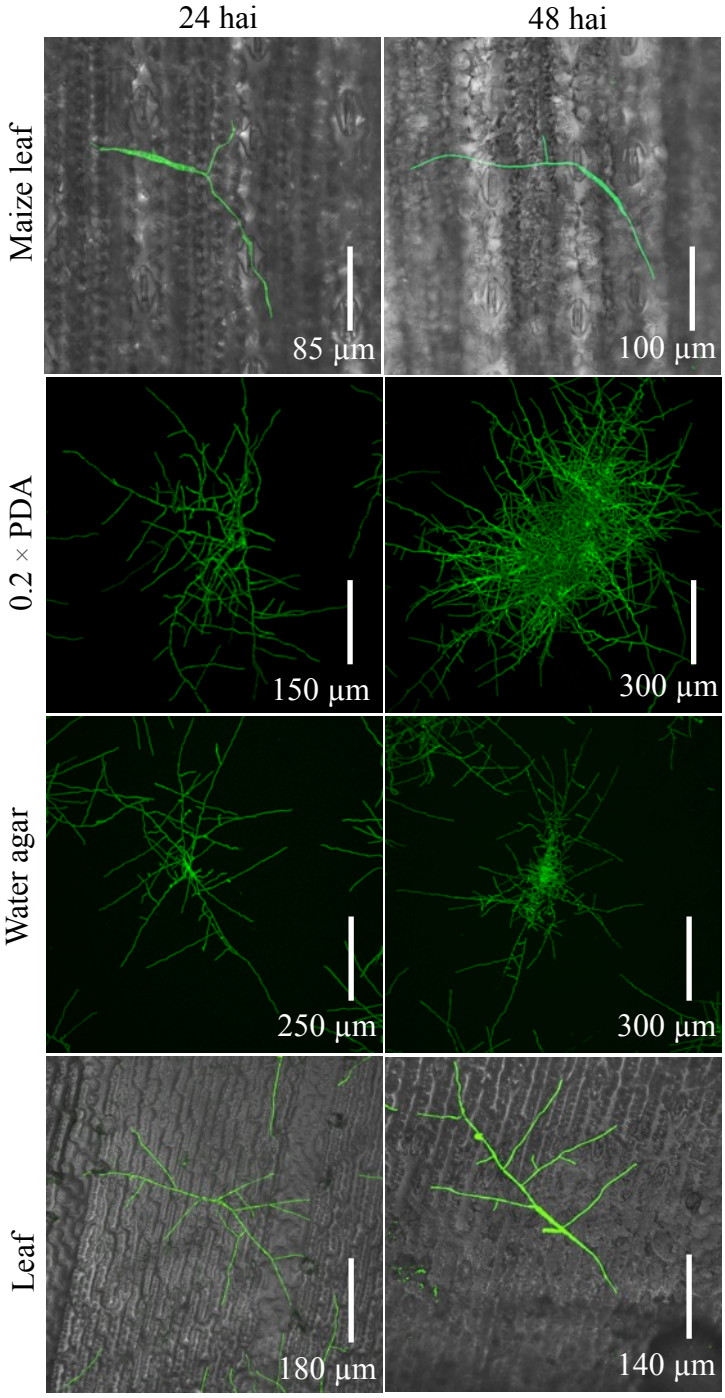

Figure 2.1. The effect of substrate on germination and mycelium formation in *C. zeae-maydis*. *C. zeae-maydis* GFP-tagged reporter strain (SCOH1-5-GFP3) was inoculated on different substrates and observed 24 and 48 hours after inoculation (hai). Following inoculation on maize leaves, conidia germinated from the conidial apices and from the intercalary cells after 24 hours, culminating in the formation of a small mycelia consisting of several hyphae after 48 hours. When inoculated on the nutrient poor 0.2 × PDA and water agar, conidia germinated and formed

mycelia by 24 hours, and dense aerial mycelia by 48 hours. However, when conidia were inoculated on a topographically accurate acrylic leaf replica, conidia germinated and formed approximately twice as many hyphae compared to the maize leaf both 24 and 48 hours after inoculation. Growth of the GFP-tagged reporter strain was observed with confocal microscopy, and representative pictures of the phenotypes observed in three separate experiments are presented.

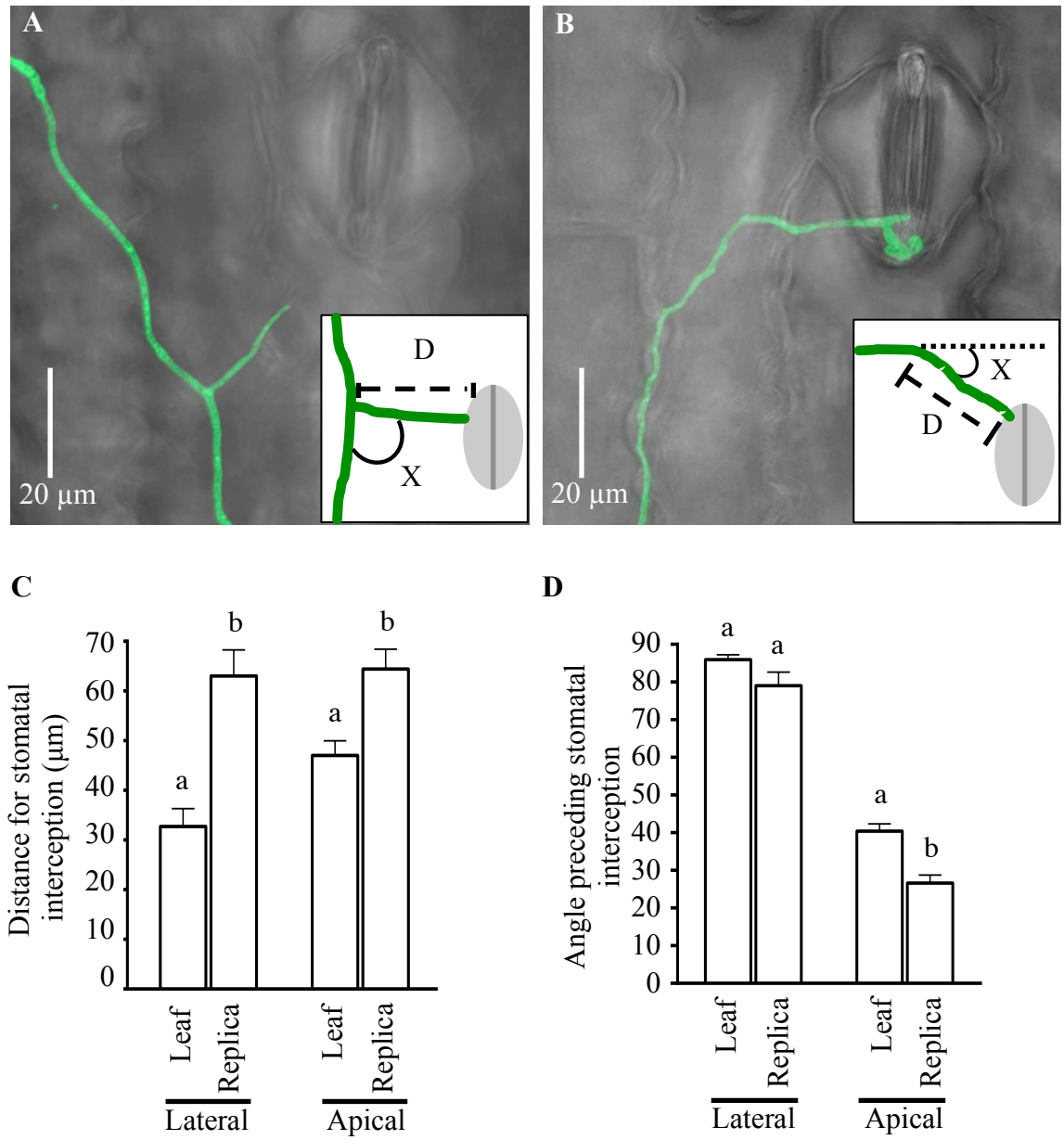

Figure 2.2. *C. zeae-maydis* exhibits lateral branch formation and apical reorientation of hypha during stomatal tropism. Maize leaves were inoculated with conidia of a GFP-tagged wild-type reporter strain and hyphal interactions with stomata were observed over seven days. A) Lateral branches were often formed in close association with host stomata during pathogenic development. The distance required for stomatal interception was determined by measuring the linear distance (D) between the location of branch initiation and the intersected stomate. The angle preceding stomatal interception was determined by measuring the acute angle (X°) formed by the parental and lateral hyphae, in the direction of growth. B) Developing hyphae also frequently reoriented apical growth toward host stomata. In cases of apical reorientation, the

distance (D) required for stomatal interception were determined by measuring the distance from the location of apical reorientation to the point of stomatal contact. The angle (X°) of apical reorientation was determined by measuring the acute angle formed by the initial axis of growth and the tropic hypha. C) Average distances required for stomatal interception for lateral branches and apically reoriented hyphae following inoculation on leaves or leaf replicas. D) Average angle formed by hyphae following tropic reorientation toward host or replicate stomata. Measurements were conducted on 100 hyphae/stomata interactions following inoculation on host leaves and topographically accurate leaf replicas, with bars showing standard error. Statistical comparisons of means were performed with an Independent Samples *t*-test ($\alpha = 0.05$; letters denote statistical significance).

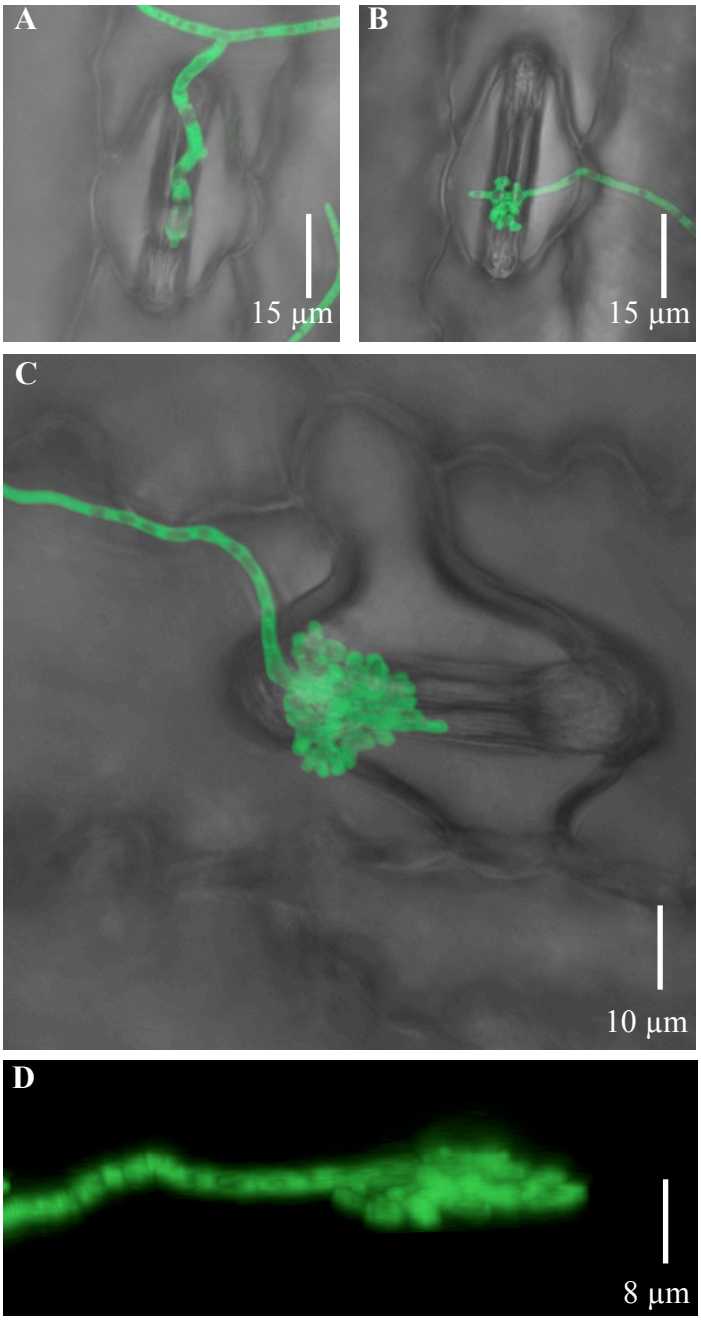

Figure 2.3. Appressorium formation in *C. zeae-maydis*. Maize leaves were inoculated and pre-infectious development was observed over several days. A) After physically encountering host stomata, hyphae typically begin to subtly swell and form small lateral growths. B) Hyphae appear to lose polarity, and the lateral growths develop into large bulbous growths spreading out from the parental hypha. C) After several hours, a mature appressorium containing several cells is formed in close association with host stomata. D) A computer-rendered lateral view of a mature appressorium shows that appressoria of *C. zeae-maydis* lay flatly against the surface of the leaf. Growth of the GFP-tagged reporter strain was observed with confocal microscopy, and representative pictures of the phenotypes observed in three separate experiments are presented.

Laterally rendered pictures were created from digitally analyzed confocal images, and the leaf surface was removed for clarity.

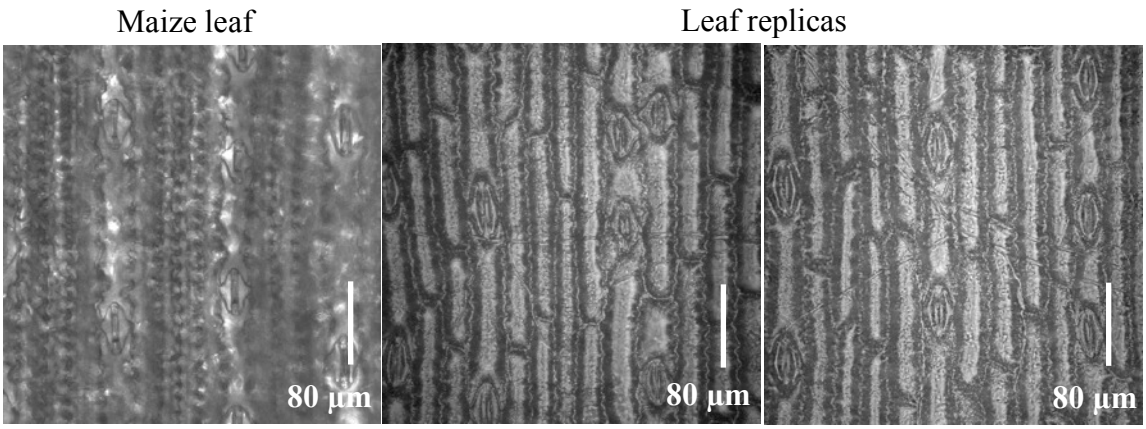

Figure 2.4. Morphological similarities between a live maize leaf and an acrylic leaf replica. Representative samples of each surface were observed with a transmitted light microscope to highlight the topographical similarities between the two surfaces.

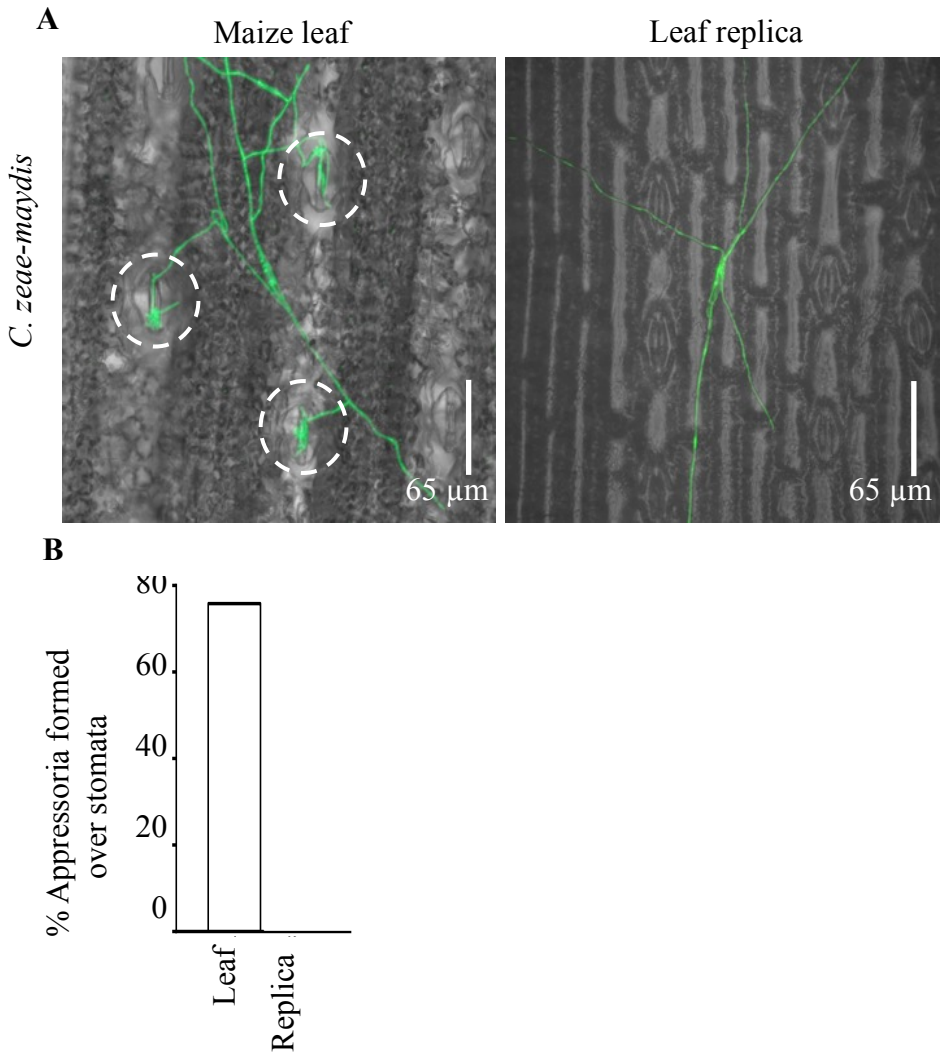

Figure 2.5. Appressorium formation is dependent on physical contact with viable host stomata. A) Conidia of a GFP-tagged *C. zeae-maydis* wild-type reporter strain were inoculated on intact maize leaves and topographically accurate leaf replicas and incubated for five days in a growth chamber. Following incubation, the wild-type reporter strain readily formed appressoria on host stomata (white circles), whereas the same strain never formed appressoria despite forming a mycelium and physically interacting with stomata. B) After inoculation on an intact maize leaf, *C. zeae-maydis* developed appressoria during 78% of hypha/stomatal interactions, while *C. zeae-maydis* failed to form appressoria on the leaf replicas following several repeated inoculations. Growth of the GFP-tagged reporter strain was observed with confocal microscopy, and representative pictures of the phenotypes observed in three separate experiments are presented. Percentage appressorium formation was calculated by observing 100 hyphal/stomatal interactions. Statistical comparisons of means were performed with an Independent Samples *t*-test ($\alpha = 0.05$; letters denote statistical significance).

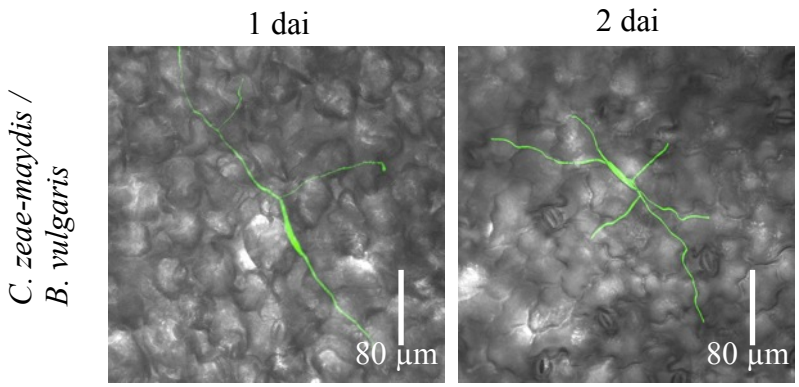

Figure 2.6. The effect of host and non-host leaves on germination and mycelium formation in *C. zeae-maydis*. Conidia germinated readily on beet leaves following one day after inoculation (dai) and two dai.

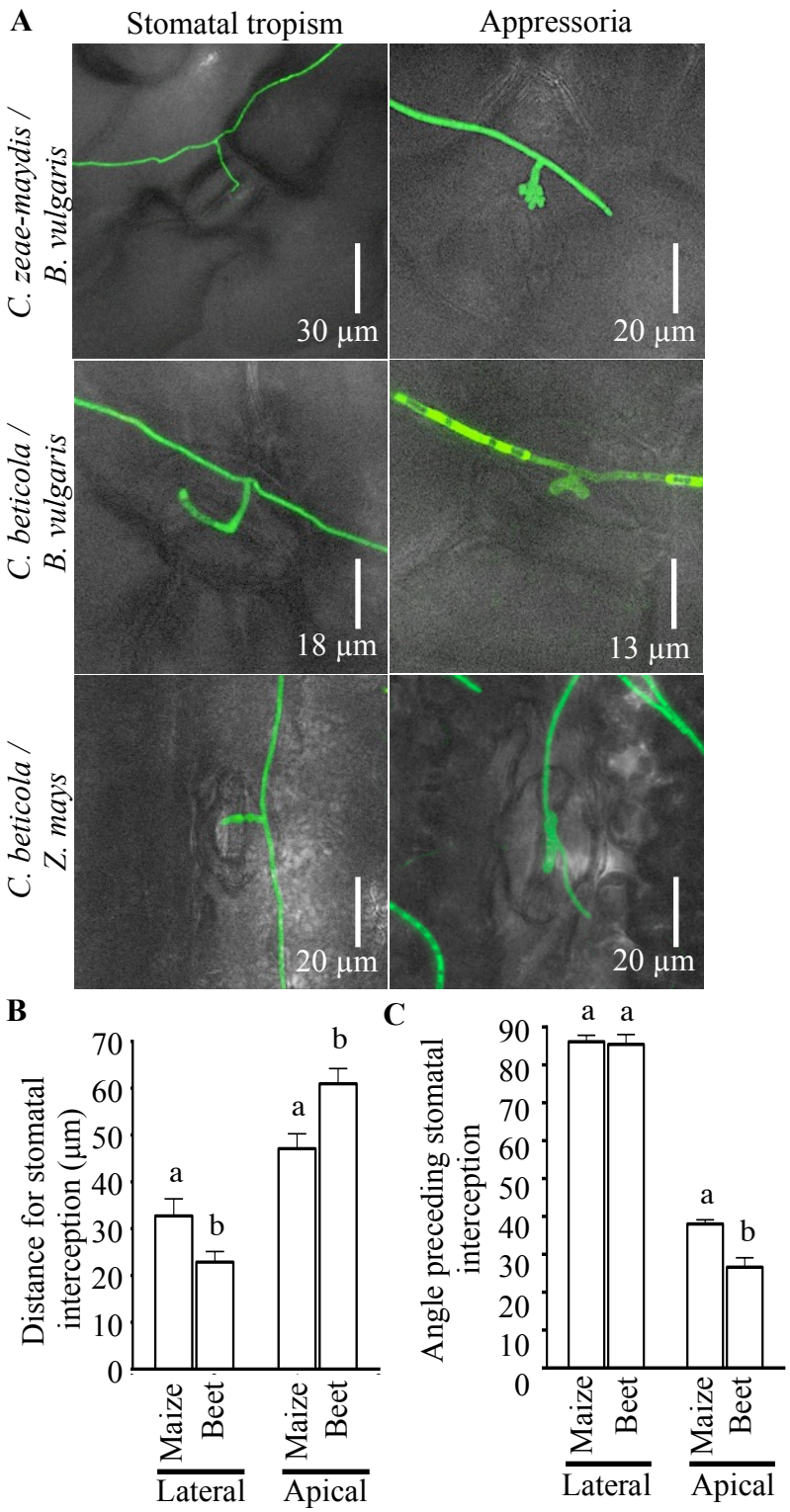

Figure 2.7. *Cercospora* species exhibit stomatal tropism and appressorium formation in response to non-host stomata. In order to determine the host-specificity of the stomatal attractant, *C. zeae-maydis* and the beet foliar pathogen *C. beticola* were cross-inoculated on beet (*B. vulgaris*) or maize (*Z. mays*), respectively. A) Following inoculation, *C. beticola* exhibited

similar lateral branching and appressorium formation on beet and maize. *C. zeae-maydis* also formed lateral branches and appressoria in response to non-host beet stomata. B) Average distances required for stomatal interception for lateral branches and apically reoriented hyphae following inoculation of *C. zeae-maydis* on maize and beet leaves. C) Average angle formed by hyphae following tropic reorientation toward maize or beet stomata. Measurements were conducted on 100 hyphae/stomata interactions, with bars showing standard error. Statistical comparisons of means were performed with an Independent Samples *t*-test ($\alpha = 0.05$; letters denote statistical significance).

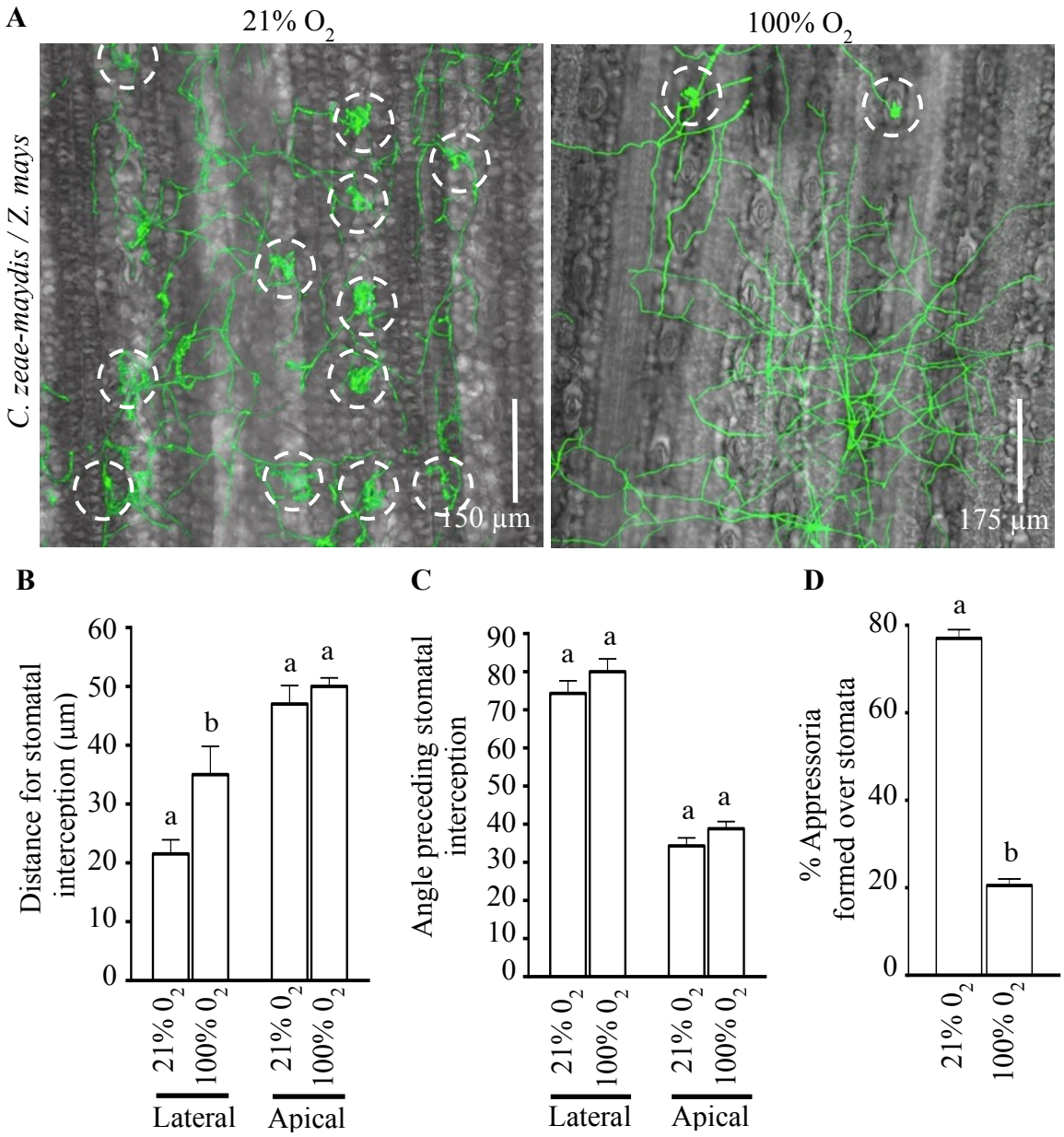

Figure 2.8. Molecular oxygen is required for appressorium formation. A) Conidia of a GFP-tagged *C. zeae-maydis* wild-type reporter strain were inoculated on maize plants, which were incubated in chambers containing air (21% O_2), or an atmosphere enriched in oxygen (100% O_2). Following incubation in air, the wild-type GFP reporter strain readily formed appressoria on host stomata, whereas the same strain formed markedly fewer appressoria when inoculated in 100% O_2 (white circles). B) Average distances required for stomatal interception for lateral branches and apically reoriented hyphae following inoculation on leaves or leaf replicas. C) Average angle formed by hyphae following tropic reorientation toward host or replicate stomata. D) Ratio of appressoria per stomate encountered during incubation in air and 100% O_2. Measurements were conducted on 100 hyphal/stomatal interactions following inoculation on host leaves and topographically accurate leaf replicas, with bars showing standard error. Statistical comparisons

of means were performed with an Independent Samples *t*-test ($\alpha = 0.05$; letters denote statistical significance).

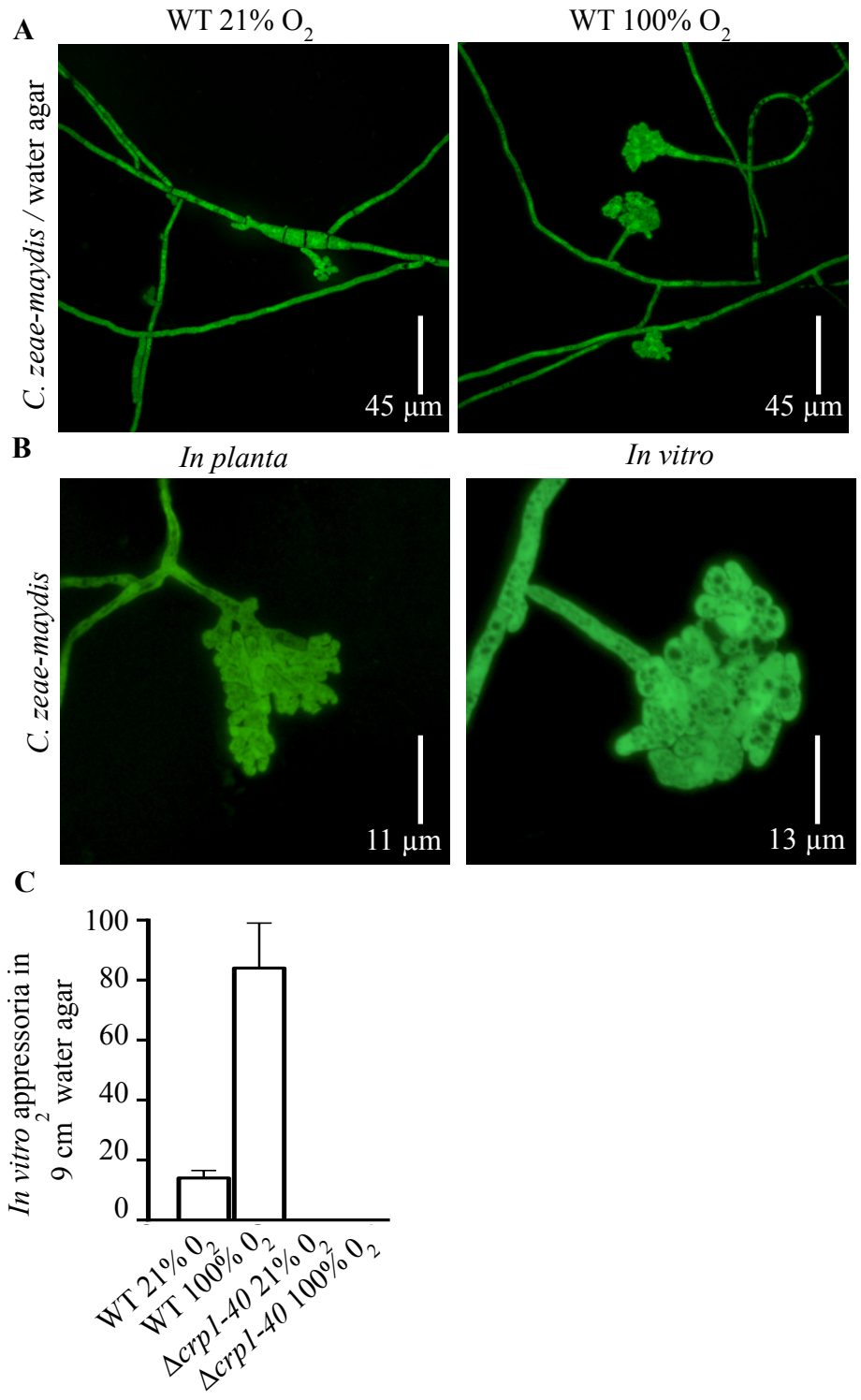

Figure 2.9. Sensing oxygen gradients is required for appressorium formation. Molten water agar was inoculated with conidia of the GFP-reporter wild-type strain and sandwiched between a microscope slide and coverslip to produce a thin layer of medium, with margins evenly exposed to the atmosphere. Thin-medium cultures were incubated in air (21% O_2) or an atmosphere

enriched in oxygen (100%) and observed after seven days. A) The wild-type strain formed small, truncated appressorium-like structures when incubated in air, but readily formed appressorium-like structures when incubated in 100 O_2. B) Appressorium-like structures formed *in vitro* in 100% O_2 appear morphologically similar to appressoria formed in association with host stomata. For clarity, the stomata and surrounding leaf surface was removed from the image of an appressorium formed *in planta*. C) Appressorium-like structures in a 9 cm^2 area of the thin-medium oxygen gradient assay were quantified for both the wild-type and Δ*crp1-40* strains. Values represent the average of three experiments and bars represent standard error.

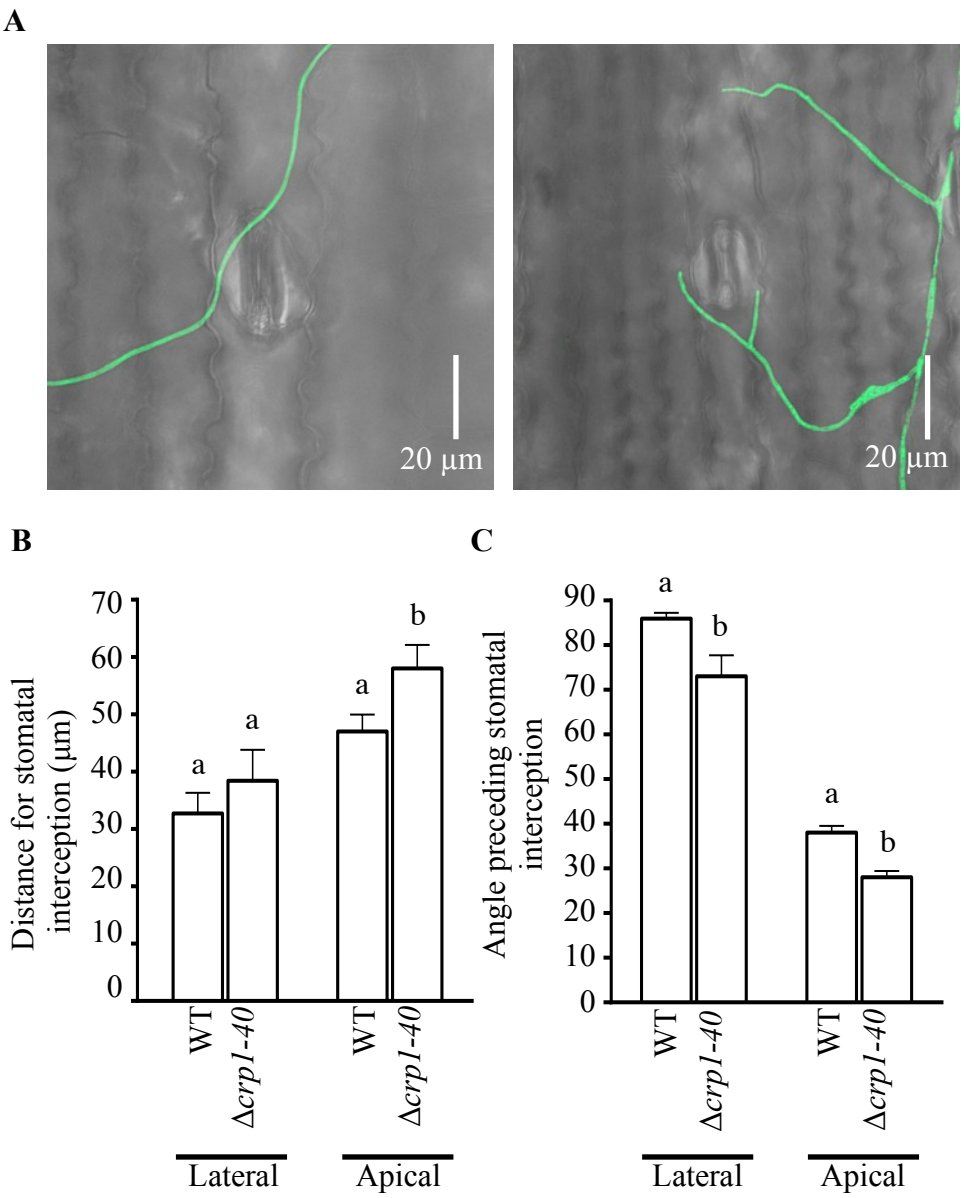

Figure 2.10. *CRP1* is required for aspects of wild type stomatal perception. A) Δ*crp1-40*-GFP was inoculated on maize and incubated for five days. The Δ*crp1-40*-GFP strain failed to form appressoria after physically encountering host-stomata. B) Average distances required for stomatal interception for lateral branches and apically reoriented hyphae following inoculation compared to the wild type. C) Average angle formed by hyphae following tropic reorientation toward host or replicate stomata. Measurements were conducted on 100 hyphal/stomatal interactions following inoculation on host leaves and topographically accurate leaf replicas, with bars showing standard error. Statistical comparisons of means were performed with an Independent Samples *t*-test ($\alpha = 0.05$; letters denote statistical significance).

Tables

Table 2.1. Germination of *C. zeae-maydis* conidia on different surfaces

Strain[a]	Substrate[b]	1 dai		2 dai	
		Branches[c]	Length[d]	Branches[c]	Length[d]
WT	Maize, 21% O_2	2.78 ± 0.09	244 ± 10	3.29 ± 0.13	247 ± 13
WT	Replica	3.89 ± 0.11[A]	319 ± 12[B]	6.39 ± 0.48	520 ± 45
WT	Beet	3.81 ± 0.18[A]	313 ± 20[B]	4.68 ± 0.25	441 ± 26
WT	Maize, 100% O_2	4.02 ± 0.26[A]	408 ± 38	7.43 ± 0.58	856 ± 82
WT	H_2O agar	na[e]	na	na	na
WT	0.2 × PDA	na	na	na	na

[a] Conidia were inoculated onto each surface and data recorded every day after inoculation (dai).

[b] All substrates were incubated in a growth chamber under 14:10 L:D with high humidity.

[c] Reported as number of germ tubes emerging from each conidia and the number of subsequent hyphal branches. Data are the mean values of 100 conidia ± SE.

[d] Reported as μm of all germ tubes and hyphae borne from a single conidium. Data are the mean values of 100 conidia ± SE. All values were calculated by ANOVA with Tukey's HSD test at a cutoff of $p = <0.05$, and letters signify statistical significance.

[e] Measurements listed as "na" represent dense, flocculent mycelia wherein it was impossible to measure individual hypha.

Table 2.2. Percent hyphal branches or apically reoriented hyphae prior to physical contact with stomata[a]

Hyphae	WT on maize	WT on beet	Δ*crp1* on maize	WT on replica
Lateral Branch	40.6% ± 0.1% b	43.6% ± 0.1% b	23.1% ± 0.1% c	28.0% ± 0.1% bc
Apical Reorientation	59.4% ± 0.1% b	56.4% ± 0.1% b	76.9% ± 0.1% c	72.0% ± 0.1% bc

[a] The proportion of lateral branch formation versus apical reorientation varied as a function of condition as measured by a chi-square test of independence with Cramer's V as the nominal correlation statistic. Post-hoc comparisons conducted using a Bonferroni correction for multiple comparisons are presented. Values presented are the mean ± standard error with letters signifying statistical significance.

Table 2.3. Percent hyphal branches or apically reoriented hyphae prior to physical contract with stomata during oxygen enrichment incubations with the wild-type (WT) strain[a]

Hyphae	WT / 21% O_2	WT / 100% O_2
Lateral Branch	38.3% ± 0.1% b	29.8%± 0.1% b
Apical Reorientation	61.7% ± 0.1% b	70.2%± 0.1% b

[a] The proportion of lateral branch formation versus apical reorientation varied as a function of condition as measured by a chi-square test of independence with Cramer's V as the nominal correlation statistic. Post-hoc comparisons conducted using a Bonferroni correction for multiple comparisons are presented. Values presented are the mean ± standard error with letters signifying statistical significance.

CHAPTER III: AN ORTHOLOG OF THE CIRCADIAN OSCILLATORY GENE FREQUENCY IS REQUIRED FOR STOMATAL INFECTION IN CERCOSPORA ZEAE-MAYDIS

Summary

Cercospora zeae-maydis causes gray leaf spot of maize, a foliar disease of concern in most maize-producing regions of the world. Hyphae of *C. zeae-maydis* exhibit stomatal tropism and form appressoria over host stomata before penetrating leaves. Recently, the blue-light photoreceptor *CRP1* was shown to be required for stomatal tropism, appressorium formation, and lesion development. Orthologs of *CRP1* in *Neurospora crassa* and other fungi regulate innate circadian rhythms by modulating the expression of the *frequency* gene (*FRQ*), a core clock component. In this study, transcriptional analysis of circadian gene expression established the presence of a *frequency*-mediated circadian clock in *C. zeae-maydis*. To elucidate the role of circadian regulatory genes in the development of gray leaf spot, the *frequency* ortholog *FRQ* in *C. zeae-maydis* was identified and disrupted, and deletion mutants were compared to wild type during growth on leaf surfaces prior to stomatal penetration. Interestingly, *FRQ* deletion mutants were significantly disrupted in their ability to form infection structures relative to the wild-type strain when inoculated on maize leaves. These findings demonstrate a unique role for a fungal circadian clock in regulating disease development, and illuminates the complexities underlying the interplay between environmental sensing and fungal pathogenesis.

Introduction

Molecular clocks allow organisms to anticipate and respond to many environmental factors, including the diurnal transition from night to day. In some cases, the rhythmic patterns of gene expression regulated by light are called "circadian" rhythms (Latin: 'circa' *about*, and 'dies' *day*), and they must satisfy three characteristics: 1) complete one period of oscillation in approximately 24 hours, 2) persist in the absence of the stimulus (i.e., rhythmic light exposure), and 3) compensate for environmental stress (e.g., temperature changes; Dunlap et al., 2004; McClung, 2006). Plants, animals, fungi and bacteria all have circadian clocks that regulate important biological processes and responses to environmental stimuli (Young and Kay, 2001). Despite the prevalence of circadian clocks in most organisms, the lack of clear homology between the core oscillatory proteins of cyanobacteria, prokaryotic, and eukaryotic clocks points towards independent evolution of different clock mechanisms (Young and Kay, 2001). Early investigations of circadian regulation began in *Drosophila* in the 1970's (Konopka and Benzer, 1971), and have matured into the development of well-characterized model systems representing a broad cross-section of diverse taxonomic groups including plants and fungi (Loudon et al., 2000)

Emerging evidence indicates that circadian clocks regulate important aspects of plant defense against pathogens. Many plant genes relating to growth and metabolism are expressed in a circadian rhythm (reviewed by McClung 2001, 2006), and recent research in Arabidopsis has elucidated the circadian regulation of basal metabolic gene expression and resistance-gene expression in response to pathogen invasion. The central circadian oscillator in Arabidopsis is comprised of several genes including CIRCADIAN CLOCK ASSOCIATED1 (CCA1) and its homolog LATE ELONGATED HYPOCOTYL (LHY), which act as transcription factors that regulate multiple feedback loops and mediate clock activity (Lu et al., 2009; Mizoguchi et al.,

2002; Alabadi et al., 2002). Arabidopsis exhibits daily fluctuations in susceptibility to infection by the bacterium *Pseudomonas syringae*, which is altered following overexpression of CCA1 (Bardwaj et al., 2011). Following inoculation with *P. syringae* and the oomycete pathogen *Hyaloperonospora arabidopsidis,* CCA1 and LHY act synergistically to regulate basal defense by altering stomatal aperture and by eliciting the expression of pathogen-specific resistance genes (Wang et al., 2011; Zhang et al., 2013). An intriguing but uncharacterized component of circadian basal- and induced-defense gene expression is the role of circadian regulation of pathogenesis or virulence-related genes in the plant pathogen, and the subsequent interaction between the pathogen and host during infection.

Circadian regulation of pathogenesis in fungi is poorly understood. However, the circadian clock in the model fungus *Neurospora crassa* has been studied extensively and serves as a model for fungal chronobiology. In *N. crassa*, circadian rhythms are driven by daily changes in expression of the central oscillator *frequency* (reviewed by Baker et al., 2011). *Frequency* expression is regulated by the heterodimeric White Collar Complex (WCC) formed by the GATA-family transcription factors *white collar-1* and *white collar-2* (Crosthwaite et al., 1997; Linden and Macion, 1997; Ballario et al., 1998; Cheng et al., 2002). In late evening (after several hours in the absence of sunlight), the WCC binds to the *frequency* promoter to drive *frequency* expression, which peaks in the early morning. Frequency proteins form functional homodimers via a coiled-coil domain (Cheng et al., 2001a,b) and enter the nucleus to repress *frequency* transcription by interacting with the WCC (Luo et al., 1998). The negative feedback loop of the *N. crassa* circadian cycle begins in late morning and reduces *frequency* expression to basal levels by evening, when the cycle repeats itself during the next light cycle (Gooch et al., 2008).

The maize foliar pathogen *Cercospora zeae-maydis* causes gray leaf spot of maize and requires light to sense its host (Kim et al., 2011a,b). After conidia germinate on maize leaves, developing hyphae of *C. zeae-maydis* display a complex series of morphological steps during growth on the leaf surface, including growth toward stomata and the formation of appressoria in association with host stomata (Kim et al., 2011a, Chapter Two). Following appressorium formation on stomata and penetration into the sub-stomatal cavity, it is postulated that hyphae asymptomatically colonize leaf tissue for several days until an unknown cue triggers a transition to necrotrophy which leads to lesion formation (Kim et al., 2011a). Conidia develop from conidiophores arising from stomata, resulting in the generation of secondary inocula and the continuation of the disease cycle (Kim et al., 2011a). Recently, the *white collar-1* ortholog in *C. zeae-maydis* (*CRP1*) was shown to be required for pathogenic development during infection (Kim et al., 2011b). *CRP1* deletion mutants were unable to locate host stomata, failed to form wild type levels of appressoria after physical contact with stomata, and did not cause lesions. While numerous *white collar-1* orthologs and other light responsive genes have been characterized in fungi, very little is known regarding the downstream effectors of light sensing and the circadian regulation of plant pathogenesis.

The current study sought to elucidate the function of a circadian-related regulatory gene (*FRQ*) during stomatal perception and appressorium formation. Specifically, a component of the molecular clock in *C. zeae-maydis* was shown to regulate stomatal infection during foliar pathogenesis. The *frequency* ortholog in *C. zeae-maydis* (*FRQ*) was identified by sequence homology, and transcriptional analysis showed that *FRQ* was expressed in a rhythmic manner and regulated by *CRP1*. Gene-deletion mutants of *FRQ* failed to form appressoria after stomatal interception. This study represents the first report of a circadian clock-related gene regulating

disease development in a plant pathogenic fungus. These findings resulted in the discovery of novel regulatory mechanisms governing fungal environmental sensing and pathogenesis during the development of foliar disease.

Materials and Methods

Strains and culture conditions. A wild-type strain of *C. zeae-maydis* (SCOH1-5) was isolated from symptomatic maize plants collected in Scott County, Ohio in 1995. SCOH1-5 GFP reporter strain SCOH1-5-GFP3 was generated in Chapter Two. The *CRP1* deletion strain Δ*wc-40* was generated in a previous study (Kim et al., 2011b). *C. zeae-maydis* strains Δ*frq*-5, Δ*frq*-6, Δ*frq*-33, and reporter strains expressing GFP (Δ*frq*-5gfp1, Δ*frq*-6gfp1, and Δ*frq*-33gfp1) were created for this study and are described in greater detail below. All strains were maintained on V8 agar medium, incubated at room temperature in the dark, and sub-cultured on fresh media every four days to promote conidiation. Conidia were harvested with sterile water and quantified with a hemocytometer for the inoculation studies.

Nucleic acid manipulations and fungal transformation. Plasmid gGFP was obtained from the Fungal Genetics Stock Center (Kansas City, MO; McClusky et al., 2003). Plasmid pBYR48 containing the *GFP* gene driven by the *trpC* promoter and geneticin resistance gene, GEN^R, driven by the *gpdA* promoter was acquired from the Bluhm lab plasmid stocks. pBYR48 was transformed into protoplasts of the appropriate mutant strain as previously described (Shim and Dunkle, 2003). Plasmid pTA-HYG containing the hygromycin resistance gene, HYG^R, driven by the *trpC* promoter was acquired from the Bluhm lab plasmid stocks. Transformants expressing GFP in the presence of geneticin selection were identified with the DFP-1 Dual Fluorescent Protein Flashlight (NightSea, Bedford Md) and subsequently cultured on V-8 medium amended with 400 μg/ml geneticin. Genomic analysis was performed utilizing the

genomic sequence of the wild-type strain SCOH1-5 available at <genome.jgi.doe.gov/Cerzm1/Cerzm1.home.html>

Disruption of *FRQ* in *C. zeae-maydis.* A disruption cassette was constructed via split-marker PCR (Table 3.1; Fu et al., 2006; Ridenour et al., 2012). DNA fragments corresponding to 5' upstream (762 bp) and 3' downstream (973 bp) regions flanking *FRQ* were amplified from *C. zeae-maydis* with primer sets CZM FRQ F1/CZM FRQ F2, and CZM FRQ F3/CZM FRQ F4; respectively. To create the split selectable marker, 1 kb portions of the 1.4 kb hygromycin B phosphotransferase (HYG^R) gene cassette were amplified from pTA-HYG with primers M13F/HY1 and M13F/YG1. Two fusion products combining the 5' flank to HY, and the 3' flank to YG, were created with primers CZM FRQ F1n/HY2 and CZM FRQ F4n/YG2. Protoplasts of *C. zeae-maydis* strain SCOH1-5 were transformed according to Kim et al. (2011b). After seven days, transformants were subcultured on V8 medium containing 150 µg/mL hygromycin and sub-cultured every four days to increase colony size. DNA was extracted following standard protocols (Doyle and Doyle, 1992) and transformants were screened by PCR with primers CZM FRQ A1/ HYG SCRN B and CZM FRQ A1/ CZM FRQ F2. Four of the isolates that tested positive for a targeted disruption were subjected to a more comprehensive PCR screen with primers CZM FRQ A1/ CZM FRQ F2, CZM FRQ A1/HYG SCRN B, CZM FRQ A2/CZM FRQ F3, and CZM FRQ A2/HYG SCRN C to identify strains disrupted in *FRQ*. Three isolates that tested positive for disruption of *FRQ* by PCR were designated Δ*frq*-5, Δ*frq*-6, Δ*frq*-33.

Evaluation of the infection process. The maize cultivar Silver Queen was inoculated when plants were approximately three weeks old. Plants were inoculated with 10 ml of a conidium suspension (10^5 conidia/ml) with 0.01% Triton X-100 utilizing an atomizer attached to

an air compressor. Mock-inoculated control plants were sprayed with a 0.01% Triton X-100 solution containing no conidia. Plants were then placed individually in incubation chambers made of wire mesh wrapped in opaque plastic to maintain free moisture on plants and increase humidity, and placed in a large growth chamber. The growth chamber was maintained at 23°C with a 14:10 light:dark photoperiod with a light intensity at leaf level of 300 μmol m^{-2} s^{-1}. Five separate infection assays were performed to evaluate the phenotype of the wild-type GFP-reporter strain and the GFP-reporter *FRQ*-deletion strains (Δ*frq*-5gfp1, Δ*frq*-6gfp1, and Δ*frq*-33gfp1) during growth on the leaf surface. For each inoculation, three plants for each strain and mock solution were inoculated and incubated as outlined above. Small leaf sections (1.5 cm × 4.0 cm) were excised from each plant and hyphal branching and appressorium formation were recorded five days following inoculation as performed previously (Chapter Two). The level of humidity appeared to affect conidial germination following inoculation, so trial inoculations established the correct incubation parameters that increased humidity to a sufficiently high level for uniform conidia germination. For example, placing a clear plastic bag over the inoculated plants did not yield consistent results, in part because the leaves would frequently touch the side of the bag and become waterlogged. In order to create a large humid area and reduce the likelihood of leaves becoming waterlogged, an 18 cubic foot chamber was constructed with Plexiglas sheets and placed in the greenhouse. Inoculated plants were placed in the chamber and the chamber was sealed for five days to increase humidity. Despite multiple incubation attempts over several months, the Plexiglas chamber did not yield any successful inoculations. The incubation condition that yielded the most consistent results was a wire cage wrapped in clear plastic. The wire cage chambers facilitated a large covered area for multiple inoculated plants, and provided a humid environment conducive for conidia germination and disease development.

After conditions were optimized, a final experiment was performed utilizing the inoculation parameters stated above (three plants x four strains and negative control, 15 plants total) and data from that experiment are presented herein.

Histological observation of hyphae on the leaf surface. Infected leaves were collected five days after inoculation to observe fungal growth and development on the leaf surface. Leaves were examined with a Nikon Eclipse 90i for routine observations and measurements, and a Nikon Eclipse 90i C1 confocal microscope for confocal imagery. Hyphal characteristics were measured with the digital image analysis program ImageJ as performed previously (Chapter Two). Briefly, digital images of hyphae from each strain exhibiting tropic growth toward distant stomata were collected and analyzed with ImageJ < http://imagej.nih.gov/ij/>. Appressorium formation was quantified by identifying 50 hypha/stomate interactions and observing the percent of events that resulted in the formation of appressoria on host stomata.. Statistical analysis of 50 measurements per strain were performed with the software program SPSS. Confocal images were edited for color and clarity in either Adobe Photoshop or NIS Elements.

Quantitative PCR. Total RNA was extracted with Trizol reagent (Invitrogen) and treated with DNase (Promega Corp.) following manufacturer recommendations. For analysis of gene expression, cDNA was generated with random primers by GoScript Reverse Transcription System (Promega Corp.). Expression of *FRQ* (forward primer Frq_rt_F4, reverse primer Frq_rt_R3) and the endogenous control *Beta-actin* (forward B-actin_rt_F1, reverse primer B-actin_rt_R1) was measured by quantitative PCR. Reactions were performed in an MXP-3000 real-time PCR system (Stratagene), and the reactions were performed as described previously (Bluhm and Dunkle, 2008). Expression of *FRQ* was normalized to *Beta-actin* expression and

calculated as fold differences in expression relative to expression in the wild type under the same light exposure. The calculation was based on the $2^{-\Delta\Delta Ct}$ method.

Results

The genome of *C. zeae-maydis* contains a putative ortholog of the fungal circadian oscillator gene *FRQ*. Observations that *CRP1* is involved in light-mediated signal transduction and pathogenesis in *C. zeae-maydis* led to the identification of potential downstream regulatory components (Kim et al., 2011b). Analysis of the *C. zeae-maydis* genome identified gene 111252 (designated *FRQ*), a putative ortholog of *frequency* of *N. crassa*. Based on the annotated genomic information available from the Joint Genome Institute, conceptual translations of *FRQ* indicated that the gene contained an open reading frame (ORF) of 3,109 bp. Additionally, annotation of *FRQ* indicated that the *FRQ* ORF contained one intron (97 bp) starting 2807 bp from the start site of the ORF (Fig. 3.1 A). Conceptual translation of *FRQ* also revealed a predicted protein of 944 amino acid residues (Fig. 3.1 B). Global comparison of the amino acid residues of *FRQ* and *frequency* of *N. crassa* indicated the two proteins shared 76% similarity and 29% identity. *FRQ* was predicted to contain a coiled coil domain from amino acids 170-203, and a large Frequency domain from amino acids 13-944 (Cheng et al., 2001a,b; Baker et al., 2009). The high e-value of the Frequency domain comparison (5.10e-118), combined with amino acid similarity between *frequency* of *N. crassa* and *FRQ* of *C. zeae-maydis* indicated that *FRQ* was a homolog of the central circadian oscillator gene and a valid target for functional characterization.

***C. zeae-maydis* displays rhythmic fluctuations of gene expression.** In *N. crassa*, circadian regulation of gene expression has been confirmed with race tube assays and transcriptional profiling (Baker et al., 2011). However, *C. zeae-maydis* grows much more slowly than *N. crassa* in culture, and thus circadian regulation of gene expression was investigated at the

transcriptional level. To this end, transcription of *FRQ* in *C. zeae-maydis* was investigated over a 48-hour time period. Similarly to the *FRQ* homolog in *N. crassa, FRQ* in *C. zeae-maydis* displayed the hallmark characteristics of circadian expression based on qPCR analysis (Fig 3.2 A). *FRQ* transcripts were most abundant at subjective dawn (12-16 hai), and exhibited a periodicity of approximately 24 hours in free-running conditions (Fig 3.2 A). Patterns of *FRQ* expression *in C. zeae-maydis* were consistent with circadian expression of *FRQ* in *N. crassa* (Baker et al., 2011).

To determine if *FRQ* transcription in *C. zeae-maydis* was regulated by the WCC, a similar time-course experiment was performed to determine the transcriptional expression of *FRQ* in the *CRP1* deletion strain. Consistent with the hypothesis that *N. crassa* and *C. zeae-maydis* both utilize the WCC to regulate *FRQ* expression, *FRQ* transcripts did not exhibit oscillations in the *CRP1* deletion background over a 24-hour time course (Fig 3.2 B). Taken together, the two experiments show that *C. zeae-maydis* contains a *FRQ* ortholog that is regulated by an ortholog of the WCC in *N. crassa*.

***FRQ* is required for appressorium formation.** To further dissect the role of a potential circadian clock component in pathogenesis, *FRQ* was deleted in the *C. zeae-maydis* wild-type strain by homologous recombination (Fig. 3.3 A). Gene-deletion strains were recovered from colonies originating from single conidia, verified by PCR, and transformed with GFP for histological analysis (Fig. 3.3 B). Three independent gene-deletion mutants of *FRQ* were created (Δ*frq*-5*,* Δ*frq*-6*,* Δ*frq*-33) that were morphologically indistinguishable from the wild-type strain in culture media (Fig. 3.3 C). To elucidate the role of *FRQ* in appressorium formation, the efficiency of appressorium formation was measured during hyphal/stomatal interactions following inoculation. During pre-penetration infectious growth, the wild-type strain formed

appressoria on 78% ± 2% of the stomata that were physically encountered by hyphae (Fig. 3.4 A, B). However, the *FRQ* deletion strains formed appressoria at a greatly reduced frequency (<4%; Fig 3.4 A, B). These findings indicated that *FRQ* of *C. zeae-maydis* is required for wild-type levels of appressorium formation during infection of maize, which is a known requirement for leaf penetration and subsequent tissue colonization.

Discussion

Light responsiveness and circadian regulation of gene expression in fungi has been studied extensively, but the regulatory function of fungal clock components during pathogenesis is poorly understood. This study documents the first molecular confirmation that fungi utilize circadian rhythm-associated genes to regulate early infection processes. Fungal biologists have long observed the rhythmic banding of cultures during growth in laboratory medium in association with daily changes in light and dark cycles, and early investigations into light-responsiveness established fungi like *Phycomyces*, (a zygomycete) and *Coprinus* species (basidiomycetes) as model systems of photo-biology (Kues, 2000; Cerda-Olmedo, 2001). The discovery and eventual characterization of the *N. crassa frequency*-mediated circadian clock led to the establishment of the field of fungal chronobiology, which delved deeper into light responses and elucidated intricate genetic mechanisms through which fungi tell time and interact with their environment (Jinhu and Yi, 2010). Despite the advancements achieved in *N. crassa*, the different lifestyles and ecological niches of plant pathogenic fungi compared to non-pathogenic saprotrophs has recently led to emerging hypotheses regarding how pathogens interact with daily changes in host condition and environment (Bluhm et al., 2010; Kim et al., 2011a,b). While no prior research has elucidated the circadian regulation of pathogenesis during plant/fungal interactions, the cumulative data of this investigation provides compelling evidence

that *C. zeae-maydis* anticipates diurnal changes in light in order to facilitate host penetration and the eventual development of disease.

Based on the conservation of core clock components and other regulatory genes involved in clock-mediated gene expression in many fungi, *FRQ* likely regulates pathogenesis-related genes in a circadian manner similar to what is observed in *N. crassa* (Salichos and Rokas, 2010). In *C. zeae-maydis*, *FRQ* transcripts exhibited expression oscillations comparable to the period and relative *FRQ* mRNA levels observed in *N. crassa* during similar clock assays (Baker et al., 2011), which established the presence of a functional circadian clock. However, due to the inherently slow radial growth of *C. zeae-maydis in vitro* (~1 cm every 14 days) and the requirement for culture incubation in darkness to induce conidiation, direct physiological comparisons between circadian regulation of conidia production and pigment biosynthesis in the two systems was not feasible. The molecular machinery required for circadian rhythmicity is conserved in several classes of fungi (Salichos and Rokas, 2010), and *C. zeae-maydis* contains presumed homologs of most core and peripheral clock components required for the maintenance of clock function in *N. crassa* (Chapter Five; Baker et al., 2011). However, recent evidence suggests that while many fungi possess similar clock components, individual species exhibit variability in the regulation of clock oscillations (Dunlap and Loros, 2006; Salichos and Rokas, 2010, Baker et al., 2011). One intriguing piece of evidence supporting alternate regulation of circadian oscillations by *C. zeae-maydis* compared to *N. crassa* is the apparent absence of a homolog to the *vivid* gene, which is required for the maintenance of clock periodicity and photo-entrainment in *N. crassa* and also present in many other fungi (Hall et al., 1993; Heintzen et al., 2001; Lombardi and Brody, 2005, genome.jgi.doe.gov/Cerzm1/Cerzm1.home.html). The possibility also exists that the circadian clock functions are fundamentally different in *C. zeae-*

maydis compared to *N. crassa*. This novel hypothesis deviates from the current understanding of *FRQ*-mediated circadian regulation of gene expression in filamentous fungi, but represents an intriguing avenue for future research as the knowledge of fungal biological clocks matures to encompass broader definitions of diverse regulatory mechanisms.

The identification of a biological clock in *C. zeae-maydis* provides a molecular foothold to further dissect the regulation of important morphological transitions that occur during pathogenesis. The genetic regulation of stomatal tropism and appressorium formation is poorly understood in *C. zeae-maydis*, but this study uncovered potential mechanisms that could uncouple the two related, but potentially distinct, physiological processes. An important finding of this research was that the *FRQ* deletion strains rarely formed appressoria following multiple inoculations. One hypothesis explaining this apparent discrepancy is that stomatal tropism and appressorium formation are regulated by separate sensory mechanisms that function synergistically to produce appressoria during growth on host tissue. With this model, a receptor on the exterior of the hyphal membrane that relies on a functioning WCC transcription factor senses the stomatal attractant, and transduces that signal to initiate a new hyphal branch or reorient apical polarity in the direction of the attractant. Upon reaching stomata, uncharacterized genes regulated by *FRQ* elicit appressorium formation. Since *CRP1* likely regulates *FRQ* transcription in a manner similar to *N. crassa*, neither stomatal tropism nor appressorium formation occurs in the *CRP1* deletion mutant strain, while the *FRQ*-deletion strains likely maintain the ability to sense stomata due to a functional WCC acting upon a separate regulatory system. This model depends on circadian regulated genes interacting with an unknown stomatal signal separate from the cue that elicits stomatal tropism, so a thorough identification of the

genes regulated by *FRQ* would provide putative targets for functional characterization and an opportunity to elucidate the intricacies of appressorium formation apart from stomatal tropism.

At the molecular level, plants and plant pathogens undergo complex interactions culminating in either plant resistance or the establishment of disease, especially during the transitions between night and day. Recent investigations into the circadian regulation of plant innate- and R-gene mediated immunity against microbial pathogens have added greatly to the discussion regarding how plants defend against pathogens during the process of infection. Under free-running circadian conditions, Arabidopsis exhibits periodic fluctuations in susceptibility to *Pseudomonas syringae* infection that are disrupted by altering the circadian clock (Bhardwaj et al., 2011). In Arabidopsis, circadian expression of the core clock genes CCA1 and LHY are required for resistance to the bacterium *P. syringae* and the oomycete *Hyaloperonospora arabidopsidis* (Zhang et al., 2013). Innate-defense genes that elicit stomatal closure in response to natural changes in light availability and pathogen pressure interact synergistically with resistance-genes to reduce infection by both bacterial and oomycete pathogens following ectopic inoculation with *P. syringae* and *H. arabidopsis* and leaf infiltration with *P. syringae* (Wang et al., 2011; Zhang et al., 2013). The specific interaction between *C. zeae-maydis* and maize stomata during infection presents an intriguing interplay between the pathogen and host. Hyphae of *C. zeae-maydis* exhibit stomatal tropism toward distant host stomata, and grow toward an increasing concentration of molecular oxygen has been hypothesized to be involved in the maintenance of stomatal tropism (Chapter Two). Circadian regulation of stomatal tropism may have evolved in response to changes in stomatal aperture and the dynamic release of stomatal exudates throughout the day. Under normal environmental circumstances, maize stomata reach maximum aperture early in the morning and close slowly throughout the day (reviewed by

Mansfield et al., 1990). Based on this model, maize stomata attain their greatest aperture in the morning, and presumably exude more volatile chemicals that may act as chemoattractants to distant hyphae. *C. zeae-maydis* "anticipates" the recurring patterns of increased stomatal aperture that are conducive for stomatal sensing and pathogenic development via circadian-regulated changes in gene expression, and transcribes pathogenesis-related genes in the morning corresponding to the decreased innate immunity of the host. This hypothesis is difficult to test, in part because any changes in light regimes following inoculation would affect both the fungus and the plant, thus altering normal diurnal changes in stomatal physiology and plant defense gene expression. An alternative to manipulating light throughout the experiment is to identify different maize lines with defects in stomatal physiology, such as lines with altered fluctuations of stomatal aperture or lines containing deficiencies in volatile organic stomatal emissions, and observe pre-infectious fungal development following inoculation.

Additional questions remain regarding why *C. zeae-maydis* may have evolved a circadian regulatory system to anticipate diurnal changes in sunlight and what additional components of pathogenesis are regulated in a *FRQ*-dependent manner. Similar to many fungi, *C. zeae-maydis* exhibits a period of symptomless colonization of the host leaf prior to the formation of lesions called hemibiotrophy (Münch et al., 2008; Kim et al., 2011a). The mechanisms through which fungi regulate the transition from biotrophic colonization to necrotrophic growth and host tissue degradation is an intriguing aspect of fungal biology that remains poorly understood. Given the evidence that plants exhibit circadian oscillations of defense genes (McClung, 2001, 2006; Wang et al., 2011; Zhang et al., 2013), it is plausible that *C. zeae-maydis* and other pathogens have evolved finely tuned virulence mechanisms that react in active opposition to daily changes in plant susceptibility to increase the likelihood of successful establishment within the host. To this

end, a hemibiotrophic lifestyle would allow the fungal pathogen to thoroughly colonize host tissue while evading host detection, and in response to a developmental trigger during a period of increased host susceptibility, overwhelm plant defense mechanisms resulting in rapid necrosis and the biogenesis of conidia to infect additional plants. While the slow growth of *C. zeae-maydis* excludes the measurement of conidial banding patterns in laboratory medium, the scalariform conidial bands visible in gray leaf spot lesions *in planta* is similar to the rhythmic patterns of circadian conidial development observed in *N. crassa* during growth in race tubes (Baker et al., 2011). Circadian patterns of conidial banding were recently shown in the soybean pathogen *Cercospora kikuchii*, a close relative of *C. zeae-maydis*, which supports the hypothesis that temporal oscillations in conidiation are regulated by circadian rhythms across diverse classes of fungi and are important for the development of inoculum preceding plant disease epidemics (Bluhm et al., 2010; Greene et al., 2003). This hypothesis is difficult to test due to the absence of a dependable conidia infiltration technique that bypasses the inability of the *FRQ* deletion strains to form appressoria and penetrate host tissue. However, future identification of clock-controlled genes in *C. zeae-maydis* can be compared with established EST libraries identifying genes upregulated during growth in conditions conducive for conidiation (Bluhm et al., 2008), which will identify potential targets for future investigations.

The role of light and fungal pathogenesis has been discussed for more than 100 years, and this study uncovered a novel and important mechanism through which light regulates host/pathogen interactions. The observation of a functional circadian-related regulatory gene in a plant pathogen and the establishment that a core clock component is required for appressorium formation represents the first report of a fungus utilizing potential circadian rhythms to mediate pathogenesis. The evidence that plant pathogenic fungi have evolved mechanisms to sense and

anticipate both diurnal environmental changes and daily fluctuations in host susceptibility has established new molecular and biological footholds through which to elucidate the complex interactions between hosts, pathogens and their environment.

References

Alabadi, D, Yanovsky, M. J., Mas, P, Harmer, S. L., Kay, S. A. 2002. Critical role for CCA1 and LHY in maintaining circadian rhythmicity in Arabidopsis. *Curr Biol* 12: 757–761.

Baker, C. L., Loros, J. L. Dunlap, J. C. 2011. The circadian clock of *Neurospora crassa. FEMS Microbiol Rev* 36: 95-110.

Baker, C.L., Kettenbach, A.N., Loros, J.J., Gerber, S.A., Dunlap, J.C. 2009. Quantitative proteomics reveals a dymanic interactome and phase-specfiic phosphorylation in the *Neurospora* circadian clock. *Mol Cell* 34:354-363.

Ballario, P., Talora, C., Galli, D., Linden, H., Macino, G. 1998. Roles in dimerization and blue light photo response of the PAS and LOV domains of *Neurospora crassa* white collar proteins. *Mol Microbiol* 29: 719–729.

Bhardwaj V, Meier S, Petersen L. N., Ingle, R.A., and Roden L.C. 2011. Defense responses of *Arabidopsis thaliana* to infection by *Pseudomonas syringae* are regulated by the circadian clock. *PLoS One* 6: e26968.

Bluhm, H. B., Dhillon, B., Lindquist, E. A., Kema, G. H. J., Goodwin, S. B. and Dunkle, L. D. 2008. Analysis of expressed sequence tags from the maize foliar pathogen *Cercospora zeae-maydis* identify novel genes expressed during vegetative, infectious, and reproductive growth. *BMC Gen* 9:523.

Bluhm, B. H., Burnham, A. M. and Dunkle, L. D. 2010. A circadian rhythm regulating hyphal melanization in *Cercospora kikuchii*. *Mycologia* 102:1221-1228.

Cerdá-Olmedo E. 2001. *Phycomyces* and the biology of light. *FEMS Microbiol Reviews* 25: 503–512.

Cheng, P., Yang, Y., Heintzen, C. and Liu, Y. 2001a. Coiled-coil domain-mediated FRQ–FRQ interaction is essential for its circadian clock function in *Neurospora*. *EMBO J* 20: 101–108.

Cheng, P., Yang, Y. and Liu, Y. 2001b. Interlocked feedback loops contribute to the robustness of the *Neurospora* circadian clock. *P Natl Acad Sci USA* 98: 7408–7413.

Cheng, P., Yang, Y., Gardner, K. H. and Liu, Y. 2002. PAS domain mediated WC-1/WC-2 interaction is essential for maintaining the steady-state level of WC-1 and the function of both proteins in circadian clock and light responses of *Neurospora*. *Mol Cell Biol* 22: 517–524.

Correa, A., Lewis, Z.A., Greene, A.V., March, I.J., Gomer, R.H., and Bell-Pedersen, D. 2003. Multiple oscillators regulate circadian gene expression in *Neurospora. Proc. Natl Acad. Sci. USA.* 100:13597-10602.

Crosthwaite, S. K., Dunlap, J. C. and Loros, J. J. 1997. *Neurospora wc-1* and *wc-2*: transcription, photoresponses, and the origins of circadian rhythmicity. *Science* 276:763-769.

Dunlap, J. C., Loros, J. J., and DeCoursey, P. 2004. Chronobiology: Biological Timekeeping. (Sunderland, MA: Sinauer Associates).

Fu, J., Hettler, E., and Wickes, N. L. 2006. Split marker transformation increased homologous integration frequency in *Cryptococcus neoformans*. *Fungal Genet Biol* 43: 100-121.

Gardner, G. F. and Feldman, J. F. 1980. The frq locus in *Neurospora crassa*: a key element in circadian clock organization. *Genetics* 96: 877-886.

Gooch, V. D., Mehra, A., Larrondo, L. F., Fox, J., Touroutoutoudis, M., Loros, J. J. and Dunlap J. C. 2008. Fully codon-optimized luciferase uncovers novel temperature characteristics of the *Neurospora* clock. *Eukaryot Cell* 7: 28–37.

Greene, A.V., Keller, N., Haas, H., and Bell-Pedersen, D. 2003. A circadian oscillator in *Aspergillus* spp. regulates daily development and gene expression. *Eukary Cell* 2:231-237.

Hall, M.D., Bennett, S.N. and Krissinger, W.A. Characterization of a newly isolated pigmentation mutant of *Neurospora crassa*. *Georgia J. Sci*. 51, 27 (1993)

Heintzen, C., Loros, J. J. and Dunlap, J. C. 2001. The PAS protein VIVID defines a clock-associated feedback loop that represses light input, modulates gating, and regulates clock resetting. *Cell*. 104:453-464.

Idnurm, A., Heitman, J. 2005. Light controls growth and development via a conserved pathway in the fungal kingdom. *PLoS Biol* 3: e395. doi:10.1371/journal.pbio.0030095.

Jinhu, G. and Yi, L. 2010. Molecular mechanism of the *Neurospora* circadian oscillator. *Protein Cell* 1: 331–341.

Kim, H., Ridenour, J. B., Dunkle, L. D. and Bluhm, B. H. 2011a. Regulation of pathogenesis by light in *Cercospora zeae-maydis*: An updated perspective. *Plant Pathol J* 27:103-109.

Kim, H., Ridenour, J. B., Dunkle, L. D. and Bluhm, B. H. 2011b. Regulation of stomatal tropism and infection by light in *Cercospora zeae-maydis*: Evidence for coordinated host/pathogen responses to photoperiod? *PLoS Pathog* 7(7): e1002113.

Konopka, R. J. and Benzer, S. 1971. Clock mutants of *Drosophila melanogaster*. *Proc. Natl Acad. Sci. USA* 68: 2112-2116.

Kües, U. 2000. Life history and development processes in the basidiomycete *Coprinus cinereus*. *Microbiol Mol Biol Rev* 64: 316–353.

Linden, H. and Macino, G. 1997. White collar 2, a partner in bluelight signal transduction,

controlling expression of light regulated genes in *Neurospora crassa*. *EMBO J* 16: 98–109.

Liu, O.W., Chun, C.D., Chow, E.D., Chen, C., Madhani, H.D. et al. 2008. Systematic genetic analysis of virulence in the human fungal pathogen *Cryptococcus neoformans*. *Cell* 135: 174–188.

Lombardi, L.M., and Brody, S. 2005. Circadian rhythms in *Neurospora crassa*: clock gene homologues in fungi. *Fungal Genet Biol*. 42:887-892.

Loudon, A. S. I., Semikhodskii, A. G., Crosthwaite, S. K. 2000. A brief history of circadian time. *Trend. Gen*. 16: 477-481.

Lu, S. X., Knowles, S. M., Andronis, C., Ong, M. S., Tobin E. M. 2009. CIRCADIAN CLOCK ASSOCIATED1 and LATE ELONGATED HYPOCOTYL function synergistically in the circadian clock of Arabidopsis. *Plant Physiol* 150: 834–843.

Luo, C., Loros, J.J. and Dunlap J.C. 1998. Nuclear localization is required for function of the essential clock protein FRQ. *EMBO J* 17: 1228–1235.

Mansfield, T.A., Hetherington, A.M., and Atkinson, C.J. 1990. Some current aspects of stomatal physiology. *Annu Rev Plant Physiol Plant Mol Biol* 41:55-75.

McCluskey, K. 2003. The fungal genetics stock center: from molds to molecules. *Adv Appl Microbiol* 52:245-262.

McClung C.R. 2001. Circadian rhythms in plants. *Annu Rev Plant Physiol Plant Mol Biol* 52:139-162.

McClung, C.R. 2006. Plant Circadian Rhythms. *Plant Cell* 18:792-803.

Mizoguchi T, Wheatley K, Hanzawa Y, Wright L, Mizoguchi M, et al. (2002) LHY and CCA1 are partially redundant genes required to maintain circadian rhythms in Arabidopsis. *Dev Cell* 2: 629–641.

Münch, S., Lingner, U., Floss, D. S., Ludwig, N., Sauer, N., Deising, H.B. 2008. The hemibiotrophic lifestyle of *Colletotrichum* species. *J Plant Phys* 165:41-51.

de Paula, R.M., Lewis, Z.A., Greene, A.V., Seo, K.S., Morgan, L.W., Vitalini, M.W., Bennett, L., Gomer, R.H. and Bell-Pedersen, D. 2006. Two circadian timing circuits in *Neurospora crassa* cells share components and regulate distinct rhythmic processes. *J Biol Rhythm*. 21:159-168.

Roenneberg, T., Kantermann, T., Juda, M., Vetter, C., Allebrandt, KV. 2013. Light and the human circadian clock. *Circadian Clocks. Handbook of Experimental Pharmacology*. 217:311-331.

Ridenour, J.B., Hirsch, R.L. and Bluhm B.H. 2012. Identifying genes in *Fusarium verticillioides* through forward and reverse genetics. *Methods Mol Biol* 835: 457-479.

Ruiz-Roldan, M.C., Garre, V., Guarro, J., Marine, M. and Roncero, M.I.G. 2008. Role of the white collar 1 photoreceptor in carotenogenesis, UV resistance, hydrophobicity, and virulence of *Fusarium oxysporum*. *Eukaryot Cell* 7: 1227–1230.

Salichos, L. and Rokas, A. 2010. The diversity and evolution of circadian clock proteins in fungi. *Mycologia* 102:269-278.

Shim, W-B. and Dunkle, L.D. 2003. *CZK3*, a MAP kinase kinase kinase homolog in *Cercospora zeae-maydis*, regulates cercosporin biosynthesis, fungal development, and pathogenesis. *Mol Plant-Microbe Interact* 16:760-768.

Smith, K.M., Sancar, G., Dekang, R., Sullivan, C.M., Li, S., Tag, A.G. et al. 2010. Transcription factors in light and circadian clock signaling networks revealed by genomewide mapping of direct targets for Neurospora White Collar Complex. *Eukary Cell*:10:1549-1556.

Tseng, Y-Y., Hunt, S.M., Heintzen, C., Crosthwaite, S.K. and Schwartz, J-M. 2012. Comprehensive modeling of the *Neurospora* circadian clock and its temperature compensation. *PLoS Comput Biol* 8(3): e1002437

Wang, W., Barnaby, J.Y., Tada, Y., Li, H., Tor, M., et al. 2011. Timing of plant immune responses by a central circadian regulator. *Nature* 470: 110-114.

Young, M.W. and Kay, S.A. 2001. Time zones: a comparative genetics of circadian clocks. *Nat Rev Genet*. 2:702-715.

Zhang, C., Xie, Q., Anderson, R.G., Ng, G., Seitz, N.C., et al. 2013. Crosstalk between the circadian clock and innate immunity in Arabidopsis. *PLoS Pathog* 9(6): e1003370. doi:10.1371/journal.ppat.1003370

Figures

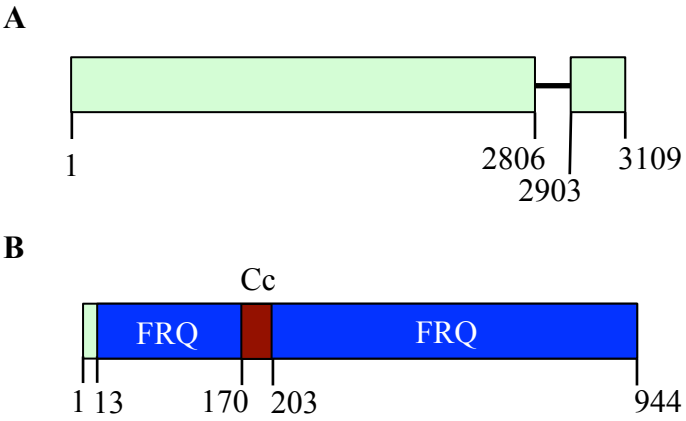

Figure 3.1. Identification and characterization of the *FRQ* gene and predicted protein. A) The *FRQ* gene *in C. zeae-maydis* is 3109 nucleotides in length with a single 97 bp intron near the 3' flank. B) Analysis of the predicted protein shows a protein containing 944 amino acids with a coil-coiled (Cc) domain between amino acids 170 and 203, and a large Frequency clock domain (FRQ) from amino acids 13 to 944.

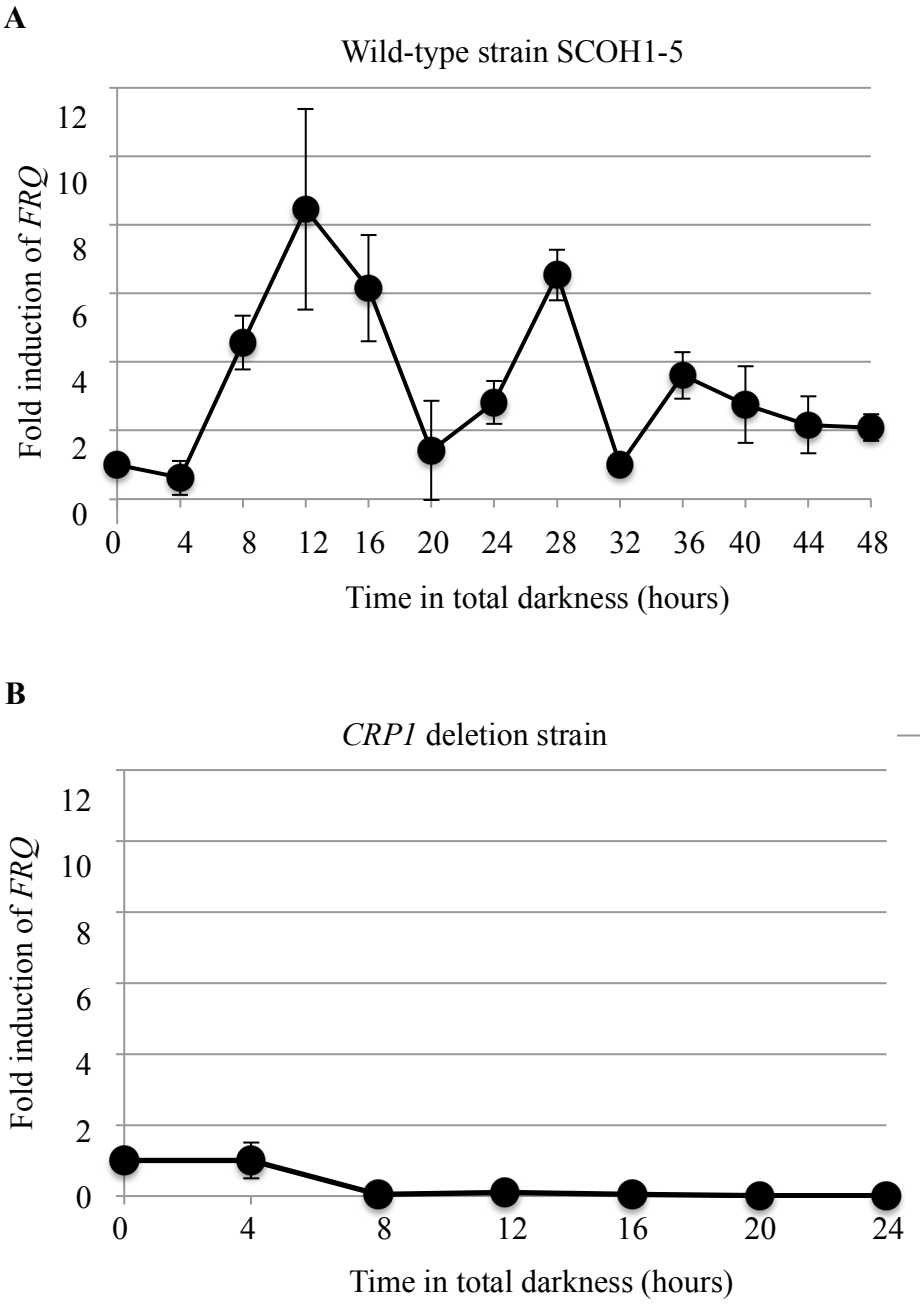

Figure 3.2. Transcriptional analysis of the expression levels of *FRQ* by quantitative PCR. Conidia of the wild-type strain SCOH1-5 or the *CRP1*-deletion strain were inoculated on V8 medium and incubated in continuous light for two days to uniformly repress the transcription of *FRQ*. Following incubation, cultures were quickly moved to and maintained in total darkness and sampled every four hours. A) *FRQ* transcripts in the wild-type strain under free-running clock conditions were expressed in a circadian fashion up to 48 hours following incubation in total darkness. B) *FRQ* transcripts were not detectable in the *CRP1* deletion strain during free-running clock conditions over 24 hours, suggesting that *CRP1* regulates *FRQ* expression in a manner similar to the homologous circadian regulatory mechanism in *N. crassa*. Data points

represent *FRQ* expression levels relative to the housekeeping gene Beta-actin, and the bars represent the range of expression. Expression values were calculated with the $2^{-\Delta\Delta Ct}$ method.

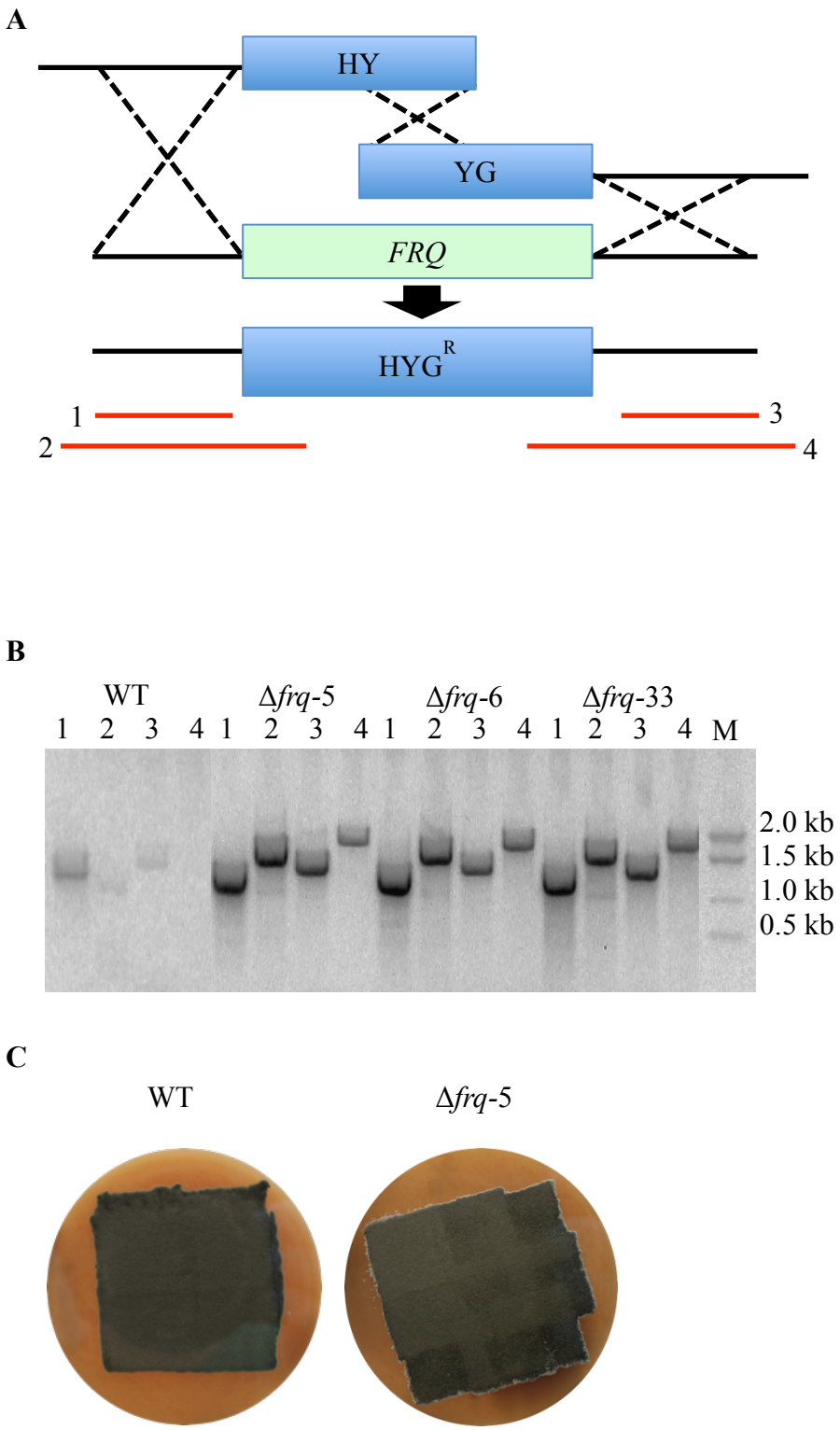

Figure 3.3. Gene deletion strategy for the *FRQ* locus. A) A hygromycin resistance gene split-marker triple homologous recombination approach was utilized for this study. Amplicons 1 and 3 represent positive controls, while amplicons 2 and 4 are expected in the presence of the hygromycin resistance gene integrated into the correct genomic locus. B) Three independent deletion strains of the *FRQ* gene Δ*frq*-5, Δ*frq*-6, Δ*frq*-33, contain amplicons consistent with a

successful gene replacement attempt. C) The wild-type and Δ*frq-5* strains on V8 medium after incubation for four days in the dark. Strain Δ*frq-5* was selected as a representative mutant strain to illustrate the phenotypic similarity between the different strains during growth in culture.

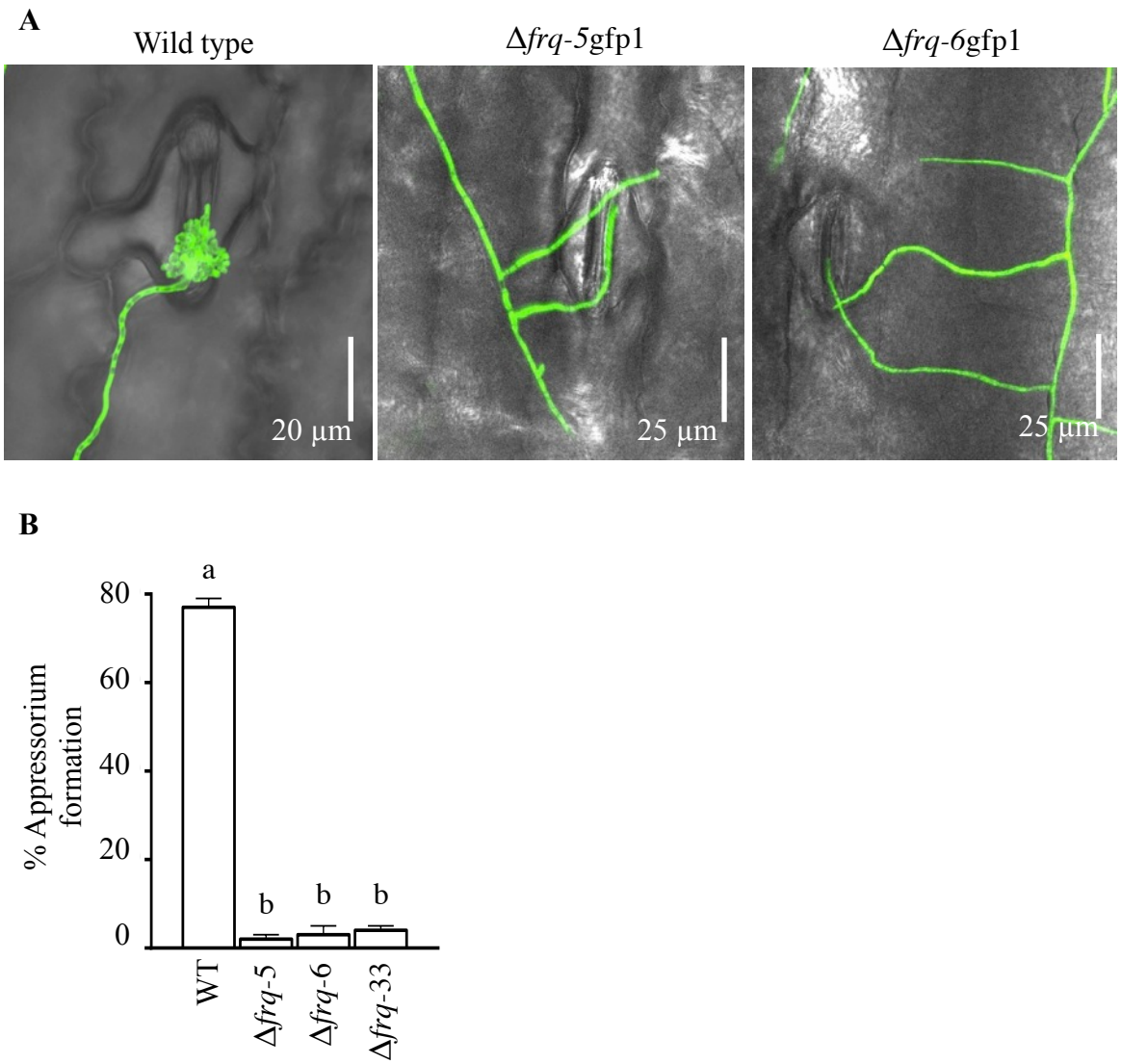

Figure 3.4. *FRQ* is required for wild type levels of appressorium formation. A) Following tropic growth toward host stomata, the wild-type strain readily formed appressoria, while the Δ*frq*-5, Δ*frq*-6, Δ*frq*-33 strains rarely formed appressoria. B) Percent appressorium formation measurements were conducted by counting how many appressoria were formed after 50 hyphal/stomatal interactions, with bars representing standard error. Statistical comparisons of means were performed with a Tukey's Honestly Significant Difference analysis ($\alpha = 0.05$; letters denote statistical significance).

Tables

Table 3.1 Primers utilized in this study

Name	Sequence
CZM FRQ A1	GCAGGGCATCGAACGG
CZM FRQ F1	ATCGTCGATGGCTCACAC
CZM FRQ F1n	GCTCCCGTCTGATGCTG
CZM FRQ F2	ATTACAATTCACTGGCCGTCGTTTTACATGGGCGGCATTGCTG
CZM FRQ F3	CGTAATCATGGTCATAGCTGTTTCCTGGACGAGATGGGAGATGGCTA
CZM FRQ F4n	TCGCCAGCGTTTCGTC
CZM FRQ F4	TGCTGCTCTCGGTGCT
CZM FRQ A2	GGACTTACCGACTCATTCTTGG
M13spmrkF	GTAAAACGACGGCCAGTGAATTGTAA
M13spmrkR	CAGGAAACAGCTATGACCATGATTAC

CHAPTER IV: DEFINING THE TRANSCRIPTOME OF *CERCOSPORA ZEAE-MAYDIS* DURING PRE-PENETRATION INFECTIOUS DEVELOPMENT

Summary

Cercospora zeae-maydis is a ubiquitous foliar pathogen of maize, significantly increasing management costs and reducing annual maize yields. Despite the importance of *C. zeae-maydis* to global agriculture, little is known regarding the genetic regulation of pathogenesis. To investigate and identify the transcriptome underlying pathogenesis, RNA from tissue samples representing pre-penetration infectious growth and growth in axenic culture was extracted and sequenced with Illumina HiSeq. Sequence analysis identified 3283 genes that were differentially expressed during growth on a maize leaf as compared to axenic culture samples. Analysis of the transcriptome from infectious tissue identified an increase in the expression of genes involved in responses to stress, cell communication, and cellular response to stimuli. To identify specific genes related to infectious growth, 200 genes differentially expressed during infection were selected for individual analysis. The collection included genes encoding carbohydrate and protein degrading enzymes, cell signaling, transcriptional regulation and responses to host defense mechanisms compared to growth in laboratory medium. Furthermore, the analysis identified multiple sensory mechanisms that are putatively involved in sensing the host environment during infection. In summary, this effort represented the first transcriptome-wide investigation of infection in *C. zeae-maydis* and identified several novel targets for future genomic studies.

Introduction

Plant pathogenic fungi display a wide range of infection strategies, which are underscored by the complexities underlying gene transcription during disease initiation. Many fungi have evolved mechanisms to first attach to the host surface and subsequently infect their hosts. For example, conidia of the rice blast fungus *Magnaporthe oryzae* adhere to surfaces and germinate shortly after contact (Gilbert et al., 1996; Flaishman and Kolattukudy, 1994; Lee and Dean, 1993). As conidia germinate, *M. oryzae* displays major transcriptional reprogramming as the developing germ tubes form appressoria in response to surface hydrophobicity (Takano et al., 2003; Gowda et al., 2006; Oh et al., 2008). Identifying the genes involved in critical development steps during pathogenesis in *M. oryzae* and other fungi has highlighted the conservation of important signaling networks like mitogen-activated protein kinases and cyclic AMP (Xu and Hamer, 1996; D'Souza and Heitman, 2001). Also, these studies identified novel, species-specific genes that regulate pathogenesis (Gowda et al., 2006; Oh et al., 2008). In other pathosystems, similar gene expression studies characterized global changes in gene expression by the rust fungus *Uromyces fabae* (Jakupovic et al., 2006) and the cotton vascular wilt pathogen *Fusarium oxysporum* f. sp. *vasinfectum* (McFadden et al., 2006) during host infection. *F. oxysporum* f. sp. *vasinfectum* expressed a putative oxidoreductase gene 500-fold higher during vascular infection of cotton compared to expression vegetative mycelium, and the expression of the oxidoreductase gene correlated with isolate virulence as measured by vascular browning (McFadden et al., 2006). Changes in gene expression associated with infectious growth are major determinants of pathogenesis and are important targets of current research.

Next-generation RNA sequencing has revolutionized the study of transcriptomics by increasing sequencing depth and allowing for the identification of rare transcripts and splice

variants (Wang et al., 2009; Horn et al., 2012). Initially, next-generation sequencing characterized transcriptomes in humans, yeast, and rice, but the technology is now also commonly utilized for filamentous fungi. Recently, transcriptomes were described for *Cordyceps militaris, Trichoderma reesei, Fusarium graminearum, Colletotrichum* spp., *Magnaporthe oryzae* and *Zymoseptoria tritici* (O'Connell et al., 2012, Soanes et al., 2012, Yin et al., 2012; Zhao et al., 2013), unveiling novel mechanisms underlying infection-related metabolic transitions and the transcriptional reprogramming associated with pathogenic development. In *M. oryzae*, genome-wide transcriptional profiling identified genes involved in fungal defense against bacterial antagonists (Mathioni et al., 2012) as well as large-scale gene expression changes during appressorium development, including genes implicated in autophagy, lipid metabolism and melanin production (Soanes et al., 2012). Analysis of plant infection by *Colletotrichum higginsianum* and *Colletotrichum graminicola* indicated that both fungi produce effectors and secondary metabolism enzymes before penetration and during biotrophic growth, and rapidly increase the expression of hydrolases and transporters during the switch to necrotrophy (O'Connell et al., 2012). However, since the infection process of *C. zeae-maydis* differs from previously sequenced fungi in terms of stomatal tropism and appressorium formation, comparisons with established model systems may not be sufficient to address important biological questions. As such, the current study sought to characterize the unique transcriptome of *C. zeae-maydis* during pathogenesis and identify potential targets for molecular characterization.

The transcripts underlying infection by *C. zeae-maydis* were sequenced with the Illumina HiSeq platform and analyzed with CLC Genomics Workbench. Analysis of sequenced transcripts during early stages of the infection process on maize and from axenic culture

identified 3283 genes differentially expressed during fungal growth and development on a host leaf surface. Functional annotations were utilized to investigate the global function of each transcriptome. Furthermore, the 200 highest differentially upregulated genes during infectious growth were selected for additional analysis. The analysis presented in this study enriches the current understanding of pathogenesis in *C. zeae-maydis*, and identifies putative regulatory mechanisms involved in disease development.

Materials and Methods

Strains and culture conditions. The GFP-reporter strain SCOH1-5-GFP3 was generated in a previous study (Chapter Two), and utilized for this study. Strains were maintained on V8 agar medium in the darkness, and sub-cultured on to fresh V8 medium every four days to promote conidiation. For experiments to establish basal gene expression, strains were grown on Complete Medium (CM), 0.2 × Potato Dextrose Agar (0.2 × PDA) or V8 agar medium covered with a layer of cellophane to simplify fungal tissue collection. Cellophane (Fisher Scientific Catalog number 45-001-623)-overlaid media plates were inoculated with 10^5 conidia in one ml of ddH_20 and evenly spread across the surface of each Petri dish with a sterile plastic tool in order to establish a uniform thallus. Conidia for inoculations were harvested by flooding a 4-day old V8 culture with 10 ml sterile ddH_20 and gently agitating the mycelium with a sterile tool to disturb conidia. Conidia concentrations were quantified with a hemocytometer.

Plant inoculation parameters. Maize cultivar Silver Queen was inoculated when plants were approximately three-weeks old. Ten plants were inoculated with 10 ml of conidia suspension of strain SCOH1-5-GFP3 (10^7 conidia/ml) with 0.01% Triton X-100 by an atomizer attached to an air compressor until inoculum runoff. Inoculated plants were covered in small wire cages wrapped in opaque plastic to increase humidity. Covered and inoculated plants were

then incubated in a growth chamber at 23°C with a 12:12 light:dark photoperiod with a light intensity at leaf level of 300 μmol m^{-2} s^{-1}.

Tissue preparation and nucleic acid manipulations. Following incubation for five days, one inoculated leaf was collected from each of the ten inoculated plants. Fungal tissue growing on the surface of maize leaves was collected from heavily inoculated leaves at 4°C by submerging each of the ten leaves in 50mL sterile ddH_2O with 0.01% Triton X-100 and brushed with a stiff-bristled brush to dislodge the fungal mycelium. To create the stiff-bristled brush, the bristles on a two-inch wide paintbrush were cut to a length of one inch. The bristle stiffness was sufficient to dislodge fungal tissue from the leaf surface without destroying the underlying leaf tissue. To verify that the fungal tissue collected from the leaf surface contained infection-related structures, a sample of the tissue was observed on an epifluorescence microscope. Histological observation of dislodged conidia, germinated conidia, hyphae and appressoria confirmed the presence of infection-related tissue in the sample. The collected fungal tissue from all ten inoculated leaves was pelleted by centrifugation, and ground with a mini-pestle in a 1.7 ml microcentrifuge tube in the presence of 0.5 ml Trizol reagent (Invitrogen, Grand Island, NY). For the axenic cultures, tissue was harvested from each medium (CM, V8, and 0.2 × PDA) in triplicate by gently peeling the cellophane layer off the surface of the medium. Prior to RNA extraction, three colonized cellophane overlays from each medium were combined and ground to a fine powder in liquid nitrogen. Low temperature was maintained in liquid nitrogen or at -80°C for storage. RNA was extracted from 0.1 g of fungal tissue with Trizol reagent following manufacturer specifications. RNA samples were treated with RNase-Free DNase (Qiagen) and purified with the RNeasy MinElute Cleanup Kit (Qiagen) following manufacturer specifications.

Transcriptome sequencing and analysis. RNA was shipped on dry ice to the Purdue Genomics Core Facility, West Lafayette, Indiana for sequencing. Samples were sequenced on an Illumina HiSeq 2500 platform and data was accessible via a secure Internet portal. Adapter-trimmed sequence data was analyzed with the CLC Genomics Workbench platform, and genomic data of *C. zeae-maydis* was obtained from DOE-JGI (http://genome.jgi-psf.org/Cerzm1/Cerzm1. home.html). Differential gene expression was determined by transcript count and significant differences were detected by the normalized *p*-value ($p < 0.05$). For the non-infectious tissue condition, transcripts from each medium and incubation condition were combined and analyzed as independent biological replications, and standardized to the infectious tissue sample with the Kal Z and Baggerly statistical tests. Functional annotation by gene ontology (GO) was performed with Blast2GO <http://blast2go.com/b2ghome>. Evaluation of 200 genes with the highest differential expression levels during growth on maize leaves were performed by analyzing the predicted protein sequence and domain homology with NCBI BLAST (Altschul et al., 1990, 1997) and SMART (Schultz et al., 1998; Letunic et al.,2009) searches.

Results

Transcriptomic analysis identified genes differentially regulated during leaf infection. RNA representing genes expressed during pre-penetration growth on the maize leaf surface during the initial stages of infection or growth in defined media (non-infectious growth) were sequenced with Illumina HiSeq. The sequenced transcripts were analyzed for differential expression to identify transcriptional reprogramming associated with pathogenesis. After quality filtering by the bioinformatics program CLC Genomics Workbench, 349,359 and 5,337,843 reads were obtained from tissue harvested from the leaf surface and growth in culture;

respectively (Table 4.1). Approximately 6.76% of reads from infective tissue could be mapped to the *C. zeae-maydis* genome and 6.59% mapped to the gene, while 70.48% of reads from the non-infectious samples to the genome and 70.47% to a gene. Almost all reads were mapped to unique positions in the genome except a small percentage (0.01% for infectious samples and 0.17% for the non-infectious samples) that mapped to multiple loci (Table 4.1). The CLC Workbench analysis software predicted that a sufficient amount of transcriptomic data was obtained for the identification of differentially expressed genes.

A collection of 6817 differentially expressed genes was identified after analytical comparisons ($p = <0.05$) between infectious and non-infectious samples (Fig 4.1). However, many of the identified genes exhibited minor expression changes (less than two-fold expression difference) between the conditions. In order to identify genes with large changes in gene expression, a two-fold expression filter was applied to the transcriptome, resulting in a collection of 3283 differentially expressed genes. Between samples representing infectious tissue on the leaf surface and growth in culture, 2170 genes were upregulated during infectious development on the leaf, while 1113 genes were upregulated in culture compared to growth on the leaf surface prior to infection.

Transcriptome-wide analysis highlights broad changes in gene expression based on metabolic status. In order to characterize global changes in gene expression that occur during pathogenesis and growth in culture, the two collections of differentially expressed genes were analyzed with Blast2GO. The Blast2GO software assigned predicted functions based on conserved sequence homology to known and characterized proteins. Consistent with the limited nutrient availability on a leaf surface and exposure to environmental stresses, the transcriptome from infectious tissue contained more genes related to stress response (3%) than the

transcriptome from non-infectious tissue (0%), yet revealed a decrease in genes involved in primary (18%) and cellular (14%) metabolic processes (Fig 4.2 A). Perhaps most significant was the observation that the transcriptome from infectious tissue contained genes involved in the cellular response to stimuli (4%) while the transcriptome from non-infectious tissue did not contain any stimuli response-related genes (Fig 4.2 A). The transcriptome from non-infectious tissue displayed an increase in primary (23%) and cellular (18%) metabolic processes, consistent with growth in nutrient-rich media compared to growth on the leaf surface (Fig 4.2 B). Taken together, the comparisons of the functionally annotated transcriptomes indicated that *C. zeae-maydis* exhibited transcriptional reprogramming during growth on leaves, which likely resulted in directed growth toward stomata, appressorium formation, and the initiation of disease.

In order to characterize transcriptional reprogramming by *C. zeae-maydis* during the initial phases of pathogenesis in further detail, the 200 highest differentially upregulated genes during infectious growth were selected for analysis. Predicted gene functions were assigned based on sequence homology and domain similarity to characterized genes. The genes were organized based on predicted biological function (Yang et al., 2013), and represented differential expression levels ranging from 1676- to 14-fold higher during infection (Table 4.2). Comparisons of the different functional classes revealed that genes implicated in transport (13%), metabolism (26%), and stress responses (9%) were highly expressed during infection (Fig 4.3). The largest single group of enzymes identified in the collection was chloroperoxidases, including five that were upregulated more than 100-fold during infection and likely scavenge reactive oxygen species produced defensively by the host plant. Of the 27 genes involved in transport, twelve were predicted to encode members of the Major Facilitator Superfamily (MFS) class of transport proteins, which facilitate movement of small solutes across cell membranes in

response to osmotic gradients (Pao et al., 1998). Related to genes involved in mediating intracellular solute transport, genes containing signal peptides were prominently upregulated during infection. The *C. zeae-maydis* genome is predicted to encode 1266 signal peptide-containing proteins, representing 9.4% of the total genes. However, 46% of the 200 highest differentially upregulated genes during infection contained signal peptides, implicating secretory pathway-dependent movement of peptides and effector proteins throughout the cell as a crucial component of infectious development (Table 4.2). In addition, genes encoding enzymes involved in carbohydrate, amino acid, and lipid metabolism were actively transcribed during infection compared to growth in culture (Table 4.2). Five genes encoding carbohydrate degrading glycoside hydrolase-family enzymes were expressed during growth on the leaf, encoding enzymes predicted to degrade pectin and hemicellulose, two major components of plant cell walls. In addition to plant cell degrading enzymes, genes encoding aspartic proteases, serine proteases and peptidase enzymes utilized in protein degradation and metabolism were upregulated during growth on the leaf surface (Table 4.2). Taken together, these findings emphasize the metabolic reprogramming and molecule transport required for disease development and the establishment of infection.

To identify potential mechanisms of signal transduction and host sensing during foliar infection, genes encoding signaling and pathogenesis-related proteins were identified from the collection of highest differentially upregulated genes (Fig 4.3; Table 4.2). Interestingly, membrane-associated sensory proteins including three Ca2+-modulated nonselective cation channel polycystins implicated in fungal mechanosensing and two G protein-coupled receptors (GPCRs) were upregulated during infection, including a GPCR expressed more than 1000-fold compared to growth in culture. Furthermore, sequence comparisons identified a homolog to the

nuclear pore complex subunit Nro1, which is involved in oxygen sensing during growth and development in *Schizosaccharomyces pombe* (Lee et al., 2009). In addition to genes implicated in signaling, several groups of genes involved in aspects of pathogenesis in related fungi were upregulated during growth on maize leaves. Membrane-associated genes like galactomannoproteins and hydrophobins with known roles in fungal attachment and pathogenesis were upregulated during infection, including a homolog of the cell wall protein Mp1 in *Aspergillus fumigatus* (Woo et al., 2003). Furthermore, genes encoding heterokaryon incompatibility proteins involved in hyphal interaction and the formation of mycelia were upregulated during growth on the leaf surface. Lastly, the collection of genes upregulated during infection contained several putative effector proteins that may play roles in masking fungal infection or reducing host defense responses following pathogen perception (Table 4.3; Giraldo and Valent, 2013). A SCP-like extracellular protein homologous to effector protein 14 in *Venturia ineaqualis* was expressed 28-fold higher during growth on the leaf, along with eleven uncharacterized small secreted, cystine-rich proteins, which bear the hallmark structural qualities of fungal effectors (Donofrio and Raman, 2012; Table 4.3). In sum, the gene expression data from infectious tissue indicated that *C. zeae-maydis* expressed a diverse array of pathogenesis and virulence-associated genes along with a suite of genes encoding putative effector proteins that may be involved in infection.

Discussion

The transcriptional reprogramming associated with foliar pathogenesis is poorly understood in fungi, and is likely dependent on many uncharacterized mechanisms regulating the outcomes of host-pathogen interactions. Numerous next-generation RNA sequencing projects have studied fungi that enter host leaves via stomata or penetrate the leaf cuticle directly through

massive turgor pressure generated by appressoria (Oh et al., 2008; Kleeman et al., 2012; Soanes et al., 2012). *C. zeae-maydis* displays the uncommon ability to sense and reorient hyphae toward distant stomata and form bulbous appressoria in association with the stomatal pore (Kim et al., 2011a,b), which represents potentially novel mechanisms of host and environmental sensing not frequently observed in other model fungi. This study characterized the transcriptional reprogramming underlying infection, and identified regulatory genes potentially involved in stomatal tropism and the morphological transition from hyphae to appressoria prior to stomatal penetration.

Characterizing the transcriptome of *C. zeae-maydis* during stomatal tropism and appressorium formation adds to the emerging narrative regarding how Dothideomycete fungi interact with their hosts during infection. Dothideomycetes is the largest and most diverse class of fungi containing 1,300 genera and more than 19,000 species, many of which infect plants across all agricultural areas of the world (Kirk et al., 2008; Lumbsch and Huhndorf, 2010; Zhang et al., 2011). Plant pathogenic Dothideomycet*e* fungi utilize many strategies to infect their hosts, including the poorly described transition from biotrophic to necrotrophic growth that culminates in disease development (Ohm et al., 2011). Comparative genomic analysis of 18 *Dothideomycete* species, including biotrophic, hemi-biotrophic and necrotrophic fungi, revealed similarities in the number of genes involved in aspects of pathogenesis (carbohydrate-active enzymes, peptidases, and small secreted proteins; Ohm et al., 2011). The analysis also highlighted differences in the infection-related protein arsenals between fungi exhibiting different modes of pathogenesis. For example, the capacity for effector synthesis by biotrophic fungi compared to necrotrophic fungi was greatly reduced, which likely allows biotrophic fungi to evade host detection during stealth pathogenesis by producing less host-reactive compounds

(Goodwin et al., 2011; Ohm et al., 2011). The elucidation of transcriptional reprogramming associated with infection by the wheat foliar pathogen *Zymoseptoria tritici* (teleomorph *Mycosphaerella graminicola*) has uncovered the complex nature of foliar infection and hemi-biotrophic host colonization. Recent transcriptomic and proteomic studies identified host-specificity during infection (Kellner et al., 2014) and the secretome associated with infection of wheat by *Z. tritici* (Morais do Amaral et al., 2012), along with the expression profiles of post-penetration biotrophic growth and the switch to necrotrophy (Yang et al., 2013). The transcriptomes characterized in this study parallel the patterns of global transcriptomic reprogramming exhibited by *Z. tritici* during infection in terms of functional classes of expressed genes involved in metabolism, signaling, transport and stress tolerance (Morais do Amaral, et al. 2012; Yang et al., 2013; Kellner et al., 2014). However, the collection of the 200 highest differentially upregulated genes during infectious growth identified several novel targets for host sensing and the initiation of pathogenesis not observed during comparable stages of infection by *Z. tritici* (Morais do Amaral, et al. 2012; Yang et al., 2013; Kellner et al., 2014). *Z. tritici* has not been conclusively shown to exhibit stomatal tropism during pre-infectious growth on host leaf surfaces, and penetrates stomata directly without the formation of morphologically distinct structures like appressoria (Kema et al., 1996; Duncan and Howard, 2000). However, *z. tritici* has been observed forming lateral hyphal branches in association with stomatal guard cells, and occasionally formed indistinct hyphal swellings associated with the stomatal pore (Kema et al., 1996; Duncan and Howard, 2000). In contrast, *C. zeae-maydis* displays stomatal tropism in a non-thigmotropic manner toward distant stomata and forms bulbous, multi-lobed appressoria on stomata (Kim et al., 2011a,b). These similar processes in related fungi could indicate that stomatal tropism and appressorium formation in *C. zeae-maydis* may not require a substantial

number of novel response pathways or biosynthetic genes, but may rather be a finely tuned manifestation of subtle processes that occur during foliar pathogenesis in other Dothideomycete fungi. Therefore, while the transcriptomes of early infectious development by *C. zeae-maydis* and *Z. tritici* overlap in conserved areas of biological function, the transcriptome of *C. zeae-maydis* represents reprogramming associated with poorly elucidated morphological and physiological transitions which are uncommon among plant pathogenic fungi..

The expression of genes involved in protein and carbohydrate metabolism and transport prior to foliar penetration demonstrates an important metabolic transition during infection by *C. zeae-maydis*. An intriguing finding of this study was that some of the highest differentially upregulated genes during growth on the leaf surface encoded proteins involved in host cell wall degradation. Called carbohydrate activity enzymes, CAZymes are broadly conserved across fungi and are utilized to degrade plant polysaccharides to gain nutrition or cause infection (Zhao et al., 2013). Among the CAZyme families present in fungi, glycoside hydrolases were significantly upregulated during growth on the leaf surface by *C. zeae-maydis*. Glycoside hydrolases hydrolyze the glycosidic bond between two or more carbohydrate molecules, or between a carbohydrate molecule and another moiety, such as a lipid or protein (Cantarel et al., 2009). Six glycoside hydrolases belonging to families 16, 31, 43, 53, and 54 encode proteins involved in the degradation of β-glycans, pectin, and hemicellulose, which are key structural components of plant cells and therefore represent enzymatic targets for pathogens (Zhao et al., 2013). The expression of genes encoding CAZymes by *C. zeae-maydis* prior to host infection and several days before symptoms begin to develop points toward a previously uncharacterized preparatory step of the initiation of host tissue degradation. For example, secreted oligosaccharide-degrading enzymes are upregulated during appressorium maturation in *M.*

oryzae and *Colletotrichum higginsianum*, likely in preparation for host cuticle penetration and subsequent colonization of the underlying foliar tissue (Wilson and Talbot, 2009a,b; O'Connell et al., 2012; Soanes et al., 2012; Kleeman et al., 2012). However, a major disparity between the time course of infection displayed by *M. oryzae* and *C. higginsianum* compared to *C. zeae-maydis* is the temporal differences during the transitions from appressorium initiation to the necrotrophic growth phase. *C. zeae-maydis* grows asymptotically within the host for several days while the other pathogens rapidly colonized infected tissue and cause necrosis. Applying the model from established fungi, *C. zeae-maydis* begins to express and synthesize CAZymes in preparation of the switch to necrotrophy several days in advance, cultivating a large amount of available enzymes that can be secreted quickly and overwhelm plant defenses leading to rapid lesion formation. While this hypothesis requires experimental validation, the gene expression data from a collection of detached conidia, hyphae and appressoria in this study clearly shows that *C. zeae-maydis* expresses a distinct group of CAZymes that likely play important but unknown roles during the initial stages of maize infection.

Foliar tissue is comprised of numerous macromolecules other than carbohydrates that plant pathogens metabolize during infection, and the breakdown of plant proteins likely plays an important role in infection by *C. zeae-maydis*. Many fungi express proteases during plant infection, and proteases are regarded as virulence factors required for pathogenesis by many fungi (Gowda et al., 2006; Yike, 2011; Yang et al., 2013; Kellner et al., 2014). During growth on the leaf surface, *C. zeae-maydis* expressed several different classes of proteases, including two aspartic proteases, five serine proteases and two additional proteases with multiple catalytic domains. While some of the proteases are likely involved in proteolysis of host peptides during infection, proteolytic enzymes serve diverse roles ranging from the mobilization of storage

proteins, the selective breakdown of mis-folded or damaged proteins, and post-translational modification of catalytic and regulatory proteins (Bank et al., 2000; Schaller, 2004; Yike, 2011). Therefore, the specific functions and target molecules of these proteases remains to be determined. However, a majority of the proteases expressed by *C. zeae-maydis* during infection contained a signal peptide sequence, and could be secreted as extracellular molecules which could interact with and degrade host tissue. Despite evidence of secretion in response to a pathogenic elicitor, research in model fungi like *Aspergillus nidulans* and *A. niger* demonstrated that the production of extracellular proteases is regulated by carbon, nitrogen, sulfur metabolite repression and pH control (Jarai and Buxton, 1994; Katz et al., 1996), which could affect proteolytic enzyme production by *C. zeae-maydis* on the nutrient-poor leaf surface regardless of host signals. Lastly, appressoria may function as storage repositories for proteases (and other digestive enzymes) prior to foliar penetration, so the synthesis of host tissue-degrading enzymes during growth on the leaf surface may contribute to virulence.

Hyphal fusion (anastomosis) is important for the formation of mycelia and general colony homeostasis, but the role of anastomosis during foliar infection by plant pathogens is poorly understood. The non-self rejection of incompatible fungi occurs after hyphae containing different *het* loci (heterokaryon incompatibility) undergo cell fusion and exchange genetic material (Saupe, 2000; Glass and Dementhon, 2006; Aanen et al., 2010). Despite the broad coverage of mycelia on a maize leaf following inoculation, separate hyphae rarely compete over a single stomate during appressorium formation, even when part of a physically different mycelium (Chapter Two; Kim et al., 2011a). It is possible that prior to appressorium formation, hyphae communicate with each other via uncharacterized mechanisms before or after anastomosis to avoid forming appressoria on the same stomate (Leeder et al., 2011). Similar

interactions have been observed in *N. crassa* prior to anastomosis (Fu et al., 2011), and in yeast prior to mating (Gooday and Adams 1993; Daniels et al. 2006). Furthermore, anastomosis was shown to be required for virulence by the fungal necrotroph *Alternaria brassicocola* (Craven et al., 2008), implicating heterkaryon compatibility in aspects of fungal pathogenesis. Despite what is known regarding hyphal fusion events and the formation of a mycelium, the dynamics of hyphal communication on a leaf surface during plant infection remain poorly characterized (Brand and Gow, 2009).

Fungal hyphae are surrounded in a proteinaceous surface coating called the rodlet layer that acts as a molecular barrier to prevent cell damage or aid in propagule dispersal (Wessels et al., 1991). This study identified two hydrophobin class II proteins (categorized by sequence homology), and one hydrophobin-like protein that were upregulated during infection and likely aided in fungal attachment to the leaf surface. Hydrophobins are low molecular mass secreted proteins that contain eight conserved cysteine residues and are present only in fungi (Bayry et al., 2012). Arial hyphae and conidia often are covered in hydrophobins, which aid in spore dispersal and prevent water logging in moist environments (Wang et al., 2005). During pathogenesis, hydrophobins have been implicated as host sensors and host attachment mechanisms. For example, the hydrophobin Mpg1 in *M. oryzae* putatively functions as a developmental sensor for appressorium initiation on host and non-host hydrophobic surfaces (Talbot et al., 1996). Loss of *MPG1* results in reduced virulence, and the deletion of a separate hydrophobin, *MHP1,* leads to a reduced infection capacity on susceptible hosts (Kim et al., 2005). Furthermore, in the entomopathogenic fungus *Beauveria bassiana*, hydrophobic interactions between conidia-associated hydrophobins and the insect cuticle were required for the fungus to initiate pathogenesis (Zhang et al., 2011). Interestingly, *C. zeae-maydis* displays similar biological traits

to other fungi containing characterized hydrophobin-like proteins, and may utilize hydrophobins in a similar manner. After conidia dispersal, *C. zeae-maydis* may mediate hyphal growth depending on substrate (host leaves, non-host leaves and hydrophobic acrylic surfaces), which could be regulated by physical associations with hydrophobin-like proteins. Furthermore, uncharacterized thigmotropism may be involved in the formation of appressoria or penetration into the substomatal cavity. In sum, the three hydrophobins identified in this study are potentially involved in surface sensing or attachment, which may facilitate mycelial development and the initiation of pathogenesis.

Effector proteins are pathogen molecules that modify host cell structure, alter metabolism, or interfere with signaling pathways that mediate host invasion or trigger host resistance (de Jong et al., 2011; Donofrio and Raman, 2012; Giraldo and Valent, 2013). Initially discovered in Oomycetes, effector proteins are also produced by diverse groups of fungi and appear to play crucial roles during pathogenesis (Tyler et al., 2006; Donofrio and Raman, 2012). Effector proteins are generally identifiable by size (<200 amino acids), content (often containing more than 5% cysteine residues), location (secreted), and they display no significant sequence or domain homology to other characterized proteins (Donofrio and Raman, 2012). Furthermore, effectors are thought to function as pathogenesis and virulence determinants during infection, and are often species specific with poor homology to other predicted effectors in related pathogens (Dodds and Rathjen, 2010; de Jong et al., 2011). The effector suite of *C. zeae-maydis* is currently uncharacterized, but this study identified eleven candidate effectors based on the application of the current size, amino acid content and homology parameters (de Jong et al., 2011). Since host plants initiate defense responses prior to pathogen infection, it is reasonable to hypothesize that pathogens also initiate pathogenic responses to the host prior to infection

(Giraldo and Valent, 2013). For example, during infection of Arabidopsis leaves, *C. higginsianum* produces discrete waves of secreted effector proteins during specific stages of infection (Kleeman et al., 2012). Wave 1 effectors were only expressed in appressoria prior to cuticle penetration, while Wave 2 effectors were expressed before and during penetration (Kleeman et al., 2012). Interestingly, candidate *C. higginsianum* effectors Chec6 and Chec36 were secreted from the appressorial pore, the point of membrane contact between the pathogen and host cuticle layer where initial penetration occurs (Howard and Valent, 1996; Kleeman et al., 2012). It is plausible to hypothesize that *C. zeae-maydis* produces waves of secreted proteins (including effectors) during different stages of penetration in a similar fashion to *C. higginsianum* via appressoria, and during biotrophic and necrotrophic growth similarly to *Z. tritici* (Kleeman et al., 2012; Yang et al., 2013). Furthermore, the discovery and characterization of effector proteins produced by *C. zeae-maydis* prior to stomatal penetration will inform the dynamics of appressorium formation, colonization of the stomatal pore, and growth throughout leaf tissue during the initial stages of foliar infection.

Fungi have evolved the ability to sense and respond to minute changes in their environment, and the unknown physical and chemical cues that trigger drastic changes in hyphal growth and development during infection by *C. zeae-maydis* are likely perceived by receptors on the cell surface. This study identified two G protein-coupled receptors (GPCRs) that potentially function as sensory mechanisms involved in pathogenesis. G protein-coupled receptors represent the largest family of fungal transmembrane receptors, and transmit extracellular signals to the cellular interior after stimuli by a diverse range of signals including light, Ca^{2+}, odorants, fatty acids, amino acids, nucleotides, proteins and steroids (Maller, 2003; Xue et al., 2008). Signals are transmitted from GPCRs through intracellular space by G protein subunits, which act upon

downstream effectors to elicit changes in gene expression (reviewed by Li et al., 2007). G protein signaling is an important and conserved signal transduction mechanism in fungi. Identifying the specific GPCR that triggers the release of G protein subunits to facilitate downstream reactions is critical to elucidating the G protein signaling cascade and gain a molecular foothold to further unravel the intricacies of environmental sensing (Tuteja, 2012; Katritch et al., 2013). Recently, surveys of the diversity of GPCRs in fungi have focused on genome-wide analysis of basiodiomycetes and filamentous saprophytic ascomycetes like *Trichoderma* spp., *N. crassa* and *A. nidulans*, (Gruber et al., 2013; Krishnan et al., 2012, Xue et al., 2008; Lafon et al., 2006) and several studies have examined GPCR-like receptors in plant pathogenic fungi like *M. oryzae, Verticillium dahlia, Verticillium albo-atrum* (Zheng et al, 2011; Kulkarni et al., 2005). Fungi contain 13 distinct classes of GPCRs organized by sequence homology (Borkovich et al., 2004; Kulkarni et al., 2005; Lafon et al., 2006; Xue et al., 2008), but both presumed GPCRs identified in this study belong to the *PTH11*-like GPCR class, referring to the well characterized GPCR-like protein *PTH11* of *M. oryzae*. Following conidial germination on hydrophobic surfaces, *PTH11* regulates appressorium formation and acts upstream of the cAMP pathway (DeZwaan et al., 1999). *PTH11* contains a cysteine-rich Common in Fungal Extracellular Membrane (CFEM) domain, which is present in many other fungal membrane proteins and is hypothesized to mediate aspects of host-pathogen interaction and virulence (Kulkarni et al., 2003). For example, in *C. albicans* and *C. parapsilosis*, the CFEM domain-containing proteins Rbt5/Rbt51, Cfem2/Cfem3, and Cfem6 are involved in haemoglobin-iron and haemin utilization, and deletion of CFEM-encoding genes Rbt5/Rbt51/Csa1 results in increased sensitivity to cell-wall damaging chemicals and a reduction in biofilm formation in *C. albicans* (Weissman and Kornitzer, 2004; Weissman et al., 2008; Ding et al., 2011). However,

the three CFEM-domain containing proteins in the human pathogen *A. fumigatus* were recently shown to affect cell-wall stability but not virulence (tested individually or as a family) in insect and mice models (Vaknin et al., 2014), representing an exception to the CFEM dogma and highlighting the necessity to further elucidate the specific role of CFEM domain-containing *PTH11*-like GPCRs in fungal pathogenesis. Recent research characterized the three Gα subunits in *C. zeae-maydis*, and identified *GPA2* as required for stomatal tropism and appressorium formation (Chapter Five), thus providing a direct link between G protein signaling and pathogenesis. The putative GPCRs identified in this study represent potential molecular footholds in dissecting host sensing and responsiveness in an important pathogenic fungus with direct correlations to other pathogenic fungi

Many fungi initiate pathogenic development after sensing changes in leaf surface topography associated with guard cell margins and the stomatal pore, however the role of mechanosensing by *C. zeae-maydis* during stomatal infection remains unknown. In fungi, mechanosensitive ion channels (MS channels) open in response to physical stimuli that affect the membrane, such as hyphal bending associated with growth on topographically dynamic surfaces (Booth et al., 2007; Kloda et al., 2008). Changes in ion concentration gradients associated with mechanical open and closing of the channels triggers different physiological responses, and is a primary method for thigmotropism in fungi (Kumamoto, 2008). For example, during growth on bean leaves and artificial surfaces, hyphae of the bean rust fungus *Uromyces appendiculatus* sense changes in calcium ion concentrations to initiate the formation of appressoria (Hoch et al., 1987). Experimental observations on artificial surfaces showed that hyphae of *U. appendiculatus* were able to form appressoria preferentially on 0.5 μm ridges, which correlated to the average height of bean stomatal guard cells (Hoch et al., 1987). Supporting this

hypothesis, treatment with the MS channel-inhibitory chemical gadolinium blocked appressorium differentiation by *U. appendiculatus* (Zhou et al., 1991). Previous studies established that changes in surface topography are not sufficient to trigger appressorium differentiation by *C. zeae-maydis (*Chapter 2), but it is plausible that *C. zeae-maydis* utilizes Ca+ ion-mediated mechanosensing in conjunction with a separate method of stomatal perception to elicit appressorium formation. Within this model, hyphae must sense both the chemical signal and topographical features associated with stomata (i.e. an unknown volatile chemical and the ridge of a stomatal guard cell) in order to form appressoria, thus reducing the amount of errantly formed appressoria. Relatedly, hyphal perception of host leaf topography may play an important role in maintaining pathogenic development on host leaves in the absence of stomatal signals. Prior to stomatal tropism, hyphae of *C. zeae-maydis* grow without discernable pattern (Chapter 2), yet do not begin to initiate micro-cycle conidiogenesis as is observed on non-host trichomes and inert surfaces (Lapaire and Dunkle, 2003). In sum, *C. zeae-maydis* likely utilizes MS channel proteins (in addition to other sensory mechanisms) to sense physical host cues during growth on the leaf surface and sense topographical features, like stomatal guard cells on the leaf surface to initiate disease.

In conclusion, this study reported and analyzed the difference between pre-infection stages on maize and vegetative growth in axenic culture of *C. zeae-maydis* by transcriptomic analysis. Functional analysis of the identified transcripts revealed that genes involved in cell communication, response to stress, and cellular responses to stimuli were more actively transcribed during pre-infection stages on maize compared to vegetative growth. The expression of putative environmental sensors like novel GPCRs and MS ion channels implicate chemical and physical cues in mediating pathogenesis. Lastly, this study identified several pathogenesis-

related genes involved in pre-penetration infectious growth on the leaf surface, including hydrophobins, anastomosis-related *het* genes and a previously undiscovered suite of putative effector proteins. The characterized transcriptional reprogramming associated with growth on the leaf surface, stomatal sensing and appressorium formation broadens the understanding of pathogenesis in an important plant pathogen, and establishes novel targets to functionally characterize signaling mechanisms underlying infection.

References

Altschul, S.F., Gish, W., Miller, W., Myers, E.W., and Lipman, D.J. 1990. Basic local alignment search tool. *J Mol Biol* 215: 403-410.

Altschul, S. F., T. L. Madden, A. A. Schäffer, J. Zhang, Z. Zhang et al. 1997. Gapped BLAST and PSI-BLAST: a new generation of protein database search programs. *Nucleic Acids Res* 25: 3389–3402.

Aanen, D.K., Debets, A.J. M., Glass, N.L. and Saupe, S.J. 2010. Biology and Genetics of vegetative incompatibility in fungi, pp. 274-288 in Cellular and Molecular Biology of Filamentous Fungi, edited by K. A. Borkovich and D. J. Ebbole. ASM Press, Washington, D.C.

Bahn, Y-S., Xue, C., Idnurm, A., Rutherford, J.D., Heitman, J. 2007. Sensing the environment: lessons from fungi. *Nature Rev Microbiol* 5:57-69.

Bank U, Kruger S, Langner J, Roessner A. 2000. Review: peptidases and peptidase inhibitors in the pathogenesis of diseases. Disturbances in the ubiquitin-mediated proteolytic system. Protease-antiprotease imbalance in inflammatory reactions. Role of cathepsins in tumor progression. *Adv Exp Med Biol*. 477:349-378.

Bayry, J., Aimanianda, V., Guijarro, J.I., Sunde, M., Latge, J.P. 2012. Hydrophobins—unique fungal proteins. *PLoS Pathog* 8(5): e1002700.

Bluhm, H.B., Dhillon, B., Lindquist, E.A., Kema, G.H.J., Goodwin, S.B. et al. 2008. Analysis of expressed sequence tags from the maize foliar pathogen *Cercospora zeae-maydis* identify novel genes expressed during vegetative, infectious, and reproductive growth. *BMC Gen* 9:523.

Booth, I.R., Edwards, M.D., Black, S., Schumann, U. and Miller, S. 2007. Mechanosensitive channels in bacteria: signs of closure? *Nature Rev Microbiol*: 5:431-440.

Borkovich, K.A., Alex, L.A., Yarden, O., Freitag M., Turner, G.E., et al., 2004. Lessons from the genome sequence of Neurospora crassa: tracing the path from genomic blueprint to multicellular organism. *Microbiol Mol Biol Rev* 68:1-108.

Brand, A. and Gow, N.A.R. 2009. Mechanisms of hypha orientation in fungi. *Curr Opin Microbiol* 12:350-357.

Breakspear, A. and Momany, M. 2007. The first fifty microarray studies in filamentous fungi. *Microbiology* 153: 7-15.

Cantarel, B.L., Coutinho, P.M., Rancurel, C., Bernard, T., Lombard, V., Henrissat, B. 2009. The Carbohydrate-Active EnZymes database (CAZy): an expert resource for Glycogenomics. *Nucleic Acids Res* 37:D233–D238.

Craven, K.D., Velez, H., Cho, Y., Lawrence, C.B., Mitchell, T.K. 2008. Anastomosis is required for virulence of the fungal necrotroph Alternaria brassicicola. *Eukaryotic Cell* 7:675-683.

D'Souza, C.A., Heitman, J. 2001. Conserved cAMP signaling cascades regulate fungal development and virulence. *FEMS Microbiol Rev.* 25:349-364.

Daniels, K.J., Srikantha, T., Lockhart, S.R., Pujol, C. and Soll, D.R. 2006. Opaque cells signal white cells to form biofilms in *Candida albicans*. *EMBO J* 25:2240-2252

de Jong, R., Bolton, M.D., and Thomma, B.P.H.J. 2011. How filamentous pathogens co-opt plants: the ins and outs of fungal effectors. *Cur Opin Plant Biol* 14:400-406.

DeRisi, J.L., Iyer, V.R. and Brown, P.O. 1997. Exploring the metabolic and genetic control of gene expression on a genomic scale. *Science* 278:680-686.

DeZwaan, T.M., Carroll, A.M., Valent, B., and Sweigard, J.A. 1999. Magnaporthe grisea Pth11p is a novel plasma membrane protein that mediates appressorium differentiation in response to inductive substrate cues. *Plant Cell* 11:2013-2030.

Ding, C., Vidanes, G.M., Maguire, S.L., Guida, A., Synnott, J.M., Andes, D.R., Butler, G. 2011. Conserved and divergent roles of Bcr1 and CFEM proteins in *Candida parapsilosis* and *Candida albicans. PLoS One* 6, e28151.

Dodds, P.N., Rathjen, J.P. 2010. Plant immunity: towards an integrated view of plant–pathogen interactions. *Nat Rev Genet* 11:539-548.

Donofrio, N.M., Oh, Y., Lundy, R., Pan, H., Brown, D.E., et al. 2006. Global gene expression during nitrogen starvation in the rice blast fungus, *Magnaporthe grisea*. *Fungal Genet Biol* 43: 605–617

Donofrio, N.M., and Raman, V. 2012. Roles and delivery mechanisms of fungal effectors during infection development: common threads and new directions. *Curr Opin Microbiol* 15:692-698.

Flaishman, M.A., Kolattukudy, P.E. 1994. Timing of fungal invasion using hosts ripening hormone as a signal. *Proc Natl Acad Sci USA*. 91:6579-6583.

Fu, C., Iyer, P., Herkal, A., Abdullah, J., Stout, A. and Free, S.J. 2011. Identification and characterization of genes required for cell-to-cell fusion in *Neurospora crassa. Eukaryot Cell* 10:1100-1109.

Gilbert, R.D., Johnson, A.M., Dean, R.A. 1996. Chemical signals responsible for appressorium formation in the rice blast fungus *Magnaporthe grisea. Physiol Mol Plant Pathol.* 48:335-346.

Giraldo, M.A., and Valent, B. 2013. Filamentous plant pathogen effectors in action. *Nat Rev Microbiol* 11:800-814.

Glass, N.L., and K. Dementhon. 2006. Non-self recognition and programmed cell death in filamentous fungi. *Curr Opin Microbiol* 9:553-558.

Gooday, G.W. and Adams, D.J. 1993. Sex hormones and fungi. *Adv Microb Physiol* 34:69-145.

Goodwin, S.B., M'Barek, S.B., Dhillon, B., Wittenberg, A.H., Crane, C.F., et al. 2011. Finished genome of the fungal wheat pathogen Mycosphaerella graminicola reveals dispensome structure, chromosome plasticity, and stealth pathogenesis. *PLoS Genet* 7: e1002070.

Gowda, M., Venu, R.C., Raghupathy, M.B., Nobuta, K., Li, H., et al. 2006. Deep and comparative analysis of the mycelium and appressorium transcriptomes of *Magnaporthe grisea* using MPSS, RL-SAGE, and oligoarray methods. *BMC Genomics* 7: 310

Gruber, S., Sman, M. and Zeilinger, S. 2013. Comparative analysis of the repertoire of G protein-coupled receptors of three species of the fungal genus *Trichoderm*a. *BMC Microbiol* 13:108.

Hoch, H.C., Staples, R.C., Whitehead, B., Comeau, J. and Wolf, E.D. 1987. Signaling for growth orientation and cell differentiation by surface topography in *Uromyces*. *Science* 235:1659-1662.

Horn, F., Heinekamp, T., Kniemeyer, O., Pollmächer, J., Valiante, V., and Brakhage, A.A. 2012. Systems biology of fungal infection. *Front Microbiol* 3**:**118.

Howard, R.J., and Valent, B. 1996. Breaking and entering: host penetration by the fungal rice blast pathogen *Magnaporthe grisea. Annu Rev Microbiol* 50:491-512.

Jakupovic´, M., Heintz, M., Reichmann, P., Mendgen, K. and Hahn, M. 2006. Microarray analysis of expressed sequence tags from haustoria of the rust fungus *Uromyces fabae*. *Fungal Genet Biol* 43:8-19.

Jarai, G., and Buxton, F. 1994. Nitrogen, carbon, and pH regulation of extracellular acidic proteases of *Aspergillus niger. Curr Genet* 26:238-44.

Katritch, V., Cherezov, V. and Stevens, R.C. 2013. Structure-function of the G protein-coupled receptor superfamily. *Annu Rev Pharm Tox* 53: 531-556.

Katz, M.E., Flynn, P.K., van Kuyk, P.A., Cheetham, B.F. 1996. Mutations affecting extracellular protease production in the filamentous fungus *Aspergillus nidulans. Mol Gen Genet* 250:715-724.

Kellner, R., Bhattacharyya, A., Poppe, S., Hsu, T.Y., Brem, R. and Stukenbrock, E.H. 2014. Expression profiling of the wheat pathogen *Zymoseptoria tritici* reveals genomic patterns of transcription and host-specific regulatory programs. *Genome Biol Evol* 14:1353-1365.

Kema, G., D. Yu, F. Rijkenberg, M. Shaw, and R. Baayen, 1996. Histology of the pathogenesis of *Mycosphaerella graminicola* in wheat. *Phytopathology* 86:777-786.

Kim, S.,Ahn, I.P., Rho, H.S., Lee, Y.H. 2005. MHP1, a *Magnaporthe grisea* hydrophobin gene, is required for fungal development and plant colonization. *Mol Microbiol* 57: 1224-1237.

Kim, H., Ridenour, J.B., Dunkle, L.D. and Bluhm, B.H. 2011a. Regulation of pathogenesis by light in *Cercospora zeae-maydis*: An updated perspective. *Plant Pathol J* 27:103-109.

Kim, H., Ridenour, J.B., Dunkle, L.D. and Bluhm, B.H. 2011b. Regulation of stomatal tropism and infection by light in *Cercospora zeae-maydis*: Evidence for coordinated host/pathogen responses to photoperiod? *PLoS Pathog* 7(7): e1002113.

Kirk, P., Cannon, P., Minter, D., and Stalpers, J. 2008. Ainsworth and Bisby's dictionary of the Fungi, 10th ed. Wallingford, UK: CAB International.

Kleemann, J., Rincon-Rivera, L.J., Takahara, H., Neumann, U., Ver Loren van Themaat, E. et al. 2012. Sequential delivery of host-induced vrulence effectors by appressoria and Iintracellular hyphae of the phytopathogen *Colletotrichum higginsianum*. *PLoS Pathog* 8(4): e1002643.

Kloda, A. Petrov, E., Meyer, G.R., Nguyen, T., Hurst, A.C., Hool, L., and Marinac, B. 2008. Mechanosensitive channel of large conductance. *Int J Biochem Cell Biol* 40:64-169.

Krishnan, A., Almén, M.S., Fredriksson, R. and Schiöth, H.B. 2012. The Origin of GPCRs: Identification of mammalian-like *Rhodopsin, Adhesion, Glutamate* and *Frizzled* GPCRs in Fungi. *PLoS One* 7(1):e29817.

Kulkarni, R.D., Kelkar, H.S., and Dean, R.A. 2003. An eight-cysteine-containing CFEM domain unique to a group of fungal membrane proteins. *Trends Biochem* Sci. 28:118-121.

Kulkarni, R.D., Thon, M.R., Pan, H. and Dean, R.A. 2005. Novel G-protein-coupled receptor-like proteins in the plant pathogenic fungus *Magnaporthe grisea.* *Genome Biol* 6:R24.

Kumamoto, C.A. 2008. Molecular mechanisms of mechanosensing and their roles in fungal contract sensing. *Nat Rev Microbiol* 6:667-673.

Lafon A, Han, K-H., Seo, J-A., Yu, J-H., and d'Enfert C. 2006. G-protein and cAMP-mediated signaling in *Aspergilli*: a genomic perspective. *Fungal Gen Biol* 43:490-502.

Lapaire, C.L., and Dunkle, L.D. 2003. Microcycle conidiation in *Cercospora zeae-maydis.* *Phytopathology* 2:193-199.

Lashkari, D.A., DeRisi, J.L., McCusker, J.H., Namath, A.F., Gentile, C., Hwang, S. Y. et al. 1997. Yeast microarrays for genome wide parallel genetic and gene expression analysis. *Proc Natl Acad Sci USA* 94:13057-13062.

Lee, Y-H., Dean, R.A. 1993. Stage-specific gene expression during appressorium formation of *Magnaporthe grisea*. *Exp Mycol*. 17:215-222.

Lee, C.Y., Stewart, E.V., Hughes, B.T., and Espenshade, P.J. 2009. Oxygen-dependent binding of Nro1 to the prolyl hydroxylase Ofd1 regulates SREBP degradation in yeast. *EMBO J.* 28:135-143.

Leeder, A.C., Palma-Guerrero, J. and Glass N.L. 2011 The social network: deciphering fungal language. *Nat Rev Microbiol* 9:440-451.

Letunic, I., Doerks, T., and Bork, P. 2009. SMART 6: recent updates and new developments. *Nucleic Acids Res* 37:229-232.

Li, L., Wright, S.J., Krystofova, S., Park, G. and Borkovich, K.A. 2007. Heterotrimeric G protein signaling in filamentous fungi. *Annu Rev Microbiol* 61:423-452.

Lumbsch, H.T., and Huhndorf, S.M. 2010. Myconet Volume 14. Part One. Outline of Ascomycota—2009. Part Two. Notes on Ascomycete Systematics. Nos. 4751–5113. Fieldiana Life and Earth Sciences 1–64.

Maller, J.L. 2003. Signal transduction. Fishing at the cell surface. *Science* 300:594-595.

Mathioni, S.M., Patel, N., Riddick, B., Sweigard, J.A., Czymmek, K.J. et al. 2013. Transcriptomics of the rice blast fungus *Magnaporthe oryzae* in response to the bacterial antagonist *Lysobacter enzymogenes* reveals candidate fungal defense response genes. *PLoS ONE* 8(10): e76487.

Marioni, J.C., Mason, C.E., Mane, S.M., Stephens, M. and Gilad, Y. 2008. RNA-seq: an assessment of technical reproducibility and comparison with gene expression arrays. *Genome Res* 18:1509-1517

McFadden, H.G., Wilson, I.W., Chapple, R.M. and Dowd, C. 2006. Fusarium wilt (*Fusarium oxysporum* f. sp. *vasinfectum*) genes expressed during infection of cotton (*Gossypium hirsutum*). *Mol Plant Pathol* 7:87–101.

Morais do Amaral, A., Antoniw, J., Rudd, J.J., Hammond-Kosack, K.E. 2012. Defining the predicted protein secretome of the fungal wheat leaf pathogen *Mycosphaerella graminicola*. *PLoS ONE* 7(12): e49904.

O'Connell, R.J., Thon, M.R., Hacquard, S., Amyotte, S.G., Kleeman, J. et al. 2012. Lifestyle transitions in plant pathogenic C*olletotrichum* fungi deciphered by genome and transcriptome analysis. *Nat Gen* 44:1060-1065.

Oh, Y., Donofrio, N., Pan, H., Coughlan, S., Brown, D.E., et al. 2008. Transcriptome analysis reveals new insight into appressorium formation and function in the rice blast fungus *Magnaporthe oryzae*. *Genome Biol* 9:R85

Ortiz-Bermudez, P., Srebotnik, F. and Hammel. 2003. Chlorination and cleavage of lignin structures by fungal chloroperoxidases. *Appl Environ Microbiol* 69:5015-5018.

Pao, S.S., Paulsen, I.T., Sair, M.H. 1998. Major facilitator superfamily. *Microbiol Mol Biol Rev*

62:1-34.

Saupe, S. J. 2000. Molecular genetics of heterokaryon incompatibility in filamentous ascomycetes. *Microbiol Mol Biol Rev* 64: 489-502.

Schaller, A. 2004. A cut above the rest: the regulatory function of plant proteases. *Planta* 220:183–97.

Schultz, J., Milpetz, F., Bork, P., and Ponting, C.P. 1998. SMART, a simple modular architecture research tool: identification of signaling domains. *PNAS* 95:5857-5864.

Soanes, D.M. and Talbot, N.J. 2006. Comparative genomic analysis of phytopathogenic fungi using expressed sequence tag (EST) collections. *Mol Plant Pathol* 1:61-70.

Soanes, D.M., Chakrabarti, A., Paszkiewicz, K.H., Dawe, A.L., and Talbot, N.J. 2012. Genome-wide transcriptional profiling of appressorium development by the rice blast fungus *Magnaporthe oryzae*. *PLoS Pathog* 8(2): e1002514.

Takano, Y., Choi, W.B., Mitchell, T.K., Okuno, T. & Dean, R.A. 2003. Large-scale parallel analysis of gene expression during infection-related morphogenesis of *Magnaporthe grisea*. *Mol Plant Pathol* 4:337-346.

Talbot, N.J., Kershaw, M.J., Wakley, G.E., De Vries, O., Wessels, J., et al. 1996. MPG1 encodes a fungal hydrophobin involved in surface interactions during infection-related development of *Magnaporthe grisea. Plant Cell* 8:985-999.

Tyler, B.M., Tripathy, S., Zhang, X.M., Dehal, P., Jiang, R.H.Y., Aerts, A., Arredondo, F.D., Baxter, L., Bensasson, D., Beynon, J.L. et al. 2006. *Phytophthora* genome sequences uncover evolutionary origins and mechanisms of pathogenesis. *Science* 313:1261-1266.

Tuteja, N. 2009. Signaling through G protein-coupled receptors. *Plant Sig Behav* 4:942-947.

Vaknin, Y., Shadkchan, Y., Levdansky, E., Morozov, M., Romano, J, and Osherov, N. 2014. The three *Aspergillus fumigatus* CFEM-domain GPI-anchored proteins (CfmA-C) affect cell-wall stability but do not play a role in fungal virulence. *Fungal Gen Biol* 63:55-64.

Wang, X., Shi, F., Wosten, H.A., Hektor, H., Poolman, B., et al. 2005. The SC3 hydrophobin self-assembles into a membrane with distinct mass transfer properties. *Biophys J* 88: 3434-3443.

Wang, Z., Gerstein, M. and Snyder, M. 2009. RNA-Seq: a revolutionary tool for transcriptomics. *Nat Rev Genet* 10:57-63.

Weissmann, Z. and Kornitzer, D. 2004. A family of *Candida* cell surface haem-binding proteins involved in haemin and haemoglobin-iron utilization. *Mol. Microbiol*. 53:1209-1220.

Weissman, Z., Shemer, R., Conibear, E., Kornitzer, D. 2008. An endocytic mechanism

for haemoglobin-iron acquisition in *Candida albicans*. *Mol Microbiol* 69:201-217.

Wessels, J., De Vries, O., Asgeirsdottir, S.A., Schuren, F. 1991. Hydrophobin genes involved in formation of aerial hyphae and fruit bodies in *Schizophyllum*. *Plant Cell* 3:793-799.

Wilson, R.A., Talbot, N.J. 2009a. Under pressure: investigating the biology of plant infection by *Magnaporthe oryzae*. *Nat Rev Microbiol* 7:185-195.

Wilson, R.A., Talbot, N.J. 2009b. Fungal physiology - a future perspective. *Microbiology* 155: 3810-3815

Woo, P.C., Chong, K.T., Leung, A.S., Wong, S.S., Lau, S.K., and Yuen, K.Y. 2003. AFKMP1 encodes an antigenic cell wall protein in *Aspergillus flavus.* *J Clin Microbiol* 41:841-850.

Xue, C., Hsueh, Y.P. and Heitman, J. 2008. Magnificent seven: roles of G protein-coupled receptors in extracellular sensing in fungi. *FEMS Microbiol Rev* 32:1010-1032.

Yin, Y., Yu, G., Chen, Y., Jiang, S., Wang, M. et al. 2012. Genome-wide transcriptome and proteome analysis on different developmental stages of *Cordyceps militaris*. *PLoS ONE* 7(12): e51853.

Zhang Y, Crous P, Schoch C, Bahkali A, Guo L, et al. 2011. A molecular, morphological and ecological re-appraisal of *Venturiales* - a new order of *Dothideomycetes*. *Fungal Div* 51:249-277.

Zhang, P. and Min, X.J. 2005. EST data mining and applications in fungal genomics. *Appl Mycol Biotech* 5:33-70.

Zhao, C., Wallwijk ,C., de Wit, P.J.G.M., Tang D., and van der Lee, T. 2013. RNA-Seq analysis reveals new gene models and alternative splicing in the fungal pathogen *Fusarium graminearum.* *BMC Genomics* 14:21.

Zhao, Z., Liu, H., Wang, C. and Xu, J-R. 2013. Comparative analysis of fungal genomes reveals different plant cell wall degrading capacity in fungi. *BMC Genomics* 14:274.

Zhang, S., Xia, Y.X., Kim, B., Keyhani, N.O. 2011. Two hydrophobins are involved in fungal spore coat rodlet layer assembly and each play distinct roles in surface interactions, development and pathogenesis in the entomopathogenic fungus, *Beauveria bassiana. Mol Microbiol* 80:811-826.

Zheng, H., Zhou, L., Dou, T., Han, X., Cai, Y., Zhan, X. et al. 2011. Genome-wide prediction of G protein-coupled receptors in *Verticllium* spp. *Fungal Biol* 114:359-368.

Zhou, X. L., Stumpf, M. A., Hoch, H. C. & Kung, C. 1991. A mechanosensitive channel in whole cells and in membrane patches of the fungus *Uromyces*. *Science* 253:1415-1417.

Figures

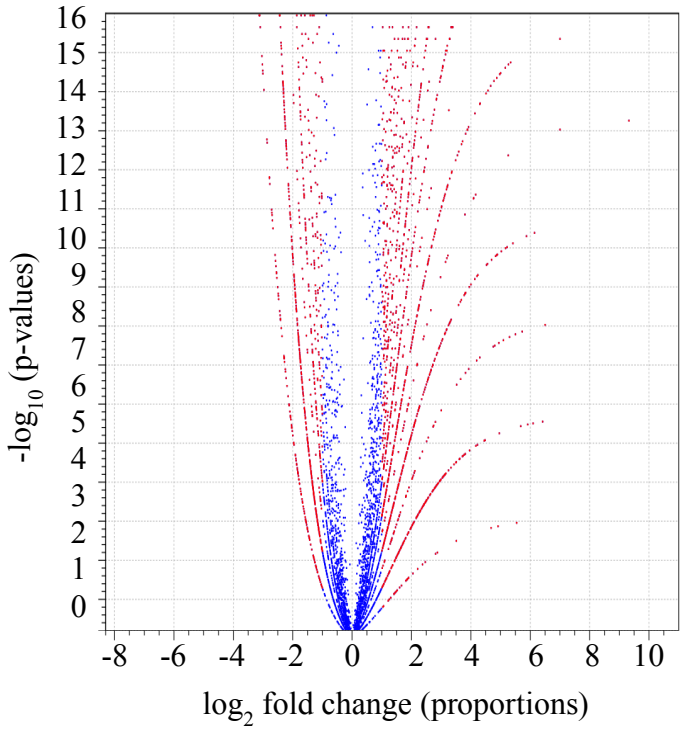

Figure 4.1. Differentially expressed genes during infection and vegetative growth in nutrient media. The volcano plot was produced by mapping individually identified genes base on the –log of the p-value on the y-axis, and the $\log_2$ fold change of expression on the x-axis (Kal's Test). Blue dots represent mapped reads expressing less than a 2-fold difference between the two transcriptomes, and red dots represent mapped reads expressing 2-fold greater differential expression.

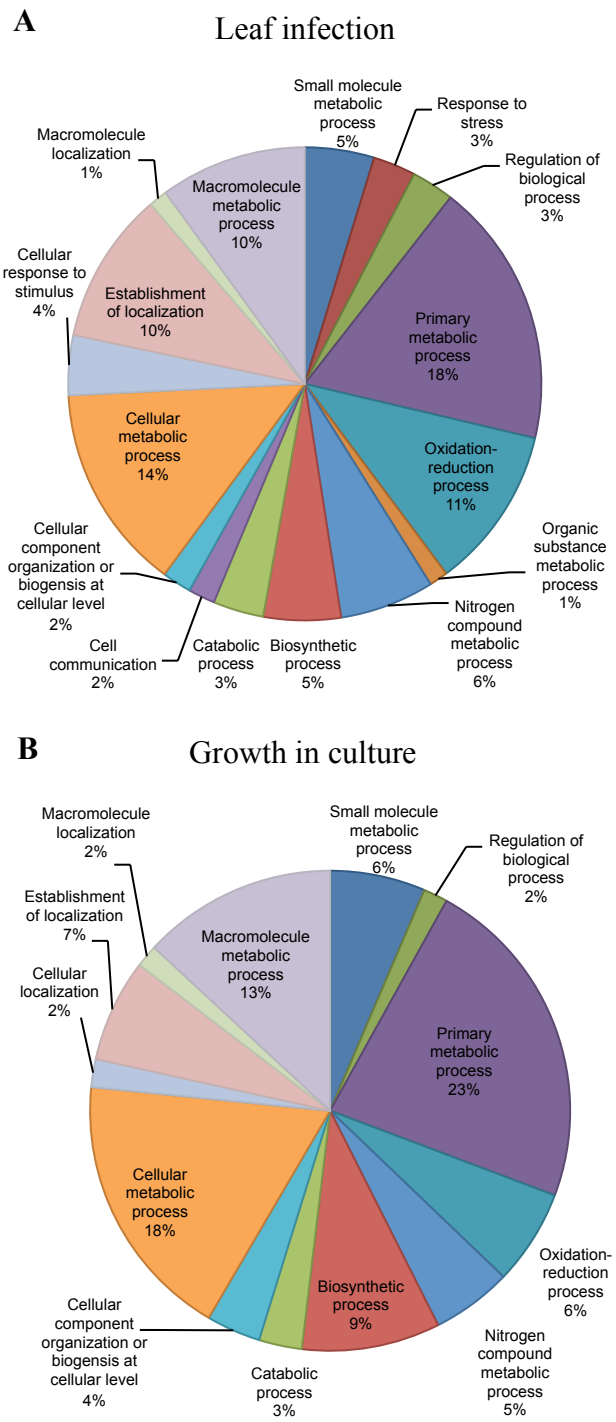

Figure 4.2. Functional annotation of the transcriptomes utilized in this study. Blast2GO analyses were conducted at the level-four hierarchical cutoff and functional annotations are represented as pie charts for the A) transcriptome of infectious growth, and B) the transcriptome of non-infectious growth. GO functional groups are highlighted, with a percentage of total transcripts belonging to the GO group presented for each transcriptome.

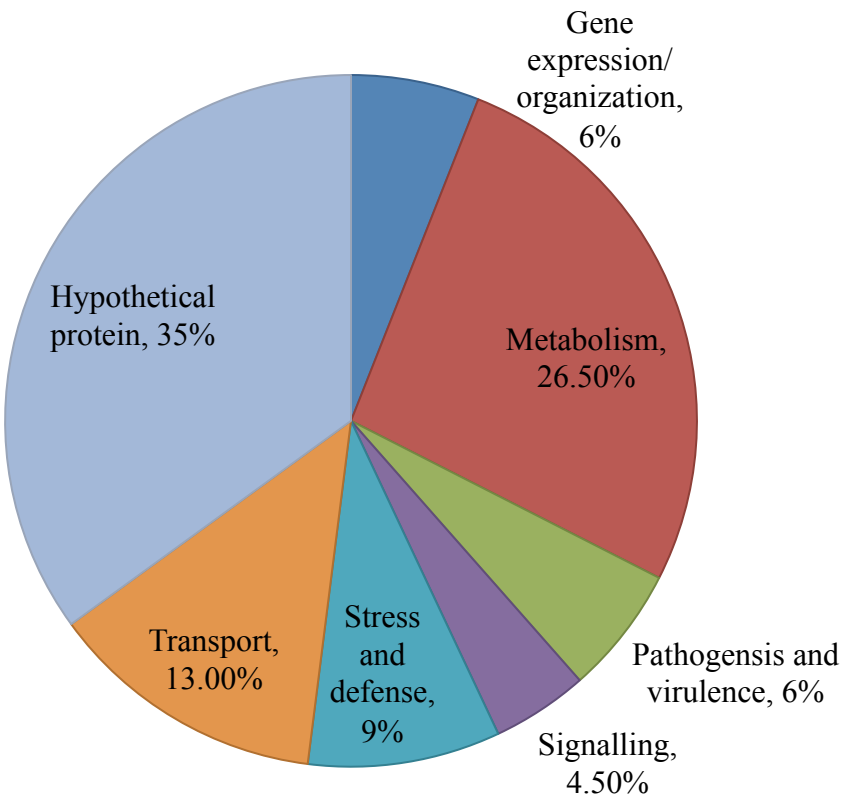

Figure 4.3. Functional annotation of the 200 highest differentially upregulated genes during infection. The 200 genes were analyzed based on sequence and domain homology of the predicted protein sequences utilizing BLAST and SMART searches. Genes were grouped based on predicted biological function.

Tables

Table 4.1. Mapping statistics from transcriptomic sequencing

Condition	Total Reads	All mapped reads	Uniquely matched reads	Multi-position match[a]	Unmapped reads
Non-infectious growth	5337834	3769879 (70.62%)	3762446 (70.49%)	7433 (0.13%)	1567955 (29.38%)
Infectious growth	349359	23620 (6.76%)	23040 (6.59%)	580 (0.17%)	325739 (93.24%)

[a] Transcripts displayed homology to multiple loci in the genome, and were not included in transcriptomic analyses

Table 4.2. Collection of 200 genes upregulated during infection

Protein ID	Annotation	Biological process	SignalP
82338	Argonaut-like protein	Gene expression	No
5765	BTB/PO-like transcriptional repressor	Gene expression	No
56487	bZIP transcription factor-like	Gene expression	No
51543	C2H2-type zinc finger transcription factor	Gene expression	No
101833	Chromosome segregation ATPase; SMC protein	Gene expression	No
81126	F-box, cyclin-like	Gene expression	No
93904	LexA-like protein	Gene expression	No
37127	Like-Sm ribonucleoprotein	Gene expression	Yes
30742	MYB DNA-binding protein domain-containing protein	Gene expression	No
120690	NF-H1 Zn finger-like	Gene expression	Yes
96285	NmrA-like transcriptional regulator	Gene expression	No
30389	Zinc finger, C2H2-type protein	Gene expression	No
115073	2-dehydropantoate 2-reductatse	Metabolism	Yes
40715	2OG-Fe(II) oxygenase	Metabolism	No
102307	3-hydroxymethyl-3-methylglutaryl-Coenzyme A lyase	Metabolism	No
66196	4-coumarate-CoA ligase	Metabolism	Yes
44020	7-alpha-ceph-methylase-like	Metabolism	No
30940	Acetyl-CoA synthase FacA (A. fumigatus)	Metabolism	No
45105	Acid phosphatase-like	Metabolism	No
101378	Acyltransferase	Metabolism	No
97333	Aldehyde dehydrogenase	Metabolism	No
72046	Amidohydrolase	Metabolism	No
45446	Aromatic aminotransferase	Metabolism	No
82538	Aspartic protease	Metabolism	Yes
113850	Cellobiose dehydrogenase	Metabolism	Yes

Table 4.2 Cont. Collection of 200 genes upregulated during infection

Protein ID	Annotation	Biological process	SignalP
50616	Cyclohexanone-monooxygenase	Metabolism	No
42584	Endoribonuclease L-PSP	Metabolism	No
108623	Ferredoxin reductase-like	Metabolism	No
109427	Flavin-binding monooxygenase-like protein	Metabolism	No
49440	Flavin-binding monooxygenase-like protein	Metabolism	No
70336	Flavin-containing amine oxidase	Metabolism	Yes
91628	GCN5-related N-acetyltransferase	Metabolism	No
63798	Glucose-methanolcholine oxidoreductase	Metabolism	Yes
64205	Glutathione-dependent formaldehyde-activating enzyme	Metabolism	No
116205	Glyceraldehyde 3-phosphate dehydrogenase	Metabolism	Yes
86744	Glycogen debranching enzyme	Metabolism	No
68501	Glycoside hydrolase family 16	Metabolism	Yes
57804	Glycoside hydrolase family 54	Metabolism	Yes
107681	Glycoside hydrolase family 43	Metabolism	Yes
31995	Glycoside hydrolase family 43	Metabolism	Yes
34408	Glycoside hydrolase family 53	Metabolism	Yes
90022	Glycosyltransferase family 31	Metabolism	No
104221	Isoprenylcysteine carboxyl methyltransferase	Metabolism	Yes
65121	Lysine 2,3-aminomutase	Metabolism	Yes
103453	Metallopeptidase	Metabolism	Yes
107483	NAD dependent epimerase dehydrase	Metabolism	No
112770	Nitriloacetate monooxygenase component A	Metabolism	No
35242	Non-ribosomal peptide synthase	Metabolism	No
35062	Oxoglutarate/iron-dependent oxygenase	Metabolism	No
48729	P450 monooxygenase	Metabolism	Yes

Table 4.2 Cont. Collection of 200 genes upregulated during infection

Protein ID	Annotation	Biological process	SignalP
115220	P540 monooxygenase	Metabolism	Yes
116362	Pectin lyase-like protein	Metabolism	No
82627	Peptidase A1 (aspartic)	Metabolism	No
81896	Serine peptidase S28 family	Metabolism	Yes
45538	Polyketide synthase	Metabolism	No
87815	Riseke 2Fe-2S family protein	Metabolism	No
102425	Serine hydrolase	Metabolism	No
47406	SMP-30/LEE domain containing protein	Metabolism	No
3513	SnoalL-like polyketide synthase	Metabolism	No
32502	Subtilisin-related protease	Metabolism	Yes
71659	Subtilisin-related protease	Metabolism	Yes
56633	Subtilisin-related protease	Metabolism	Yes
32465	Tannase	Metabolism	Yes
86904	Tryosinase	Metabolism	Yes
81786	Xanthine dehydrogenase-like	Metabolism	No
111799	Cell wall associated galactomannoprotein	Pathogenesis and virulence	Yes
90717	Cell wall associated galactomannoprotein Mp1 (*A. flavus*)	Pathogenesis and virulence	Yes
91279	Conidiation-specific protein 8 (*C. orbiculare*)	Pathogenesis and virulence	No
42723	Fasciclin-like	Pathogenesis and virulence	Yes
98067	Hemagglutinin lectin-like	Pathogenesis and virulence	Yes
87300	Heterokaryon incompatibility protein	Pathogenesis and virulence	Yes
14385	Heterokaryon incompatibility protein	Pathogenesis and virulence	No
104443	Hydrophobin II	Pathogenesis and virulence	No
86869	Hydrophobin II	Pathogenesis and virulence	No
100964	Hydrophobin-like	Pathogenesis and virulence	Yes

Table 4.2 Cont. Collection of 200 genes upregulated during infection

Protein ID	Annotation	Biological process	SignalP
93769	Plant proteinase inhibitor-like	Pathogenesis and virulence	Yes
95022	Proteophosphoglucan cell wall protein	Pathogenesis and virulence	Yes
111141	SCP-like extracellular protein	Pathogenesis and virulence	Yes
98167	StcD-like	Pathogenesis and virulence	Yes
99601	Ca^{2+} -modulated nonselective cation channel polycystin	Signaling	Yes
87532	Ca^{2+} -modulated nonselective cation channel polycystin	Signaling	Yes
95741	Ca^{2+} -modulated nonselective cation channel polycystin	Signaling	Yes
22441	GPCR (*PTH11*-like)	Signaling	No
48334	GPCR (CFEM-domain, *PTH11*-like)	Signaling	Yes
3784	Tyrosine protein phosphatase	Signaling	Yes
92520	Nuclear pore complex subunit Nro1 (*S. pombe*)	Signaling	No
111854	Chloroperoxidase	Stress and defense	Yes
109174	Chloroperoxidase	Stress and defense	Yes
87914	Chloroperoxidase	Stress and defense	Yes
70955	Chloroperoxidase	Stress and defense	Yes
55888	Chloroperoxidase	Stress and defense	Yes
39839	Chloroperoxidase	Stress and defense	No
72150	Chloroperoxidase	Stress and defense	Yes
53106	Chloroperoxidase	Stress and defense	Yes
46101	Chloroperoxidase	Stress and defense	Yes
43414	Chloroperoxidase	Stress and defense	No
85519	Cytochrome p450 E-class, group 1	Stress and defense	Yes
36547	GroES-like chaperonin 10	Stress and defense	Yes
53227	Heat shock protein Hsp70	Stress and defense	No
86670	IgE- binding protein	Stress and defense	Yes

Table 4.2 Cont. Collection of 200 genes upregulated during infection

Protein ID	Annotation	Biological process	SignalP
88230	Protein or carbohydrate binding, Apple-like protein	Stress and defense	Yes
33054	RTA-1 like protein	Stress and defense	Yes
107114	Stress response protein rds1	Stress and defense	Yes
41432	Virginiamycin B hydrolyase (defense related)	Stress and defense	Yes
48019	ABC transporter (ATP-binding cassette)	Transport	No
99788	Alkylglycerol monooxygenase	Transport	No
85555	Amino acid permease	Transport	No
57026	Aquaporin-like	Transport	Yes
115275	Aquaporin-like protein	Transport	No
10258	Cytochrome b-561 / Ferric reductase transmembrane protein	Transport	No
44499	Dynamin GTPase	Transport	No
70365	Fe3+ ABC transporter periplasmic protein	Transport	Yes
31663	GPR1/FUN34/Yaah-class plasma membrane protein	Transport	No
115779	MFS monocarboxylate transporter	Transport	No
116272	MFS sugar transporter	Transport	No
115669	MFS sugar transporter	Transport	Yes
109963	MFS transporter	Transport	No
108599	MFS transporter	Transport	No
108408	MFS transporter	Transport	Yes
102199	MFS transporter	Transport	No
84892	MFS transporter	Transport	No
66198	MFS transporter	Transport	No
61150	MFS transporter	Transport	Yes
51371	MFS transporter	Transport	No

Table 4.2 Cont. Collection of 200 genes upregulated during infection

Protein ID	Annotation	Biological process	SignalP
38318	MFS transporter	Transport	No
87204	Multidrug transporter	Transport	No
95563	Nucleoside triphosphate hydrolase	Transport	No
48711	Oligopeptide transporter protein	Transport	No
88954	VAMP-like	Transport	Yes
113425	Hypothetical protein	--	Yes
108411	Hypothetical protein	--	Yes
102911	Hypothetical protein	--	Yes
102061	Hypothetical protein	--	Yes
101414	Hypothetical protein	--	Yes
99453	Hypothetical protein	--	Yes
98586	Hypothetical protein	--	Yes
97640	Hypothetical protein	--	Yes
96315	Hypothetical protein	--	Yes
95505	Hypothetical protein	--	Yes
94159	Hypothetical protein	--	Yes
91217	Hypothetical protein	--	Yes
91190	Hypothetical protein	--	Yes
90003	Hypothetical protein	--	Yes
89435	Hypothetical protein	--	Yes
89005	Hypothetical protein	--	Yes
88538	Hypothetical protein	--	Yes
86900	Hypothetical protein	--	Yes
86659	Hypothetical protein	--	Yes
86414	Hypothetical protein	--	Yes

Table 4.2 Cont. Collection of 200 genes upregulated during infection

Protein ID	Annotation	Biological process	SignalP
85890	Hypothetical protein	--	Yes
84073	Hypothetical protein	--	Yes
83631	Hypothetical protein	--	Yes
82871	Hypothetical protein	--	Yes
82328	Hypothetical protein	--	Yes
81723	Hypothetical protein	--	Yes
80689	Hypothetical protein	--	Yes
3662	Hypothetical protein	--	Yes
3197	Hypothetical protein	--	Yes
81519	Hypothetical protein	--	Yes
121885	Hypothetical protein	--	No
103377	Hypothetical protein	--	No
102381	Hypothetical protein	--	No
101604	Hypothetical protein	--	No
100697	Hypothetical protein	--	No
99793	Hypothetical protein	--	No
99450	Hypothetical protein	--	No
99361	Hypothetical protein	--	No
98509	Hypothetical protein	--	No
97292	Hypothetical protein	--	No
97285	Hypothetical protein	--	No
96877	Hypothetical protein	--	No
94853	Hypothetical protein	--	No
94708	Hypothetical protein	--	No
94240	Hypothetical protein	--	No

Table 4.2 Cont. Collection of 200 genes upregulated during infection

Protein ID	Annotation	Biological process	SignalP
92472	Hypothetical protein	--	No
92405	Hypothetical protein	--	No
91991	Hypothetical protein	--	No
91709	Hypothetical protein	--	No
91041	Hypothetical protein	--	No
90876	Hypothetical protein	--	No
90699	Hypothetical protein	--	No
90124	Hypothetical protein	--	No
89890	Hypothetical protein	--	No
88782	Hypothetical protein	--	No
88026	Hypothetical protein	--	No
87938	Hypothetical protein	--	No
87908	Hypothetical protein	--	No
87691	Hypothetical protein	--	No
84627	Hypothetical protein	--	No
84389	Hypothetical protein	--	No
82979	Hypothetical protein	--	No
82844	Hypothetical protein	--	No
82684	Hypothetical protein	--	No
81783	Hypothetical protein	--	No
81681	Hypothetical protein	--	No
49762	Hypothetical protein	--	No
48104	Hypothetical protein	--	No
46514	Hypothetical protein	--	No

Table 4.3. Hypothetical proteins highly expressed during infection

Protein ID	SignalP	Amino acids	Cysteines	Homology	% Cysteine residues
82871	Yes	118	14	None	12%
101414	Yes	209	14	None	7%
89435	Yes	203	13	4 Fungi	6%
90003	Yes	96	6	None	6%
84073	Yes	106	6	5 *Glomerella* sp.	6%
102911	Yes	134	7	None	5%
81723	Yes	412	21	None	5%
3662	Yes	157	8	>10 Fungi	5%
83631	Yes	105	5	2 Dothideomycete spp.	5%
89005	Yes	106	5	None	5%
88538	Yes	278	13	None	5%
85890	Yes	119	4	1 Dothideomyce*t*e sp.	3%
108411	Yes	368	12	>10 Fungi	3%
97640	Yes	269	8	None	3%
102061	Yes	114	3	None	3%
86900	Yes	623	15	>10 Fungi	2%
91217	Yes	90	2	None	2%
80689	Yes	225	5	None	2%
86414	Yes	187	4	None	2%
3197	Yes	472	7	>10 Fungi	1%
81519	Yes	347	5	>10 Fungi	1%
113425	Yes	321	4	>10 Fungi	1%
86659	Yes	244	3	>10 Fungi	1%
82328	Yes	169	2	None	1%
94159	Yes	183	2	None	1%

Table 4.3 Cont. Hypothetical proteins highly expressed during infection

Protein ID	SignalP	Amino acids	Cysteines	Homology	% Cysteine residues
95505	Yes	92	1	1 Dothideomycete sp.	1%
96315	Yes	108	1	1 Dothideomycete sp.	1%
99453	Yes	551	0	None	0%
98586	Yes	159	0	1 Dothideomycete sp.	0%
91190	Yes	125	0	2 Dothideomycete spp.	0%
121885	No	247	1	>10 Fungi	0%
103377	No	246	4	3 Dothideomycete spp.	2%
102381	No	276	3	2 Dothideomycete spp.	1%
101604	No	123	4	3 Dothideomycete spp.	3%
100697	No	189	4	>10 Fungi	2%
99793	No	330	2	None	1%
99450	No	423	1	>10 Fungi	0%
99361	No	385	8	>10 Fungi	2%
98509	No	50	0	None	0%
97292	No	167	1	None	1%
97285	No	344	3	None	1%
96877	No	172	4	2 Dothideomycete spp.	2%
94853	No	209	2	None	1%
94708	No	213	3	None	1%
94240	No	325	5	>10 Fungi	2%
92472	No	272	1	>10 Fungi	0%
92405	No	66	1	None	2%
91991	No	51	1	None	2%
91709	No	171	1	1 Dothideomycete sp.	1%

Table 4.3 Cont. Hypothetical proteins highly expressed during infection

Protein ID	SignalP	Amino acids	Cysteines	Homology	% Cysteine residues
91041	No	58	7	5 *F. oxysporum* isolates	12%
90876	No	77	0	1 Dothideomycete sp.	0%
90699	No	56	4	None	7%
90124	No	55	1	None	2%
89890	No	88	2	None	2%
88782	No	101	1	None	1%
88026	No	113	0	>10 Fungi	0%
87938	No	520	8	10 *F. oxysporum* isolates	2%
87908	No	162	0	None	0%
87691	No	272	8	6 Dothideomycete spp.	3%
84627	No	177	8	>10 Fungi	5%
84389	No	335	5	1 Dothideomycete sp.	1%
82979	No	239	2	None	1%
82844	No	154	5	None	3%
82684	No	204	7	None	3%
81783	No	257	9	None	4%
81681	No	147	2	None	1%
49762	No	120	8	>10 Fungi	7%
48104	No	73	8	8 Fungi	11%
46514	No	331	6	>10 Fungi	2%

CHAPTER V: THE DISCOVERY AND CHARACTERIZATION OF NOVEL GENES INVOLVED IN STOMATAL TROPISM, APPRESSORIUM FORMATION AND INFECTION IN *CERCOSPORA ZEAE-MAYDIS* THROUGH FUNCTIONAL GENOMIC APPROACHES.

Summary

Despite the global agronomic importance of gray leaf spot of maize caused by *Cercospora zeae-maydis*, very little is known about the genetic regulation of pre-penetration infectious growth prior to leaf infection. Thus, forward and reverse genetic approaches were utilized to identify and disrupt genes involved in the preinfection phase of disease development. A collection of 1228 tagged, insertional mutants was created and assayed for defects relating to germination, growth, and appressorium formation. Ten mutants were identified with defects in stomatal tropism, appressorium formation and/or conidiation during foliar egress. The genomic lesions were defined in four of the strains. One of the mutants was disrupted in a gene orthologous to a Major Royal Jelly protein of honeybees. This gene, designated *RJP1*, is predicted to be an epigenetic regulator of gene expression. In a reverse genetics approach, thirty-one putative regulatory genes were identified and targeted for functional disruption. The reverse genetic screen characterized several genes putatively involved in signal transduction and circadian regulation. *GPA2*, a Gα subunit and a component of G protein signaling, was shown to regulate pathogenic development. However, the related Gα subunits *GPA1* and *GPA3* were dispensable for pre penetration infectious development. Together, the strains identified and characterized in this study provide novel genetic resources to help dissect pathogenesis in *C. zeae-maydis*.

Introduction

Forward and reverse genetic approaches are invaluable methods to elucidate genes involved in important biological processes in fungi. The generation of collections of genome-wide knockout mutants of the model yeasts *Schizosaccharomyces pombe* and *Saccharomyces cerevisiae* have provided a wealth of knowledge regarding the genetic regulation of important biological processes in fungi (Gleaver et al., 2002; Kim et al., 2010, Ram, 2013). For example, mutants defective in sporulation and meiosis have been identified and characterized in *S. pombe* during numerous genetic screens. Initially, *spo* mutants were discovered by screening random mutants for disruptions in sporulation (Bresh et al., 1968; Kishida and Shimoda, 1986), and more recent forward and reverse genetic approaches have identified additional genes involved both processes (Gregan et al., 2005; Martin-Castellanos et al., 2005; Ucisik-Akkaya et al., 2014). In the budding yeast *S. cerevisiae*, screening collections of random gene-deletion mutants has identified hundreds of genes involved in sporulation (Deutschbauer et al., 2002; Enyenihi and Saunders, 2003; Marston et al., 2004). Despite the success of these screens, they were not saturating and additional genes likely remain undiscovered (Ucisik-Akkaya et al., 2014). Also, about 20% of yeast genes are lethal when disrupted, which hinders functional analysis (Gleaver et al., 2002; Kim et al., 2010).

Similar screens have been conducted on filamentous fungi, which identified genes required for growth, development and pathogenesis. Temperature stress has been utilized to screen mutant collections for genes regulating nuclear division and cytoskeleton dynamics (Morris and Enos, 1992; Osmoni and Mirabito, 2004), and larger collections of *Aspergillus nidulans* temperature-sensitive mutants and *Aspergillus niger* cell wall mutants are available but limitedly characterized (Harris et al., 1994, Damveld et al., 2008). Genetic screens have also

been utilized to elucidate pathogenesis in many plant pathogenic fungi (Bolker et al., 1995; Linnemannstons et al., 1999; Kahmann and Basse, 1999; Balhadere et al., 1999; Thon et al., 2000; Covert et al., 2001; Weld et al., 2006). For example, the role of the Cystathionine beta lyase gene *CBL1* and the methionine synthase gene *MSY1* in pathogenesis was revealed by a forward screen in the maize and wheat pathogen *Fusarium graminearum*, along with the discovery and characterization of a species-specific b-ZIP transcription factor (Seong et al., 2005). The success of both forward and reverse genetic screens in filamentous fungi highlights the usefulness of these genetic tools to discover and characterize novel genes involved in important biological processes.

The filamentous ascomycete *Cercospora zeae-maydis* causes gray leaf spot of maize, a major yield-limiting disease of maize present throughout the world (Latterell and Rossi, 1983; Ward et al., 1997; Ward et al., 1999; Dunkle and Levy, 2000). Prior to leaf infection, germinating conidia of *C. zeae-maydis* exhibit hyphal reorientation toward distant stomata (Kim et al., 2011b). Stomatal tropism culminates in the formation of appressorium in physical association with the stomatal pore that are required for penetration into the underlying mesophyll tissue (Kim et al., 2011b). The apparent preference for physical contact between hyphae and stomata to elicit appressorium formation is uncommon across the fungi, and very little is known regarding how fungi sense and respond to their environment during infection (Bahn et al., 2007). This is especially true in the case of sensing distant stimuli; such as the unknown stomatal cue that triggers hyphal reorientation toward stomata (Bahn et al., 2007; Chapter 2). Despite the importance of gray leaf spot and related diseases on most agriculturally important plants, there are few promising genetic targets for functional characterization that relate to host sensing, appressorium formation and pathogenesis. *CZK3*, a mitogen-activated protein kinase kinase

kinase is required for conidiation, wild-type hyphal development and infection in *C. zeae-maydis* (Shim and Dunkle, 2003). Also, the blue-light photoreceptor *CRP1* was recently shown to regulate appressorium formation and was required for lesion formation (Kim et al., 2011b), which implicated light sensing with stomatal tropism and appressorium formation.

In this study, 1228 random insertional mutants were developed and assayed for phenotypes involved in pathogenesis. From the mutant collection, nine mutants exhibited reductions in pre-penetration development and one displayed a reduction in conidiation following lesion formation, and was catalogued for future investigation. Concurrently, 31 genes were selected for targeted disruption based on similarities to known regulatory genes and genes involved in circadian gene expression in other fungi. Together, these approaches identified several genes involved in the regulation of pathogenesis in *C. zeae-maydis*, and the strains developed in this study represent a significant increase of molecular resources for future research in this system.

Materials and Methods

Strains and culture conditions. *C. zeae-maydis* (strain SCOH1-5) was utilized as the wild-type strain for this study. The development of the GFP-reporter strain SCOH1-5-GFP3 was described in Chapter Two. The *C. zeae-maydis* targeted gene-disruption strains generated for this study are described in Table 5.1. All strains were maintained on V8 agar medium, incubated at room temperature in darkness, and sub-cultured on fresh media every four days to maintain conidiation. Conidia were harvested with 10 mL sterile water per Petri dish and quantified with a hemocytometer. All Isolates developed for this study were stored at -80°C in 25% glycerol.

Creation of randomly tagged *C. zeae-maydis* mutants. Plasmid gGFP was obtained from the Fungal Genetics Stock Center (Kansas City, MO; McClusky, 2003). Plasmid pBYR73,

containing the *GFP* gene driven by the *trpC* promoter and geneticin resistance gene, GEN^R, driven by the *gpdA* promoter was acquired from the Bluhm lab plasmid stocks (Appendix 1). Plasmid pTA-HYG containing a *trpC*-driven hygromycin resistance gene, HYG^R, was obtained from the Bluhm laboratory stocks (Appendix 2). Plasmid DNA was isolated with a Fermentas Plasmid Mini-prep kit (Thermo Fisher Scientific, Glen Burnie MA). The GFP/GEN^R cassette from pBYR48 was amplified with PCR primers M13spmkrF and M13spmkeR (Appendix 3) and concentrated by ethanol precipitation following established protocols (Sambrook and Russell, 2001). The PCR product was transformed into protoplasts of the wild-type strain SCOH1-5 as previously described (Kim et al., 2011b) to generate the random insertional mutant strains. Fungal strains expressing GFP were visually selected with the DFP-1 Dual Fluorescent Protein Flashlight (NightSea, Bedford MD) and subsequently cultured on V8 medium amended with 400 μg/ml geneticin.

Disruption of specific genes in *C. zeae-maydis*. Disruption cassettes were constructed with the split-marker PCR strategy (Appendix 3; Fu et al., 2006; Ridenour et al., 2012). In *C. zeae-maydis*, DNA fragments corresponding to a 5' upstream and 3' downstream region flanking each gene were amplified with primer sets CZM XXX F1/CZM XXX F2, and CZM XXX F3/CZM XXX F4, respectively (where "XXX" stands for the abbreviation for the targeted gene; Appendix 3). To create the split selectable marker, 1 kb portions of the 1.4 kb hygromycin B phosphotransferase (HYG^R) gene cassette were amplified from pTA-HYG with primers M13F/HY1 and M13F/YG1. Two fusion products combining 5' to HY and YG to 3' were created using primers CZM XXX F1n/HY2 and CZM XXX F4n/YG2. Protoplasts of *C. zeae-maydis* strain SCOH1-5 were transformed as previously reported (Kim et al., 2011b). After seven days, transformants were subcultured on V8 medium containing 150 μg/mL hygromycin

and sub-cultured every four days to increase colony size. Genomic DNA was extracted following standard protocols (Doyle and Doyle, 1992) and transformants were screened by PCR with primers CZM XXX A1/ HYG SCRN B and CZM XXX A1/ CZM XXX F2. The isolates that tested positive for a targeted disruption were subjected to a secondary PCR screen with primers CZM XXX A1/ CZM XXX F2, CZM XXX A1/HYG SCRN B, CZM XXX A2/CZM XXX F3, and CZM XXX A2/HYG SCRN C to identify strains disrupted in the target gene.

Genomic analysis of the C. *zeae-maydis* random insertional mutants. Fungal genomic DNA was isolated with the modified CTAB extraction method (Doyle and Doyle, 1992). Southern blot analyses were performed to characterize the integration of the mutagenesis cassette in the insertional mutant strains. The digests were fractionated by electrophoresis in 0.7% agarose gels and transferred to nylon membranes (Sambrook and Russell, 2001). To verify integration of the GFP-GEN^R (Green fluorescent Protein - geneticin resistance) cassette, the GFP probe was amplified from purified pBYR48 plasmid DNA with primers GFPpf/GFPpr. Probes were radiolabelled with the Klenow labeling procedure (Sambrook and Russell, 2001). Southern blots were performed with the alkaline transfer method (Sambrook and Russell, 2001), and washed (Flaherty et al., 2003) according to established protocols.

The Universal Genome Walker kit (Clonetech, Palo Alto, CA) was used to determine sites of cassette insertion in the random insertional mutants with the following modifications. Five libraries for each insertional mutant were created by digesting 5 µg genomic DNA with EcoRV, PvuII, ScaI, RsaI, XmnI in a 100 µl reaction and incubating at 37°C overnight. Restriction digests were terminated by incubation at 70°C for 20 minutes, purified with an equal volume of chloroform, vortexed, and centrifuged at 13,000 rpm for 5 minutes. DNA was precipitated from the aqueous phase by adding 0.1 volume of 3M sodium acetate and 2.2

volumes of 100% EtOH (-20°C), followed by gentle inversion and incubation at -20°C for an hour. Precipitated DNA was centrifuged for 5 minutes at 13,000 rpm, the supernatant was discarded, and the pellet was washed as described above with 70% EtOH. The DNA pellet was dissolved with 20 µl 65°C H_2O and adaptors were ligated as described in the kit protocol. PCR conditions outlined in the protocol were used; however, the final extended polymerization step was omitted. The site of cassette insertion required the PCR amplification of genomic DNA representing the sequence bordering the GFP and GEN^R external flanks of the mutagenesis cassette. The product of the initial PCR amplifying flanking DNA was used as template for a second PCR. This reaction utilized nested annealing sites to increase amplification specificity. Putative amplicons were extracted from the gel and purified with a Gel Extraction Kit (Fermentas, Glen Burnie, MA). Purified DNA was sequenced with primers GFPsq or GENsq depending on the expected amplicon, along with primer AP2 to provide bi-directional sequence information. Samples were sequenced by the University of Arkansas DNA Sequencing Center (Fayetteville, AR) and compared to the sequenced genome hosted by the Department of Energy-Joint Genome Institute (http://genome.jgi-psf.org/Cerzm1/Cerzm1.home.html) with the Basic Local Alignment Search Tool (BLAST) search.

Evaluation of the infection process. Maize cultivar Silver Queen was inoculated when plants were approximately three weeks old. Plants were either inoculated with 10 ml of conidia suspension (10^5 conidia/ml) with 0.01% Triton X-100 by an atomizer attached to an air compressor, or the spore suspension was applied with a clean paintbrush until inoculum run-off. Inoculated plants were covered in small wire cages wrapped in opaque plastic to maintain high humidity. Plants inoculated with *C. zeae-maydis* were incubated in a growth chamber at 23°C with a 14:10 light:dark photoperiod with a light intensity at leaf level of 300 µmol m^{-2} s^{-1}. The

pathogenicity assays were performed three times with similar results. Infected leaves were collected between three and seven days after infection. Leaves were examined with a Nikon Eclipse 90i for routine observations and measurements. Hyphal characteristics were measured with the analysis program ImageJ as performed previously (Chapter Two). Images were edited for color and clarity in either Adobe Photoshop or NIS Elements.

Results and Discussion

Creation of a random insertional mutant collection. Achieving stable, homokaryotic transformation in fungi can be achieved utilizing a variety of mechanisms. For example, many different transformation approaches have been developed for a wide range of filamentous fungi (Mullins and Kang, 2001; Ruiz-Diez, 2002; Michielse et al., 2005). Successful transformations have been performed with $CaCl_2$/polyethylene glycol (Balance et al., 1993; Lorito et al., 1993; Fitzgerald et al, 2003; Ridenour et al., 2013), electroporation (Ward et al., 1989; Ozeki et al., 1994; Kuo et al., 2004) particle bombardment (Parker et al., 1995; Te'o et al., 2002) and *Agrobacterium tumefaciens* (Michielse et al., 2005). Restriction Enzyme Mediated Integration (REMI) is a common and proven technique for creating large collection of insertional mutants, but requires specific DNA sequences containing digestion sites for restriction enzymes (Kahmann and Basse, 1999; Weld et al., 2006). The approach utilized for this study utilized random insertional approach with a linear cassette of DNA amplified by PCR. The approach produced more than a thousand transformants during the course of this study. Random insertional mutagenesis has been widely utilized in plant pathogenic fungi to generate collections of tagged mutant strains for forward genetic screens (Kahmann et al., 1999; Thon *et al.,* 2000; Shim and Woloshuk, 2001; Seong et al., 2005). For this study, the constitutive expression of GFP was crucial for the genetic screen by allowing the examination of pre-penetration infectious

development with epifluorescence microscopy. During this study, 13 separate transformation events produced 1228 individual mutant strains constitutively expressing GFP (Table 5.2), generating an average of 94.5 ± 21.1 strains per transformation. Because *C. zeae-maydis* grows slowly in culture (~0.5 cm/two weeks), strains were subcultured by transferring conidia to fresh media periodically. Thus, the lack of rapid radial growth and the necessity to produce conidia in culture selected against mutant strains reduced in conidiation, conidial germination, or other aspects of growth and development during growth on V8 medium. After the size of the mycelium was enlarged during routine subculturing for two to three weeks, strains were inoculated onto maize.

Results of the forward genetic screen. Although the majority of the mutants (99%) were indistinguishable from the wild-type strain in the preliminary pathogenicity screen, nine mutants were identified with reduced levels of appressorium formation and stomatal tropism during pre-penetration infectious growth, and one additional mutant was identified with reductions in conidiation following lesion formation (Table 5.3, Figure 5.2). Following two separate inoculations, mutants AT 51, AT 85, AT 244, AT 387, AT 458, and AT 925 displayed reductions in appressorium formation but not stomatal tropism. Mutants AT 211, AT 277, and AT 290 were reduced in appressorium formation, but also exhibited reductions in stomatal tropism (Table 5.3, Figure 5.2). The diverse phenotypes of the identified mutants will allow for the uncoupling of stomatal tropism and appressorium biogenesis in future research. For example, it is plausible to hypothesize that related but separate pathways regulate stomatal tropism and appressorium formation. Furthermore, the biology of foliar infection displayed by other model fungi differs greatly compared to *C. zeae-maydis*, and few candidate genes exist for investigation utilizing reverse genetic approaches. Since few molecular footholds exist to dissect

either stage of infection, the forward genetic approach utilized in this study allowed for the discovery of novel genes that would have likely escaped consideration utilizing sequence homology-based comparisons.

An important phenotype that was inconsistently assayed during the mutant screen was lesion formation. Lesions were difficult to induce in greenhouse conditions, despite numerous attempts utilizing several different incubation and inoculation techniques. The only incubation conditions that led to occasional lesion development involved covering the inoculated plants in a wire cage wrapped in opaque plastic and incubating the covered plants in a growth chamber. However, during the course of this research project, lesions that formed with this approach were often small and irregularly spaced. Occasionally, incubation conditions would favor the development of foliar lesions and sporulation. When lesions were present on inoculated leaves, the lesions would be observed for errant phenotypes compared to lesions produced by the wild-type strain. One mutant, AT 1074, exhibited stomatal tropism and appressorium formation similar to wild type and formed lesions, but the strain failed to form conidia from the abnormally long erumpent conidiophores arising from infected stomata (Table 5.3, Figure 5.2). Mutant AT 1074 presented an intriguing opportunity to understand the regulation of conidiogenesis, because the phenotype of the mutant strain uncoupled conidiation *in vitro* from conidiation *in planta*. While not specifically measured during the course of this mutant screen, all inoculated strains produced similar amounts of conidia when grown on V8 medium during transformation selection and routine sub-culturing. The physiological cues that regulate conidiation in *C. zeae-maydis* are unknown, but *C. zeae-maydis* does exhibit microcycle conidiation in response to growth on water droplets and soybean trichomes, which implies complex regulatory control of conidiation that remains undiscovered (Lapaire and Dunkle, 2003). Furthermore, AT 1074 represents one of

the few genetic resources currently available to dissect aspects of pathogenesis after the switch to necrotrophy and lesion formation in *C. zeae-maydis*.

Identification of the genomic lesions in selected mutants. The copy number of the mutagenesis cassette was evaluated for each of the ten mutants with the goal of identifying and functionally characterizing single-insertion mutants by Genome Walker PCR. Mutants AT 244, AT 290, and AT 646 contained multiple insertions of the mutagenesis cassette, while the remaining mutants contained a single insertion (Fig. 5.3 A, B). The genomic lesions of four single-copy insertional mutant strains were characterized by Genome Walker PCR. The mutant strains that contained multiple cassette insertions and the strains with incomplete Genome Walker PCR data were sent for isolate re-sequencing at the Beijing Genome Institute, and that data will be utilized in the future to determine the site of cassette insertion for the remaining mutants (Table 5.4).

Disrupted genes in the random insertional mutant strains. AT 211: The disruption cassette of mutant AT 211 integrated upstream of gene 84892 (designated *MFS1*), a member of the Major Facilitator Superfamily (MFS) of transporters (Fig 5.3 C). The site of insertion was upstream of the open reading frame; potentially disrupting gene transcription by altering the promoter motifs required for transcription factor binding. MFS transport proteins are taxonomically ubiquitous polypeptide secondary carriers, which transport small solutes during responses to chemiosmotic ion gradients (Walton, 1996). Putative MFS transporters homologous to *MFS1* are present in many fungal genomes, although there are no characterized orthologs. Several related transporters regulate aspects of pathogenesis in human-pathogenic fungi (reviewed by Coleman and Mylonakis, 2009). For example, fungi utilize MFS transporters to secrete secondary metabolites that may be involved in virulence, such as T-toxin, victorin,

botrydial, AF-toxin and cercosporin (Coleman and Mylonakis, 2009; Walton 1996). Within this context, *MFS1* may be involved in secondary metabolite transport prior to foliar penetration. However, despite the importance MFS transporters, their role during growth and development on host leaves prior to penetration remains poorly understood. Mutant AT 211 contains a 5' insertion of the disruption cassette downstream of gene 42437, which encodes a putative amino acid transporter (designated *AAT1;* Fig 5.3 C). BLASTp analysis of the predicted protein identified no characterized fungal homologs. However, *AAT1* shares 10 conserved transmembrane regions with the vesicular GABA transporter unc-47 in *Caenorhabditis elegans* and the putative vacuolar amino acid transporter 7 gene *AVT7* in *S. cerevisiae* (Churcher et al., 1997; McIntire et al., 1997). Amino acid transporters are broadly conserved across diverse taxa (Reviewed by Wipf et al., 2002), yet few transporters involved in fungal pathogenesis have been characterized (Pitkin et al., 1996; Hahn et al., 1997; Alexander et al., 1999; Callahan et al., 1999; Han et al., 2001; Struck et al., 2002; Choquer et al., 2007). Of the two genes flanking the genomic lesion in mutant AT 211, *MFS1* represents an intriguing target because the mutagenesis cassette may disturb promoter activity, thus negatively affecting transcription rather than functionally disrupting the gene ORF. Interestingly, transcriptomic analysis of the genes involved in infectious growth identified *MFS1* as upregulated during growth on the leaf whereas *AAT1* was not highly expressed, indicating that *MFS1* may be involved during foliar pathogenesis (Chapter Four).

AT 51: Mutant AT 51 contained a direct insertion upstream of the start codon of gene 108599, encoding a putative MFS transporter gene (designated *MFS2*). While residing outside the open reading frame, the site of cassette insertion likely disrupted the promoter sequence of *MFS2* (Fig 5.3 D). *MFS2* shares homology with predicted MFS drug efflux transport proteins

conserved across most fungi, yet no characterized orthologs exist for direct comparison (reviewed by Coleman and Mylonakis, 2009). Virulence-associated efflux pumps in pathogenic fungi are classified in two different categories (Coleman and Mylonakis, 2009). The first class is responsible in secreting secondary metabolites, low molecular weight compounds that are not required for growth but may be involved in virulence (Keller et al., 2005; Howlett, 2006). *Cercospora* species produce numerous chemicals during host infection, including the phytotoxic compound cercosporin, thus implicating MFS transporters in regulating aspects of virulence (Callahan et al., 1999; Choquer et al., 2007). The second class of transporters involved in plant virulence are involved in efflux of defensive molecules produced by the plant during infection (Coleman and Mylonakis, 2009). *MFS2* belongs to the EmrB/QacA subfamily of drug resistance transporters, based on the characterized transporters EmrB in *Escherichia coli*, FarB in *Neisseria gonorrhoeae* and TcmA in *Streptomyces glaucescens* (Guilfoile and Hutchinson, 1992; Shafer et al., 2001; Tanabe et al., 2009). The role of MFS protein-mediated chemical efflux during plant pathogenesis is poorly understood, but the MFS gene *PEP5* in the pea pathogen *Necteria heamatoccocc*a was shown to be involved in foliar infection (Han et al., 2001; Liu et al., 2003). *PEP5* was able to confer an increase in pathogenicity when transformed into a non-pathogenic isolate, although the specific mechanism by which *PEP5* contributes to virulence remains unknown (Liu et al., 2003; Coleman and Mylonakis, 2009). Since efflux pumps are postulated to regulate concentrations of plant-derived defensive compounds like phytoalexins in fungi during infection, *MFS2* may play an important role in tolerating plant defensive chemicals. Within this hypothesis, the maize plant synthesizes defensive compounds after sensing hyphae of *C. zeae-maydis* on the leaf surface, but expression of *MFS2* mediates tolerance and promotes pathogenic development. In sum, the predicted drug efflux transporter encoded by *MFS2* has no

characterized homologs in fungi, and represents a novel target to dissect chemical transport and responses to host-derived signals during infection.

AT 277: The mutagenesis cassette in AT 277 integrated into the 3' flank of gene 33055 (designated *RJP1*), a putative ortholog of the Major Royal Jelly (*MRJ*) family of proteins in honeybees (Fig. 5.3 E; (Klaudiny et al., 1994a,b; Schmitzova et al., 1998; Albert and Klaudiny 2004; Drapeau et al., 2006). In honeybees, MRJ proteins are produced in the royal jelly fed to larva that will become future colony Queens, thus acting as a determinate of caste differentiation (Colhoun and Smith, 1960; Schmitzova et al., 1998). Royal jelly and MRJ proteins are hypothesized to function as epigenetic regulators of gene expression (Guo, 2010; Shi et al., 2012) and thus provide novelty in two different avenues of genetic research: The discovery of a potential epigenetic regulator of pathogenesis in an important fungus, and the identification of a broadly conserved regulator of gene expression that serves critical biological functions between different kingdoms of organisms (Drapeau et al., 2006). Epigenetic regulation in fungi has been linked to secondary metabolism (Shwab and Keller, 2008; Stauss and Reyes-Dominguez, 2011), and morphological transitions in yeast (Halme et al., 2004), but the role of epigenetic regulation in filamentous plant pathogens has not been conclusively shown. In sum, the discovery of *RJP1* provides a molecular foothold to unravel epigenetic regulation during pathogenesis and provides fresh insight into the regulation of infection.

AT 458: Interestingly, the partial insertion of the mutagenesis cassette in AT 458 occurred in a gene-poor region of the genome, and the disrupted locus did not correspond to any coding sequence annotated on the genome (Fig. 5.3 F). Recent scholarship on fungal genomic regulatory complexity has focused on the role of non-coding upstream intergentic regions (UIRs) on gene transcription (Noble and Andrianopoulos, 2013), which points toward the important role

of UIRs and other non-coding regions in shaping the genome during transcription. Another possibility underlying the phenotype of AT 458 is an unknown genomic insertion/deletion event that occurred during the transformation process that resulted in the observed phenotype.

The detection of multiple genes involved in solute transport and chemical efflux underscores the complexity of plant-pathogen interactions. Despite the importance of intracellular chemical transport, the specific mechanisms through which fungi respond to their hosts and environment during infection remains poorly elucidated. Furthermore, the identification of a novel epigenetic regulator of gene expression in fungi represents a new and potentially formative target to more thoroughly characterize the regulation of fungal pathogenesis.

Creation of a mutant collection by targeted mutagenesis. For this study, 31 *C. zeae-maydis* genes homologous to characterized fungal genes involved in signal transduction, environmental sensing and circadian rhythmicity were identified for disruption (Table 5.1). Split-marker constructs were successfully constructed by PCR for a majority of the genes of interest, and 640 transformants were generated for 22 of the 31 genes selected for functional disruption and characterization (Table 5.5). PCR analysis identified independent deletion strains for genes *GPA1, GPA2, GPA3, HAP3, UBL1, OS-2, PKA, FWD1, SRBA, PP4, WC2* and *NOP1* (Table 5.7; Fig 5.4; Fig 5.5). Strains containing partial insertions of the split-marker construct in the *FAC1, PTH11, FRH, PIC-5, PP1,* and *PP2* loci were also assayed by PCR (Table 5.7; Fig 5.5). For the putative *FAC1, PTH11, FRH, PIC-5, PP1,* and *PP2* disruption strains, integration of the split-marker construct was confirmed by PCR on a single flanking region of the target locus, and the strains were cataloged for future investigation (Table 5.7; Fig 5.5).

Genes involved in signal transduction and regulation of biological processes. Fungi sense environmental stimuli through numerous mechanisms, but stimuli responses through G protein signaling are broadly conserved and well characterized during pathogenesis (Liu et al., 2007, Lengeler et al., 2000). In eukaryotes, G protein heterotrimers are composed of α, β, and γ subunits that associate with the plasma membrane (Li et al., 2007). Filamentous fungi generally possess three distinct groups of α subunits (Group I, II, III), which are involved in triggering the activity of different downstream effectors during signaling (Bolker, 1998; Kays and Borkovich, 2004). In fungal G protein signaling, one of the three Gα subunits forms a heterotrimer with a Gβγ dimer (Liu et al., 2007; Neves et al., 2002). The Gα subunit is bound to a G protein-coupled receptor (GPCR), and the heterotrimer is released from the GPCR following the activation of the receptor. After release from the GPCR, the Gα subunit dissociates from the Gβγ heterodimer (Li et al., 2007). After subunit dissociation, the Gα and Gβγ moieties regulate downstream effector proteins in a variety of cellular systems (Li et al., 2007). A regulator of G protein signaling catalyzes the re-association of the Gα subunit with the Gβγ heterodimer, thus reforming the heterotrimer in association with the GPCR and completing the cycle (Li et al., 2007). While the G protein subunits are broadly conserved among fungi, the functions of individual Gα subunits during pathogenesis are variable. *C. zeae-maydis* is predicted to contain three Gα subunits, *GPA1* (Group I), *GPA2* (Group II) and *GPA3* (Group III) that were disrupted and the resulting gene deletion mutants were characterized.

GPA1: *GPA1* is a Group I Gα protein subunit with homologs that are putatively involved in extra-cellular signaling and pathogenesis in other fungi (Li et al., 2007; Kays and Borkvich, 2004). In the chestnut blight fungus *Cryphonectria parasitica,* the *GPA1* ortholog Cpg-1 is downregulated in response to members of the viral genus *Hypovirus*, leading to a delay in

MAPK activation that negatively affects virulence (Choi et al., 1995; Turina et al., 2006). In the rice blast pathogen *Magnaporthe oryzae*, the heterotrimers are formed by the Group I Gα subunit MagB (Class I Gα subunit), Mgb1 (Gβ), and the putative Gγ subunit Mgg1, and regulates appressorium formation (Liang et al., 2006; Liu and Dean, 1997; Nishimura et al., 2003). Furthermore, MagB is required for cAMP-dependent sensing of the hydrophobic leaf surface during appressorium initiation (Nishimura e al., 2003). Group I Gα proteins in *Botrytis cinerea* (Bcg1), *Fusarium oxysporum* (Fga1), *Colletotrichum trifolii* (Ctg-1*), Stagonospora nodorum* (Gna1) and *Alternaria alternata* (Aga1) also play important roles in plant pathogenesis (Truesdell et al., 2000; Gronover et al., 2001; Jain et al., 2002; Solomon et al., 2004; Tamagishi et al., 2006; Li et al., 2007). Despite the essential role of Group I Gα subunits in many plant pathogenic fungi, the deletion of *GPA1* in *C. zeae-maydis* did not affect stomatal tropism or appressorium formation prior to stomatal penetration. A common mechanistic thread exists between Class I Gα subunits Bcg1, Fga1 and Aga1 and cAMP-dependent signaling during pathogenesis (Gronover et al., 2001; Jain et al., 2001; Yamagishi et al., 2005). Since cAMP-dependent signaling regulates diverse processes in fungi through a variety of other signaling pathways (Lee et al, 2003), cAMP signaling may operate through novel pathways in *C. zeae-maydis*. Furthermore, post-penetration infectious growth was not assayed in the *GPA1* mutant strains, and *GPA1* may regulate important aspects of growth following penetration, or the switch from biotrophic to necrotrophic growth. During growth in culture, mycelia of the Δ*gpa1* strains formed fewer aerial hyphae on V8 medium and appeared dark green in color compared to the wild-type strain. The subtle growth phenotype *in vitro* did not affect culture viability during multiple rounds of routine subculturing, and the importance of the phenotype to growth and development remains unknown.

GPA2: The Group II Gα proteins are not as broadly conserved across filamentous fungi as the Group I and Group III Gα subunits, and few are considered to be involved in pathogenesis in plant pathogenic fungi (Li et al., 2007). For example, the Group II homolog MagC in *M. oryzae* regulates conidiation (Liu and Dean, 1997), and *GNA-2* in *Neurospora crassa* is involved in mycelial development on poor carbon sources (Li and Borkovich, 2006). Of the investigated Group II Gα proteins, only Bcg-2 of *B. cinerea* affects disease development, with deletion mutants exhibiting slightly reduced pathogenicity (Gronover et al., 2001). In contrast to what has been observed in filamentous fungi, *GPA2* is required for appressorium formation during pre-infectious growth of *C. zeae-maydis*. Over the course of multiple inoculations, the *GPA2* deletion mutants consistently failed to exhibit stomatal tropism and form appressoria in association with host stomata (Fig 5.7). The structural diversity of Class II Gα subunits in fungi combined with the lack of characterized pathogenesis-related orthologs to *GPA2* underscores the novelty of these results.

GPA3: Group III Gα subunits are highly conserved in filamentous fungi, and many regulate cAMP levels during host infection (Bolker, 1998; Li et al., 2007). In the maize smut pathogen *Ustilago maydis*, Gpa3 regulates mating, cAMP production, and pathogenicity by transducing extracellular signals to the cAMP signaling pathway (Kruger et al., 1998; Muller et al., 2004). In *C. zeae-maydis*, the Δ*gpa3* mutant strains exhibited stomatal tropism and appressorium formation following multiple inoculations on maize; therefore *GPA3* does not appear to regulate stomatal sensing and appressorium morphogenesis. Group III Gα alpha subunits Bcg3 of *B. cinerea* and Fga2 of *F. oxysporum* are required for virulence (Jain et al., 2005; Doehlemann et al., 2006), which suggests that *GPA3* can be involved in post-penetration development during the switch from biotrophic to necrotrophic growth.

Characterization of the three Gα subunits (*GPA1, GPA2 and GPA3*) established a model framework to further dissect signal transduction in *C. zeae-maydis*. The discovery that *GPA2*, but not *GPA1* or *GPA3*, is involved in pathogenic development implicated a specific signaling molecule involved in pathogenesis. Furthermore, the characterization of *GPA2* during stomatal tropism and appressorium formation indicated that G protein subunits function differently in *C. zeae-maydis* compared to other plant pathogenic fungi (Li et al., 2007). Within this model, *GPA2* is bound to a specific GPCR that senses the stomatal cue, and upon activation, releases the *GPA2*-bound heterotrimer to trigger downstream expression of pathogenicity genes. This hypothetical model would be better informed by the discovery of the downstream effectors regulated by *GPA2*, and especially the discovery of the GPCRs that respond to the stomatal cue and elicit pathogenic development.

HAP3: The Heme Activator Protein (HAP) complex in *S. cerevisiae* is an important heteromeric transcriptional regulator composed of the DNA binding components Hap2p, Hap3p and Hap5p, and the activator Hap4p (Hahn and Guarente, 1988; Frosburg and Guarente, 1989; Hahn et al., 1988; McNabb et al., 1995; McNabb and Pinto, 2005). The HAP complex regulates the expression of genes and putative transcriptional activators, suggesting that the HAP complex is a global regulator of gene expression (Buschlen et al., 2003). Despite the importance of HAP complex-mediated transcriptional regulation in yeast, surprisingly little is known regarding the role of the HAP complex during pathogenesis by filamentous fungi. HapX (the Hap4 ortholog in filamentous fungi) was recently shown to interact with the core complex to affect virulence in the vascular wild fungus *Fusarium oxysporum* (Lopez-Berges et al., 2012). Recently, the HAP complex subunit *HAP3* in *Fusarium verticillioides* was shown to regulate aspects of growth, morphogenesis, secondary metabolism and pathogenesis (Ridenour and Bluhm, 2014). To

investigate the role of the HAP complex in *C. zeae-maydis,* the predicted ortholog was identified and deleted from the wild-type *C. zeae-maydis* strain. Surprisingly, the Δ*hap3 C. zeae-maydis* strain did not exhibit any measureable deficiencies in growth in axenic culture, stomatal tropism or appressorium formation during foliar infection. While the possibility exists that the HAP complex functions differently in *C. zeae-maydis* compared to other fungi, only one gene-deletion strain was developed for the *HAP3* locus. Since only one deletion strain was generated and the deletion strain was not complimented, definitive conclusions from the phenotypic observations are premature and require further research.

UBL1: During protein ubiquitination, a target protein is tagged for destruction by the 28 S proteasome with ubiquitin moieties by the coordinate action of E1, E2 and E3 enzymes. In the maize pathogens *F. verticillioides* and *F. graminearum*, *UBL1* encodes a putative E3 ubiquitin ligase that is involved in environmental sensing, carbon metabolism, G protein signaling and virulence (Ridenour et al., 2014), thus making *UBL1* a promising target for disruption in *C. zeae-maydis*. However, none of the three independent gene deletion *UBL1* strains in *C. zeae-maydis* exhibited any deficiencies during growth in V8 medium, stomatal tropism or appressorium formation. The interaction between *UBL1*-mediated ubiquitination and G protein signaling in pathogenic fungi has been shown in *Fusarium* species. However, G protein signaling may operate differently in *C. zeae-maydis* and may not compare functionally to other fungi. Furthermore, the effect of *UBL1* in *C. zeae-maydis* may be observed during later stages of the infection profess, and was therefor not observed during this study.

SRBA: SRBA encodes a sterol-regulatory element binding protein that regulates ergosterol biosynthesis, hyphal morphology and virulence in the human pathogenic fungus *Aspergillus fumigatus*. The *SRBA* deletion mutants were unable to grow in hypoxic environments, and

formed bulbous hyphal apices when grown in culture (Willger et al., 2008). In order to investigate genes possibly involved in hyphal morphology and oxygen sensing in *C. zeae-maydis*, the *SRBA* homolog of *A. fumigatus* was identified and disrupted. Consistent with the expected phenotype, the resulting gene deletion mutant grew poorly in culture, and maintaining conidial development was difficult during routine subculturing. However, the *SRBA* deletion mutant was indistinguishable from the wild-type strain on maize leaves, and formed appressoria that were morphologically similar to those formed by the wild-type strain. An intriguing observation is that the loss of hyphal tip polarity in the *SRBA* deletion mutants of *A. fumigatus* appeared similar in structure to appressoria formed by *C. zeae-maydis* (Figure 5.8; Willger et al., 2008). However, a more thorough elucidation of appressorium morphology and biogenesis in *C. zeae-maydis* is required before plausible comparisons can be made between appressoria and *in vitro* mutant phenotypes of related fungi.

Genes potentially involved in circadian regulation of gene expression. *WC2:* When *N. crassa* is exposed to blue light, *white collar-1* and *white collar-2* form a heterodimeric transcription factor called the White Collar Complex (WCC), which regulates the expression of many genes including the central circadian oscillator, *Frequency* (Baker et al., 2012). Previous studies in *C. zeae-maydis* investigated this phenomenon and identified the *white collar-1* ortholog *CRP1*, which is required for stomatal tropism and appressorium formation (Kim et al., 2011b). In order to more thoroughly characterize the regulation of *Frequency* and other aspects of light-mediated gene expression, the *white collar-2* homolog was deleted from the *C. zeae-maydis* wild-type strain. All three independent deletion mutants of the *C. zeae-maydis white collar-2* homolog produced sparse, whiter mycelia compared to the other strains during growth on V8 medium (Figure 5.6). Furthermore, the Δ*wc2* mutants frequently stopped growing after 3-

4 weeks and had to be re-isolated from glycerol stocks. Interestingly, the growth and development phenotypes were in sharp contrast to the WCC component *Δcrp1* mutants, which grew similarly to the wild-type strain on V8 medium (Kim et al., 2011). Inoculation results were variable because the quality and quantity of conidia differed drastically between each experiment, due to poor growth in culture. However, appressoria were never observed after numerous inoculations. Despite the complications associated with inoculations, WC-2 is clearly involved in important aspects of development, including hyphal growth and conidiation.

FWD1: FWD1 encodes an F-Box/WD-40 repeat-containing protein in *N. crassa* that is involved in the ubiquitin-dependent degradation of the *FRQ* gene. In the *N. crassa fwd1* deletion strains, *FRQ* degradation is significantly reduced, resulting in hyperphosphorylated *FRQ* proteins that abolish normal circadian rhythms. In *N. crassa*, *FWD1* and *FRQ* physically interact *in vivo*, suggesting that *FWD1* acts as a substrate-recruitment subunit of the ubiquitin ligase responsible for targeting *FRQ (*He et al., 2003). The *FWD1* deletion strains in *C. zeae-maydis* did not differ from the wild-type strain during growth in culture or during foliar infection of maize. Despite the conservation of *FWD1* homologs in the circadian regulation of fungi and insects (He et al., 2003), *FWD1* does not appear to alter the normal physiology of *C. zeae-maydis* during growth in culture or during pathogenesis. Despite a BLASTp E-value of 2.07 E-119 and similar domain architecture between *FWD1* of *N. crassa* and the putative *C. zeae-maydis* homolog, the specific function of *FWD1* is unknown. Analysis of *FRQ* expression in the *C. zeae-maydis FWD1* deletion strains would greatly inform the hypothesis that *FWD1* genes are orthologs and both regulate *FRQ* stability in each fungus. However, further research is needed to elucidate the relationship between *FWD-1* in *C. zeae-maydis* and circadian gene expression.

PP4: The negative feedback loop of circadian gene expression in *N. crassa* depends on the phosphorylation of the core oscillatory components in order to maintain property rhythmicity (Cha et al., 2008). Protein phosphatase 4 (PP4) regulates both processes of the feedback loop by phosphorylating *FRQ* and both dephosphorylating and activating the WCC (Chat et al., 2008). In order to further elucidate the role of circadian rhythmicity on pathogenesis in *C. zeae-maydis,* the homolog of *PP4* from *N. crassa* was deleted and the resulting strains assayed for defects during growth, development and pathogenesis. The *PP4* deletion strains all exhibited similar phenotypes to the wild-type strain during routine subculturing, and readily formed appressoria on host stomata. In *N. crassa*, the PP4 deletion mutants exhibit a subtle reduction in period amplitudes, but not a total cessation of circadian rhythmicity. If *PP4* acts upon *FRQ* and WCC in a similar manner between *N. crassa* and *C. zeae-maydis*, the small alterations in circadian rhythms may not negatively affect pre-penetration infectious growth.

PKA: In *N. crassa*, cAMP-dependent Protein Kinase A (*PKA*) expression is essential for the function of the endogenous molecular clock. In order to establish a rhythmic cycle of expression, the central oscillator *FRQ* recruits casein kinases to progressively phosphorylate *FRQ* and promote *FRQ* degradation. Within this negative feedback loop, *PKA* serves as a priming kinase for the casein kinases and stabilizes *FRQ* phosphorylation throughout the cycle (Huang et al., 2007). Since *PKA* is a major component of the circadian clock in *N. crassa*, the homolog of *PKA* was identified in *C. zeae-maydis* and disrupted. The resulting transformations yielded only one strain that was confirmed by PCR, which did not exhibit any deficiencies in pathogenic growth following inoculation on maize leaves, and grew similar to wild type in culture. Despite the consistency of the observations from the single deletion strain, it is difficult to make any conclusions without multiple, independent gene-deletion strains.

OS-2: In *N. crassa*, the osmosensing pathway is mediated through the conserved stress-activated p38-type Osmotically Sensitive-2 (*OS-2*) gene. *OS-2* is a homolog of the Hog1 MAPK in yeast and the p38 MAPK from mammals (Zhang et al., 2002). *OS-2* mediates stress responses to extra-cellular osmotic pressure, oxidative stress and heat (Hohmann, 2002; Sheikh-Hamad and Gustin, 2004), and *OS-2* is rhythmically activated by the fungal circadian clock (Vitalini et al., 2007). The activation of *OS-2* signaling prior to dawn prepares *N. crassa* for the hyperosmotic stress and desiccation that is generally associated with sun exposure (Vitalini et al., 2007; Lamb et al., 2012). Furthermore, deletion of the *OS-2* homolog MgHog1 in *Z. tritici* regulated dimorphism and pathogenicity during infection of wheat (Mehrabi et al., 2006). Since hyphae of *C. zeae-maydis* are likely exposed to similar stresses during growth on the leaf surface following germination and *OS-2* was associated with circadian regulation in *N. crassa*, the *OS-2* homolog was identified and functionally disrupted. Conidia of the deletion mutants germinated and hyphae displayed stomatal tropism and appressorium formation similar to the wild-type strain. While the phenotypes of the *OS*-2 mutant strains were contrary to what was anticipated, one potential explanation for the results is the environmental conditions associated with the inoculation parameters for this experiment. During inoculation with *C. zeae-maydis*, the humidity in the incubation chamber was maintained at nearly 100% to allow for germination and hyphal development. The controlled parameters of the experiment likely reduced the stress on the fungus during growth (unlike a natural scenario, where plants and fungi undergo rapid cycles of environmental changes like sunlight exposure, heat fluctuations and desiccation). In the closely related fungus *Z. tritici*, MgHog1 appeared to affect the transition from yeast-like to filamentous growth, which does not resemble the biology of *C. zeae-maydis*. Since *C. zeae-maydis* remains as a filamentous fungus throughout infection, the lack of a dimorphic switch

could account for the disparity between the two findings (Mehrabi et al., 2006). Furthermore, *OS-2* homologs *in M. oryzae, C. lagenarium* and *Bipolaris oryzae* were dispensable for pathogenesis (Dixon et al., 1999; Kojima et al. 2004; Moriwaki et al, 2006). In *C. zeae-maydis*, another MAP kinase kinase kinase gene, *CZK3,* is a key regulator of growth, pathogenesis and secondary metabolism (Shim and Dunkle, 2003). *CZK3* deletion strains failed to produce the toxin cercosporin in culture, did not form conidia or melanized hyphae, and did not cause lesions following multiple inoculations (Shim and Dunkle, 2003). Based on these observations, *C. zeae-maydis* does require certain MAP kinase-related genes for aspects of growth, metabolism and virulence, but *OS-2* is not required for stomatal tropism or appressorium formation. However, the potential functions of *OS-2* during responses to environmental stresses and later stages of infection are unknown.

NOP1: In *N. crassa*, the putative green-light opsin photoreceptor *nop*-1 is expressed during conidiation and directly modulates carotenogenesis. Also, *nop-1* is negatively regulated by *white collar-2* in a blue-light dependent manner (Biezke et al., 1999; Bieszke and Borkovich, 2007). In order to further elucidate the role of broad-spectrum light sensing on pathogenesis of *C. zeae-maydis*, the homolog of the *N. crassa nop-1* gene was disrupted in the *C. zeae-maydis* wild-type strain. The Δ*nop1* strain grew on V8 media and exhibited wild-type levels of stomatal tropism and appressorium formation on maize leaves, indicating that *NOP1* is not involved in aspects of growth and pathogenesis. Surprisingly, despite the characterized role in conidiation in *N. crassa,* the *C. zeae-maydis* Δ*nop1* strain did not produce abnormal amounts of conidia during routine subculturing on V8 media throughout the experiment.

In summary, this study utilized both forward and reverse genetic approaches to identify several previously uncharacterized genes in *C. zeae-maydis* involved in pathogenesis. A forward

genetic screen yielded ten candidate mutants for future characterization, and subsequent analysis identified genes involved in solute transport and a broadly conserved regulatory gene putatively involved in epigenetic regulation of pathogenesis. Targeted deletion and characterization of the Gα subunits unveiled the role of *GPA2* in pathogenesis, and identified an important signaling pathway that appears to function somewhat uniquely in *C. zeae-maydis* compared to other model fungi. Furthermore, several conserved regulatory genes in related fungi had limited impact on growth, development and pathogenesis of *C. zeae-maydis*, which suggests that the genetic models elucidated in non-pathogenic fungi may not be broadly conserved among plant pathogens. Lastly, the developed but uncharacterized strains produced by this study represent a significant resource for future functional genomics experiments in *C. zeae-maydis*, and promises to continue to produce novel discoveries for the foreseeable future.

References

Albert, S. and Klaudiny, J. 2004. The MRJP/YELLOW protein family of *Apis mellifera*: Identification of new members in the EST library. *J. Insect Physiol*. 50: 51–59.

Alexander, N., McCormick, S., and Hohn, T. 1999. TRI12, a trichothecene efflux pump from*Fusarium sporotrichioides*: gene isolation and expression in yeast. *Mol Gen Genet* 261:977-984.

Bahn, Y-S., Xue, C., Idnurm, A., Rutherford, J.D., Heitman, J. 2007. Sensing the environment: lessons from fungi. *Nature Rev Microbiol* 5:57-69.

Balhadere, P.V., Foster, A.J., Talbot, N.J. 1999. Identification of pathogenicity mutants of the rice blast fungus *Magnaporthe grisea* by insertional mutagenesis. *Mol Plant Microbe Interact* 12:129-142.

Ballance, D.J., Buxton, F.P., and Turner, G.. 1983. Transformation of *Aspergillus nidulans* by the ornithine-5'-phosphate decarboxylase gene of *Neurospora crassa. Biochem Biophys Res Commun* 112:284-289.

Ballario P. and Macino G. 1997. White collar proteins: PASsing the light signal in *Neurospora crassa*. *Trends Microbiol*. 5: 458–462.

Bieszke J.A., Braun E.L., Bean L.E., Kang S., Natvig D.O. et al. 1999. The nop-1 gene of *Neurospora crassa* encodes a seven transmembrane helix retinal-binding protein homologous to archaeal rhodopsins. *Proc Natl Acad Sci USA* 96: 8034–8039.

Bieszke J.A. and Borkovich K.A. 2007. The fungal opsin gene nop-1 is negatively-regulated by a component of the blue light sensing pathway and influences conidiation-specific gene expression in *Neurospora crassa. Curr Genet* 52:149-157.

Bolker, M., Bohnert,, H.U., Braun, K.H., Gorl, J., Kahmann, R. 1995. Tagging pathogenicity genes in *Ustilago maydis* by restriction enzyme mediated integration (REMI). *Mol Gen Genet* 248:547-552.

Bolker M. 1998. Sex and crime: heterotrimeric G proteins in fungal mating and pathogenesis. *Fungal Genet Biol*. 25:143–56

Brand A., Shanks S., Duncan V.M.S., Yang M., Mackenzie K., Gow N.A.R. 2007. Hyphal orientation of *Candida albicans* is regulated by a calcium-dependent mechanism. *Curr Biol* 17:347–352.

Bresch, C.,G., Muller, Egel, R. 1968. Genes involved in meiosis and sporulation of a yeast. *Mol Gen Genet* 102:301-306.

Buschlen S., Amillet J-M., Guiard B., Fournier A., Marcireau C., Bolton-Fukuhara M. 2003. The *S. cerevisiae* HAP complex, a key regulator of mitochondrial function, coordinates nuclear and mitochondrial gene expression. *Comp Funct Genom* 4: 37-46.

Busov V.B., Meilan R., Pearse D.W., Ma C., Rood S.B., Strauss S.H. 2003. Activation tagging of a dominant gibberellin catabolism gene (GA 2-oxidase) from Poplar that regulates tree structure. *Plant Phys* 132: 1283-1291.

Callahan, T.M., Rose, M.S., Meade, M.J., Ehrenshaft, M., and Upchurch, R.G. 1999. CFP, the putative cercosporin transporter of *Cercospora kikuchii*, is required for wild type cercosporin production, resistance, and virulence on soybean. *Mol Plant-Microbe Interact* 12:901-910.

Cha J., Chang S.S., Huang G., Cheng P. and Liu Y. 2008. Control of WHITE COLLAR localization by phosphorylation is a critical step in the circadian negative feedback process. *EMBO J* 27: 3246–3255.

Cheng P., He Q., Wang L. and Liu Y. 2005. Regulation of the *Neurospora* circadian clock by an RNA helicase. *Gene Dev* 19: 234–241.

Choquer, M., Lee, M., Bau, H., Chung, K. 2007. Deletion of a MFS transporter-like gene in *Cerospora nicotianae* reduces cerosporin toxin accumulation and fungal virulence. *FEMS Letters* 581:489-494.

Choi G.H., Chen B., Nuss D.L. 1995. Virus-mediated or transgenic suppression of a G protein a subunit and attenuation of fungal virulence. *Proc. Natl. Acad. Sci. USA* 92:305–9

Choi Y.E. and Xu JR. 2010. The cAMP signaling pathway in *Fusarium verticillioides* is important for conidiation, plant infection, and stress responses but not fumonisin production. *Mol Plant Microbe Interact*. 23:522-533.

Churcher, C.M., Bowman, S., Badcock, K., Bankier, A.T., Brown, D. et al. 1997. The nucleotide sequence of Saccharomyces cerevisiae chromosome IX. *Nature* 387: 84-87.

Colhoun, E.H. and Smith, M.V. 1960. Neurohormonal properties of royal jelly. *Nature* 188: 854–855.

Coleman, J.J. and Mylonakis, E. 2009. Efflux in fungi: La Piece de Resistance. *PLoS Pathol* 5(6): e1000486

Covert, S.F., Kapoor, P., Lee, M.H., Briley, A., and Nairn, C.J. 2001 *Agrobacterium tumefaciens*-mediated transformation of *Fusarium cirinatum*.*Mycol Res* 105:259-64.

Damveld R.A., Franken A., Arentshorst M., Punt P.J., Klis F.M., et al. 2008. A novel screening method for cell wall mutants in *Aspergillus niger* identifies UDP-galactopyranose mutase as an important protein in fungal cell wall biosynthesis. *Genetics*. 178: 873-881.

DeZwaan T.M., Carrol A.M., Valent B. and Sweigard J.A. 1999. *Magnaporthe grisea* pth11p is a novel plasma membrane protein that mediates appressorium differentiation in response to inductive substrate cues. *Plant Cell* 11:2013-2030.

Dixon, K. P., Xu, J. R., Smirnoff, N., and Talbot, N. J. 1999. Independent signaling pathways

regulate cellular turgor during hyperosmotic stress and appressorium-mediated plant infection by *Magnaporthe grisea. Plant Cell* 11:2045-2058.

Doehlemann G, Berndt P, Hahn M. 2006. Different signaling pathways involving a G alpha protein, cAMP and a MAP kinase control germination of *Botrytis cinerea* conidia. *Mol Microbiol* 59:821-35

Doyle J.J. and Doyle J.L. 1990. A rapid total DNA preparation procedure for fresh plant tissue. *Focus* 12: 13-15.

Drapeau M.D., Albert S., Kucharski R., Prusko C., and Maleszka R. 2006. Evolution of the Tellow/Major Royal Jelly Protein family and emergence of social behavior in honey bees. *Gen Res* 16: 1385-1394.

Fitzgerald, A.M., Mudge, A.M., Gleave, A.P., Plummer, K.M.. 2003. *Agrobacterium* and PEG-mediated transformation of the phytopathogen *Venturia inaequalis*. *Mycol Res* 107:803-810.

Flaherty J.E., Pirttila A.M., Bluhm B.H. and Woloshuk C.P. 2003. PAC1, a pH- regulatory gene from *Fusarium verticillioides*. *Appl Environ Microbiol* 9: 5222-5227.

Forsburg S.L. and Guarente L. 1989. Communication between mitochondria and the nucleus in regulation of cytochrome genes in the yeast *Saccharomyces cerevisiae. Ann Rev Cell Biol* 5: 153-180.

Froehlich A.C., Noh B., Vierstra R.D., Loros J., Dunlap J.C. 2005. Genetic and molecular analysis of phytochromes from the filamentous fungus *Neurospora crassa*. E*ukaryot Cell* 4:2140-2152.

Fu J., Hettler E., Wickes N.L. 2006. Split marker transformation increased homologous integration frequency in *Cryptococcus neoformans*. *Fungal Genet Biol* 43: 100-121.

Glaever G., Chu A.M, Ni L., Connelly C., Riles .L, et al. 2002. Functional profiling of the *Saccharomyces cerevisiae* genome. *Nature* 418:387-391.

Gorl M., Merrow M., Huttner B., Johnson J., Roenneberg T. & Brunner M. 2001. A PEST-like element in FREQUENCY determines the length of the circadian period in *Neurospora crassa. EMBO J* 20: 7074–7084.

Gregan, J., Rabitsch, P.K., Sakem, B., Csutak, O., Latypov, V., Lehmann, E., Kohli, J., Nasmyth, K. 2005. Novel genes required for meiotic chromosome segregation are identified by a high-throughput knockout screen in fission yeast. *Curr Biol* 15:1663-1669.

Gronover CS, Kasulke D, Tudzynski P, Tudzynski B. 2001. The role of G protein a subunits in the infection process of the gray mold fungus *Botrytis cinerea*. *Mol Plant Microbe Interact* 14:1293–302

Guilfoile, P.G., and Hutchinson, C.R. 1992. The *Streptomyces glaucescens* TcmR protein represses transcription of the divergently oriented tcmR and tcmA genes by binding to an intergentic operator region. *J. Bacteriol*. 174:3659-3666.

Guo, X.Q. 2010. The development and molecular mechanism of queen-worker differentiation, the miRNAs of royal jelly make a difference to queen-worker differentiation. *National Science Library, Chinese Academy of Sciences.*156.

Hahn, S., Guarente, L.. 1988. Yeast HAP2 and HAP3: transcriptional activators in a heteromeric complex. *Science* 240:317-321.

Hahn, S., Pinkham, J., Wei, R., Miller, R., and Guarente, L. 1988. The HAP3 regulatory locus of *Saccharomyces cerevisiae* encodes divergent overlapping transcripts. *Mol Cell Biol* 8, 655–663.

Hahn, M., Neef, U., Struck, C., Gottfert, M., and Mendgen K. 1997. A putative amino acid transporter is superficially expressed in haustoria of the rust fungus *Uromyces fabae. Mol Plant Microbe Interact* 4:438-445.

Halme A., Bumgarner S., Styles C. and Fink. G.R. 2004. Genetic and epigenetic regulation of the FLO gene family generates cell-surface variation in yeast. *Cell* 116: 405-415.

Han, Y., Liu, X., Benny, U., Kistler, H.C., VanEtten, H.D. 2001. Genes determining pathogenicity to pea are clustered on a supernumerary chromosome in the fungal plant pathogen *Nectria haematococca*. *Plant J* 25:305-314.

Harris S.D., Morrell J.L. and Hamer J.E. 1994. Identification and characterization of *Aspergillus nidulans* mutants defective in cytokinesis. *Genetics*. 136: 517-532.

He Q., Cheng P., Yang Y., Yu H. and Liu Y. 2003. FWD1-mediated degradation of FREQUENCY in *Neurospora* establishes a conserved mechanism for circadian clock regulation. *EMBO J* 22: 4421–4430.

Howlett, B.J. 2006. Secondary metabolite toxins and nutrition of plant pathogenic fungi. *Curr Opin Plant Biol* 9:371-375.

Huang G., Chen S., Li S. et al. 2007. Protein kinase A and casein kinases mediate sequential phosphorylation events in the circadian negative feedback loop. *Gene Dev* 21: 3283–3295.

Jain S, Akiyama K, Mae K, Ohguchi T, Takata R. 2002. Targeted disruption of a G protein alpha subunit gene results in reduced pathogenicity in Fusarium oxysporum. Curr. Genet. 41:407–13

Jain, S., Akiyama, K., Takata, R., Ohguchi, T. 2005. Signaling via the G protein alpha subunit FGA2 is necessary for pathogenesis in *Fusarium oxysporum*. *FEMS Microbiol Lett* 243:165-172

Kahmann R., Basse C., Feldbrugge M. 1999. Fungal-plant signaling in the *Ustilago maydis*-maize pathosystem. *Curr Opin Microbiol* 2: 647-650.

Kays, A.M., Borkovich, K.A. 2004. Signal transduction pathways mediated by heterotrimeric G proteins. In The Mycota, Vol. III: Biochemistry and Molecular Biology, ed. R Brambl, G.A.

Marzluf, pp. 175–207. Berlin-Heidelberg: Springer-Verlag.

Keller, N.P., Turner, G., Bennett, J.W. 2005 Fungal secondary metabolism - from biochemistry to genomics. *Nat Rev Microbiol* 3:937-947.

Kim D.U., Hayles J., Kim D., Wood V., Park H.O., et al. 2010. Analysis of a genome-wide set of gene deletions in the fission yeast *Schizosaccharomyces pombe*. *Nat Biotechnol*. 28: 617-623.

Kim, H., Ridenour, J. B., Dunkle, L. D. and Bluhm, B. H. 2011a. Regulation of pathogenesis by light in *Cercospora zeae-maydis*: An updated perspective. *Plant Pathol J* 27:103-109.

Kim, H., Ridenour, J. B., Dunkle, L. D. and Bluhm, B. H. 2011b. Regulation of stomatal tropism and infection by light in *Cercospora zeae-maydis*: Evidence for coordinated host/pathogen responses to photoperiod? *PLoS Pathogens* PLoS Pathog 7(7): e1002113.

Kishida, M., Shimoda, C. 1986. Genetic mapping of eleven spo genes essential for ascospore formation in the fission yeast *Schizosaccharomyces pombe. Curr Genet* 10: 443-447.

Klaudiny J., Kulifajova J., Crailsheim K. and Simuth J. 1994a. New approach to the study of division of labour in the honeybee colony (*Apis mellifera* L.). *Apidologie (Celle)* 25: 596–600.

Klaudiny J., Hanes J., Kulifajova J., Albert S., and Simuth J. 1994b. Molecular cloning of two cDNAs from the head of the nurse honey bee (*Apis mellifera* L.) for coding related proteins of royal jelly. *J. Apic. Res*. 33: 105–111.

Kojima, K., Takano, Y., Yoshimi, A., Tanaka, C., Kikuchi, T., and Okuno, T. 2004. Fungicide activity through activation of a fungal signaling pathway. *Mol Microbiol* 53:1785-1796.

Kruger, J., Loubradou, G., Regenfelder, E., Hartmann, A., Kahmann, R. 1998. Crosstalk between cAMP and pheromone signaling pathways in *Ustilago maydis. Mol. Gen. Genet*. 260:193-98.

Kuo, C.Y., Chou, S.Y., and Huang, C.T..2004. Cloning of glyceraldehyde-3- phosphate dehydrogenase gene and use of the gpd promoter for transformation in *Flammulina velutipes. Appl Microbiol Biotechnol* 65:593-599.

Lamb, T.M., Finch, K.E., and Bell-Pedersen, D. 2012. The *Neurospora crassa* OS-MAPK pathway-activated transcription factor ASL-1 contributes to circadian rhythms in pathway responsive clock-controlled genes. *Fungal Gen Biol* 49:180-188.

Lapaire, C.L., and Dunkle, L.D. 2003. Microcycle conidiation in *Cercospora zeae-maydis*. *Phytopathology* 93:193-199.

Latterell, F.M., and Rossi, A.E. 1983. Gray leaf spot of maize: A disease on the move. *Plant Dis* 67:842-847.

Lee, N., D'Souza, C.A., Kronstad, J. 2003. Of smuts, blasts, mildews, and blights: cAMP

signaling in phytophathogenic fungi. *Ann Rev Phytopathol* 41:399-427.

Lengeler KB, Davidson RC, D'Souza C, Harashima T, Shen WC, et al. 2000. Signal transduction cascades regulating fungal development and virulence. *Microbiol. Mol. Biol. Rev.* 64:746–85

Li L,. and Borkovich KA. 2006. GPR-4 is a predicted G-protein-coupled receptor required for carbon source-dependent asexual growth and development in *Neurospora crassa. Eukaryot.Cell* 5:1287–300

Li Z., Vizeacoumar F.J., Bahr S., Li J., Warringer J., et al. 2011. Systematic exploration of essential yeast gene function with temperature-sensitive mutants. *Nat Biotechnol*. 29: 361-367.

Li L., Wright S.J., Krystofova S., Park, G. and Borkovich K.A. 2007. Heterotrimeric G protein signaling in filamentous fungi. *Annu Rev Microbiol* 61:423-452.

Liang S, Wang ZY, Liu PJ, Li DB. 2006. A Gg subunit promoter T-DNA insertion mutant: A1-412 of *Magnaporthe grisea* is defective in appressorium formation, penetration and pathogenicity. *Chin. Sci. Bull*. 51:2214–18

Lindsey K., Wei W., Clarke M.C., McArdle H.F., Rooke L.M. and Topping J.F. 1993. Tagging genomic sequences that direct transgene expression by activation of a promoter trap in plants. *Transgen Res* 2: 33-47.

Linnemannstons, P., Voss, T., Hedden, P., Gaskin, P., Tudzynski, B.. 1999. Deletions in the gibberellin biosynthesis gene cluster of *Gibberella fujikuroi* by restriction enzyme-mediated integration and conventional transformation-mediated mutagenesis. *Appl Environ Microbiol* 65:2558-2564.

Liu S, Dean RA. 1997. G protein a subunit genes control growth, development, and pathogenicity of *Magnaporthe grisea*. *Mol. Plant Microbe Interact. 10:1075–86*

Liu, X., Inlow, M., VanEtten, H.E.D. 2003. Expression profiles of pea pathogenicity (*PEP*) genes in vivo and in vitro, characterization of the flanking regions of the *PEP* cluster and evidence that the *PEP* cluster region resulted from horizontal gene transfer in the fungal pathogen *Nectria haematococca*. *Curr Genet* 44:95-103.

Lorito, M., Hayes, C.K., Di Pietro, A., Harman, G.E. 1993. Biolistic transformation of Trichoderma harzianum and Gliocladium virens using plasmid and genomic DNA. Curr Genet 24: 349-356.

López-Berges, M.S., Capilla, J., Turrà, D., Schafferer, L., Matthijs, S., Jöchl, C., Cornelis, P., Guarro, J., Haas, H., Di Pietro, A., 2012. HapX-mediated iron homeostasis is essential for rhizosphere competence and virulence of the soilborne pathogen *Fusarium oxysporum. Plant Cell* 24:3805-3822.

Martin-Castellanos, C. Blanco, M., Rozalen, A.E., Perez-Hidalgo, L., Garcia, A.I., Conde, F., Mata, J., Ellermeier, C., Davis, L., San-Segundo, P., Smith, G.R., Moreno. 2005. A large-scale

screen in *S. pombe* identifies seven novel genes required for critical meiotic events. *Curr Biol* 15:2056-2062.

McClung C.R., Fox B.A. and Dunlap J.C. 1989. The *Neurospora* clock gene frequency shares a sequence element with the Drosophila clock gene period. *Nature* 339: 558–562.

McCluskey K. 2003. The fungal genetics stock center: from molds to molecules. *Adv Appl Microbiol* 52:245-262.

McIntire, S.L., Reimer, R.J., Schuske, K., Edwards, R.H. and Jorgensen, E.M. 1997. Identification and characterization of the vesicular GABA transporter. *Nature* 389: 870-876.

McNabb, D.S., and Pinto, I., 2005. Assembly of the Hap2p/Hap3p/Hap4p/Hap5p-DNA complex in *Saccharomyces cerevisiae. Eukaryot Cell* 4:1829-1839.

McNabb, D.S., Xing, Y., Guarente, L. 1995. Cloning of yeast HAP5: a novel subunit of a heterotrimeric complex required for CCAAT binding. *Genes Dev* 9:47-58.

Mehrabi, R., Zwiers, L.H., de Waard, M.A., Kema, G.H. 2006. MgHog1 regulates dimorphism and pathogenicity in the fungal wheat pathogen *Mycosphaerella graminicola*. *Mole Plant Microbe Interact*. 19:1262-1269.

Michielse, C.B., Hooykaas, P.J.J., van den Hondel, C.A.M.J.J., and Ram, A.F.J. 2005. *Agrobacterium*-mediated transformation as a tool for functional genomics in fungi. *Curr Genet*: 48:1-17.

Moriwaki, A., Kubo, E., Arase, S., and Kihara, J. 2006. Disruption of *SRM1*, a mitogen-activated protein kinase gene, affects sensitivity to osmotic and ultraviolet stressors in the phytopathogenic fungus *Bipolaris oryzae*. *FEMS Microbiol Lett* 257:253:261.

Morris N.R. and Enos A.P. 1992. Mitotic gold in a mold: *Aspergillus* genetics and the biology of mitosis. *Trends Genet*. 8: 32-37.

Mullins, E.D., and Kang, S. 2001. Transformation: a tool for studying fungal pathogens of plants. *Cell Mol Life Sci* 58:2043-2052.

Muller P, Leibbrandt A, Teunissen H, Cubasch S, Aichinger C, Kahmann R. 2004. The G-beta-subunit-encoding gene bpp1 controls cyclic-AMP signaling in *Ustilago maydis*. *Eukaryot. Cell* 3:806-14

Neves, S.R., Ram, P.T., Iyengar, R..2002. G protein pathways. *Science* 296:1636-1639.

Nishimura M, Park G, Xu JR. 2003. The G-b subunit MGB1 is involved in regulating multiple steps of infection-related morphogenesis *in Magnaporthe grisea. Mol. Microbiol*. 50:231-43.

Noble, L.M. and Adrianopoulos, A. 2013. Fungal genes in context: Genome architecture reflects regulatory complexity and function. *Genome Biol Evol* 5: 1336-1352.

Osmani S.A. and Mirabito P.M. 2004. The early impact of genetics on our understanding of cell cycle regulation in *Aspergillus nidulans*. *Fungal Genet Biol*. 41: 401-410.

Ozeki, K., Kyoya, F., Hizume, K., Kanda, W., Hamachi, M., and Nunokawa, Y. 1994 Transformation of intact *Aspergillus niger* by electroporation. *Biosci Biotechnol Biochem* 58:2224-2227.

Park G., Xue C., Zhao X., Kim Y., Orbach M. and Xu JR. 2006. Multiple upstream signals converge on the adaptor protein Mst50 in *Magnaporthe grisea*. *Plant Cell*: 18:2822-2835.

Parker, D.M., Hilber, U.W., Bodmer, M., Smith,F.D., Yao, C., and Koller, W. 1995. Production and transformation of conidia of *Venturia inaequalis*. *Phytopathology* 85:87-91.

Pitkin, J., Panaccione, D., Walton, J. 1996. A putative cyclic peptide efflux pump encoded by the *TOXA* gene of the plant-pathogenic fungus *Cochliobolus carbonum*. *Microbiology* 142:1557-1565.

Pregueiro A.M., Liu Q., Baker C.L., Dunlap J.C. and Loros J.J. 2006. The Neurospora checkpoint kinase 2: a regulatory link between the circadian and cell cycles. *Science* 313: 644–649.

Ram A.F.J. 2013. Modern Technologies Boost Classical Genetics: Whole Genome Sequencing Revives Forward Genetic Mutant Screens in Filamentous Fungi. *Fungal Genom Biol* 3: e105. doi:10.4172/2165-8056.1000e105.

Ridenour J.B., Hirsch R.L. and Bluhm B.H. 2012. Identifying genes in *Fusarium verticillioides* through forward and reverse genetics. *Methods Mol Biol* 835: 457-479.

Ridenour J.B., Smith, J.E., Hirsch, R.H., Horevaj, P., Kim, H., Sharma, S., Bluhm, B.H. 2013. UBL1 of *Fusarium verticillioides* links the N-end rule pathways to extracellular sensing and plant pathogenesis. *Environ Microbiol* 16:2004-2022.

Ridenour, J.B., and Bluhm, B.H. 2014. The HAP complex in *Fusarium verticillioides* is a key regulator of growth, morphogenesis, secondary metabolism, and pathogenesis. *Fungal Gen Biol* 69:52-64.

Riggle P.J. and Kumamoto C.A. 1998. Genetic analysis in fungi using restriction-enzyme-mediated integration. *Curr Opin Microbiol* 1:395-399.

Ruiz-Diez B.2002. Strategies for the transformation of filamentous fungi. *J Appl Microbiol* 92:189-195

Sambrook J., and Russell D.W. 2001. Molecular cloning: A laboratory manual. 3rd ed. Cold Spring Harbor Laboratory Press.

Sagaram U.S. and Shim WB. 2007. *Fusarium verticillioides* GBB1, a gene encoding heterotrimeric G protein beta subunit, is associated with fumonisin B biosynthesis and hyphal development but not with fungal virulence. *Mol Plant Pathol* 8:375-384.

Schmitzova J., Klaudiny J., Albert S., Schroeder W., Schreckengost W., Hanes J., Judova J., and Simuth J. 1998. A family of major royal jelly proteins of the honeybee *Apis mellifera* L. *Cell. Mol. Life Sci*. 54: 1020–1030.

Seong K., Hou S., Tracy M., Kistler H.C. and Xu J. 2005. Random insertional mutagenesis identifies genes associated with virulence in the wheat scab fungus *Fusarium graminearum*. *Phytopathology* 95: 744-750.

Shafer, W.M., Veal, W.L., Lee, E-H., Zaraontelli, L., Balthazar, J.T., and Rouquette, C. 2001. Genetic organization and regulation of antimicrobial efflux systems possessed by *Neisseria gonorrhoeae* and *Neisseria meningitides*. *J Mol Microbiol Biotechnol* 3:219-224.

Shi, Y.Y., Wu, X.B., Huang, Z.Y., Wang, Z.L., Yan, Y.Y., Zeng, Z.J. 2012. Epigenetic modification of gene expression in honey bees by heterospecific gland secretions. *PLoS ONE* 7(8): e43727.

Shim, W-B. and Dunkle, L.D. 2003. CZK3, a MAP kinase kinase kinase homolog in *Cercospora zeae-maydis*, regulates cercosporin biosynthesis, fungal development, and pathogenesis. *Mol Plant-Microbe Interact* 16:760-768.

Shim W-B., Woloshuk C.P. 2001. Regulation of fumonisin B1 biosynthesis and conidiation in *Fusarium verticillioides* by a Cyclin-like (C-type) gene, FCC1. *Appl Environ Microbiol* 4: 1607-1612.

Shwab E.K. and Keller N.P. 2008. Regulation of secondary metabolite production in filamentous ascomycetes. *Mycol Res* 112: 225-230.

Solomon PS, Tan KC, Sanchez P, Cooper RM, Oliver RP. 2004. The disruption of a Ga subunit sheds new light on the pathogenicity of *Stagonospora nodorum* on wheat. *Mol. Plant-Microbe Interac*t. 17:456–66

Strauss J. and Reyes-Dominguez Y. 2011. Regulation of secondary metabolism by chromatin structure and epigenetic codes. *Fungal Gen Biol* 1: 62-69.

Struck, C., Ernst, M., and Hahn, M. 2002. Characterization of a developmentally regulated amino acid transporter (AAT1p) of the rust fungus *Uromyces fabae. Mol Plant Pathol* 3:23-30.

Tanabe, M., Szakonyi, G., Brown, K.A., Genderson, P.J., Nield, J., and Byrne, B. 2009. The multidrug resistance efflux complex, EmrAV from *Escherichia coli* forms a dimer *in vitro*. *Biochem Biophys Res Commun* 6:338-342.

Te'o, V.S., Bergquist, P.L., Nevalainen, K.M.2002.Biolistic transformation of *Trichoderma*

reesei using the Bio-Rad seven barrels Hepta Adaptor system. *J Microbiol Methods* 51:393-399.

Thon M.R., Nuckles E.M., Vaillancourt L.J. 2000. Restriction enzyme-mediated integration used to produce pathogenicity mutants of *Colletotrichum graminicola*. *Mol Plant- Microbe Interact* 13: 1356-1365.

Teichert S., Wottawa M., Shoning B. and Tudzynski B. 2006. Role of *Fusarium fujikuroi* TOR kinase in nitrogen regulation and secondary metabolism. *Eukaryot Cell* 5:1807-1819.

Truesdell GM, Yang ZH, Dickman MB. 2000. A Ga subunit gene from the phytopathogenic fungus *Colletotrichum trifolii* is required for conidial germination. *Physiol. Mol. Plant Pathol*. 56:131–40

Turina M, Zhang L, Van Alfen NK. 2006. Effect of *Cryphonectria hypovirus* 1 (CHV1) infection on Cpkk1, a mitogen-activated protein kinase kinase of the filamentous fungus *Cryphonectria parasitica. Fungal Genet. Biol*. 43:764–74

Ucisik-Akkaya, E., Leatherwood, J.K. Neiman, A.M. 2014. A genome-wide screen for sporulation-defective mutants in Schizosaccharomyces pombe. *Genes Genom Genet* 4:1173-1182.

Vitalini M.W., de Paula R.M., Goldsmith C.S., Jones C.A., Borkovich K.A. and Bell-Pedersen D. 2007. Circadian rhythmicity mediated by temporal regulation of the activity of p38 MAPK. *P Natl Acad Sci* USA 104: 18223–18228.

Walton, J.D. 1996. Host-selective toxins: agents of compatibility. *Plant Cell* 8:1723-1733.

Ward, M., Kodama, K.H., and Wilson, L.J. 1989. Transformation of *Aspergillus awamori* and *A. niger* by electroporation. *Experimental Mycol* 13:289-293.

Ward, J.M.J., Laing, M.D. and Rijkenbert, F.H.J. 1997. Frequency and timing of fungicide applications for the control of gray leaf spot of maize. *Plant Dis* 81:41-48.

Ward, J. M. J., Stromberg, E. L., Nowell, D. C., and Nutter, F. W. 1999. Gray leaf spot: A disease of global importance in maize production. *Plant Dis* 83:884-895.

Weld R.J., Plummer K.M., Carpenter M.A. and Ridgway H.J. 2006. Approaches to functional genomics in filamentous fungi. *Cell Res* 16: 31-44.

Willger S.D., Puttikamonkul S., Kim K.H., Burritt J.B., Grahl N., et al. 2008. A sterol-regulatory element binding protein is required for cell polarity, hypoxia adaptation, azole drug resistance, and virulence in *Aspergillus fumigatus*. *PLoS Pathog* 4: e1000200.

Wipf, D., Ludweig, U., Tegeder, M., Rentsch, D., Koch, W. and Frommer, W.B. 2002. Conservation of amino acid transporters in fungi, plants and animals. *Trend Biochem Sci*. 27:139-147.

Yamagishi, D., Otani, H., Kodama, M. 2006. G protein signaling mediates developmental processes and pathogenesis of *Alternaria alternata. Mol. Plant-Microbe Interact*. 19:1280–88

Yang, Y., Cheng, P., Zhi, G., Liu, Y. 2001. Identification of a calcium/calmodulin-dependent protein kinase that phosphorylates the *Neurospora circadian* clock protein FREQUENCY. *J Biol Chem* 276: 41064–41072.

Yang, Y., Cheng, P. and Liu Y. 2002. Regulation of the Neurospora circadian clock by casein kinase II. *Gene Dev* 16: 994–1006.

Yang, Y., He, Q., Cheng, P., Wrage, P., Yarden, O., Liu, Y. 2004. Distinct roles for PP1 and PP2A in the Neurospora circadian clock. *Gene Dev* 18: 255–260.

Yu H.Y., Seo J.A., Kim J.E., Han K.H., Shim W.B., Yun S.H. and Lee Y.W. 2008. Functional analysis of heterotrimeric G protein G alpha and G beta subunits in *Gibberella zeae. Microbiology* 154: 392-401.

Zhang H., Xue C., Kong L., Li G. and Xu JR. 2011. A Pmk1-interacting gene is involved in appressorium differentiation and plant infection in *Magnaporthe oryzae. Eukaryot Cell* 10:1062-1070.

Zhang, Y., Lamm, R., Pillonel, C., Lam, S., and Xu, J.R. 2002. Osmoregulation and fungicide resistance: the *Neurospora crassa* os-2 gene encodes a HOG1 mitogen-activated protein kinase homologue. *Appl Environ Microbiol*. 68:532-538.

Figures

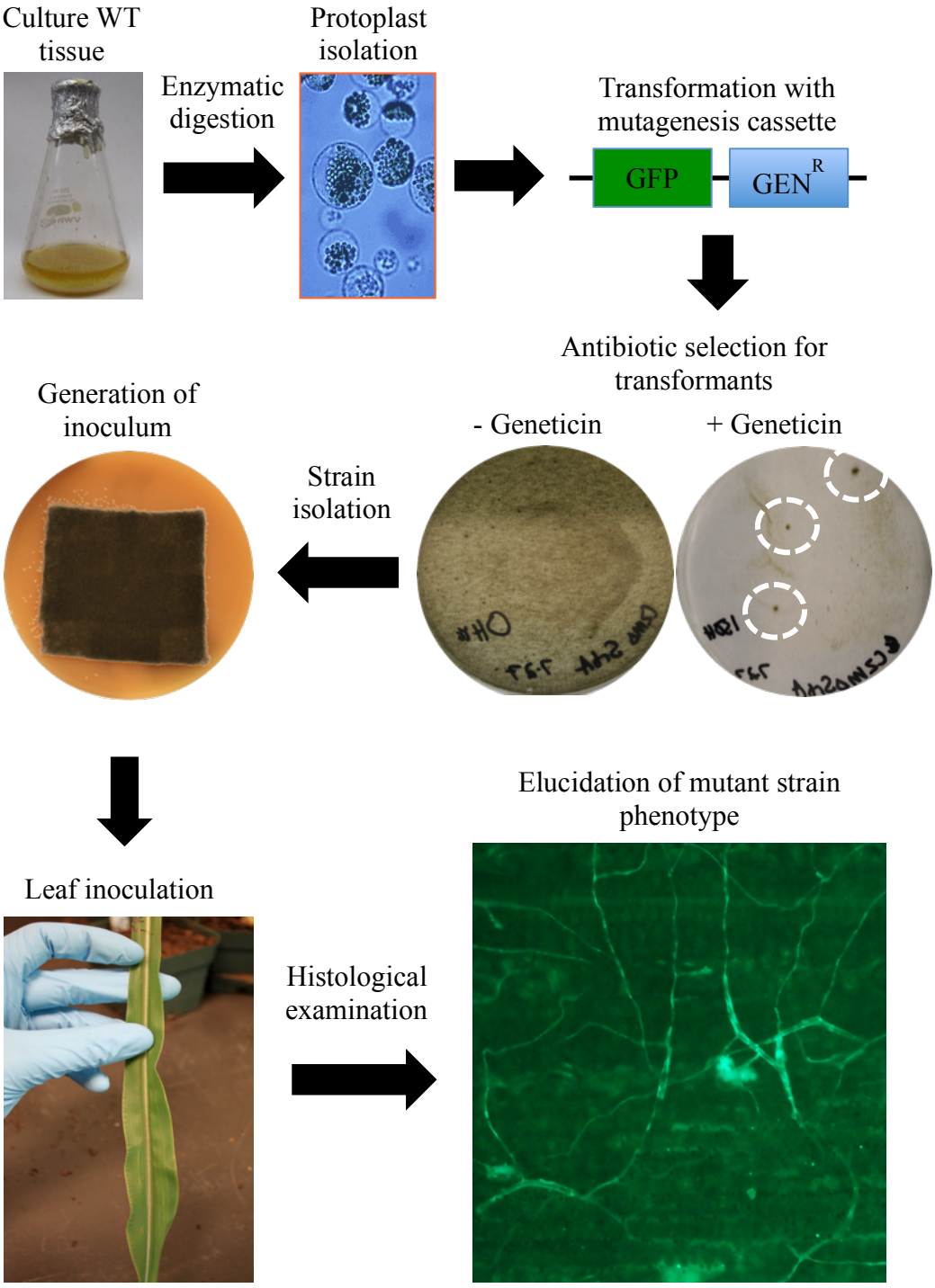

Figure 5.1. Generation of an insertional mutant collection utilized in this study. Conidia were collected from sporulating cultures and inoculated onto YEPD medium and cultured for three days. Tissue was then digested with an enzyme solution to produce fungal protoplasts. Protoplasts were collected and transformed with a GFP/GEN^R construct. Following transformation, protoplasts were inoculated onto nutrient rich medium either containing

geneticin for selection of putative transformants, or no selection for a positive control. Regenerating colonies were isolated and propagated on V8 medium until enough conidia was produced for inoculation. Individual maize leaves were inoculated with each strain and incubated for 5 days. Following inoculation, leaf sections inoculated with each strain were observed with epifluorescence microscopy to identify mutants disrupted in pre-infectious growth and development.

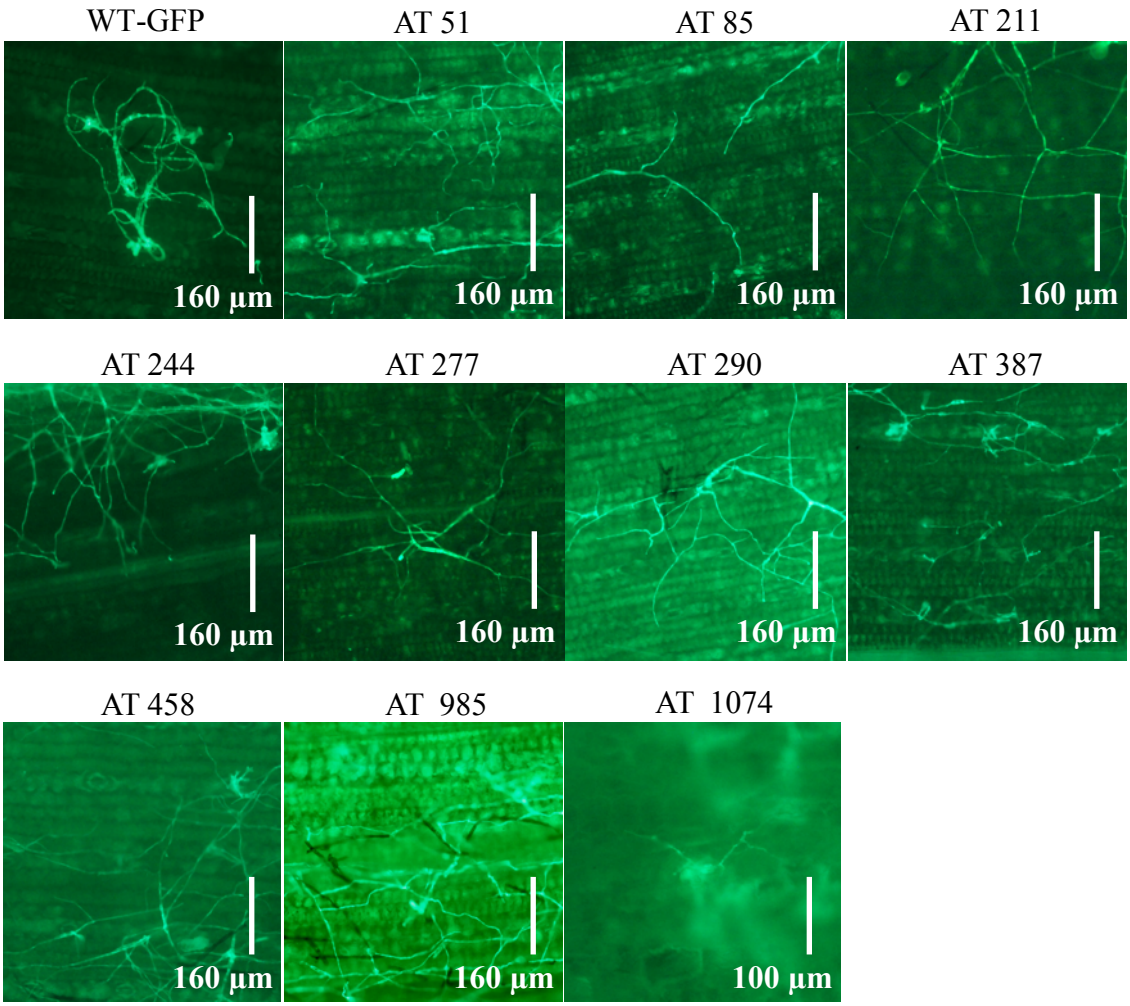

Figure 5.2. Random insertional mutant strains disrupted in infectious development. Mutant strains expressing GFP were inoculated onto a susceptible maize cultivar and growth was observed after five days with epifluorescence microscopy. Mutant strains AT 51, AT 85, AT 211, AT 244, AT 277, AT 290, AT 387, AT 458, and AT 985 displayed reduced stomatal tropism and appressorium formation compared to wild-type strain (WT-GFP), while strain AT 1074 failed to form conidia from the erumpent conidiophores arising from host stomata.

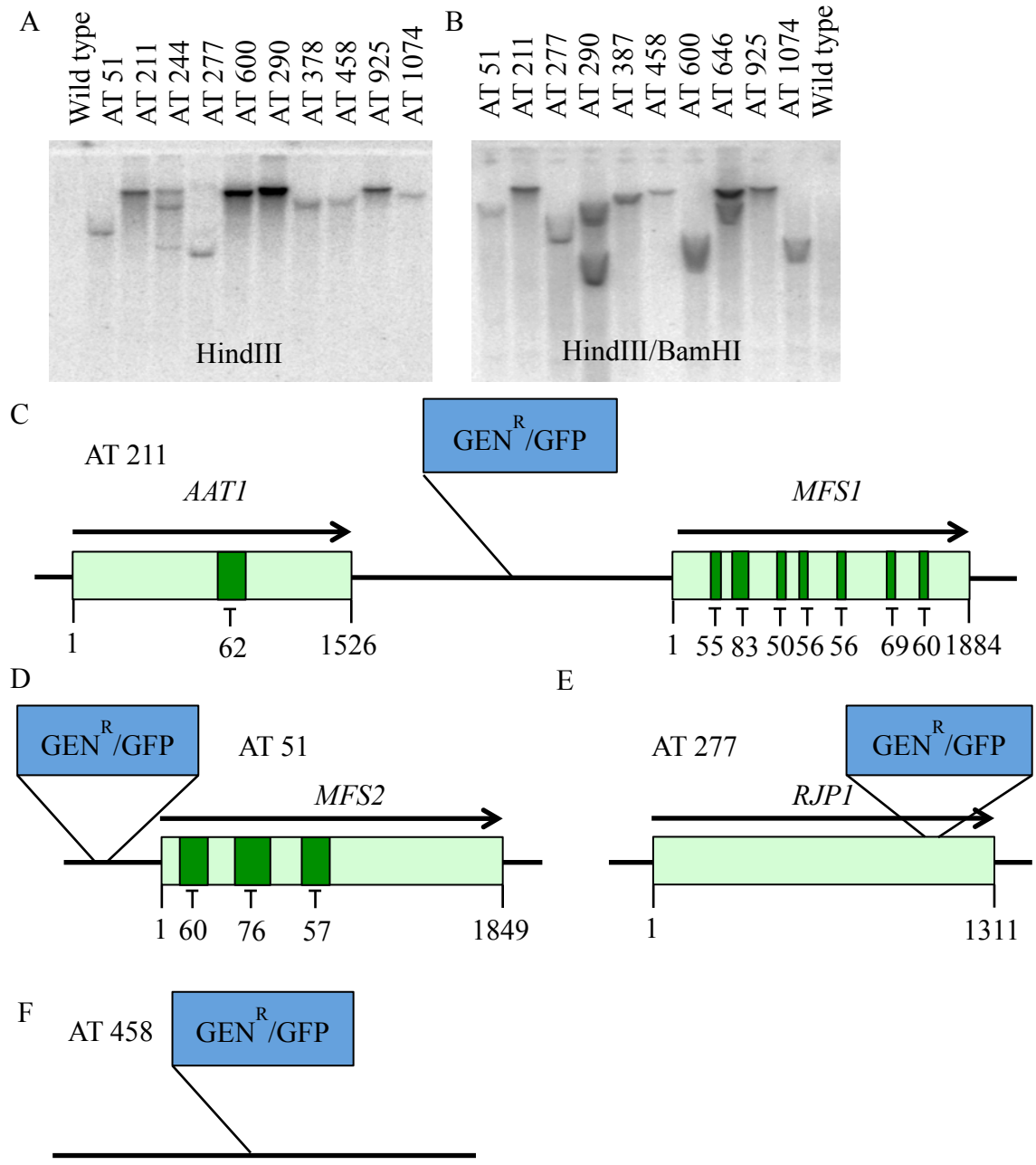

Figure 5.3. Identification and characterization of mutations present in the random mutagenesis strain collection. A) Genomic DNA of mutant strains exhibiting reductions in stomatal tropism or appressorium formation were digested with HindIII and labeled with a GFP probe to determine copy-number of the insertional cassette. Strain AT 244 contained multiple integrations of the insertional cassette, while the other strains appeared to contain only one insertion. B) To confirm that the remaining ten strains contained a single insertion, genomic DNA was double digested with HindIII and BamHI to produce smaller fragments of DNA. Hybridization with a GFP probe revealed that strains AT 290 and AT 646 contained multiple integrations of the insertional cassettes. C) The genomic lesions of four mutant strains were characterized by Genome Walker PCR. In mutant 211, the mutagenesis cassette integrated

between *AAT1*, a putative amino acid transporter, and gene *MFS1*, a member of the Major Facilitator Superfamily (MFS) of transporters. D) Mutant 51 contained a direct insertion upstream of the start codon of gene *MFS2*, a putative MFS transporter gene, and likely disrupted the promoter sequence of *MFS2*. E) The mutagenesis cassette in AT 277 integrated into the 3' flank of gene *RJP1*, a putative ortholog of the Major Royal Jelly (*MRJ*) family of proteins in honeybees, known epigenetic regulators of behavior and caste differentiation. F) Partial insertion of the mutagenesis cassette in AT 458 occurred in a gene-poor region of the genome, and the disrupted locus did not correspond to any coding sequence annotated on the genome.

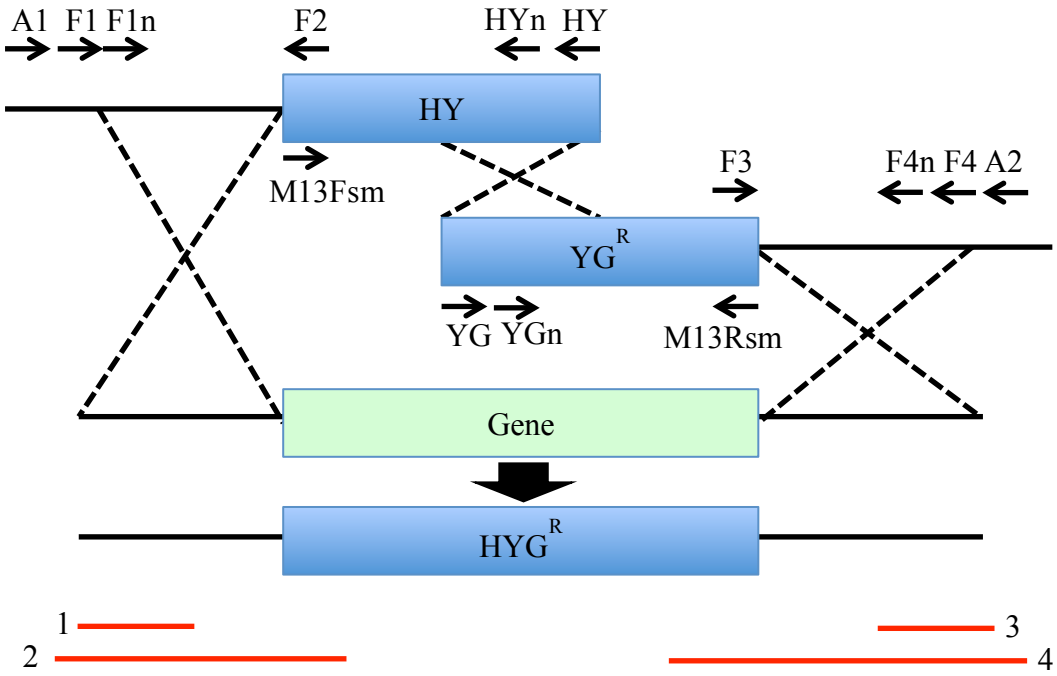

Figure 5.4. Targeted disruption of specific genes in *C. zeae-maydis*. A) Strategy for split-marker gene disruption by amplifying genomic flanks and fusing them to portions of the HYG^R gene conferring resistance to the antibiotic hygromycin. Generation of the gene deletion constructs required the amplification of 5' (F1/F2) and 3' (F3/F4) genomic flanking regions and fusing them to fragment HY or YG of the HYG^R cassette, respectively, to form the split-marker constructs A and B. Putative transformants were screened by PCR by amplifying fragments 1 and 3 as positive genomic controls, and fragments 2 and 4 to confirm successful integration of the split-marker fragments on both genomic flanks.

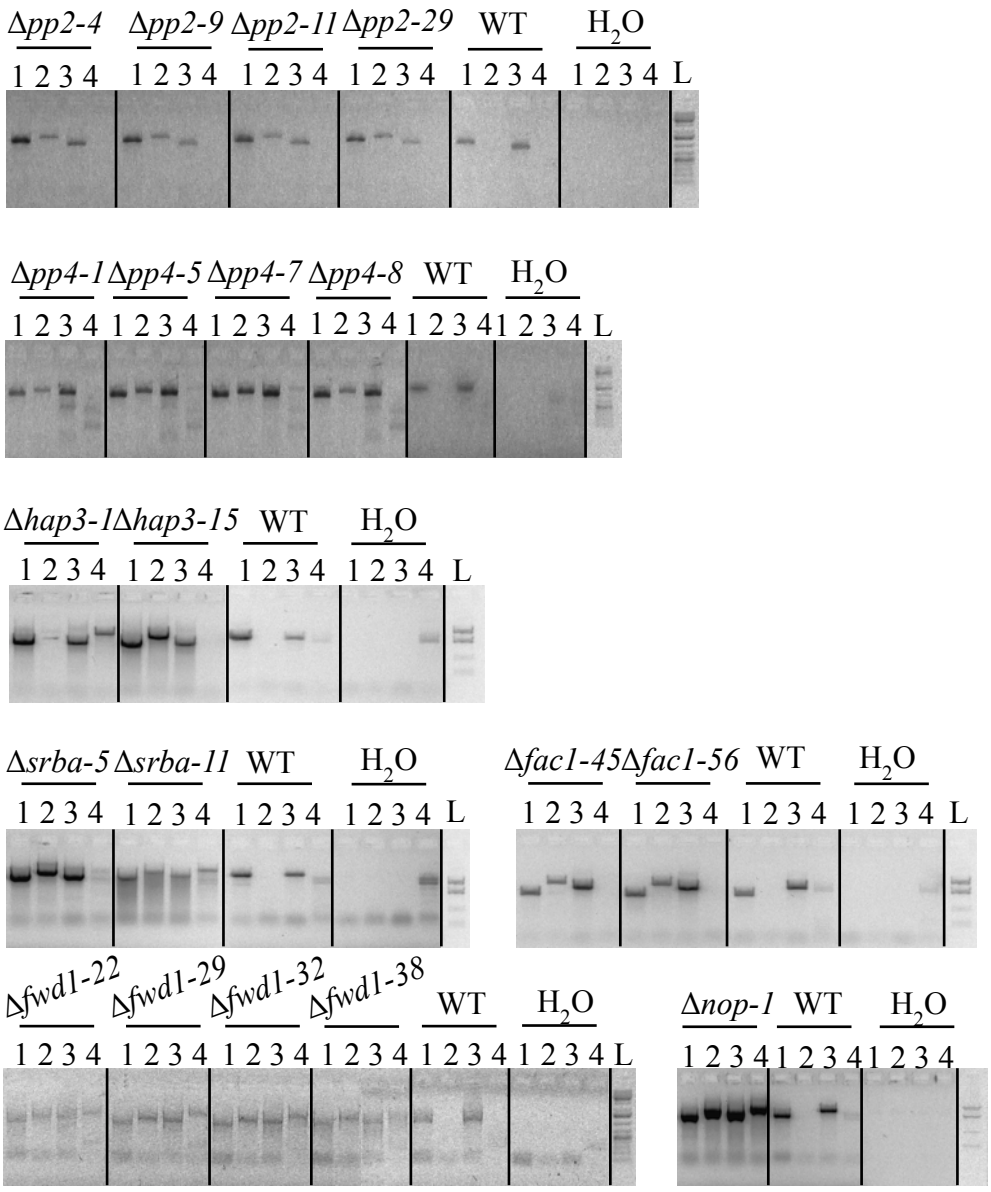

Figure 5.5. PCR validation of putative gene-deletion mutant strains. Independent gene deletion strains for *PP2, PP4, HAP3, SRBA, FAC, FWD1,* and *NOP1.* Amplicons 1 and 3 represent positive controls for DNA quality and quantity, while amplicons 2 and 4 were only be expected in the presence of the hygromycin resistance gene integrated into the 5' and 3' genomic flank, respectively. PCR markers represent, in descending order, 2.0 kb, 1.5 kb, 1.0kb and 0.5 kb.

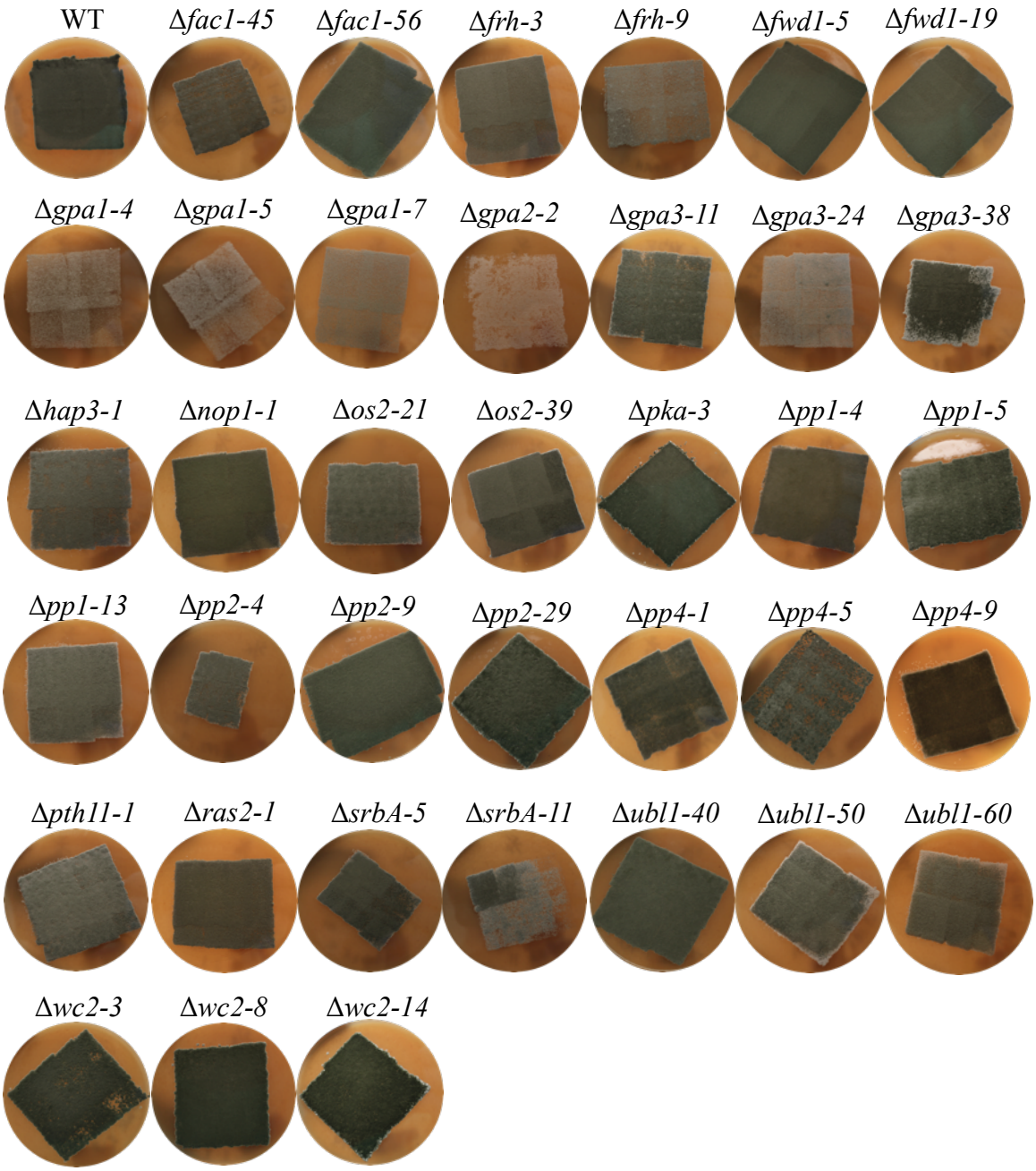

Figure 5.6. Phenotypes of the targeted gene-deletion mutants grown on V8 medium. Strains were subcultured onto fresh V8 medium by physically transferring a dense mat of conidia from one culture to a fresh culture and incubated in the dark for four days before observation. Differences in colony size are to due to variability in sub culturing, and not indicative of changes in growth.

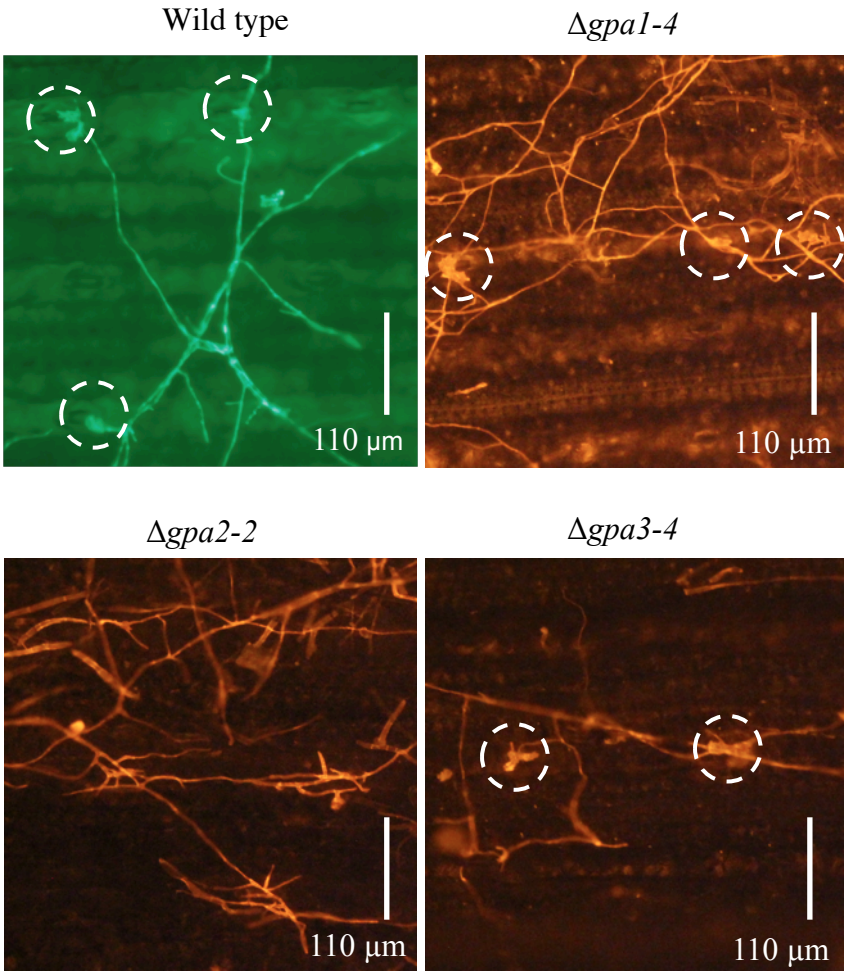

Figure 5.7. *GPA2* is required for appressorium formation during foliar infection of maize by *C. zeae-maydis*. The wild-type GFP strain, Δ*gpa1-4, Δgpa2-2* and Δ*gpa3-4* were inoculated on maize and observed after five days of incubation. The wild-type, Δ*gpa1-4, and* Δ*gpa3-4* strains formed appressoria (white circles) after physically encountering stomata, but Δ*gpa2-2* failed to form appressoria on maize stomata. The wild-type GFP strain was observed with GFP expression, and the *GPA2* mutant strains were stained with Congo Red and observed with epifluorescence microscopy.

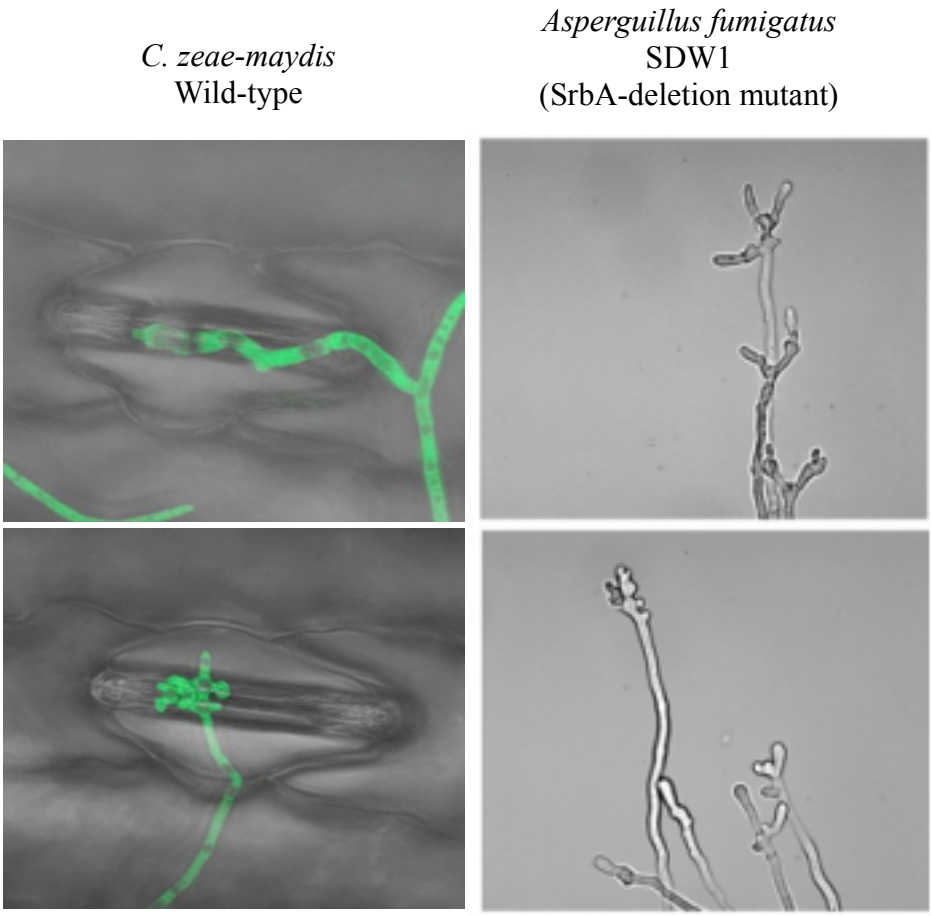

Figure 5.8. Morphological similarities between apical hyphal swelling displayed by SrbA-deletion mutants of *A. fumigatus* and the wild-type strain of *C. zeae-maydis* during pathogenesis. After hyphal tips physically touch host stomata, hypha of *C. zeae-maydis* display an apical swelling that develops into an appressorium. Hypha of the SrbA-deletion strain SWD1 of *A. fumigatus* develop similar apical swellings during growth on minimal medium overnight. Images of *A. fumigatus* from Williger et al., 2008.

Tables

Table 5.1. Genes investigated during this study

Gene name	Strain name	Location (scaffold:bp-bp)	Homologous to	Predicted function	Citation
OS-2	Δ*os2-x*	10:921191-918275	*N. crassa*	Osmotic stress MAP kinase	Vitalini et al., 2007.
PP4	Δ*pp4-x*	2:2052003-2050662	*N. crassa*	Phosphatase	Cha et al., 2008.
FRH	Δ*frh-x*	22:284207-287499	*N. crassa*	Phosphoprotein-binding	Cheng et al., 2005.
FWD-1	Δ*fwd1-x*	5:384801-387353	*N. crassa*	F-box/WD-40 repeat	He et al., 2003.
PP2	Δ*pp2-x*	29:472240-471106	*N. crassa*	Phosphatase	Yang et al., 2004.
PP1	Δ*pp1-x*	5:589257-585751	*N. crassa*	Phosphatase	Yang et al., 2004.
PKA	Δ*pka-x*	8:469441-467933	*N. crassa*	Protein kinase A	Huang et al., 2007.
CAMK-1	Δ*camk1-x*	1:887506-886166	*N. crassa*	Ca2+/CaM-dep kinase-1	Yang et al., 2001.
Prd-4	Δ*prd4-x*	11:230029-227898	*N. crassa*	Checkpoint kinase-2	Pregueiro et al., 2006.
CK2	Δ*ck2-x*	6:527272-525989	*N. crassa*	Acidic-directed casein kinase	Yang et al., 2002.
CK1a	Δ*ck1-x*	17:254782-258951	*N. crassa*	Acidic-directed casein kinase	Gorl et al., 2001.
CCH-1	Δ*cch1-x*	18:166306-172446	*C. albicans*	High affinity Ca^{2+} channel	Brand et al., 2007.
PHY1	Δ*phy1-x*	18:228620-233210	*N. crassa*	Phytochrome 1	Froehlich et al., 2005.
HHK2p	Δ*hhk2p-x*	51:172767-178814	*N. crassa*	Histidine kinase	http://genome.jgi-psf.org
HHk6p	Δ*hhk6p-x*	1:1253261-1257641	*N. crassa*	Histidine kinase	http://genome.jgi-psf.org
ERG K+	Δ*ergk-x*	6:504308-506122	*N. crassa*	Potassium channel protein	http://genome.jgi-psf.org
WC-2	Δ*wc2-x*	4:254077-255534	*N. crassa*	White Collar Complex	Ballario and Macino, 1997.
SrbA	Δ*srba-x*	6:876803-879688	*A. fumagatus*	Sterol regulator	Willger et al., 2008.
NOP-1	Δ*nop1-x*	38:330575-331623	*N. crassa*	Opsin	Bieszke et al., 1999.

Table 5.1 Cont. Genes investigated during this study

Gene name	Strain name	Location (scaffold:bp-bp)	Homologous to	Predicted function	Citation
TOR	Δ*tor-x*	19:716635-709337	*F. fujikori*	Nitrogen related kinase	Teichert et al., 2006.
HAP3	Δ*hap3-x*	1:949093-951187	*F. verticillioides*	CCAAT-binding protein	Ridenour and Bluhm, 2014.
PIC5	Δ*pic5-x*	12:751855-752024	*M. oryzae*	Pmk-1 interacting protein	Zhang et al., 2011.
FAC1	Δ*fac1-x*	51:166415-170770	*F. verticillioides*	Adenylate cyclase	Choi and Xu, 2010.
RAS2	Δ*ras2-x*	9:197439-196666	*M. oryzae*	Reacts with Mst50 complex	Park et al, 2006.
GPA1	Δ*gpa1-x*	24:439277-440365	*G. zeae*	G protein signaling	Yu et al., 2008.
GPA2	Δ*gpa2-x*	10:922214-923436	*G. zeae*	G protein signaling	Yu et al., 2008.
GPA3	Δ*gpa3-x*	24:91609-90381	*G. zeae*	G protein signaling	Yu et al., 2008.
GPB1	Δ*gpb1-x*	3:412121-410867	*F. verticillioides*	G protein signaling	Sagaram and Shim, 2007.
UBL1	Δ*ubl1-x*	51:133408-140094	*F. verticillioides*	E3 Ubiquitin ligase	Ridenour et al., 2013.
PTH11	Δ*pth11-x*	32:188594-192053	*M. oryzae*	Integral membrane protein	DeZwaan et al., 1999.

Table 5.2. Transformations performed to create the random mutant collection utilized in this study.

Transformation number	Subcultured strains
1	95
2	26
3	28
4	23
5	155
6	5
7	7
8	87
9	55
10	94
11	107
12	291
13	255
Total	1228

Table 5.3. Phenotypes of the random insertional mutants exhibiting reduced pre-infectious development phenotypes.

Strain	% Appressoria	Stomatal tropism
WT	75	Yes
51	20	Yes
85	10	Yes
211	10	No
244	30	Yes
277	10	No
290	1	No
387	40	Yes
458	10	Yes
925	10	Yes
1074	70	Yes

Table 5.4 Methodology for the characterization of genomic lesions in the random insertional mutant collection.

Mutant strain	Characterization method
AT 51	Genome Walker PCR
AT 211	Genome Walker PCR
AT 244	Isolate resequencing
AT 277	Genome Walker PCR
AT 290	Isolate resequencing
AT 387	Isolate resequencing
AT 458	Genome Walker PCR
AT 600	Isolate resequencing
AT 646	Isolate resequencing
AT 925	Isolate resequencing
AT 1074	Isolate resequencing

Table 5.5. Length of split-marker genomic flanks utilized in this study.

Gene	5' Flank (bp)	3' Flank (bp)
CAMK	1309	1355
FWD-1	1145	1410
NOP-1	1138	1484
PHYHK	1347	1080
CK2b	1397	1354
UBL1	759	853
FAC1	578	1001
FRH	1312	1008
FRQ	762	973
GPA1	728	679
GPA2	639	873
GPA3	819	781
HAP3	810	590
OS-2	1218	1130
PIC5	731	591
PP4	739	1205
PRD4	1354	1319
PKA	1310	1356
PTH11	931	713
RAS2	945	762
SRBA	1366	1384
TOR	823	1295
WC2	1291	1322
HHK6P	1374	1295
HHK2P	1415	1267
CCH1	1440	1027
PP1	1382	1552
PP2	1361	1161
KERG	1341	1050
GPB1	705	658

Table 5.6. Generation of the split-marker constructs and total number of gene transformants.

	Constructs created				Total
Gene	F1/F2	F3/F4	A	B	strains
CAMK	Yes	Yes	Yes	Yes	0
FWD-1	Yes	Yes	Yes	Yes	40
NOP-1	Yes	Yes	Yes	Yes	1
PHY1	Yes	No	Yes	No	0
CK2b	Yes	Yes	Yes	Yes	0
UBL1	Yes	Yes	Yes	Yes	81
FAC1	Yes	Yes	Yes	Yes	117
FRH	Yes	Yes	Yes	Yes	40
FRQ	Yes	Yes	Yes	Yes	41
GPA1	Yes	Yes	Yes	Yes	13
GPA2	Yes	Yes	Yes	Yes	26
GPA3	Yes	Yes	Yes	Yes	53
HAP3	Yes	Yes	Yes	Yes	50
OS-2	Yes	Yes	Yes	Yes	60
PIC5	Yes	Yes	Yes	Yes	4
PP4	Yes	Yes	Yes	Yes	35
PRD4	Yes	Yes	No	No	0
PKA	Yes	Yes	Yes	Yes	40
PTH11	Yes	Yes	Yes	Yes	5
RAS2	Yes	Yes	Yes	Yes	5
SRBA	Yes	Yes	Yes	Yes	18
TOR	Yes	Yes	No	Yes	0
WC2	Yes	Yes	Yes	Yes	35
HHK6P	Yes	Yes	Yes	Yes	6
HHK2P	Yes	Yes	Yes	Yes	0
CCH1	Yes	Yes	Yes	Yes	0
PP1	Yes	Yes	Yes	Yes	37
PP2	Yes	Yes	Yes	Yes	31
KERG	Yes	Yes	No	No	0
GPB1	Yes	Yes	Yes	No	2
CK1a	Yes	Yes	No	Yes	0
CCH-1	Yes	Yes	Yes	No	0

Table 5.7. Putative gene deletion mutant strains created for this study and assayed by PCR[a].

Strain name	5' flank	3' flank
Δgpa1-4	YES	YES
Δgpa1-5	YES	YES
Δgpa1-7	YES	YES
Δgpa1-12	YES	YES
Δgpa1-13	YES	YES
Δgpa2-2	YES	YES
Δgpa3-4	YES	YES
Δgpa3-11	YES	YES
Δgpa3-17	YES	YES
Δgpa3-24	YES	YES
Δgpa3-30	YES	YES
Δgpa3-31	YES	YES
Δgpa3-33	YES	YES
Δgpa3-34	YES	YES
Δgpa3-38	YES	YES
Δgpa3-53	YES	YES
Δhap3-1	YES	YES
Δhap3-15	YES	NO
Δhap3-40	YES	NO
Δubl1-40	YES	NO
Δubl1-50	YES	YES
Δubl1-60	YES	YES
Δubl1-61	NO	YES
Δubl1-64	YES	NO
Δubl1-68	NO	YES
Δfac1-45	YES	NO
Δfac1-56	YES	NO
Δfac1-84	NO	NO
Δras2-1	YES	NO
Δos2-21	YES	YES
Δos2-39	YES	YES
Δpth11-1	YES	NO
Δfrh-3	YES	NO
Δfrh-9	YES	NO
Δfrh-16	YES	NO
Δfrh-34	YES	NO
Δpka-3	YES	YES
Δpka-12	YES	NO

Table 5.7 Cont. Putative gene deletion mutant strains created for this study and assayed by PCR[a].

Strain name	5' flank	3' flank
Δpka-16	YES	NO
Δpka-17	YES	NO
Δpka-21	YES	NO
Δpka-27	YES	NO
Δpka-36	YES	NO
Δfwd1-5	YES	YES
Δfwd1-7	YES	NO
Δfwd1-11	YES	NO
Δfwd1-14	YES	YES
Δfwd1-19	YES	NO
Δfwd1-20	YES	NO
Δfwd1-21	YES	NO
Δfwd1-22	YES	YES
Δfwd1-28	YES	YES
Δfwd1-29	YES	YES
Δfwd1-32	YES	YES
Δfwd1-38	YES	YES
Δfwd1-40	YES	NO
ΔsrbA-5	YES	NO
ΔsrbA-7	YES	NO
ΔsrbA-9	YES	NO
ΔsrbA-11	YES	YES
Δpic5-3	YES	YES
Δpp1-4	YES	NO
Δpp1-5	YES	NO
Δpp1-13	YES	NO
Δpp1-17	YES	NO
Δpp1-18	YES	NO
Δpp1-20	YES	NO
Δpp1-23	YES	NO
Δpp1-27	YES	NO
Δpp1-29	YES	NO
Δpp1-30	YES	NO
Δpp1-36	YES	NO
Δpp2-4	YES	NO
Δpp2-9	YES	NO
Δpp2-11	YES	NO
Δpp2-29	YES	NO

Table 5.7 Cont. Putative gene deletion mutant strains created for this study and assayed by PCR[a].

Strain name	5' flank	3' flank
Δpp4-1	YES	YES
Δpp4-5	YES	YES
Δpp4-7	YES	YES
Δpp4-8	YES	NO
Δpp4-9	YES	YES
Δpp4-10	YES	NO
Δpp4-12	YES	YES
Δpp4-13	YES	YES
Δpp4-26	YES	YES
Δwc2-3	YES	NO
Δwc2-8	YES	YES
Δwc2-14	YES	NO
Δwc2-21	YES	YES
Δwc2-24	YES	YES
Δnop1-1	YES	YES

[a] "YES" denotes a positive PCR result. "NO" denotes the absence of expected amplicons during PCR screens to confirm the integration of the split-marker mutagenesis cassette.

Appendix

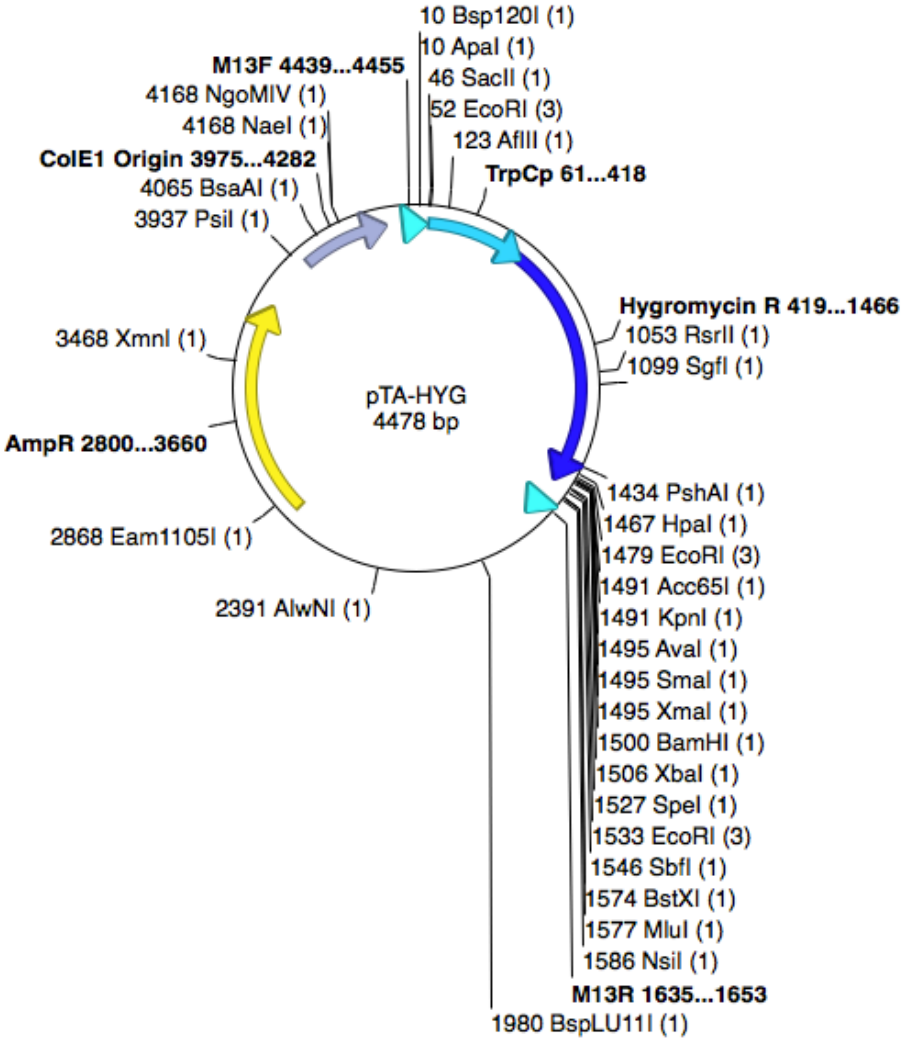

Appendix 1. Plasmid map of pTA-HYG

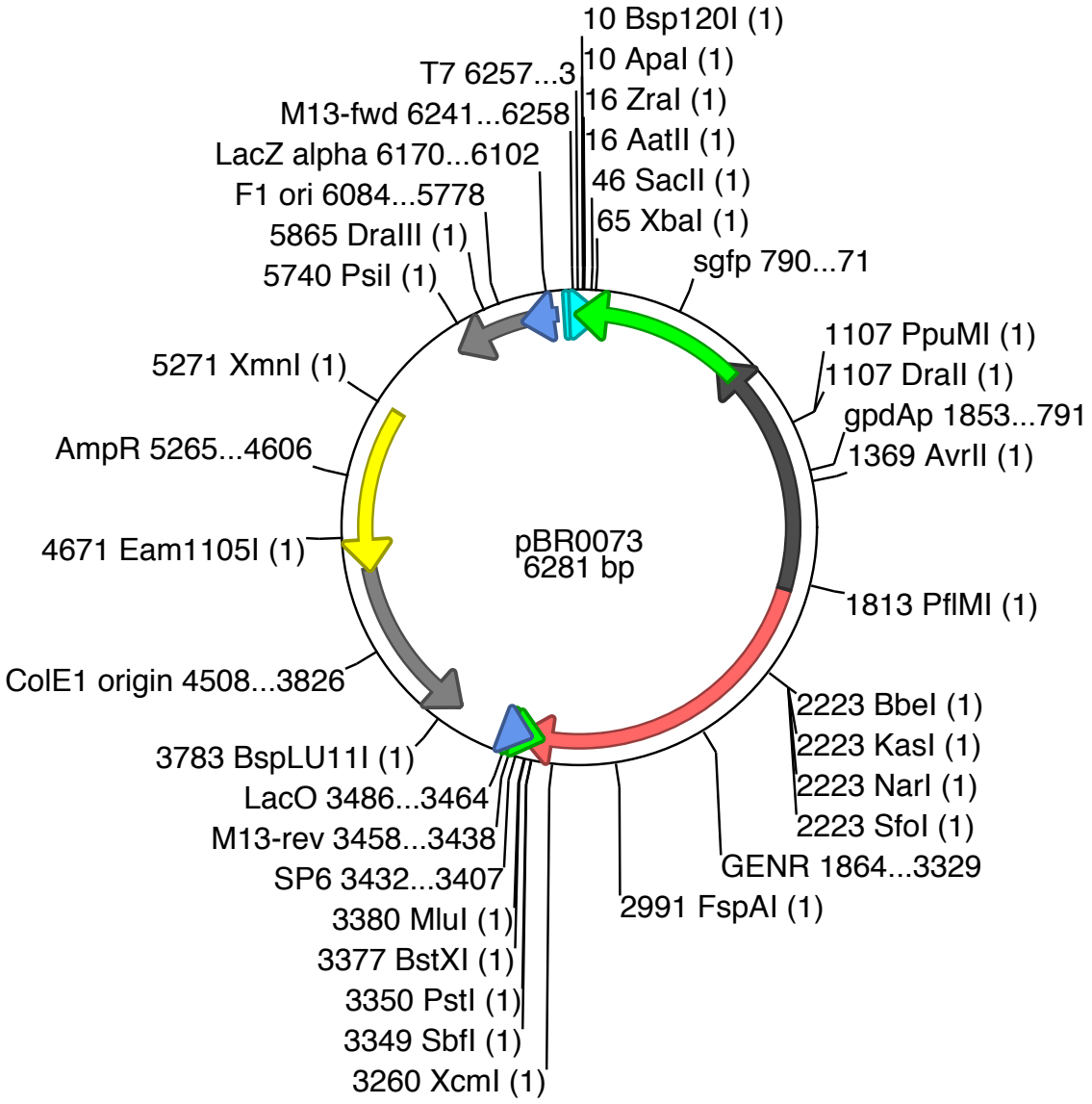

Appendix 2. Plasmid map of pBR0073

Appendix 3. Primers utilized in this study.

Name	Sequence
CZM UBL1 A1	AGGCATTGGCTGATGTGG
CZM UBL1 F1	CGTGAAGAAAAGGAGCGACTG
CZM UBL1 F1n	AGCAGTGCATTTGATGTTACCG
CZM UBL1 F2	ATTACAATTCACTGGCCGTCGTTTTACGCTCTGCTTCTCCAACCTTG
CZM UBL1 F3	CGTAATCATGGTCATAGCTGTTTCCTGTTGAAGAATTGCTTGCTGGAGTC
CZM UBL1 F4n	CCTATGCGAATGCCAAACTGTC
CZM UBL1 F4	CGTCTTCTTGCTCGATGTGC
CZM HAP3 A1	CAGGTTGTGGCATGGAGAG
CZM HAP3 F1	GCACAGAGTGGTGAAGCTC
CZM HAP3 F1n	GCGATGTGAGCAGCGA
CZM HAP3 F2	ATTACAATTCACTGGCCGTCGTTTTACAGACCCGTTTTGTGTAAGCG
CZM HAP3 F3	CGTAATCATGGTCATAGCTGTTTCCTGGCTGCCCGATATAGAGTGCT
CZM HAP3 F4n	CGCATTGACTTGAGATTCTTCCG
CZM HAP3 F4	ACGATAACGTAGAATTGCGACG
CZM GPA1 A1	ACTGTCTTGTAGGTAGTAGTGTCG
CZM GPA1 F1	GCAGGAGCGTTCATTCACC
CZM GPA1 F1n	CATCGCCATCACCATACCG
CZM GPA1 F2	ATTACAATTCACTGGCCGTCGTTTTACCGATGGCGTGTTGGACA
CZM GPA1 F3	CGTAATCATGGTCATAGCTGTTTCCTGATCGGAGCGGAAAAAGTGG
CZM GPA1 F4n	AGCAAAAGCAGCGTCTCAC
CZM GPA1 F4	CGGTGCCATTTCAGGAATG
CZM GPA2 A1	TGTGGCGTGGTTGGG
CZM GPA2 F1	CGTTCATGCTCTCTTCGCT
CZM GPA2 F1n	GCCGTCTCCACCTTGG
CZM GPA2 F2	ATTACAATTCACTGGCCGTCGTTTTACCGACGACCCCAAACCG
CZM GPA2 F3	CGTAATCATGGTCATAGCTGTTTCCTGCACTTTCTCCATTTACAGAGCCA
CZM GPA2 F4n	GCCGTCTTCCACCAAGG
CZM GPA2 F4	GGTTTGATGGCGGAAGTGTG
CZM GPA3 A1	CTCTTTCGCTGTGACGGT
CZM GPA3 F1	GGCTGAAAACTGGGTCGTG
CZM GPA3 F1n	CAGGTTCGCCGTGAGG
CZM GPA3 F2	ATTACAATTCACTGGCCGTCGTTTTACTCCCAAATGCCATCAATACCG
CZM GPA3 F3	CGTAATCATGGTCATAGCTGTTTCCTGCCATTCTTGTGATACCCAACAGC
CZM GPA3 F4n	CGAGCGAGCAAACAAAGAACC

Appendix 3 Cont. Primers utilized in this study.

Name	Sequence
CZM GPA3 F4	TGAAGCCAACCGTTTTGCG
CZM GPB1 A1	GCCACTCCTCCAGACCA
CZM GPB1 F1	AGGCGTGTCGGCACA
CZM GPB1 F1n	CAGATCACACAGGCTGGGA
CZM GPB1 F2	ATTACAATTCACTGGCCGTCGTTTTACGGAACAAGCACGCACCAG
CZM GPB1 F3	CGTAATCATGGTCATAGCTGTTTCCTGATTGGCGAACCTGTGTGC
CZM GPB1 F4n	CACAGTTGATGCTATTGAGGGC
CZM GPB1 F4	CGTACTGTACTGTACCTCGCA
CZM RAS2 A1	ACGCCACGGAAAGGTGT
CZM RAS2 F1	AGCGGAGATGGACTGGAC
CZM RAS2 F1n	ACAGGACGAGACGAGACG
CZM RAS2 F2	ATTACAATTCACTGGCCGTCGTTTTACGGTCTATCGCTCGTGTG
CZM RAS2 F3	CGTAATCATGGTCATAGCTGTTTCCTGCAAAACCTCACAGCATTCGGA
CZM RAS2 F4n	TCTGGATCGCAAAAGATGAGC
CZM RAS2 F4	CTGCTTTGGTCTCGTCGTC
CZM FAC1 A1	CTTCTCCACCGTGCGAA
CZM FAC1 F1	GTAGTGTGGGGAGACGCA
CZM FAC1 F1n	CCAGACTGCTGCGGAAC
CZM FAC1 F2	ATTACAATTCACTGGCCGTCGTTTTACGCATCATCGCATCGTTCATCG
CZM FAC1 F3	CGTAATCATGGTCATAGCTGTTTCCTGAAGCGAGCGATTTCTTGTCAC
CZM FAC1 F4n	GACGACGAATCCGAATGAGC
CZM FAC1 F4	CCTACTCCTCTTCTTGTCATCCAC
CZM PTH11 A1	GCTGTGATGGTTTTCCGCT
CZM PTH11 F1	GGACTTTAGTTCATCAGCGACTC
CZM PTH11 F1n	ACATACCCGCCTTTGCC
CZM PTH11 F2	ATTACAATTCACTGGCCGTCGTTTTACGGGATGCCACAGACAAGC
CZM PTH11 F3	CGTAATCATGGTCATAGCTGTTTCCTGCCAACACCGCAAGTGAAGC
CZM PTH11 F4n	GTCGTCTTCGTCGTTGTCG
CZM PTH11 F4	TGGTGGGTAGTCTTCAAATGGAG
CZM PIC5 A1	GGAGGAGGCAATGACCG
CZM PIC5 F1	AAGATTGATGTCGTTGCTGGTG
CZM PIC5 F1n	CTATCGGCGGCTATATGCG
CZM PIC5 F2	ATTACAATTCACTGGCCGTCGTTTTACGCTTATGAAGAGTTTGATATGGCATCG
CZM PIC5 F3	CGTAATCATGGTCATAGCTGTTTCCTGTTTGTATAATGAGAGTGTGGTGAGC

Appendix 3 Cont. Primers utilized in this study.

Name	Sequence
CZM PIC5 F4n	GCTAGGCAAGAGTTGGAAAGG
CZM PIC5 F4	ATGCCCAGCGAAGCG
CZM UNKN3 A1	CCGCTCATTCTTTGTTGCTG
CZM UNKN3 F1	GTGACAACTTCTCCCGCATC
CZM UNKN3 F1n	CCCTAAGCGGAAATCTGAACAG
CZM UNKN3 F2	ATTACAATTCACTGGCCGTCGTTTTACCTGGTATGTTTGCGACTTGAGG
CZM UNKN3 F3	CGTAATCATGGTCATAGCTGTTTCCTGTTCGTTTGATGATGCTGTGGT
CZM UNKN3 F4n	GCTGAAGATGGTCTGCTTGTC
CZM UNKN3 F4	TCTGGTCGCACAGTCTTCC
CZM UNKN6 A1	CTTGGGATGGATGTGTCGT
CZM UNKN6 F1	GTGTGCCTGCCTTCTGC
CZM UNKN6 F1n	CCGACCGTGGATGGC
CZM UNKN6 F2	ATTACAATTCACTGGCCGTCGTTTTACGGTGCCCGCTTCAGG
CZM UNKN6 F3	CGTAATCATGGTCATAGCTGTTTCCTGGAACGAAACGGAAGAAATGACCA
CZM UNKN6 F4n	CTGAATAGGAGGCTGCGACTC
CZM UNKN6 F4	GCTCTGGGTGCTTGAGG
CZM UNKN7 A1	GGAACAGATGAATGGTCTACGG
CZM UNKN7 F1	GGAAGCGAGAGCAGCC
CZM UNKN7 F1n	GGTTCTGCGATACCTTCTCC
CZM UNKN7 F2	ATTACAATTCACTGGCCGTCGTTTTACAGATTGCCCTGACTTTGGAG
CZM UNKN7 F3	CGTAATCATGGTCATAGCTGTTTCCTGCATCTTCGGGCGTTTCTCTG
CZM UNKN7 F4n	CACTCAGCCTAGACCTGCTC
CZM UNKN7 F4	TGAGGTAGGTGCTGTGAGC
CZM FRQ A1	GCAGGGCATCGAACGG
CZM FRQ F1	ATCGTCGATGGCTCACAC
CZM FRQ F1n	GCTCCCGTCTGATGCTG
CZM FRQ F2	ATTACAATTCACTGGCCGTCGTTTTACATGGGCGGCATTGCTG

Appendix 3 Cont. Primers utilized in this study.

Name	Sequence
CZM FRQ F3	CGTAATCATGGTCATAGCTGTTTCCTGGACGAGATGGGAG ATGGCTA
CZM FRQ F4n	TCGCCAGCGTTTCGTC
CZM FRQ F4	TGCTGCTCTCGGTGCT
CZM FRQ A2	GGACTTACCGACTCATTCTTGG
CZM TOR A1	AGTAGGCATACTAGGCGTTAGAG
CZM TOR F1	GGCAGTATAAGGACGGAAGGTAG
CZM TOR F1n	AGCCTAGCCCGTAATACTACC
CZM TOR F2	ATTACAATTCACTGGCCGTCGTTTTACCGTGCTTGCGATGC G
CZM TOR F3	CGTAATCATGGTCATAGCTGTTTCCTGCGAAAGCGGATGAA CAAGTTCG
CZM TOR F4n	CTCTCCATCCTCTTCATCTACGG
CZM TOR F4	TGACATCTTCAGTTGGTTGCTG
CZM TOR A2	GCTTGGCTTTCATCAACTTGG
HYGSCRN D	GTACACAAATCGCCCGCAGAAG
HYGSCRN A	CTACTGCTACAAGTGGGGCTGA
HYGSCRN B	AGGCTTTTTCATTTGGATGCTTGGG
HYGSCRN C	TCTTCTGGAGGCCGTGGTT
CZM OS-2 A1	GTCGCAGCATCCTCCT
CZM OS-2 F1	CACGACACCGCAGTCG
CZM OS-2 F1n	GTACGCACCCGTCTTGC
CZM OS-2 F2	ATTACAATTCACTGGCCGTCGTTTTACAGGTGGGGTCGTTC TCG
CZM OS-2 F3	CGTAATCATGGTCATAGCTGTTTCCTGGCGACATCCCACGA ACC
CZM OS-2 F4n	CGTCACTACCTTGACCTGGTC
CZM OS-2 F4	GGTGGCATCAGCTTGTCG
CZM OS-2 A2	GCTGCGCGACTAGCTC
CZM PP4 A1	GACGCCACGCTCTTCG
CZM PP4 F1	GCTGACTCGACGCATCTC
CZM PP4 F1n	TCTTACCCATCGCGATGC
CZM PP4 F2	ATTACAATTCACTGGCCGTCGTTTTACGTGCGTGGTACGTT CCTC
CZM PP4 F3	CGTAATCATGGTCATAGCTGTTTCCTGCCGTTTTGGTTATGC AGCG
CZM PP4 F4n	ATCGCATCCTGTCAAGTTCC
CZM PP4 F4	CGGCTCTGCCATACGAC
CZM PP4 A2	GATGGCAAGGAGGTCAGC
CZM NOP-1 A1	GGTGCCATTTGACGAAC
CZM NOP-1 F1	CGGCACGTTGTTGAGGTC
CZM NOP-1 F1n	CGACTTGGACACGAAAGAGG
CZM NOP-1 F2	ATTACAATTCACTGGCCGTCGTTTTACGTGCTTCCCGGAAG ATGG

Appendix 3 Cont. Primers utilized in this study.

Name	Sequence
CZM NOP-1 F3	CGTAATCATGGTCATAGCTGTTTCCTGACGAGGGTGCTTAAATGCG
CZM NOP-1 F4n	CGATCCCATGCTACATCACG
CZM NOP-1 F4	CCACAACAGCACCTTCCAC
CZM NOP-1 A2	GTCCCAGAAAGAGTACGTGAG
CZM PhyHK A1	CAGACCATTCCGCGAGCA
CZM PhyHK F1	CAGCAGGTCTTGCACGATC
CZM PhyHK F1n	GATGGAGGCAAAGACGACGT
CZM PhyHK F2	ATTACAATTCACTGGCCGTCGTTTTACGCAGTTGCTACTGCAGCG
CZM PhyHK F3	CGTAATCATGGTCATAGCTGTTTCCTGGACACGACAGCACGATGC
CZM PhyHK F4n	CGATCTCCGTGTGCTCGT
CZM PhyHK F4	GTCGTAGTCGATGTGTGCG
CZM PhyHK A2	TTGGCGATCTGCAGCCA
CZM srbA A1	GTCTCGCCTTCTGCTCTG
CZM srbA F1	TGATACACCTGAACCTCCGA
CZM srbA F1n	ACAAGCCGTCCATCAGC
CZM srbA F2	ATTACAATTCACTGGCCGTCGTTTTACTCGCAGTCGCGTTTCTG
CZM srbA F3	CGTAATCATGGTCATAGCTGTTTCCTGGCGTGGAGCAAAATGACC
CZM srbA F4n	GGTGATGCTTCTGCAACTCA
CZM srbA F4	GGACAAAACAGCCACGGC
CZM srbA A2	TGGAGAGAGCGGATCGTATG
CZM WC2 A1	AAGTCCTTGGGCGGAGA
CZM WC2 F1	TTGGCCACAGTGAAGTCTC
CZM WC2 F1n	GCATTCGCGGCATGATCG
CZM WC2 F2	ATTACAATTCACTGGCCGTCGTTTTACGTCAGCACTCATCATGCC
CZM WC2 F3	CGTAATCATGGTCATAGCTGTTTCCTGTTGCACTGGGCTTCCAG
CZM WC2 F4n	CCAGAGCACCAACGACAA
CZM WC2 F4	GTCTGCTTGCCGATGAGC
CZM WC2 A2	CGAGATGTCATGTCTGGGC
CZM HHK6P A1	GCTTGACCACAGAGGCGAT
CZM HHK6P F1	TGCGCAAGAGAAGAAGAGC
CZM HHK6P F1n	GGTGTTGAAGAGGGACTCG
CZM HHK6P F2	ATTACAATTCACTGGCCGTCGTTTTACGTAGCCATCATCGGTGCC

Appendix 3 Cont. Primers utilized in this study.

Name	Sequence
CZM HHK6P F3	CGTAATCATGGTCATAGCTGTTTCCTGTCAGACCAATGGGTTTCACG
CZM HHK6P F4n	TGGAGACGACGGTGATGG
CZM HHK6P F4	GCTTGCTCAGTGCCGAA
CZM HHK6P A2	CCAGTCGACCAGAGCTTG
CZM HHK2P A1	TCACGCACTGTTCAGGTG
CZM HHK2P F1	TGCTCACTAAGCGGACGT
CZM HHK2P F1n	GAACGACGACGTGTAGGTC
CZM HHK2P F2	ATTACAATTCACTGGCCGTCGTTTTACTCTGGCACTTTGCCCAG
CZM HHK2P F3	CGTAATCATGGTCATAGCTGTTTCCTGACGACCAACGAATGCACAC
CZM HHK2P F4n	GCTTGCTTCGGAAGCGA
CZM HHK2P F4	GACCTGTGACCTGGCTT
CZM HHK2P A2	AAGGGCGTTCGTTCGGT
CZM CCH-1 A1	ACGCTGAGACAGTTGGGT
CZM CCH-1 F1	GTGATCATGTAGGGCCGAAC
CZM CCH-1 F1n	ATTGGCCGTCGATCTGC
CZM CCH-1 F2	ATTACAATTCACTGGCCGTCGTTTTACCACCTGGGGACACAAACG
CZM CCH-1 F3	CGTAATCATGGTCATAGCTGTTTCCTGTGCGATACCGCACGCAA
CZM CCH-1 F4n	ACCACCGACACACGCTG
CZM CCH-1 F4	CCTCTCCACCACCATCAT
CZM CCH-1 A2	GAAGCTACTACGTGCCCG
CZM ERG K+ A1	TTGGAGTCACGGGCTCT
CZM ERG K+ F1	CGCTGGTTCTTGTTTCGTG
CZM ERG K+ F1n	CGAAAACGCCAGCACAC
CZM ERG K+ F2	ATTACAATTCACTGGCCGTCGTTTTACCTTCGTTCCATGCATGCAC
CZM ERG K+ F3	CGTAATCATGGTCATAGCTGTTTCCTGAGGTAGTCGCAAGCTTGC
CZM ERG K+ F4n	GTAGGCGCATAGGCCATC
CZM ERG K+ F4	GGTCAAGGTGGCAATTGTG

Appendix 3 Cont. Primers utilized in this study.

Name	Sequence
CZM ERG K+ A2	GGTACAAAGAAGCGCGACA
CZM FRH A1	CGGGTAGAGCGTTTGCG
CZM FRH F1	TTCTGCGCTGTAGTATCGC
CZM FRH F1n	AGTTGTGGGATCGGTCGT
CZM FRH F2	ATTACAATTCACTGGCCGTCGTTTTACCGGCGTGGCAGTCTC
CZM FRH F3	CGTAATCATGGTCATAGCTGTTTCCTGCCGCGACGGATATACAGG
CZM FRH F4n	CGTCACAACGAAGAGCAACTC
CZM FRH F4	CGCGAAGCATGGTTGAGATG
CZM FRH A2	TACCATCCCCAACCAGATCC
CZM Prd4 A1	ATCGTCCATGTCCACCTC
CZM Prd4 F1	GCCTGGATCGTTTCGATGG
CZM Prd4 F1n	TCGATCCCAGCAAACAGC
CZM Prd4 F2	ATTACAATTCACTGGCCGTCGTTTTACAGCAGAGCTGCACGATG
CZM Prd4 F3	CGTAATCATGGTCATAGCTGTTTCCTGGACGAAAAGTTGGGCGCAT
CZM Prd4 F4n	CGTCTGCCCAATATACAGCA
CZM Prd4 F4	CTCCTTCGCATCACCCATC
CZM Prd4 A2	CTCCAAATCCTCCACGAGC
CZM CAMK-1 A1	CTGCTTCCTTGGCACCTAC
CZM CAMK-1 F1	TCGACATTCTGCACAGGAC
CZM CAMK-1 F1n	ACAGATGATGCCGTTGCTG
CZM CAMK-1 F2	ATTACAATTCACTGGCCGTCGTTTTACCATGTCGTGCAGACTCAGG
CZM CAMK-1 F3	CGTAATCATGGTCATAGCTGTTTCCTGAGCATTGTAGAAGGCTGGAG
CZM CAMK-1 F4n	CTGGACTGGAATGGACTCAC
CZM CAMK-1 F4	TGCTTGTAGGCGCTGCA
CZM CAMK-1 A2	GCTTGCTCGATGGAGCATG
CZM CK2 A1	TTCAGCGGCAGACGATG
CZM CK2 F1	GCGATGATGAGAGCGACGA
CZM CK2 F1n	TCACTGCCAACGAAGCTG
CZM CK2 F2	ATTACAATTCACTGGCCGTCGTTTTACTCGAGCGCGACTTGATGC

Appendix 3 Cont. Primers utilized in this study.

Name	Sequence
CZM CK2 F3	CGTAATCATGGTCATAGCTGTTTCCTGTCGCGCTCAGAACG AAG
CZM CK2 F4n	GCCAGATCAGCAGCAAGG
CZM CK2 F4	GGACGAGACGTACAGACG
CZM CK2 A2	TGAAGCGAAGCCAGGAG
CZM CK1a A1	ACGAGGGCGTTTCGCAT
CZM CK1a F1	AATGGGTGCACGCTTCG
CZM CK1a F1n	GCGCTTGCTACCGGATG
CZM CK1a F2	ATTACAATTCACTGGCCGTCGTTTTACTTCTACCGAGAGCG AGCAG
CZM CK1a F3	CGTAATCATGGTCATAGCTGTTTCCTGGGGGCTGCCATTCA CTC
CZM CK1a F4n	CGCGCGAAAACTCAACTGG
CZM CK1a F4	TACCCCGCTCCTTCAGCA
CZM CK1a A2	AAACGCCAAGGCCACGT
CZM PKA A1	AACCCCATCCGGATAGCGA
CZM PKA F1	GGCTGCAAACGATGTATGCG
CZM PKA F1n	AAGCAATCGGCGTGTTGC
CZM PKA F2	ATTACAATTCACTGGCCGTCGTTTTACGGCGGTGTTGCTAT CTGT
CZM PKA F3	CGTAATCATGGTCATAGCTGTTTCCTGAGGATCGCCGGATT CGTC
CZM PKA F4n	AGGAGGGCGATTTACCG
CZM PKA F4	GGCCGAATTGGATCGTAGC
CZM PKA A2	AGAGAATTTCCCGAGCAGAC
CZM PP1 A1	CGATCGCTGTCGATGAGTG
CZM PP1 F1	CGTGGTGTGTTGCTATGCAG
CZM PP1 F1n	CGCCAAAGGCATACAGTTCG
CZM PP1 F2	ATTACAATTCACTGGCCGTCGTTTTACAGGCCTGGGTGTAC TTGG
CZM PP1 F3	CGTAATCATGGTCATAGCTGTTTCCTGGCGAGAGAGCGAA AGCTG
CZM PP1 F4n	CGTAGCATCCGCAATCTCC
CZM PP1 F4	CACTGTCCACCGTCGAC
CZM PP1 A2	CGAATCCCTTGCCCTCTG
CZM PP2 A1	CTCTCGTCGCTTTGTCTCG
CZM PP2 F1	GGCAATGACGGACTTGTGC
CZM PP2 F1n	GGATGTACTGGCGTCGGAT
CZM PP2 F2	ATTACAATTCACTGGCCGTCGTTTTACCGGCGCTGTCAAAC ACAG
CZM PP2 F3	CGTAATCATGGTCATAGCTGTTTCCTGCTGGCCACGAAGAT TCGG
CZM PP2 F4n	ACAAGTGGCTCACTTCACC
CZM PP2 F4	AAGCGAGGTGATCTGTGC

Appendix 3 Cont. Primers utilized in this study.

Name	Sequence
CZM PP2 A2	CGCTGCTTGCTAGCT
CZM FWD-1 A1	CCCCATCTTGGCAAGACG
CZM FWD-1 F1	CGGTGAAGTCGAAGTCTCG
CZM FWD-1 F1n	ATGGCACCTCAGTTACAGTG
CZM FWD-1 F2	ATTACAATTCACTGGCCGTCGTTTTACCGGCGAAGTGGTGTGTC
CZM FWD-1 F3	CGTAATCATGGTCATAGCTGTTTCCTGGGACTTTGCCAACGGAGAC
CZM FWD-1 F4n	TCAGGACGAAACGAGAACG
CZM FWD-1 F4	ACGAAGAGGGCAAGAAGC
CZM FWD-1 A2	CCGAACCGGATAGACAAGC
CZM PHYHK F3v2	CGTAATCATGGTCATAGCTGTTTCCTGTGATACAGGTGGTGATTGACAG
CZM PHYHK F4nv2	TGCGAGAGGGGAGGATG
CZM PHYHK F4v2	GGTGCTGGTGGTCGATG
CZM PHYHK A2v2	CAGGGCAGCACCTACTC
CZM CCH-1 F3v2	CGTAATCATGGTCATAGCTGTTTCCTGGTTGCTCGGAAGATGAGAGG
CZM CCH-1 F4nv2	GCCCTCTCACTACATTGCG
CZM CCH-1 F4v2	GCCGAGGTCATCAAGCAG
CZM CCH-1 A2v52	CGGAGCTGGTCTCTTGC
CZM ERG K+ F1nv2	AACGTACCGAGAGAAAGCCA
CZM ERG K+ F3v2	CGTAATCATGGTCATAGCTGTTTCCTGCATCACACAGCAAGGCTCA
CZM ERG K+ F4nv2	CTCTCTCGACCTGCATGAGA
CZM ERG K+ F4v2	CAGCGTGACCCTCTTCG
CZM ERG K+ A2v2	TGGTGTTCACACATCCACAG
CZM PP4 F1nv2	CAGTCGGCACAGGCTAC
CZM WC-2 F1nv2	CGAAGACACGCGAGCTG
CZM HHK2p F4nv2	TTTTGCTGCTGGAGGAGTC

Appendix 3 Cont. Primers utilized in this study.

Name	Sequence
CZM FRH F4nv2	CGAGTGGTTGTAGCATGTCG
CZM Prd4 F4nv2	CCTTCTTCTCCACCAACTCC
CZM GPB1 F3v2	CGTAATCATGGTCATAGCTGTTTCCTGGCGAGGAAGCATGACTGAC
CZM GPB1 F4v2	CACTCTCATCAAAAGCAGGTCG
CZM GPB1 F4nv2	CAACATACAGTGCGTAGATGCC
CZM GPB1 A2	ACAAGCATCGGGACTGAGC
CZM GPA2 A2	GCCACATGGGTGAACCG
CZM GPA3 A2	GTCAAAGTGAGTTCGCGATCAG
M13spmrkF	GTAAAACGACGGCCAGTGAATTGTAA
M13spmrkR	CAGGAAACAGCTATGACCATGATTAC

CHAPTER VI: SUMMARY AND CONCLUSIONS

The research presented in this dissertation identified novel mechanisms of pathogenesis in *C. zeae-maydis*. An important component of this work was the elucidation of stomatal tropism that allowed for the thorough characterization of hyphal responses to environmental stimuli. Prior to this study, stomatal tropism by plant pathogenic fungi was described only in qualitative terms, which limited the ability to dissect specific components of hyphal tropic reorientation. The discovery that stomatal tropism was comprised of both sensory distance and reorientation toward a stomatal cue allows for an integrative approach to study host-pathogen interactions that combines various sub-disciplines of fungal biology. For example, the process of hyphal growth and development displayed by *C. zeae-maydis* and *C. beticola* during infection can be now be directly compared with well characterized saprophytic fungi to investigate how fungi interact with their hosts and environment.

A key component of environmental sensing in *C. zeae-maydis* identified in this research was the role of oxygen during stomatal sensing, appressorium formation, and growth *in vitro*. During incubation in an atmosphere enriched in oxygen, *C. zeae-maydis* formed hyphal branches or apically reoriented hyphal growth in response to stomata but formed fewer appressoria. Little is known regarding the relationship between volatile plant emissions and fungal pathogenesis, despite the evident interplay between the two. The findings from this dissertation point toward intriguing questions about how different plant exudates, such as broadly conserved chemicals like oxygen and plant-specific exudates like uncharacterized volatile organic compounds (VOCs), affect the development of disease. Water vapor has long been hypothesized to act as a cue for

pathogens, but research investigating the effects of stomatal oxygen and VOC levels on filamentous fungi during foliar pathogenesis would more directly address hypotheses about how plants sense and perceive their host environment. Furthermore, the elucidation of the chemicals emitted by stomata prior to pathogeneses by filamentous fungi would likely identify a previously unknown suite of volatile chemicals involved in aspects of plant disease, and uncover a novel layer underlying the complexity of plant/fungal interactions. The potential chemoattractive function of different uncharacterized stomatal exudates highlighted in this study refreshes the 97-year old observation by Poole and McKay that hyphae of *C. beticola* sensed an unknown signal from stomata and initiated pathogenic development.

The post-genomics era has increased the tractability of "non-model" fungi, leading to broader appreciation of emerging fungal systems that exhibit markedly diverse physiology and infectious processes. For instance, discussions of appressorium mediated leaf penetration and the development of plant disease commonly begins with the established fungal models of rusts, *M. oryzae*, or *Colletotrichum* spp., despite their lack of applicability to other groups of pathogenic fungi. In contrast, *Cercospora* lacks a single model species for foliar pathogenesis and molecular genetics, but represents a similarly large group of fungi with a diverse range of environments, hosts and methods of pathogenesis. For example, appressoria of *C. zeae-maydis* are required for leaf penetration, but since penetration is mediated through the stomatal pore and appressoria do not possess morphology consistent with turgor generation, their specific function is unknown. Appressoria of *C. zeae-maydis* may act as biochemical reserves prior to and during infection, providing the underlying hyphae with virulence-associated products

prior to the switch from biotrophic to necrotrophic growth. The complexity underlying stomatal infection *by C. zeae-maydis* represents a novel target to dissect foundational questions in fungal genetics and biology that remains unanswered despite decades of research.

The elucidation that light sensing, light-associated gene expression, and responses to volatile chemoattractants regulate stomatal tropism and penetration informs the development of potential gray leaf spot management strategies. Since stomata are the only known portals of entry for *C. zeae-maydis*, crop improvement strategies could include selecting for maize lines that display small changes in stomatal aperture or alterations in stomatal functions that reduce disease severity while maintaining yields. Genetic resistance is often determined by lesion counts following inoculation, but research in this dissertation clearly showed that a complicated cross talk occurs between maize stomata and fungal hyphae prior to infection. While time consuming and expensive, a histopathological survey of various sources of resistance to gray leaf spot may identify lines that elicit less stomatal tropism, or promote reductions in appressorium formation on stomata. Resistance like the previously mentioned examples may not manifest in a quantifiable reduction in lesion formation when viewed as part of a field-wide survey, but may still be valuable forms of resistance that can be crossed into other resistant lines. Relatedly, fungicides are frequently applied to reduce the impact of gray leaf spot and other fungal diseases of crops, and the results from this dissertation could lead to research that will improve chemical efficacy and reduce application rates. For instance, once the chemoattractant chemicals emitted from stomata are elucidated, chemical treatments can be developed that essentially mask natural plant exudates or

otherwise disrupt stomatal tropism, thus resulting in less disease pressure. Future research will likely elucidate the role of circadian rhythms in *C. zeae-maydis* and could identify periods of the day or night when the fungus is most pathogenic. The timing of chemical treatments during the period of maximum fungal pathogenesis potential fits well within the precision agriculture movement, and could represent significant savings in areas where gray leaf spot is a major pathogen.

In conclusion, the research completed in this dissertation has increased the understanding of how *C. zeae-maydis* senses maize stomata during pre infection stages, and elucidated several regulatory mechanisms underlying initial stages of pathogenesis. The elucidation of hyphal dynamics during chemoresponsive stomatal tropism allows for more detailed studies into the genetic regulation of infection by providing an empirical framework with which to analyze infectious growth. Several novel genes were discovered that may play roles in pathogenesis, including *RJP1*, a putative epigenetic regulator of gene expression, two novel GPCRs highly expressed during pathogenic growth, and several pathogenesis-related proteins like hydrophobins and heterokaryon incompatibility proteins. Lastly, this research established that infection by *C. zeae-maydis* is regulated by a conserved clock component that is associated with circadian rhythmicity in model fungi. This observation represents one of the first reports of a potential circadian rhythm-related gene underlying pathogenesis in filamentous fungi.